University of Alberta

Crane Lifting Operation Planning and Lifted Object Spatial Trajectory Analysis

by

Jacek Olearczyk

A thesis submitted to the Faculty of Graduate Studies and Research
in partial fulfillment of the requirements for the degree of

Doctor of Philosophy

in

Construction Engineering and Management

Department of Civil and Environmental Engineering

Fall 2010
Edmonton, Alberta

Examining Committee

Dr. Mohamed Al-Hussein, Department of Civil and Environmental Engineering,
University of Alberta

Dr. Ahmed Bouferguene, Campus Saint Jean,
University of Alberta

Dr. SangHyun Lee, Department of Civil and Environmental Engineering,
University of Alberta

Dr. Josef Szymanski, Department of Mining Engineering,
University of Alberta

Dr. Pierre Boulanger, Department of Computing Science,
University of Alberta

Dr. Saad H. Al-Jibouri, Associate Professor
University of Twente, Netherlands

Dedication

This thesis is dedicated to the memory of my noble father, Wladyslaw, who motivated and supported my academic decision, my wonderful wife, Maria, and my lovely son, Karol.

ABSTRACT

Compact facility designs and retro-fitting of facilities that involve heavy lifts are often performed in congested areas. Tight schedules increase the requirement to provide detailed heavy lift analysis. The planning of every aspect of a critical lift operation is essential. Managing the behavior and trajectory of the lifted object during the lift is often left to the field crew. The rigger signalman and the crane operator communicate by radio, or by hand signals, to maneuver the lifted object between obstructions. This thesis presents advancements in the development of mathematical algorithms for the lift object trajectory path and analysis. The proposed methodology is divided into smaller manageable phases to control the process and at the same time create independent modules. Each step of the lifted object movement was algebraically-digitally tracked, starting at the lifted object pick-point through an optimum path development to the object's final position or set-point. Parameters such as the minimum distance between the lifted object and passing obstructions and the minimum clearance between the lifted object and the crane boom envelope are some of the many predefined rules that were taken into account. Each step in the developed algorithm provides a short description, partial decision flowchart, and graphical interpretation of the problem, and some sections cover mathematical calculations of a defined path. The lifted object's spatial trajectory analysis and optimization are part of the complex assignment relating to the crane selection process. The proposed methodology is tested on a case study, which is also described in this thesis in order to illustrate the essential features of the proposed methodology.

Acknowledgements

First, I would like to thank my family, especially my father Wladyslaw. He ignited the idea of expanding my personal development. I express special thanks to my wife, Maria, who greatly supported me in hard times of exams and research work.

This dissertation and attached information reflects the hard work of many of my colleagues. I would like to thank my supervisor, Dr. Mohamed Al-Hussein, and co-supervisor, Dr. Ahmed Bouferguene, for supporting the exploration of undeveloped sections of crane lift analysis and directing me over the course of study to successfully compose this considerable manuscript. I believe that our creative brainstorming sessions formed a special professional bond that has progressed from a strict academic relationship to a friendship that will continue beyond graduation. I am also grateful to Dr. Simaan M. AbouRizk for his encouragement at the beginning, during my study and research development.

I would also like to thank my colleagues at PCL Industrial Management Inc.: Engineering Manager Ulrich (Rick) Hermann, who recognized my knowledge and accomplishments over the past few years and helped me construct the final shape of this dissertation, and Construction Engineer Ali Hendi, who as a fellow student encouraged me to stay strong during my first two semesters and now as a colleague patiently explains, critiques, and fairly judges my ideas for unique solutions.

This research would not have been presented in such a way without Kullman Building Corp. Lebanon, New Jersey, USA. Particularly, I would like to thank CEO Avi Teylas, who personally monitored the research progress, and COO Roger Masciatti, who helped solidify our ideas and gave us full support in implementing them.

This research was partially funded by the Natural Sciences and Engineering Research Council of Canada (NSERC); PCL Industrial Management Inc., Edmonton, Alberta, Canada; and by the University of Alberta, Construction Engineering and Management Group.

Table of contents

List of Tables

Table of Figures

CHAPTER 1 – INTRODUCTION

1.1 Motivation of Research

On large construction sites there are usually several cranes operating to undertake material handling tasks; together they can provide overall coverage of all materials from onsite supply to demand points. Many factors influence the location of cranes. In the interest of safety and of efficiency of operations, cranes' locations are carefully selected in order to avoid collisions. However, this ideal situation is often difficult to achieve in real-world scenarios; constrained available space as well as limited capacity of cranes make it unavoidable that crane areas will overlap. As a result, interferences may be encountered at different elevations.

The analysis of complicated spatial static equipment locations is not an easy task. At present, in most construction sites, crane positions tend to be determined through a process of trial and error. A practitioner, who is responsible for crane configuration and lift analysis, makes a subjective decision about optimum crane layout relay based on experience and a general practice manual. Such interpretation of maintaining high safety standards is not economical and not competitive in this rapidly developing industry. To help engineers optimize solutions for the crane planning process, the proposed new and mathematical algorithm has been developed.

A mathematical approach to harness crane related issues is not a new concept in the construction industry; however, research usually focuses on smaller problems that solve tasks on-the-fly, but neglect the overall picture. A combination of site preparation, proper crane selection methods, and advanced object trajectory development analysis are the sequential steps of capturing knowledge and release a ready product to industry professionals.

This thesis presents advancements in the development of mathematical algorithms for the lift object trajectory path and analysis.

The proposed methodology is divided into smaller manageable phases to control the process and at the same time create independent modules. Each step of the lifted object movement was algebraically tracked, starting at the lifted object pick-point, through an

optimum path development, to the object final position or set-point. This revolutionary approach envisions most possibilities, where crane-object tandem is faced at typical construction sites. If certain, depending on the site or climatic situation, the main core of the algorithm is easy to reconfigure and remodel to custom requirements.

1.2 Research Goal and Objectives

This research concentrates on combining expert knowledge, mathematical interpretations for crane layout calculations and a spatial object transformation approach. The use of a logical approach combined with the ability to balance new technology implementation for existing products, or working processes, makes this research challenging and the outcomes rewarding.

There is a major goal for this research, as well as specific objectives within these goals.

Goal To automate construction sites crane location and lift operations.

- To provide construction industry practitioners with a constructive method of selecting crane configurations, site crane layout analysis, and crane boom clearances.
- To impart construction lift analysis engineers a tool to analyze crane boom lift objects, spatial clearances, and on object path trajectory development algorithm.

1.3 Dissertation Organization

Chapter 2 summarizes a state-of-the-art literature review of the construction application of modular construction site logistics, spatial crane layout optimization, virtual reality and 4D scheduling techniques, and mathematical optimization algorithms. Chapter 3 presents the proposed methodology and discusses the tools needed for research. Chapter 4 is divided into three sections, each of which presents a separate construction operation challenge: 1) Problems experienced during modular construction assembly; 2) Crane boom clearance analysis to the obstruction top surface slope area, and 3) A spatial trajectory analysis for crane lifting operations. All three sections are based on real-life problems; the sections show the steps involved during preparation and execution and suggest modifications based on the implemented ideas. Chapter 5 presents final remarks regarding current research findings and discusses expected contributions to the existing body of knowledge.

CHAPTER 2 – LITERATURE REVIEW

2.1 State-of-the-art Literature in Modular Construction

When a house or apartment building is divided into smaller units, manufactured at a fabrication facility on the production line, and then moved to the construction site for assembly, the whole operation is referred to as modular construction. Layout of the assembly line may involve several different stations connected to each other. However, modular construction projects are wrongly associated with modular units, which have historically provided shelters for a variety of outdoor activities at remote and urban locations. Over the last decade this method of constructing offices, dormitories, and government facilities has warranted a second look. Due to time savings and high production quality at factory assembly lines, more individual businesses and organizations are beginning to recognize the convenience of having a hotel, diner, or embassy "instantly" erected onsite. It is likely that the benefits of abbreviated construction time compared to conventional stick-built construction appeal to all parties invested in a new acquisition.

Modular construction is not new to the construction industry; however, this term is primarily associated with single family homes, or at the most low-rise, multi-family housing [Murdock 2005]. There are few studies available describing a means of automating the model development process or using robotics in modular construction, although several articles have praised the concept of modular construction with respect to the notion of adding modular units to existing construction, or in terms of its ability to significantly reduce onsite labor [Nasereddin et al. 2007, Bock 2007, Editorial Ca - Leonard 2007]. Where a large number of units is needed for international events, modular construction also plays an important role [Yoders 2005]. But the most significant niche for implementing this type of building is for school facilities, campus/dormitory living, and affordable housing [Dolan 2006, Cardenas and Domenech 2005, Atkinson et al. 2001]. These units are not limited to low-rise accommodations; in fact, the construction of high-rise facilities using a modular approach has also been considered [Cartz and Crosby 2007]. Other examples of successful implementation have been airport roofs, NASA spacecraft architecture, and health care units, from single check-up rooms to operating theatres or pharmacy centers [Veale and Postawa 2007, Smith 2006, Editorial

Health 2007, Editorial Hospital 2007, Editorial Operating 2007, Editorial Pharmacy 2008]. These facilities or units can be customized over the Internet similar to the manner in which an automobile may be customized by the purchaser [Booth 2007]. Ready modules are delivered to the site for assembly, and in this respect a heuristic algorithm can be well utilized [Da Cunha et al. 2007]. Furthermore, unskilled labor issues as well as reduction of electricity consumption by using modular technology and the benefits of off-site construction have garnered the attention of scholars [Rehfeld 2006, Riley 2007, Editorial Off-Site 2006].

2.2 Site Layout Optimization Application in Construction

Cranes are the critical tool to complete components and handle materials in costruction. There are many factors contributing to the selection of the type, number, and location of cranes and expert judgment is essential in this process. Due to the increasing complexity of crane layout, a number of computer applications have been developed to assist practitioners in the selection and utilization of cranes [Manrique 2007].

Computer layout location models were introduced more than 20 years ago. In many cases these layouts are on the critical path toward efficient assembly or production. Crane lifts also vary in complexity: some are very simple, while others present a formidable challenge to construction managers. The approach described by Tam et al. [2001] as well as by Tam and Tang [2003] analyzes a particular area and uses a genetic algorithm (GA) to optimize tower crane operations, whereas Matsuo et al. [1991] and Sivakumar et al. [2003] have concentrated on developing a path planner for two cranes lifts. Deen et al. [2005] as well as Mashood et al. [2007] have continued with this topic of research, employing GA in order to solve the problem. On the other hand, Al-Hussein et al. [2005] and Moselhi et al. [2004] have introduced an algorithm by which to choose the optimal crane with respect to lift capacity while utilizing 3D animation for visualization techniques; in this case mathematical algorithms have been integrated with a database of commercially available cranes. Zhang et al. [1999] have employed their optimization analysis on a group of tower cranes, interacting and searching for conflicts between them. The minimization of transportation travel time [Ascheuer et al. 1999, Boussedjra et al. 2004], with respect to both storage systems and to inter-modal transportation networks, is another important application of the algorithms. The same issues of minimization of travel time, walking cost, and connection between these two factors have constituted

research conducted by Ahuja [2002], who developed a polynomial time algorithm in order to control these issues. Control algorithms for the reduction of material handling cost, utilization of resources [Williams and Narayanaswamy 1997], and analysis of crane operations in warehouse systems [Amato et al. 2002] have also been explored. The optimization and analysis of crane lifts have achieved greater recognition in the sphere of 3D technology and spatial optimization algorithms in conjunction with more advanced capabilities of hardware and software for simulation algorithms [Makhanov 2007, Manrique et al. 2007, Korhonen 2003]. Del Rio-Cidoncha et al. [2007] and ElGanainy et al. [2007] have analyzed floor plan layout designs and the critical steps involved in the design process, as well as the various benefits, techniques, and interactions among these. This approach has led to significant improvements to the layout optimization method. Research exploring similar issues, but on a larger scale for site layout and floor level planning in construction, has also contributed a fair amount of knowledge to the industry [El Beltagi and Hegazsy 2001, Jang et al. 2006].

2.3 Four-Dimensional (4D) Visualization Application in Construction

4D visualization is a technique in which 3D CAD solid models are virtually relocated in a different time frame. Within the construction industry this represents the visual progression of erecting, assembling, digging, and lifting operations. A novel and unique approach, 4D modeling requires full coordination of several independent tasks where at some point each task could interfere with or supplement another. This method forces the operator to look closely at each operation from a perspective rarely seen in the construction industry. Construction business is changing and many realize that new technology will have a major impact on this sector; however, resistance toward implementation of new technology within this field is still substantial. Those pioneers who decide to implement this new approach are usually faced with costly investments in terms of hardware and software, which expectantly provide limitless benefits and savings to each project.

3D applications have a proven record of success in assisting the construction industry, providing useful information for various construction fields. Some of these applications have been used to analyze and test tower cranes [Al-Hussein. et al. 2001], as well as for construction using a tilt-up-panel method [Manrique et al. 2007]. Others have attempted to come up with additional components in order to close the gap between simulation and

visualization [Xu 2001]. Visualization of the proposed design can be of substantial assistance with respect to analysis and communication [Olearczyk and Al-Hussein 2006]. Dynamic graphical depictions, which are able to show the proposed design just as the final product would appear, give users a better understanding of the simulation results, within an environment referred to as Virtual Reality (VR). VR provides visual inside information of modeled construction operations [Messner et al. 2006], and also helps to realistically identify the proposed design [Okyere 2004]. Furthermore, educational institutions are advancing the implementation of new technology for academic purposes [Otto et al. 2005]. Over the past two decades, simulated construction operations have been visualized in several levels of detail, taking into account the given limitations and constraints [Staub-French and Khanzode 2007]. Experiments with VR have extended beyond the automotive, aerospace, and construction industries to encompass specialized fields of human brain research, such as psychotherapy [Ehrsson 2007] and psychology [Lenggenhager et al. 2007, Miller 2007].

2.4 Spatial Analysis Optimization Algorithms for Applications in Construction

Computer advancement for the design of construction equipment has brought major changes to equipment functionality, productivity, and construction practices. Mobile cranes, among other heavy industrial machinery, have increased in size, capacity, maneuverability, and versatility. The consequences of the misuse or improper planning of a crane lift can be severe. The preparation and planning of heavy lifts can be complex and involve challenging issues during lift analysis. Fast-tracked construction projects involve frequent changes to the construction plan, thereby requiring many what-if scenarios and changes to the lift plan. Due to this, the lift engineer relies on computer technology to deliver solutions faster. Virtual reality, combined with an interactive planning environment that explores human potential and computer advancement, is an efficient alternative for spatial integration. A flag article introducing spatial integration in construction [Bernold 2002] presented the historical advancement and objectives of such technology. In other studies, authors found mathematical computations that helped identify configuration space and concepts to develop tools for creating lift paths [Raghunatha et al. 2002]. In addition, two levels of heuristic searches have been implemented for 3D bin-packing problems [Raj and Srivastava 2007].

Trajectory and short-path developments are also of concern in this field. Ishigami et al. [2005] encountered issues in the proper design of an all-wheel dynamic model during a steering trajectory analysis for planetary exploration rovers: the model's contact between the rigid wheel and loose soil was based on a terra-mechanical approach. A Markov-decision process with two algorithms addressed the problem of planning the shortest path for reliable landmark-based robot navigation strategies in the presence of significant sensor uncertainties [Briggs et al. 2004]. Trajectory path analysis is also needed in applications such as tooling equipment, military rocket tracing, satellite space travel, and integrated surveying with GPS technology [Bernold 2002]. In the machine industry [Makhanov 2007], three algorithms for tool path optimization of a numerically controlled five-axis milling machine were introduced. The focus of these algorithms is the development of a flexible geometric structure that adapts itself to a certain cost function as defined on the required part's surface. 'Algorithm One' is based on the variation grid generation. 'Algorithm Two' is based on a modification of the space-filling curves technique. 'Algorithm Three' is based on the construction of vector fields composed of optimal cutting directions. For military applications [Azimov 2005], the development of analytical, approximate analytical, and numerical methods is used for solving variations when determining optimal rocket trajectories in gravitational fields and is also applied to study flight dynamics.

Yet the industry that stands most to benefit from this technology is the construction industry. A user-customized database [Al-Hussein et al. 2005, Moselhi et al. 2004] integrated with mathematical algorithms for choosing a proper crane with respect to lift capacity, while utilizing 3D animation for visualization techniques, has been developed and is available on the market. Following this development, more complicated 3D analyses were evaluated. One analysis used a 3D optimization approach for construction using a tilt-up panel method [Manrique et al. 2007]. Another analysis used a combination of advanced visualization, the above-mentioned crane selection process, and detailed schedule optimization and interactive communication techniques [Olearczyk et al. 2009].

As Weise [2008] has purported, "One of the most fundamental principles in our world is the search for an optimal state. It begins in the microcosm where atoms in physics try to form bonds in order to minimize the energy of their electrons." In general, optimization refers to the process of obtaining the best results under known conditions. Within the construction field, engineers must frequently make important technological and

managerial decisions. The result of good decision making is the minimization of effort involved in maximizing benefits. But the situation becomes more complicated when researchers face programming problems with multiple objectives (multi-criteria optimization). In the proposed study, the researcher encounters a multi-level optimization problem in which some variables are constrained by inner, or lower-level problems, and others by upper-level variables that parameterize the upper-level problem. Consequently, the upper-level problem objective function is referred to as the upper-level function, and the objective function of the lower-level problem is referred to as the lower-level function.

Some studies on the process of algorithm design have restricted themselves to a general idea of bi-level optimization, referring to both well-posed and ill-posed problems [Alexandrow and Dennis 1994]. Other studies have concentrated solely on ill-posed problems [Bergounioux and Haddou 2006], and have begun with a regional globalization strategy or have explored a new penalized Hoffman-like approach. Few practitioners have preferred to commence from real-world scenarios of decentralized planning [Bialas and Karvan 1984] with a different hierarchy objective function and decentralized design [Chanron et al. 2005], such that the mathematical framework of Game Theory [Vincent 1983] models the interaction between decision-makers (also called players). This method has been successfully implemented in the decentralized design of a space shuttle [Yoshimura et al. 2004], where a two-phase optimization procedure, which uses GAs and Sequential Quadratic Programming (SQP), was applied to the component arrangement problem. Parametric (discrete) optimization has also been investigated where a cutting plane (bound) algorithm has been used to solve a bi-level programming problem for objective linear programming (OLP) [Dempe and Richter 2000] and multiple objective integer programming (MOIP) [Klamroth 2004], with later assigned knapsack constraints [Dempe 2001]. In order to simplify intermediate computation solutions, researchers have used other algorithms to address the most difficult ones; GAs have been widely used, for example to find the shortest transportation route [Geiger 2001] or simply to solve convex quadratic bi-level programming problems [Guang-Min et al. 2002].

2.5 Simulation of Modular Building Construction

The decision to build a project using modular techniques is often motivated by the need to meet strict deadlines. Builders know that this method will result in a high quality

building in a short amount of time. The construction process, however, is still a complicated one due to the various site and crane utilization constraints. To effectively execute the construction, the construction team must have a well-designed plan in place. Once work has begun, due to time constraints and production sequence factors, there will be little opportunity to modify the sequence of construction.

Chehayeb and AbouRizk [1998] make the case for simulation modeling over CPM scheduling. They argue that while the time required to produce a simulation model is longer than that required by traditional CPM techniques, it has advantages in that it allows the project manager to analyze alternate resource and alternate execution scenarios more easily, and in that it allows processes to be modeled stochastically.

Since there is a need to understand the benefits of different construction scenarios, and due to the repetitive nature of the interacting processes, Discreet Event Simulation (DES) is a suitable candidate by which to evaluate modular construction operations. Through the use of a Special Purpose Simulation Software (SPSS) called Simphony, which utilizes a unified modeling methodology, it is possible to develop special purpose models for construction operations, Hajjar and AbouRizk [2002]. Using Simphony's General Purpose Simulation template in conjunction with onsite case data, this process can be modeled stochastically. The simulation output provides Cumulative Density Functions (CDFs) for project duration and provides valuable insight into crew utilization. Using the simulation environment, different scenarios can be tested, and their effect on productivity, duration, and utilization can be estimated.

It should be noted that while Yu, Al-Hussein, and Nasseri [2007], as well as Nasereddin, Mullens, and Cope [2007], have investigated the use of DES in improving module production in-factory, the purpose of this paper is to examine the onsite assembly aspect of the modular construction process.

2.6 Findings and Summary

Intensity of literature review in presented sections allows the thoughtful evaluation of current practices for crane position layout, as well as object lifted path in modular construction, general concept of site layout optimization, 4D application theme, spatial optimization analysis, and simulation of modular construction. These topics introduce the challenges faced by the construction industry in the aspect of crane operations. Figure 2.1

summarizes the reviewed publications in respect to different parts of the proposed methodology. It covers articles referenced in the literature review and groups them for better visualization and understanding.

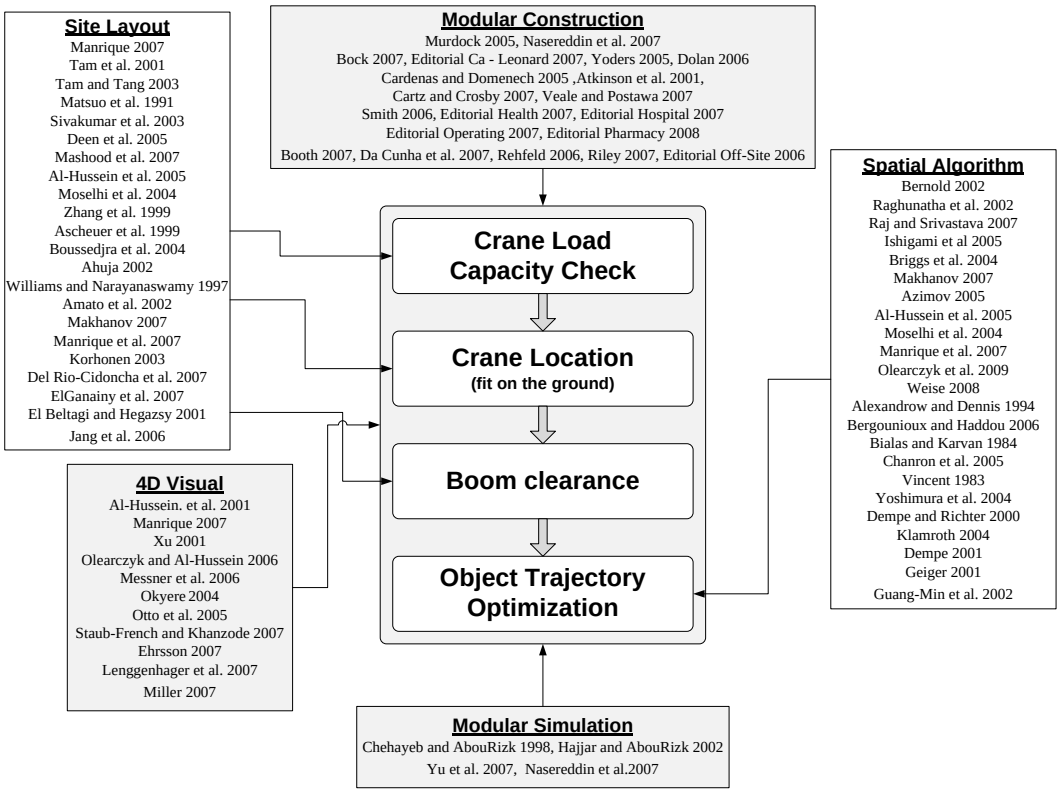

Figure 2. 1 Methodology Literature Review Flowchart.

The Site Layout group directly refers to Crane Load and Capacity Check as well as Crane Location boxes and covers 22 positions. It provides information and trends that researchers have tackled on this subject either commercially or academically. Also, this group discussed different aspects of construction site layout problems, but the majority of issues related to different crane configurations and clearance to obstructions. Only a few publications are crucial to the present research since its development is based on a concept.

The 4D Visualization Application group is not assigned to any particular methodology section due to the generality of reviewed issues and ideas that were useful to envision spatial movement with time displacement. It discussed pioneering the VR process in construction, limitations and possible routes for expansion and development. The

presented research supports the 3D-4D idea to optimize entire process mathematically, and once optimized to present the final solution again in a 3D-4D environment.

The Modular Construction group relates to the proposed methodology in general. It provides fundamental information about modular concepts in a few sectors of the industry with construction in particular. A few interesting modular concepts may dissolve the negative perception that modular complexity is not an issue. The benefits of modularity are clearly stated and presented research expands the concept even further to automating modular lifting operations.

Similar to the Modular Construction literature section, Modular Simulation references apply to the methodology in general. Similar to modular; this undeveloped part of the construction sector has few referenced publications. They discuss traditional ways of approaching similar construction challenges using the special purpose simulation software Simphony. Specific parts of the presented research may benefit implementation of this type of simulation in the future.

The core portion of this research refers to the Object Trajectory Optimization segment where 23 publications assist in evaluating current trends with successful or unsuccessful approaches. There is limited research data available about paths or trajectories in the construction industry. Extensive work was done for military or satellite tracking technology. Presented articles illustrate some concepts and methods for partial solutions to trajectory challenges. The provided information helps keep this research within its defined objectives.

CHAPTER 3 – PROPOSED METHODOLOGY

3.1 Current Practice

Preparation for lift operation is not an easy task. It requires extensive knowledge of crane configurations, lift procedures, safety, permits, etc. The list of necessary information could be as simple as lift weight and crane capacity or massive if critical heavy lifts (85% or higher crane capacity) are involved. Many industry practitioners, with the assistance of academia, try to establish rules, regulations, and penalties, but these are difficult to execute since each lift is unique. Due to so many varieties of tasks and subjective views, lift engineers establish different ways of controlling and sequencing lift preparation activities. Figure 3.1 shows examples of lift preparation and execution tasks grouping method. After each independent lift study, the list is updated, new operations are added, and those which are not applicable are not counted.

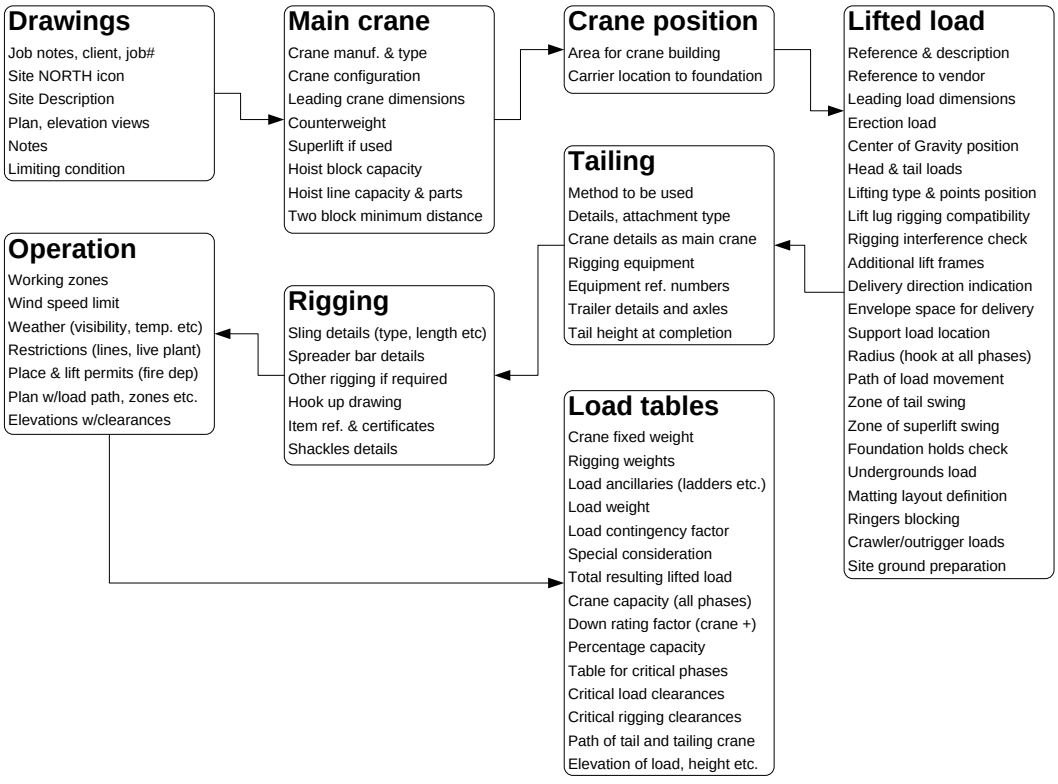

Figure 3.1 Lift preparation and execution grouping method.

Each group contains activities that are critical for that section and may be repeated in other sections. Checking and marking completed tasks shows an engineer the progress in

each section. The entire lift preparation analysis starts from the Drawings and finishes in the Load Tables section. The operation analysis is manual and time-consuming if any small changes are applied; the process must begin from the Drawings section again.

A different, more advanced method was introduced by Kuo-Liang Lin [Lin 1995] in his dissertation, "Planning for critical construction operations involving large semi-stationery equipment." He introduced a critical lift planning process model shown in Figure 3.2, which also eliminates unfeasible crane configurations.

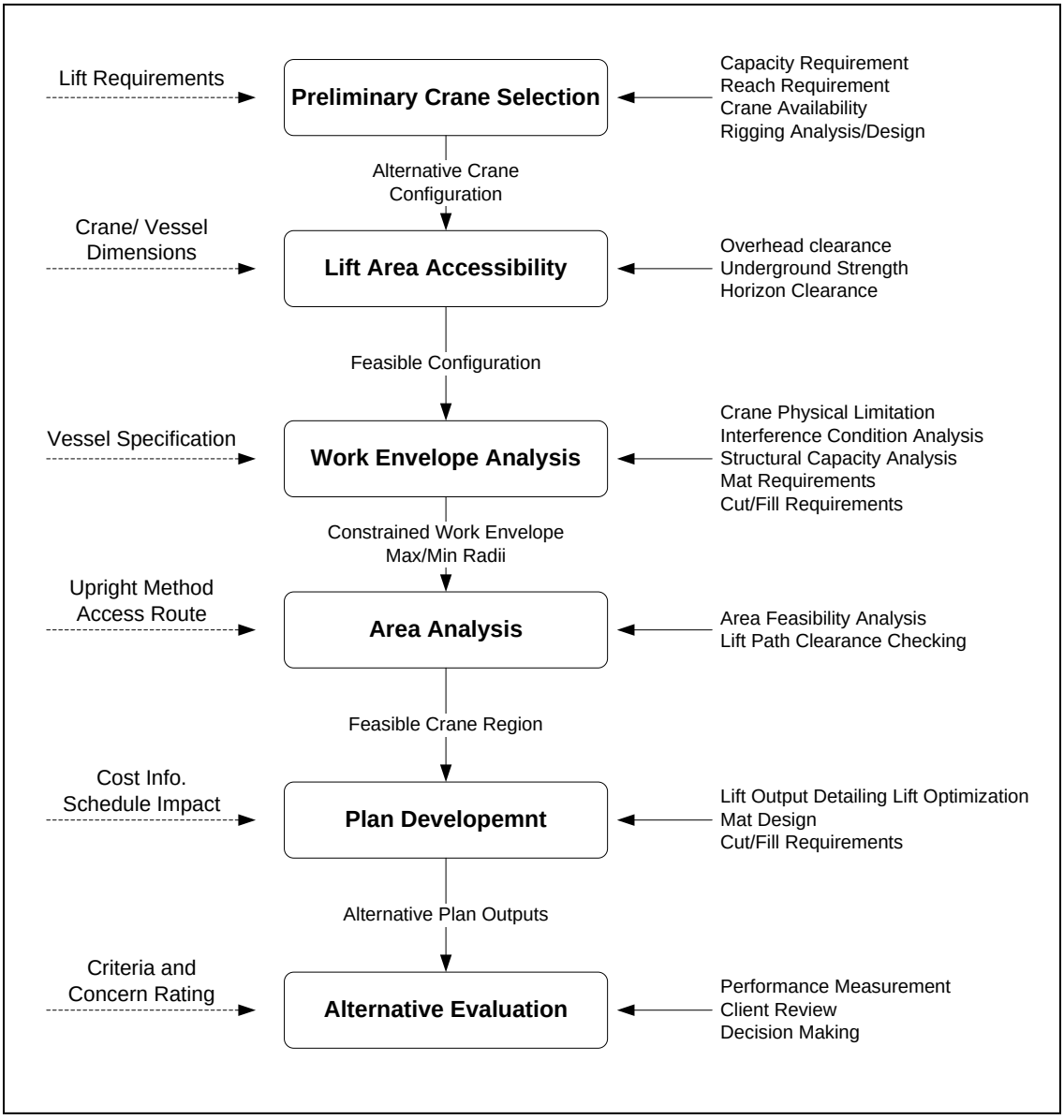

Figure 3.2 Critical Lift Planning Model [Lin 1995].

Picking alternative crane solutions based on crane capacity, reach, and rigging layout is the first evaluation criterion. Following is a lift area accessibility check, where horizontal and overhead clearances as well as underground strength are analyzed. Eliminated configurations limit the feasible cranes for lift operations. Next, the work envelope analysis segment limits those configurations that are in conflict with crane physical limitation structural capacity mats requirements or site cut/fill necessities. These limitations or modifications are associated with cost and the economic value evaluation. The area analysis study concentrates on area feasibility and lift path clearance checking. It reduces available configurations even further. Now, the lift engineer concentrates on plan development, where detail of lift optimization, final mat design, and exact cut/fill design is performed.

All performed tasks and analysis, with final design and cost comparisons, are presented in the last segment for alternative evaluation. Performance measurements and contractors' and client reviews based on criteria and concern ratings are the main evaluation factors.

Both presented current practice methods, cover almost every aspect of lift planning, but the associated cost evaluation or performance analysis is impractical. They required tedious and very time-consuming work. Although, some tasks may be automated or consolidated into a computer program, they lack fluent flow. The lift engineer is forced to compare computer outputs with manual calculation/analysis to prepare concise data for alternate evaluation.

3.2 Process Methodology

The proposed methodology, as illustrated in Figure 3.3 is built on four modules. It accepts or eliminates available crane configurations based on a crane load capacity check, crane location, boom clearance, and lifted object path optimization. The modules evaluate the project on lift specific characteristics, and site and location parameters. The main outputs of the process include object paths database, obstruction conflict ID, and proposed sequence priority. These outputs are obtained following a set of criteria including lifted object limitations, site and area restrictions, crane unit availability, and weather conditions.

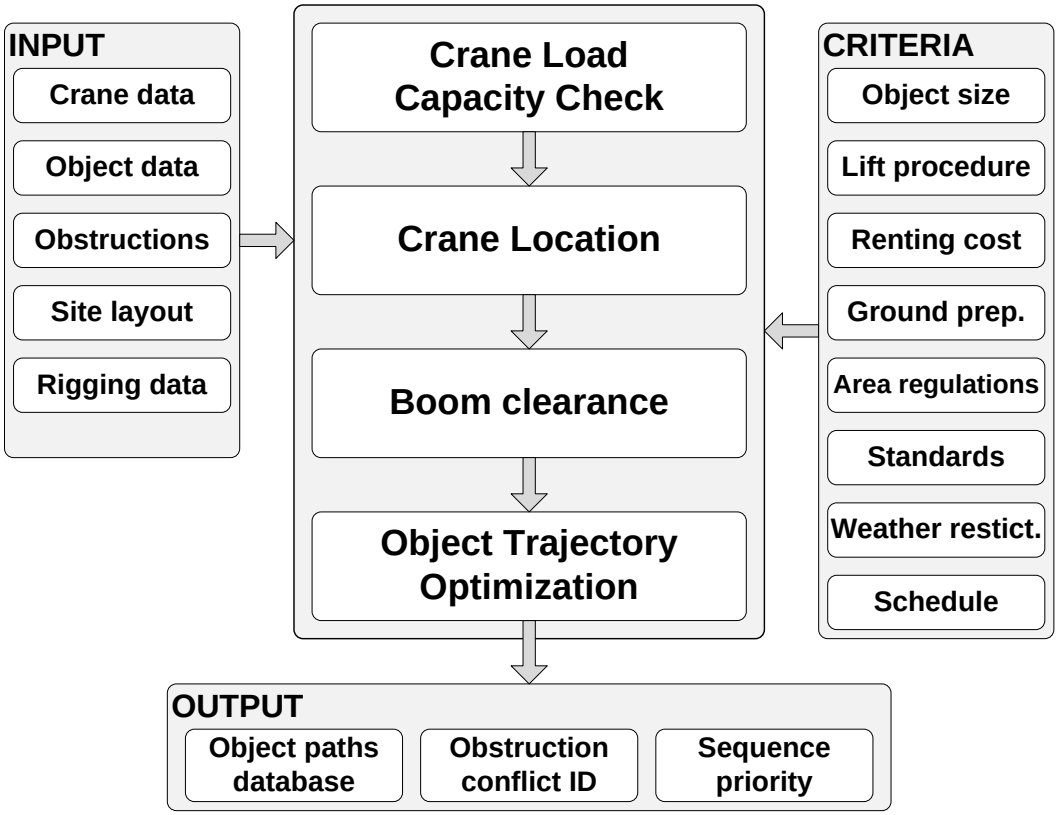

Figure 3.3 Methodology main process.

Crane Load Capacity Calculation: lift capacities are compared to the total lift weights (the weight of the lift and all of the accessories needed to hook the object to the crane), such that the crane's lifting capacity at any given configuration should be greater than or equal to the total lift weight, satisfying equation 3.1.

$$\boldsymbol{GC \geq T_w = L_W + H_W + SL_W + SB_W} \qquad \textbf{(3.1)}$$

Where:

GC - *Lift object gross capacity*
T_w - *Total lift weight*
L_w - *Lift weight*
H_w - *Hook weight*
SL_w - *Total weight of slings*
SB_w - *Total weight of spreader bar*

Figure 3.4 shows detailed parameters for each section of the crane load capacity check. Input includes crane data such as crane hook, slings, spreader bar, and jib or extensions weight. Total lifting weight may not exceed current crane configuration lifting capacity

with added industry standard safety factor. When equation (3.1) is not satisfied, crane capacity is lower than total weight, and the analyzed crane configuration is rejected. Rejection does not terminate operation but activates the re-define box section.

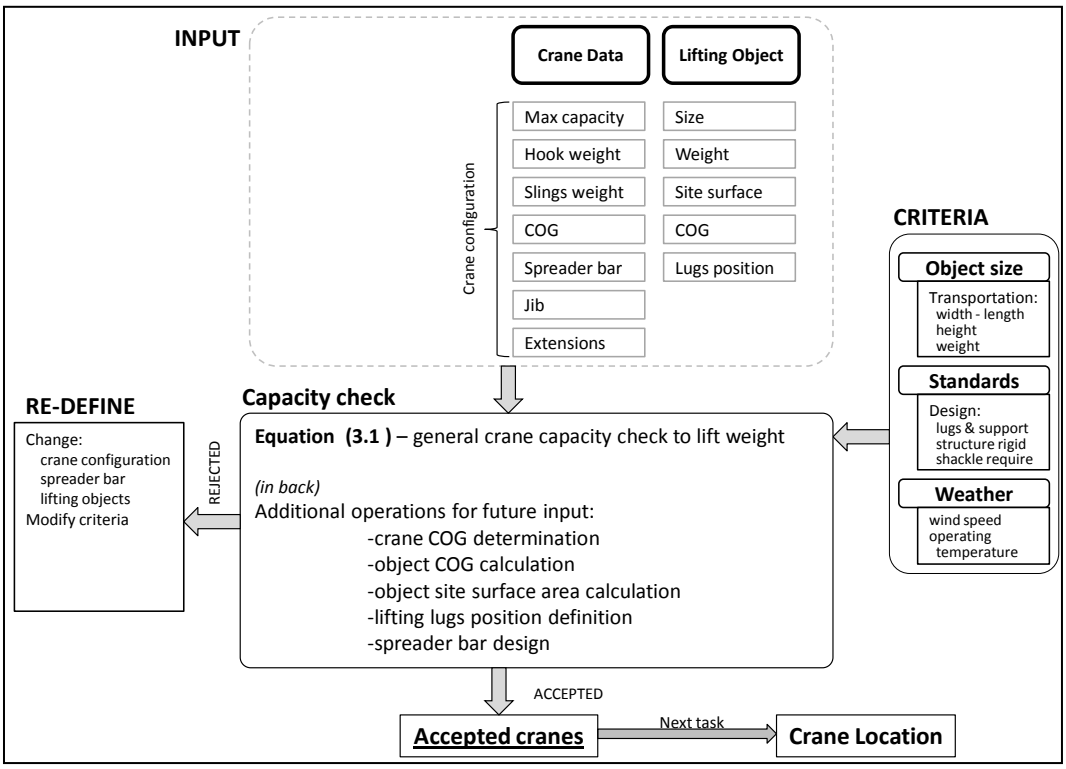

Figure 3.4 Expanded flowchart for crane load capacity check.

Re-definition poses a set of questions, which causes assigning different crane configuration, choosing a lighter spreader bar, or dividing the lifted object into smaller pieces. Capacity check activities are subject to criteria, which include object size, site regulation, building standards, or weather conditions.

Crane Placement Location: Sufficient clearance must be maintained between the surrounding buildings, the crane's carrier, the outriggers, and the counterweight in order to retain the ability to geometrically fit the crane on the construction site. Extensive work has been done on single crane lift analysis [Al-Hussein-et al. 2001 and 2005, Moselhi et al. 2004, Manrique et al. 2007] and multi-lift crane position placement [Olearczyk et al. 2007 and 2009]. Figure 3.5 displays the detailed descriptions for each section of the crane placement location. Input includes three data segments related to site, crane, and lifting object parameters. Site data provides information about available layout areas, surveying and ground density, and obstruction under and above ground level. Crane related data includes outriggers, configuration, counterweight, and superlift space requirements, as

well as spreader bar availability or boom attachment additions. Object data includes weight, geometric center (GC), lifting lugs dimensions, and additional supports for temporary storage.

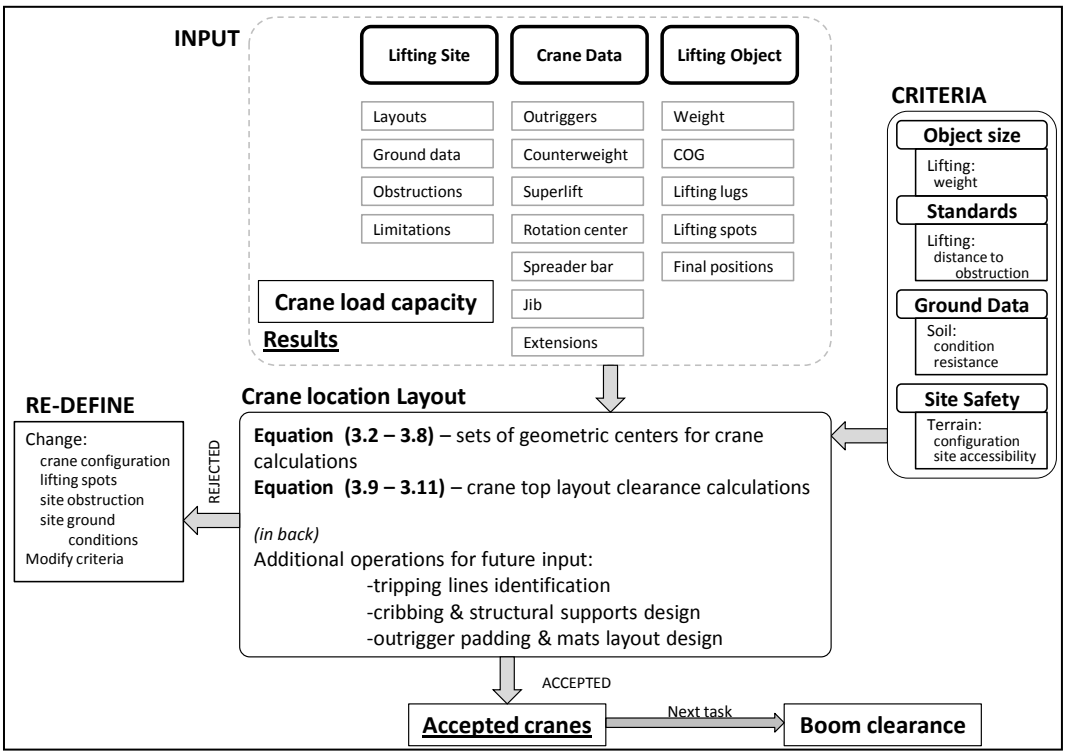

Figure 3.5 Expanded flowchart for crane placement location.

The main operation processes include equations that provide mathematical solutions to calculate geometric centers and clearance distances to nearby obstructions. If for any reason the crane configuration is rejected, the process is not terminated but re-directed for possible change implementation. The re-define option regulates the changes applied to the input data: it contains limited options strictly regulated by predefined criteria. This process starts with calculating the geometric center of all objects that are under evaluation. Figure 3.6 illustrates building layout with reference dimensions for each individual lift.

The centroid of a set of n point masses m_i located at position x_i and y_i are as follows:

$$\boldsymbol{x} = \frac{\sum_{i=1}^{n} \boldsymbol{m_i x_i}}{\sum_{i=1}^{n} \boldsymbol{m_i}} \qquad (\mathbf{3.2})$$

$$\boldsymbol{y} = \frac{\sum_{i=1}^{n} \boldsymbol{m_i y_i}}{\sum_{i=1}^{n} \boldsymbol{m_i}} \qquad (\mathbf{3.3})$$

Where:

m	*– Object mass*
n	*– Number of objects*
x	*– Plane horizontal coordinate*
y	*– Plane vertical coordinate*

Each lifted object's geometric center point is calculated satisfying equations (3.2) and (3.3). Once the calculation is complete, the next step is analyzing the maximum crane radiuses for each type of lifted object. Such analysis eliminates those crane configurations that would not be able to reach all lifts. Figure 3.7 shows the objects' maximum set-point radiuses in relation to calculated crane rotation center point.

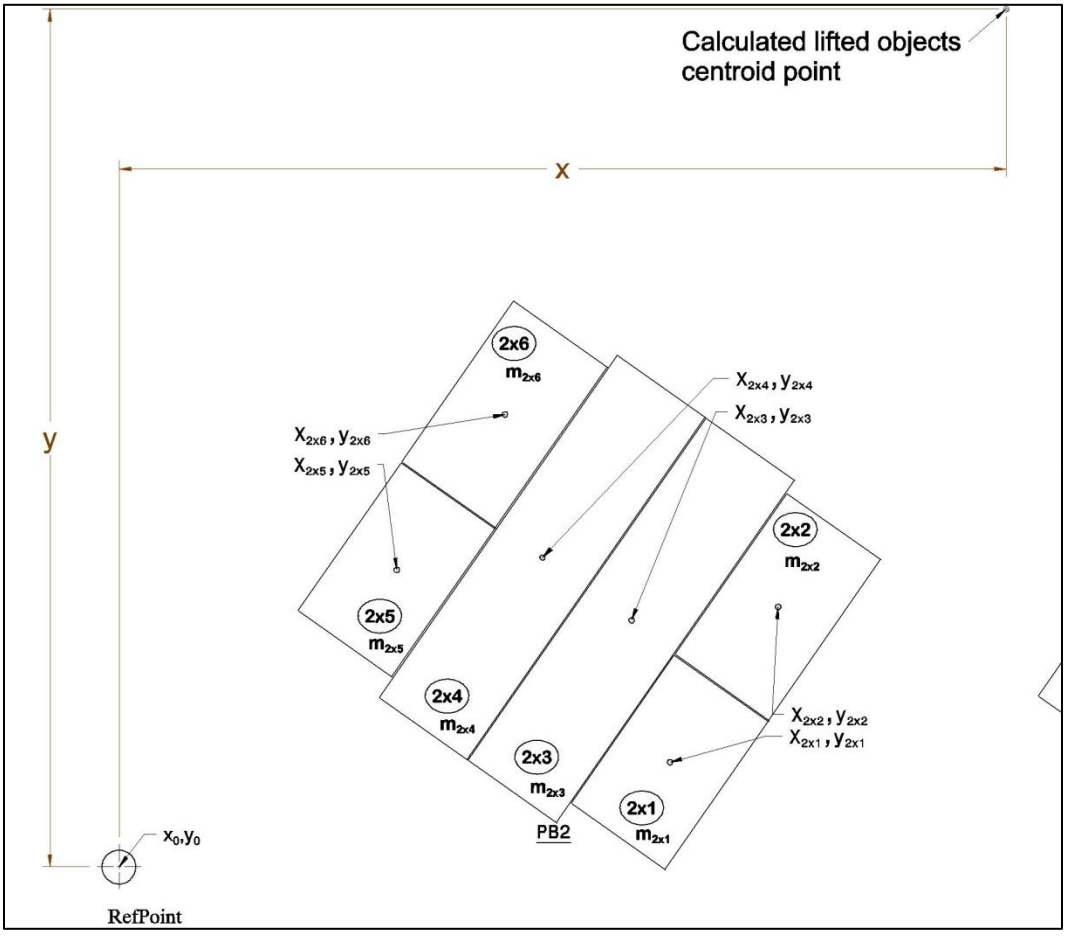

Figure 3.6 Lifted objects' centroid points.

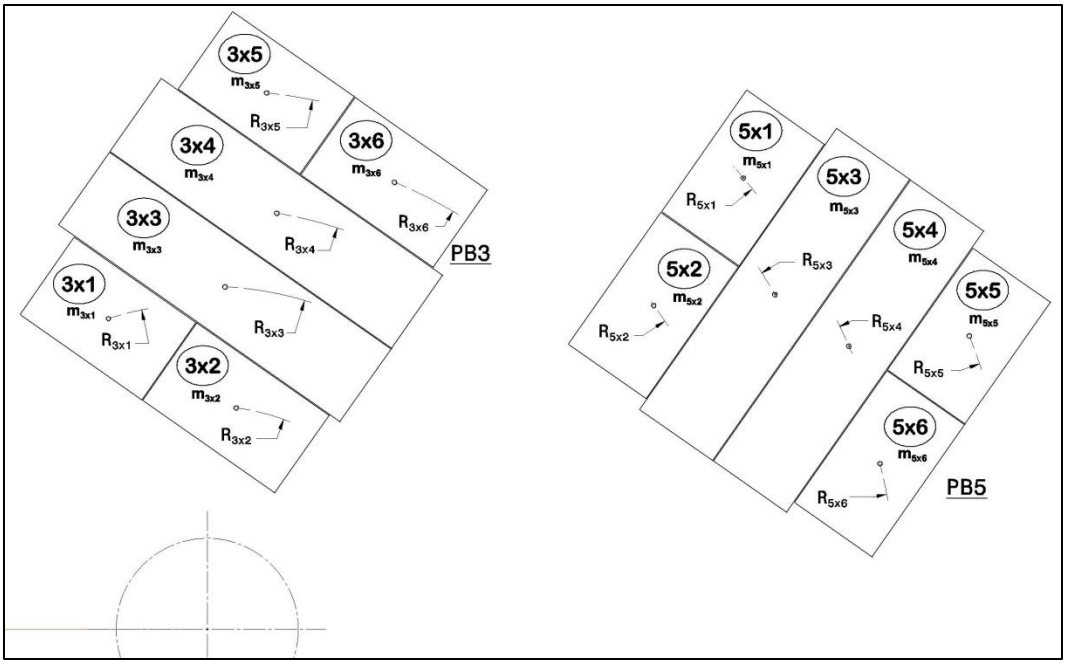

Figure 3.7 Objects' set-points radiuses.

A lifted object's geometric center in relation to the crane's radiuses together with the particular object weight must be below the chosen crane's maximum lifting capacity, satisfying equation 3.4:

$$\boldsymbol{MAX \quad R_{xxx}\ m_{xxx} \quad < R_{max}\ W} \qquad (\mathbf{3.4})$$

Where:

R_{xxx} – *Set-point radius of lifted object type*

m_{xxx} – *mass of the objects at* R_{xxx}

R_{max} – *Crane maximum radius*

W_{max} – *Crane maximum lifted weight at* R_{max}

Equation 3.4 may apply to each particular set of lifted objects, and only the one at the maximum set-point radius will govern the crane selection process. Crane manufacturers provide data, where crane boom radiuses define maximum allowable load lift weight. An algorithm for mobile crane selection [Al-Hussein at al. 2001] has been implemented to select the right unit. As an example, if the lifted object module number [5x5] (5-building, x- elevation, 5-object type), with weight m_{5x5} and set-point radius R_{5x5}, has the maximum radius for this object type, the unit data will govern crane selection operation. When all the object types are checked for maximum radiuses position and weight, and further

representative types are preselected, their maximum weight and radiuses distance control the crane selection result.

After the crane has been selected, its carrier dimension must be checked for obstruction clearances. Figure 3.8 shows the calculation of minimum clearance distance to the closest obstruction. A simple analysis of distance checking can identify the closest object to the calculated centroid point, called C_S (crane set-point). In presented analysis, unit 3x2 is the closest lifted object, with set-point (x_{3x2},y_{3x2}) and position angle ε.

From the lifted object database parameters, the length of the object (l) and the width of the object (w) are provided. The crane database provides access to counterweight radius and outrigger positions. First, the lifted object diagonal length (l_d) is calculated, satisfying equation 3.5.

$$l_d = \sqrt{\left(\frac{l}{2}\right)^2 + \left(\frac{w}{2}\right)^2} \qquad (3.5)$$

Where:

l_d – *object diagonal length*
l – *object length*
w – *object width*

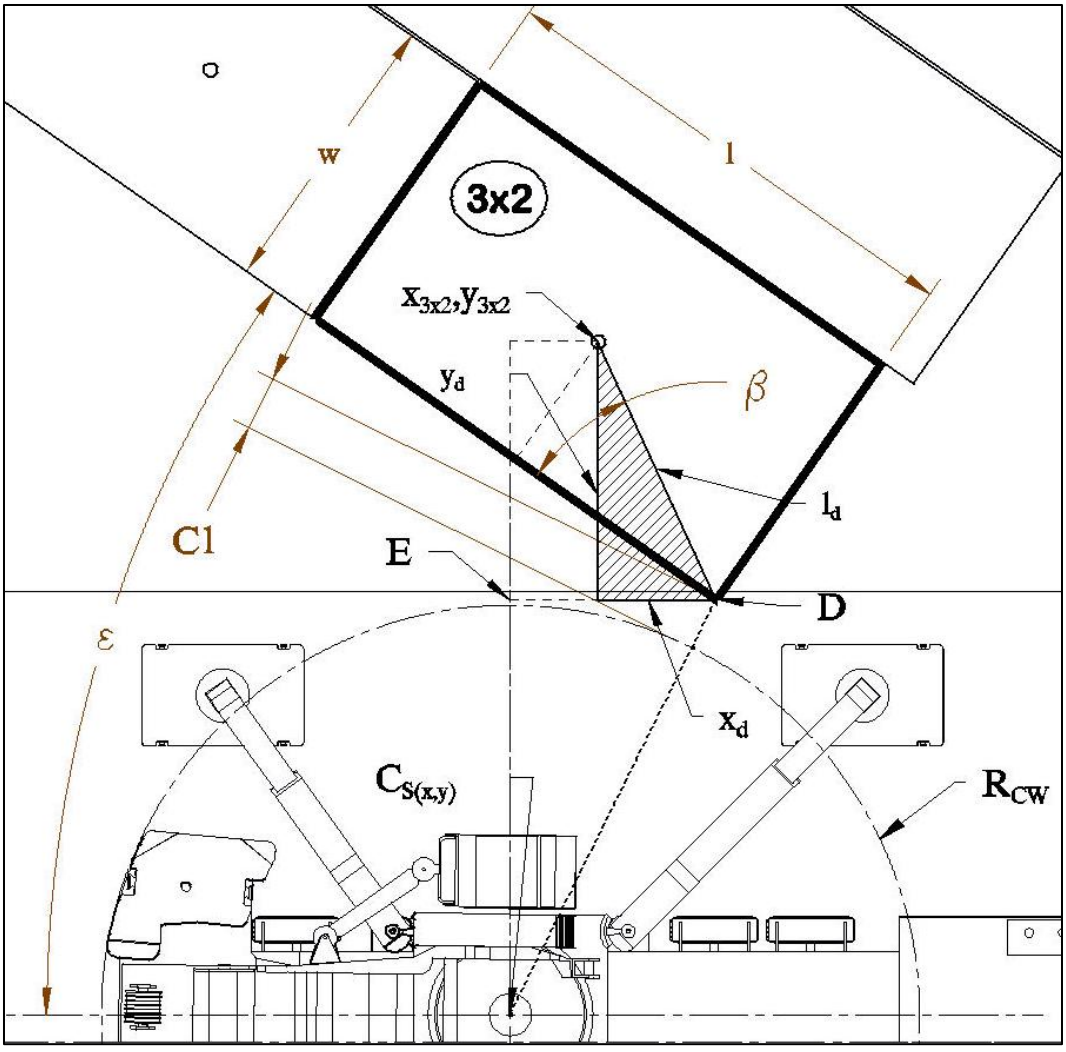

Figure 3.8 Crane carrier clearance top triangle.

Next, angle β will be calculated, satisfying equation 3.6, in order to find the common angle to the horizontal line.

$$\boldsymbol{\beta = arctg\ \frac{w}{2 * l_d}} \qquad (\mathbf{3.6})$$

Figure 3.8 shows the crane carrier clearance top triangle, where the hypotenuse is the object diagonal length (l_d) with reference angle ($\varepsilon + \beta$). Calculating adjacent (x_d) and opposite (y_d) lengths of top triangle satisfies equation 3.7 and equation 3.8, respectively.

$$\boldsymbol{y_d = l_d * sin\ \varepsilon + \beta} \qquad (\mathbf{3.7})$$

$$x_d = l_d * cos\ \varepsilon + \beta \tag{3.8}$$

Where:

l_d – *object diagonal length*

ε – *lifted object side to horizontal line angle*

β – *object diagonal length angle to its envelope side*

Identifying the bottom triangle is the next step in the clearance calculation process. Figure 3.9 shows the bottom triangle with sides C_s, D and E. Solving E, D and C_s,E sides of the presented triangle allows for calculation of hypotenuse C_s, D, satisfying equation 3.9 and equation 3.10, respectively. Calculating clearance (*Cl*) satisfies equation 3.11:

$$C_s, E = y_{3x2} - y - y_d \tag{3.9}$$

$$E, D = x_{3x2} - x + x_d \tag{3.10}$$

Where:

C_S – *crane set-point (lifted objects' centroid point)*

x,y – *Cs crane set-point coordinate values*

x_{3x2}, y_{3x2} – *3x2 object centroid point coordinate values*

x_d, y_d – *calculated lengths from eq. 3.7 and 3.8*

$$Cl = \sqrt{y_{3x2} - y - y_d\ ^2 + \ x_{3x2} - x + x_d\ ^2} - R_{CW} \tag{3.11}$$

Where:

Cl – *minimum crane carrier to obstruction clearance*

R_{CW} – *crane counterweight maximum radius*

The clearance (*Cl*) calculation is based on a particular configuration layout, but its method can be applied to any crane carrier body obstruction relation.

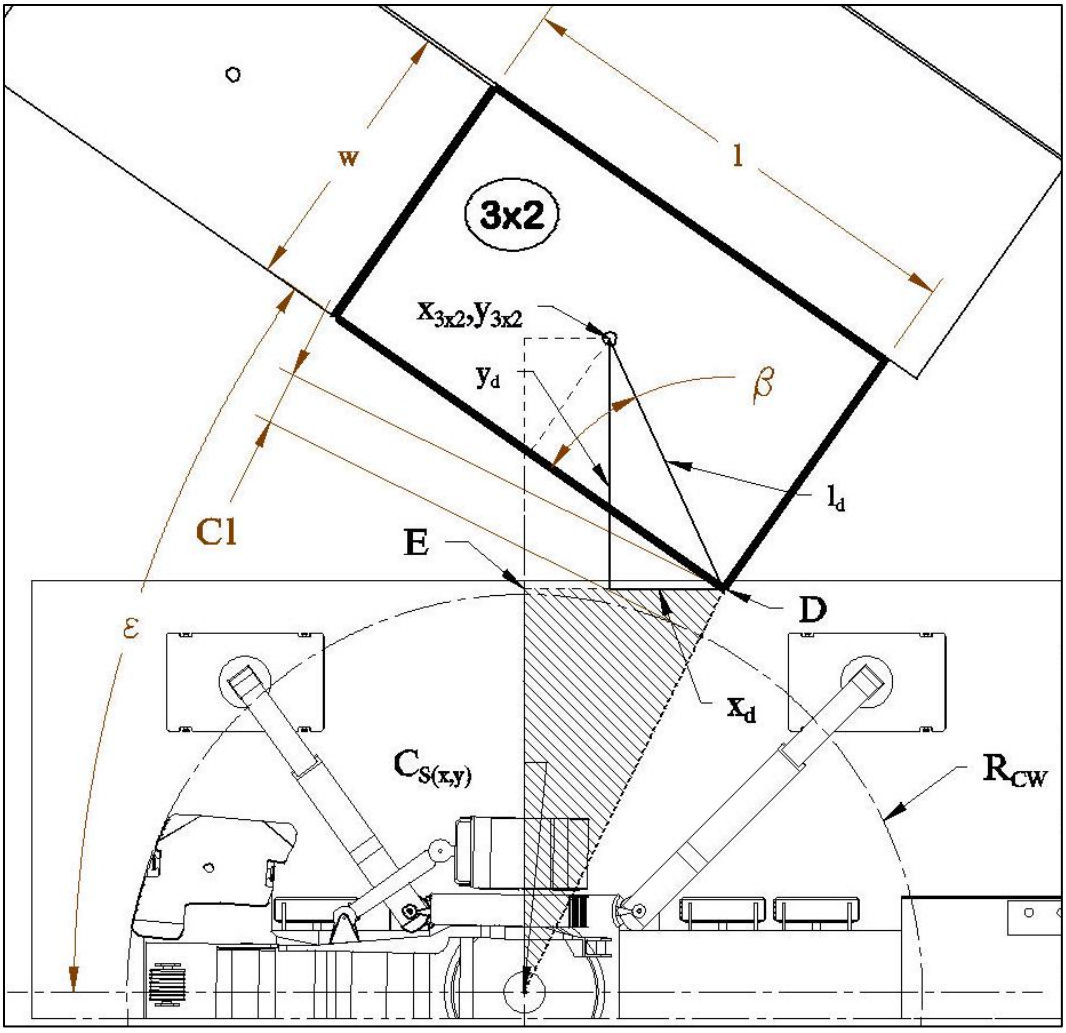

Figure 3.9 Crane carrier clearance bottom triangle.

Boom Clearance Analysis: After the crane location is defined and checked for potential carrier clearance, the crane boom clearance analysis must be performed. Table 3.1 presents the characteristics of three scenarios for which a hydraulic mobile crane can be utilized. These scenarios reflect most of the crane boom position situations at construction sites. In Scenario 1 boom angle to the ground and boom tip height is analyzed based on boom length and the lift radius. Scenarios 2 and 3 evaluate the crane boom with extension, and respectively calculate boom angle, lift radius, and tip height.

Table 3.1 Crane configuration scenarios description.

Scenario	Equipment	Given	Calculate
1	Main boom	Boom length, lift radius	Boom angle, tip height
2	Main boom, extension	Boom + extension length, lift radius	Boom angle, tip height
3	Main boom, extension	Boom + extension length, boom and extension angle	Lift radius, tip height

Figure 3.10 showcases detailed steps and equations. The input parameters include information related to the crane, its carrier dimension boom rotation offsets, as well as boom extensions dimensions, weight, and parameters that may be critical to proper and safe assembly operation. Additional input parameters include limited information related to site obstruction layout elevation dimensions, and limitation of the crane accessories assembly operation. Lifting object weight and lift operation radiuses may have a direct effect on the crane outriggers' ground pressure, and as such can require a special spot system for outriggers. Boom clearance analysis is subject to a set of criteria of ground data storing information, which is related to the minimum soil condition for heavy lifts, and special instructions about outrigger area preparation requirements.

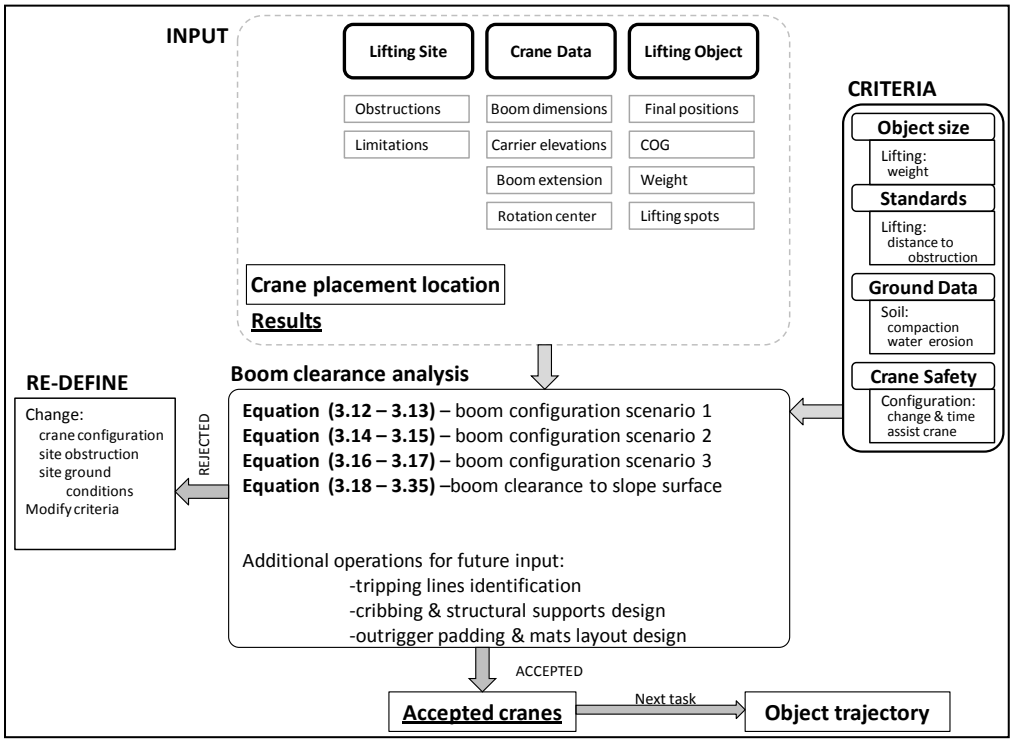

Figure 3.10 Expanded flowchart for crane boom clearance optimization.

Modifying or changing crane boom configuration must be planned carefully and in advance, and for that reason information related to safe operation with an assisted crane has its own established criteria. When part or whole equations are not satisfied, they are directed to the re-define section where changes can be made such as ground condition improvement, additional operations, or altering the current crane configuration.

Scenario 1: In this scenario (Figure 3.11) the lift is performed on the main boom without any attachments.

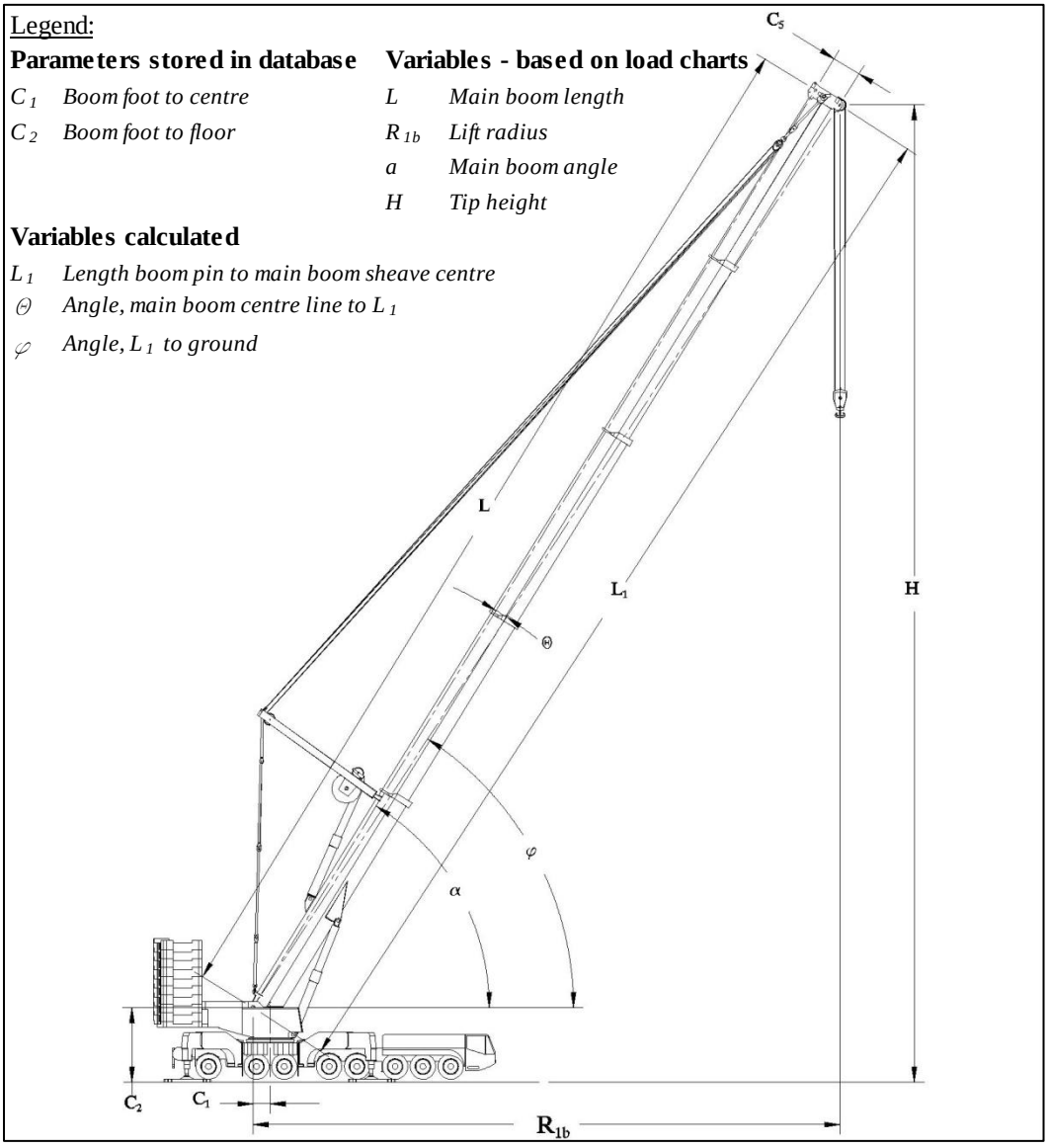

Figure 3.11 Scenario 1 graphical representation.

The known values include the main boom length (L) and the lift radius (R_{1b}); the calculated parameters include the main boom angle to the ground (α) and the lifting tip height (H), which satisfy equation 3.12 and equation 3.13, respectively.

Main boom angle

$$\boldsymbol{\alpha = \Theta + \varphi} \qquad (\mathbf{3.12})$$

and main boom tip height

$$\boldsymbol{H = C_2 + \sqrt{L_1^2 - R_{1b}^2}} \qquad (\mathbf{3.13})$$

Where:

$\boldsymbol{\varphi = arccos\frac{R_{1b}}{L}}$ *angle of L_1 line to horizontal*

$\boldsymbol{\theta = arctan\frac{C_5}{L}}$ *angle main boom center line to L_1*

$\boldsymbol{L_1 = \sqrt{L^2 + C_5^2}}$ *length boom pin to main boom sheave centre*

Scenario 2: This scenario involves lifts on the main boom's fixed extension (see Figure 3.12). In this scenario the boom length (L), lift radius (R), and extension offset (φ_{of}) are given; the main boom angle (α) and the lifting tip height (H) are calculated satisfying equation 3.14 and equation 3.15, respectively.

$$\boldsymbol{\alpha = \theta_{ex} + \varphi} \qquad (\mathbf{3.14})$$

$$\boldsymbol{H = C_2 + \sqrt{(L + C_{10})^2 - R^2}} \qquad (\mathbf{3.15})$$

Where:

$\boldsymbol{\varphi_{of} = 0}$ *boom extension offset*

$$\boldsymbol{\theta_{ex} = arctan\ \frac{C_9}{(L + C_{10})}}$$

Scenario 3: This scenario also involves lifts on the main boom's fixed extension (Figure 3.12). In this scenario the boom length (L), boom angle (α) and extension angle (φ_{ex}) are given. The lift radius (R) and lift tip height (H) are calculated satisfying equation 3.16 and equation 3.17, respectively.

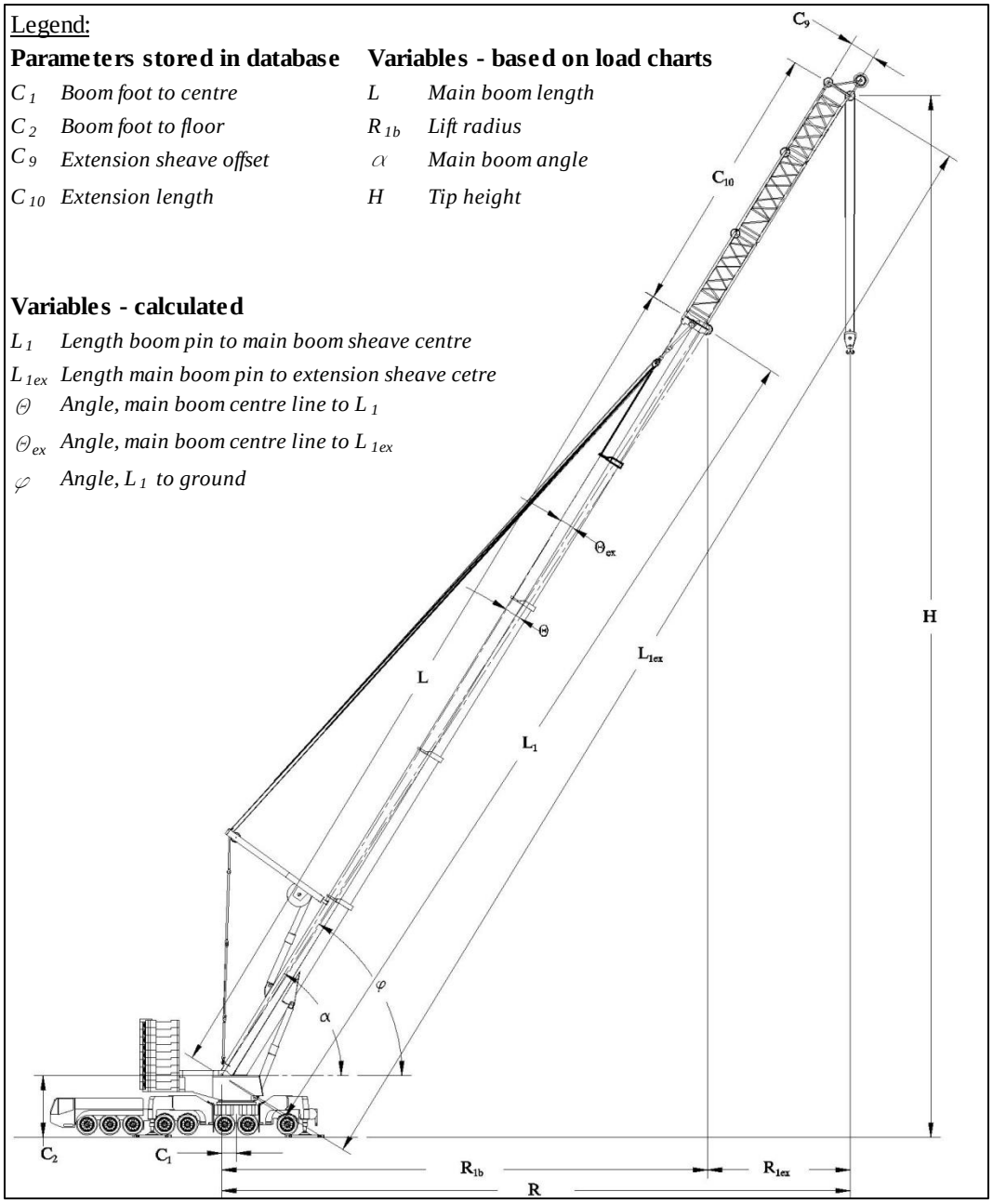

Figure 3.12 Scenario 2 and 3 graphical representation.

$$\boldsymbol{R = R_{1b} + R_{ex} - C_1} \qquad (\mathbf{3.16})$$

$$\boldsymbol{H = \sqrt{(L_{1ex} - L_1)^2 - R_{1ex}^2} + \sqrt{L_1^2 - R_{1b}^2} + C_2} \qquad (\mathbf{3.17})$$

Where:

$$\boldsymbol{R_{1ex} = \sqrt{(C_{10}^2 + C_9^2)}\cos(\propto - \theta_{ex})}$$

$$\theta_{ex} = arctan\ \frac{C_9}{(L + C_{10})}$$

$$L_{1ex} = \sqrt{(L + C_{10})^2 + (C_9)^2}$$

Boom clearance to slope surface analysis

Positioning cranes on construction sites is not a new problem for practitioners. There are a number of computer programs developed to support engineers in their planning activities. Al-Hussein et al. [2001] presents an algorithm for crane selection and location on construction sites, including boom clearance analysis. The author based his analysis on the evaluation 48 different cranes, with capacities from 20 tonnes to 880 tonnes. The number of different configurations that may be developed from that many cranes exceeds 100,000. Rigging equipment, shackles, and spreader-bars further expand the already extensive information database. To properly manage such a large amount of information, the authors developed an algorithm that incorporates a database that contains four different categories: carriers, outriggers, and counterweights; boom pin offsets in relation to main rotation axis; sheaves dimensions, jibs, and jib-sheaves dimensions with their offsets; and lift data set, radiuses, jib lengths, jibs angles and tip heights, and lifting zones. The general logic of Al-Hussein et al. [2001] was adapted in this research to all terrain hydraulic cranes with main boom and main boom with extension.

A further expansion algorithm goes beyond an analysis of the boom position in the normal plane (flat roof shape) in relation to the building, in keeping with the analysis outlined by Shapiro et al. [1999]. Figure 3.13 shows a layout of the critical crane boom position and the referenced parameters. Critical dimensions include boom obstruction calculations such as boom center line to obstruction edge angle (φ), boom radius (*R*), and boom rotation center to obstruction edges distances, horizontal (*h*) or vertical (*k*).

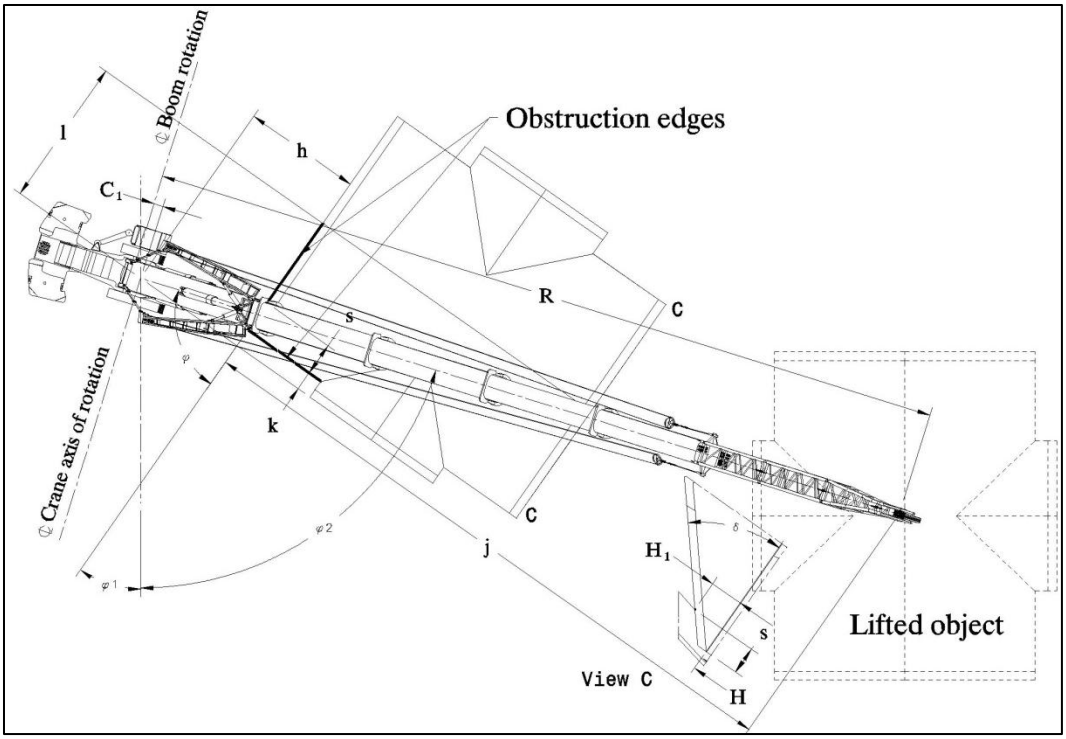

Figure 3.13 Boom-obstruction plan view.

However, while such analyses calculate the required clearances of the erected crane boom to potential obstructions, they fail to address a situation where the roof has an inclined configuration. The present study involves that particular configuration with the intent to develop a solution that addresses the situation where the crane boom position is not in the normal plane but in the inclined roof shape to the building structure. This complex geometrical configuration is supported by 2D drawings and 3D isometric layouts where the calculated minimum clearance, between the crane boom and the inclined roof, defines the exact position of the lifted roof. Such a lift configuration, where the obstruction is between the lifted object and the crane boom envelope, is common on construction sites. Engineers would like to schedule a maximum number of lifts without relocating the crane. In some situations reconfiguring the crane for one or two lifts can be more cost-effective than to disassemble-move-assemble the unit. Figure 3.14 shows an elevation boom obstruction tandem sketch, where a small-detail view shows local coordinate system arrows and triangle lines in the different planes.

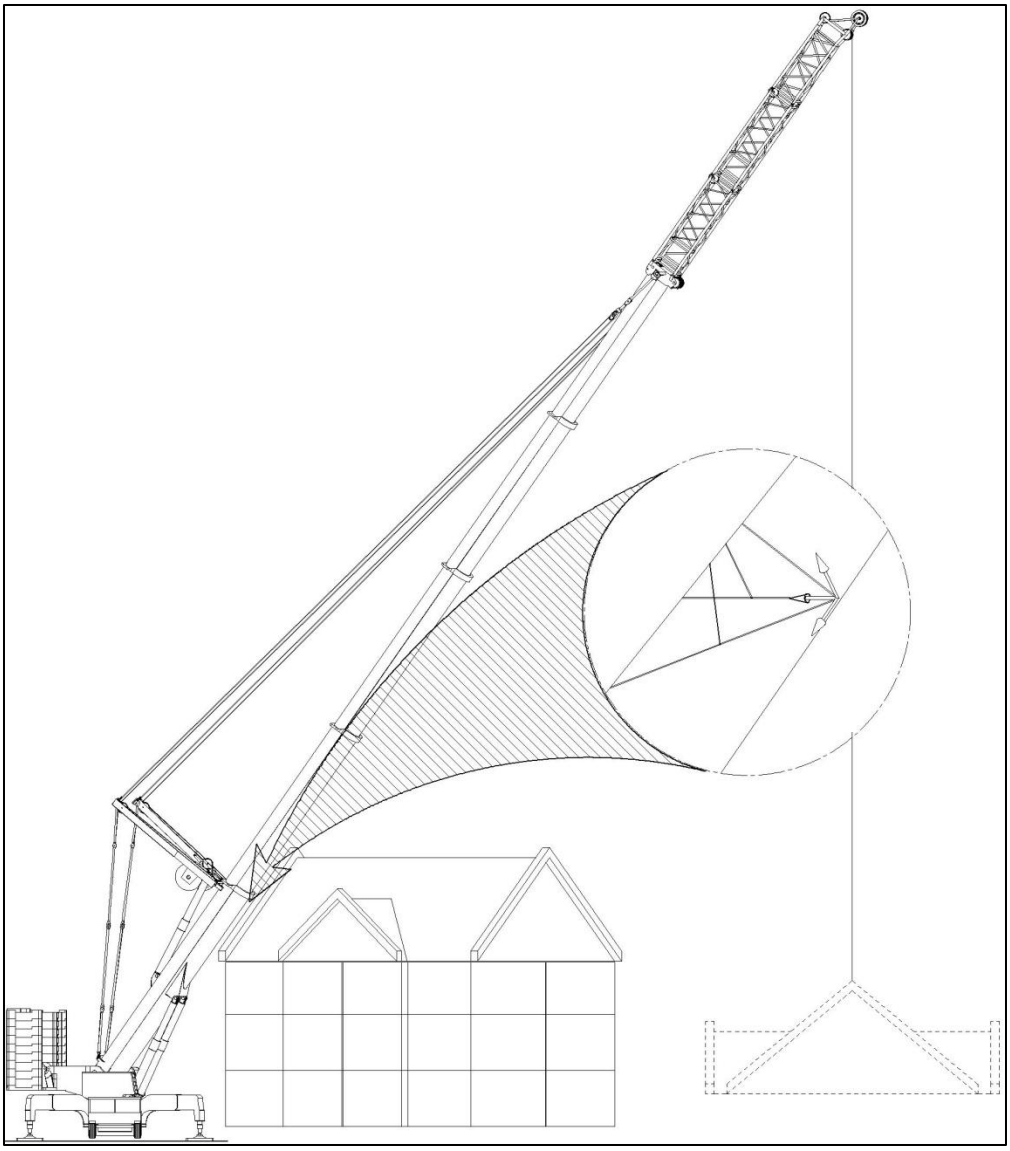

Figure 3.14 Boom elevation and Detail view.

Based on the calculated boom length (L_{1ex}) (see equation 3.17), the operation to calculate the radius satisfies equation 3.18:

$$\boldsymbol{R = L_{1ex}\, cos\ \alpha_B - C_1} \qquad (\mathbf{3.18})$$

Where:

$$\boldsymbol{\alpha_B = \alpha - \theta_{ex}}$$

R – *crane lift radius*

L_{1ex} – *crane boom length with extension*

t – *offset of the boom rotation axis*

a and Q_{ex} – *refer to Figure 3.12*

And when boom length is known the crane boom angle will be:

$$\alpha_B = cos^{-1}\ \frac{R+t}{L_{1ex}} \tag{3.19}$$

As per Figure 3.13, the horizontal angle (φ) of the crane boom obstruction is calculated to satisfy equation 3.20:

$$\varphi = sin^{-1}\ \frac{h+j}{R} \tag{3.20}$$

Where:

h	*– crane rotation axis from obstruction edge*
j	*– projected distance from crane boom tip to obstruction edge*

The roof inclined angle (δ) defines the projection point boom center to the roof envelope, and the distance (H_1) from the horizontal plane is calculated satisfying equations 3.21, 3.22 and 3.23:

$$tan\,\varphi = \frac{s+k}{h} \tag{3.21}$$

$$tan\,\delta = \frac{H_1}{s} = \frac{H_1}{h\,tan\,\varphi - k} \tag{3.22}$$

$$H_1 = tan\,\delta\ \ h\,tan\,\varphi - k \tag{3.23}$$

Where:

s	*– boom envelope edge to obstruction edge distance*
k	*– boom rotation center to obstruction edge distance*
H_1	*– elevation boom point (see Figure 3.11, View C)*
H	*– obstruction height to top surface (Figure 3.11, View C)*
d	*– roof angle (see View C)*

The distances (*h*) and (*j*) (see Figure 3.13) are taken directly from the input parameters, and they are related to the object pick-point and the crane set-point positions. The boom length (L_{1ex}) is the center line of the boom shape that is represented in Figure 3.12. The hydraulic telescopic boom is built of different-sized sections extended at the maximum height of (*L'*). In most cases the crane boom operates at its maximum extended length, and sections are automatically pinned (locked) for safe operation. The center line of the

boom shape is at constant position in all sections; however, each section has a different dimension since they must slide inside one another when they are un-pinned and retracted. For simplification and for spatial calculation, the operation envelope frame is introduced, which is presented in Figure 3.15 and Figure 3.16.

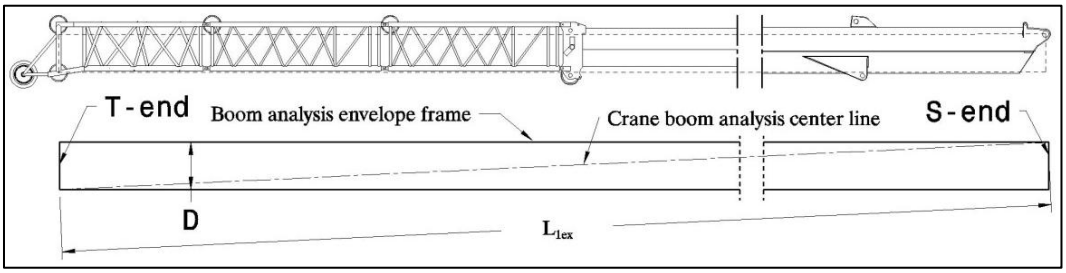

Figure 3.15 Crane boom elevation view and envelope representation.

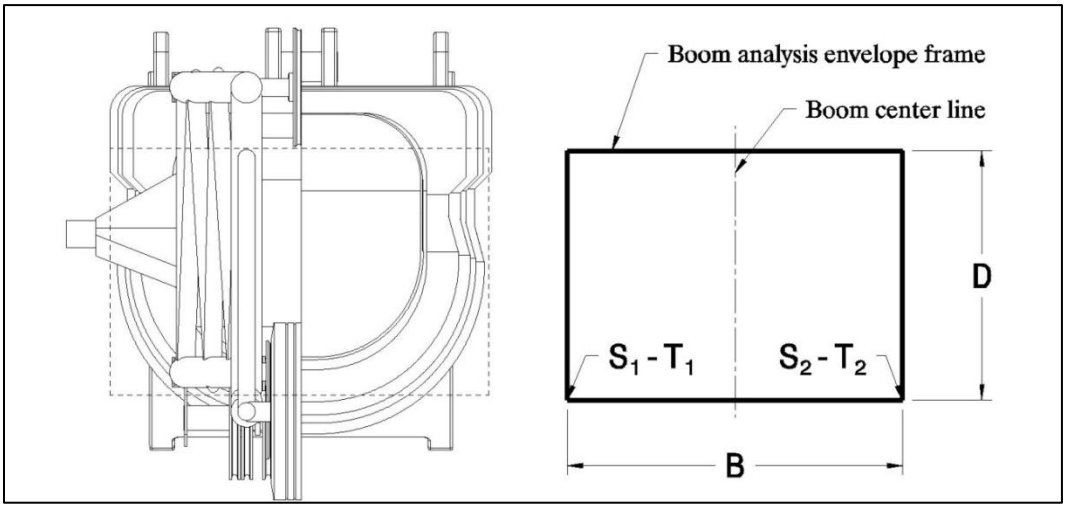

Figure 3.16 Crane boom section view and envelope representation.

In Figure 3.15 the envelope elevation ends are marked S and T, transferred to a sectional view. In Figure 3.16, and identify two critical edges of the proposed envelope, which are closest to the analyzed obstruction or other objects. Analysis will be based on S_2-T_2 line distance to the inclined roof edge structure. Figure 3.17 shows a boom-obstruction isometric research working view, with a boom envelope rectangular block shape with two vertical edges marked T_1-T_2 and S_1-S_2. The identified points create a surface, which holds important projection lines. On the right side of the Figure, dotted lines reflect the edges of the flat top obstruction surface and the portion of the roof sloped section with gable rising. There are also two circles, A and B, that illustrate graphical calculations. Detail B (Figure 3.19) presents the graphical calculation to top surface, which is described in detail in Shapiro et al. [1999], and Detail A (Figure 3.18) presents the graphical

calculation to slope surface. Clearance analysis of the boom to sloped surface is a new solution based on the same calculation principle used with a flat top surface. It includes additional sloped angle δ, which can be seen in Figure 3.20, expanded detail A clearance description.

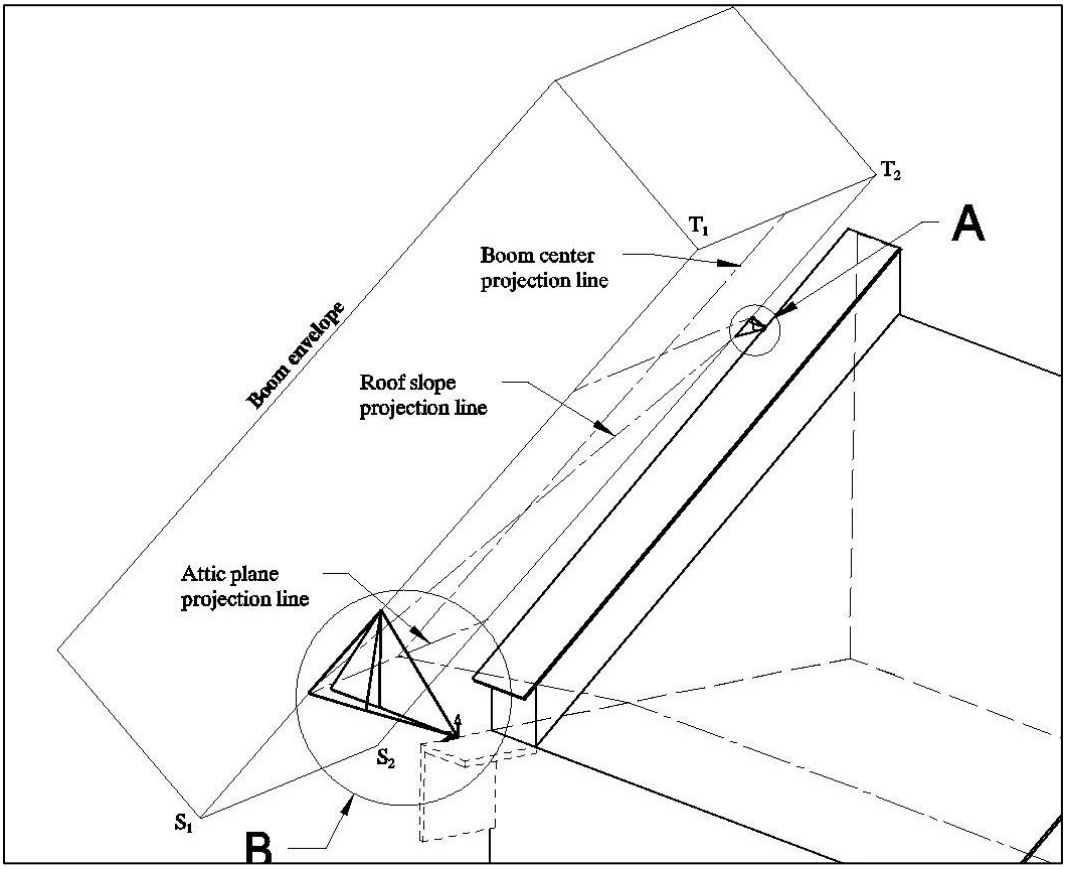

Figure 3.17 Boom-obstruction clearance analysis.

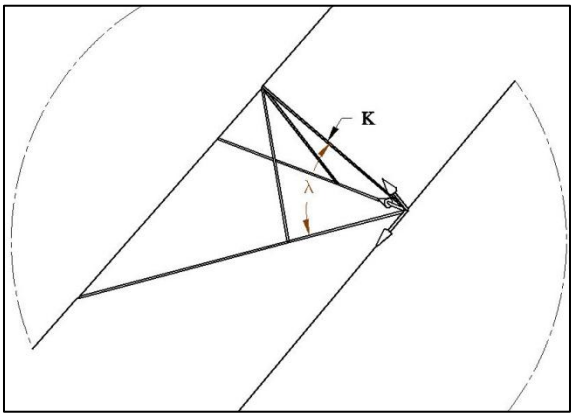

Figure 3.18 Detail A sloped roof.

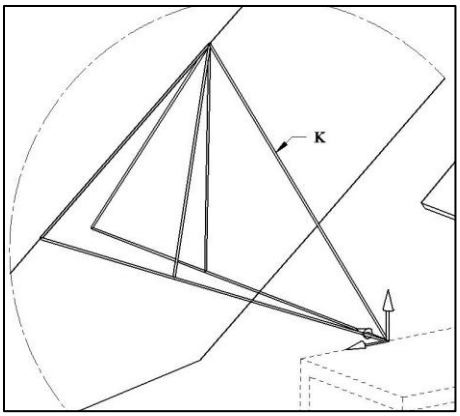

Figure 3.19 Detail B – flat roof.

For clarification, additional dotted planes (see Figure 3.20) were introduced to represent positions in a 3D environment. They include projected lengths of analyzed distances. The analysis plane is perpendicular to the obstruction is roof edge and holds an x-y coordinate of local axis definition.

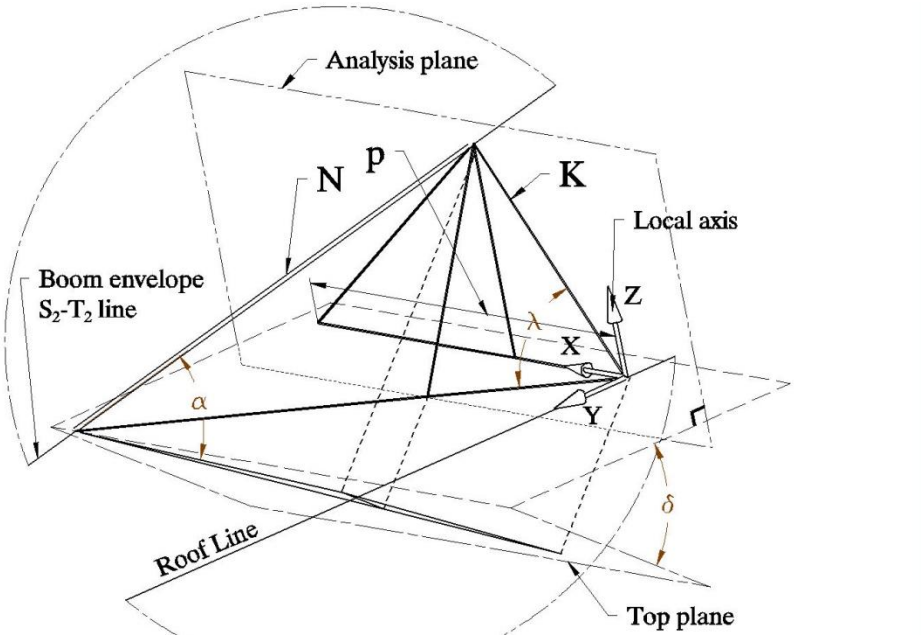

Figure 3.20 Clearance description detail A view expanded.

The clearance distance between the crane boom envelopes line S_2-T_2 and the roof slope line is defined by (*K*), which is the true length and can be seen in the first sketch of Appendix A-06. Local axis definition was created to establish a better visualization of the problem in order to help define lengths using the direction cosines mathematical method. For the true length line (*K*) direction cosines are as follows:

$$\alpha_K = \frac{X_K}{K} \qquad \beta_K = \frac{0}{K} \qquad \gamma_K = \frac{Z_K}{K} \tag{3.24}$$

The line (*N*), (see Figure 3.20) represents the edge of the boom envelope and the direction cosines are as follows:

$$\alpha_{N'} = \frac{-X_N}{N} \qquad \beta_{N'} = \frac{Y_N}{N} \qquad \gamma_K = \frac{Z_K}{N} \tag{3.25}$$

Where:

K – *clearance distance true length*

X_K – *K length projected on X axis*

Z_K – *K length projected on Z axis*

N – *boom envelope edge*

The projection of the boom envelope to the local axes in spherical coordinate form:

$$X_N = -N \sin\varphi \cos\alpha_B \sin\delta \tag{3.26}$$

$$Y_N = N \cos\varphi \cos\alpha_B \cos\delta \tag{3.27}$$

$$Z_K = N \sin\alpha_B \cos\delta \tag{3.28}$$

Direction cosines angles:

$$\alpha_{N'} = -\sin\varphi \cos\alpha_B \sin\delta \qquad \beta_{N'} = \cos\varphi \cos\alpha_B \sin\delta \quad \gamma_{N'} = \sin\alpha_B \cos\delta$$

Because line (*K*) and line (*N*) are perpendicular, the dot product of two vectors:

$$\alpha_{N'}\alpha_K + \beta_{N'}\beta_K + \gamma_{N'}\gamma_K = 0 \tag{3.29}$$

And replacing adequate values:

$$\frac{-X_K}{K} \sin\varphi \cos\alpha_B \sin\delta + \frac{Z_K}{K} \sin\alpha_B \cos\delta = 0$$

$$\frac{Z_K}{X_K} = \frac{\sin\varphi \tan\delta}{\tan\alpha_B} = \frac{h + j \tan\delta}{R \tan\alpha_B} \tag{3.30}$$

From Figure 3.20 the clearance line with inclined surface makes angle (λ), and then:

$$\tan\lambda = \frac{Z_K}{X_K} = \frac{\sin\varphi}{\tan\alpha_B} \tan\delta = \frac{h + j \tan\delta}{R \tan\alpha_B} \tag{3.31}$$

Let (p) be the shortest distance between two lines in the analysis plane:

$$p = -X_N + X_K = N \sin\varphi \cos\alpha_B \sin\delta + K \cos\lambda$$

After few substitution and manipulations:

$$p = \frac{K}{\cos\lambda} \tag{3.32}$$

Also, the distance (p) can be described as:

$$p = R - \frac{H - C_2 + K \sin\lambda \cos\delta + D/2 \cos\alpha_B}{\tan\alpha_B} - \frac{D}{2} \sin\alpha_B \sin\varphi - \frac{B}{2} \cos\varphi - j$$

$$p = R - \frac{H - C_2}{\tan \alpha_B} - \frac{D}{2 \sin \alpha_B} \sin \varphi - \frac{B}{2} \cos \varphi - j - \frac{K \sin \lambda \cos \delta \sin \varphi}{\tan \alpha_B} \quad (3.33)$$

Where:

R	*– crane boom radius*
D	*– boom envelope height dimension (see Figure 3.16)*
B	*– boom envelope width dimension (see Figure 3.16)*
H	*– obstruction height to top surface (Figure 3.13 View C)*
C_2	*– boom rotation axis ground offset (see Figure 3.12)*

Replacing (*p*) from the previous equation, clearance (*K*) is given by:

$$K = \frac{1}{W} \quad R - \frac{H - C_2}{\tan \alpha_B} - \frac{D}{2 \sin \alpha_B} \sin \varphi - \frac{B}{2} \cos \varphi - j \quad (3.34)$$

Where:

$$W = \frac{1 + \sin^2 \lambda \cos \delta}{\cos \lambda} \quad (3.35)$$

α_B	*– boom angle offset*
φ	*– boom angle to obstruction (see Figure 3.13)*
R	*– crane boom radius*
D	*– boom envelope height dimension (see Figure 3.16)*
B	*– boom envelope width dimension (see Figure 3.16)*
H	*– obstruction height to top surface (Figure 3.13 View C)*
C_2	*– boom rotation axis ground offset (see Figure 3.12)*

3.3 Object Trajectory Optimization

During the lift assembly operation, the lifted object is displaced from its pick-point, usually located at the ground level, to its final resting place, usually at a specific elevation. Although movement of crane parts can be traced in relation to the crane carrier, passage of the lifted object can be complicated and difficult to calculate. Improper assessment of clearances can cause damage to the lifted object, passed obstructions, or the operating crane. Analysis of the lifted object trajectory is critical, and the presented proposed algorithm in this section is based on the assumption that each crane action is assigned as a single operation; for example, rotation is represented as an arc, and booming up, down, and radial displacement are represented as a line. No combination movements, such as booming and rotating at the same time, are assessed.

Proposed algorithm

The proposed algorithm layout is based on extensive research on a few heavy crane lift operation projects. The algorithm will be explained step-by-step with respect to crane-object-obstruction relation movement at specific crane configuration and lifted object parameters. Figure 3.21 shows the macro-level of a linear flowchart schema with phase assignments definition names. Terminators Start and End are separated with four blocks consisting of phases where specific objectives are defined and analyzed. The sequence of operations is based on industry expert knowledge and must follow logical action consequences. Predecessor outputs, acting as an input data, are closely related to particular task operations and carry a set of evidence that are critical for this task. The macro-level flowchart is divided into four sections, which cover eight sub-sections called phases. The first section includes Phase 1, which evaluates the object pick area, and Phase 2, crane boom obstruction analysis. The second section covers Phase 3, crane superlift restriction area development, and Phase 4, crane simplified trajectory design. The third section Phase 5, elevation defining method, and Phase 6, anchored and floating obstructions development and relations. The fourth section contains Phase 7, development of elevation trajectory path, and Phase 8, optimization method for developing several paths in different elevations. At the end, the algorithm based on set-up optimization criteria and weight values, proposes an optimized road from the object pick-point to its final resting position.

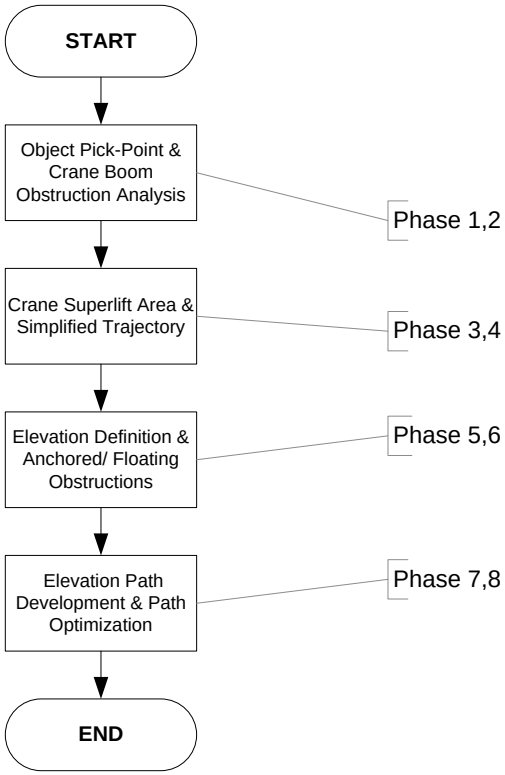

Figure 3.21 Trajectory algorithm macro-level flowchart.

Figure 3.22 shows an expanded trajectory algorithm flowchart. It consists of eight phases with clearly defined objectives and output identification direction. Phases 6 and 7 are placed in a short loop to evaluate each elevation separately and store full or partial solutions. Phase 8 analyzes developed paths to find the optimal solution and create the final trajectory path definition.

Input and criteria parameters directly involved in the algorithm are explained further in Figure 3.22. Only certain data is engaged in the process of mathematical calculations, which directly create evaluated output. Also, due to the limited information that is required for evaluation at this stage, only part of the criteria participates in filtering the desired data. The described process analyzes single iteration with the given crane position, object pick areas, and object set point location. The entire methodology concept is presented in the form of tasks and decisions blocks. Figure 3.22 shows the main process of the proposed methodology. The input parameters include essential information for the modeling process, including the object's data that contains dimensions and weight parameters, and the crane's data that includes specifications such as dimensions, radiuses, and lifting capacities. Also, the input box stores information about construction site

configuration and potential coordinate values of obstructions. Each specific parameter in the input box refers to a set of data required in order to run the algorithm operations. This section begins with a segment where data collection procedures, system configuration identification, and detailed schedule preparation create a basis for the algorithm performance and must be provided prior to initiating the algorithm operation.

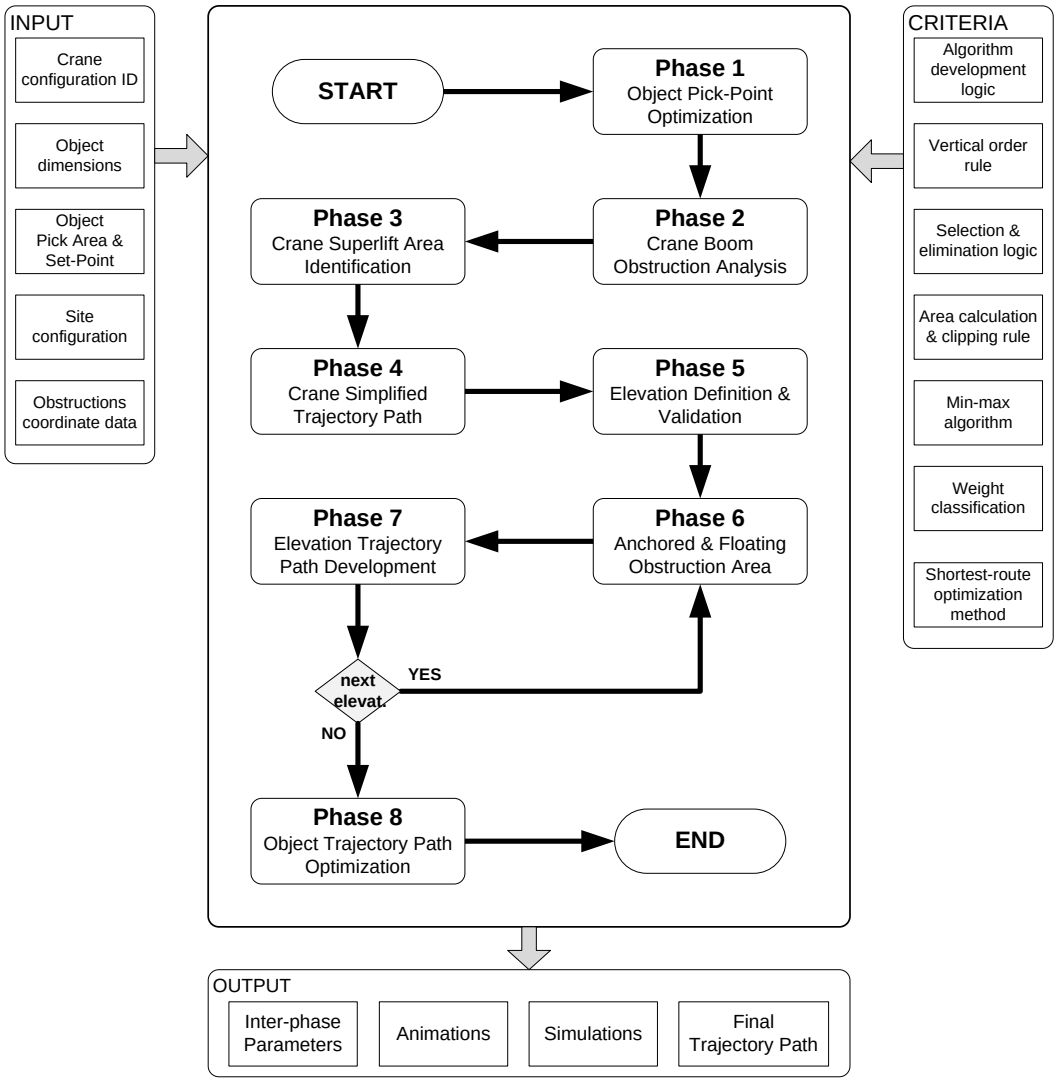

Figure 3.22 Algorithm micro-level flowchart.

The trajectory algorithm's main process phases are between the "Start" and "End" flowchart terminators. It contains eight phases, which focus on functions that are critical to develop the lifted object trajectory path. Each phase objectives are clearly defined and supported by graphical sketches. Phase 1 (object pick-point optimization) defines single pick-point coordinates from provided pick areas. Phase 2 (crane boom obstruction

analysis) and Phase 3 (crane superlift area identification) concentrate on given crane configurations such as crane boom and the crane wheeled superlift addition, respectively. These two phase outputs are restricted areas of a crane boom movement. Phase 4 (crane simplified trajectory path) is the first phase where the crane simplified trajectory (CST) path is presented. The concept introduced in this phase shows a method of translating complicated spatial crane path movement into simple 2D line arc combination polygons. Phase 5 (elevation definition & validation) shows methods of identifying *k* elevations, which are present for particular crane configurations, as well as validating critical ones. This phase deals with possible combination elevations for object pick- and set-point and crane set-point. Phase 6 (anchored & floating obstruction areas) concentrates strictly on obstructions analysis where two types of obstruction areas are developed. This phase is in a loop with its successor, Phase 7, modifying the CST path at elevations developed in Phase 5. As mentioned, Phase 7 (elevation trajectory path development) develops CST paths onto separate elevations and modifies them accordingly to recognized obstructions. Either a full or partial trajectory path is stored in the algorithm database for further analysis. When all elevations are analysed, Phase 8 (object trajectory path optimization) vertically connects the developed elevation paths and recognizes a single optimized trajectory from object pick-point to set-point based on user-defined criteria.

The presented phases and their tasks are influenced by criteria that are summarized in Figure 3.22. The criteria start with algorithm development logic, which requires certain operations to be performed prior to others, for example CST path cannot be developed before object pick-point is optimized. Some operations are exempt, (Phase 3 crane superlift area identification) from following this criterion, because a crane may not have a carrier superlift, but it must be clear when and where such exemption is allowed. The vertical order rule criterion refers to identifying working elevations from pick-point, set-point, and crane set-point vertical relations. It uses a rule when one or two working elevations can be developed from a set of three possibilities. This criterion will be presented in detail in Phase 5 (elevation definition and validation) analysis. The selection and elimination logic criterion is heavily used in three separate phases (2, 3 and 4) for selecting and eliminating obstruction shapes from areas defined by various radiuses. Either obstruction offsets or original shape data are treated and ruled by this criterion. As in the previous criterion, an area calculation and clipping rule is used on several occasions in the algorithm set-up. It starts operation in Phase 3 and finishes in Phase 6, where subtraction, union, or intersection operations are performed. It consists of a short

algorithm that is implemented at any time of need. The min-max algorithm criterion sets the rule for developed elevations and organizes them in the min-max sequence. The least weight optimization method is the default rule used in Phase 8, where the object trajectory path optimization operation is performed. If the user does not specify a different method of optimizing the developed path, this criterion is applied to show the least weight path from pick-point to set-point. The preceding criteria are either short algorithms supporting a specific task in separate phases or predefined knowledge-based rules. They may apply to different phases for several operational tasks.

The output section in the Figure 3.22 flowchart contains four boxes, where each output is defined. Inter-phase parameter is collecting information related to each phase. Each phase is output must clearly be defined and stored (see Appendix A-01). The algorithm flow addresses major components, which play a significant role in judging the next step. Developed output is stored temporarily in the algorithm database for down-the-road operation. Phase 1 stores pick point coordinate values. Phase 2 tasks analyze and store restricted crane boom regions (CSR). Cranes that are equipped with wheeled superlift parts are directed for analysis to Phase 3 for restricted area crane wheeled superlift region (CSR). Phase 4 final tasks store crane simplified trajectory path to develop a crane elevation plane. Phase 5 analyzes either one or two stored elevation planes, depending on the vertical trajectory order rule, and deposits elevation planes associated with recognized obstruction heights. Phase 6 also has two separate output parts: one connected to modify CST paths and a second to identify anchored or floating obstruction offsets areas. Stored obstructions offset areas reflect analysis at each recognized elevation in two horizontal directions, A (outside modified CST path) and B (inside modified CST path). Phase 7 modifies stored CST paths by recognized obstruction offsets and also predecessor phase output record un-modified paths into A and B directions. Phase 8 stores one intermediate result of concatenated partials and optimized trajectory final path. The output sections' data used to create animation and simulation is also stored in the separate boxes that may be used for visualization purposes.

Phase 1;-Object Pick-Point Optimization: The objective is to identify object's pick-point coordinates from available input pick area region(s). To meet objective requirements there are three different methods of selection available to the user: (1) area centroid method, (2) area boundary point shortest radius method, and (3) area boundary point shortest angle method. The phase input box includes all parameters required to evaluate

the main operation process to meet defined objectives. It contains crane data, such as R_{min} value, and the crane set-point position. It also includes object set-point coordinates and selected areas where the lifted object will be delivered. Phase criteria define algorithm rule logic where Method A is predefined as the default method for object pick-point selection. The phase output delivers the chosen pick-point coordinate position. Figure 3.23 shows Phase 1 flowchart with input, output, and criteria boxes.

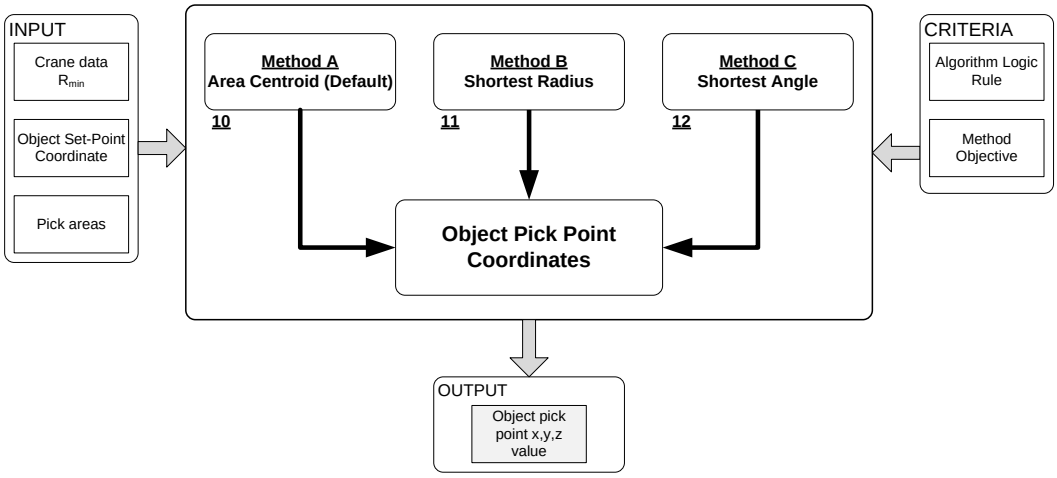

Figure 3.23 Object pick-point selection flowchart (Ph-1).

Each method will be discussed separately. Default Method A evaluates centroid of the analyzed area. The centroid of an area is similar to the geometric center (GC) of a body. To calculate the centroid only, the geometric shape of an area is involved. Integration formulas for calculating the centroid are as follows:

$$C_x = \frac{xdA}{A} \qquad C_y = \frac{ydA}{A} \qquad A = \int x\, dx \qquad (3.36)$$

Figure 3.24 shows graphical interpretation (10) of the centroid calculation method. It is referenced from the flowchart (bottom left corner) with number 10 representing the analyzed task.

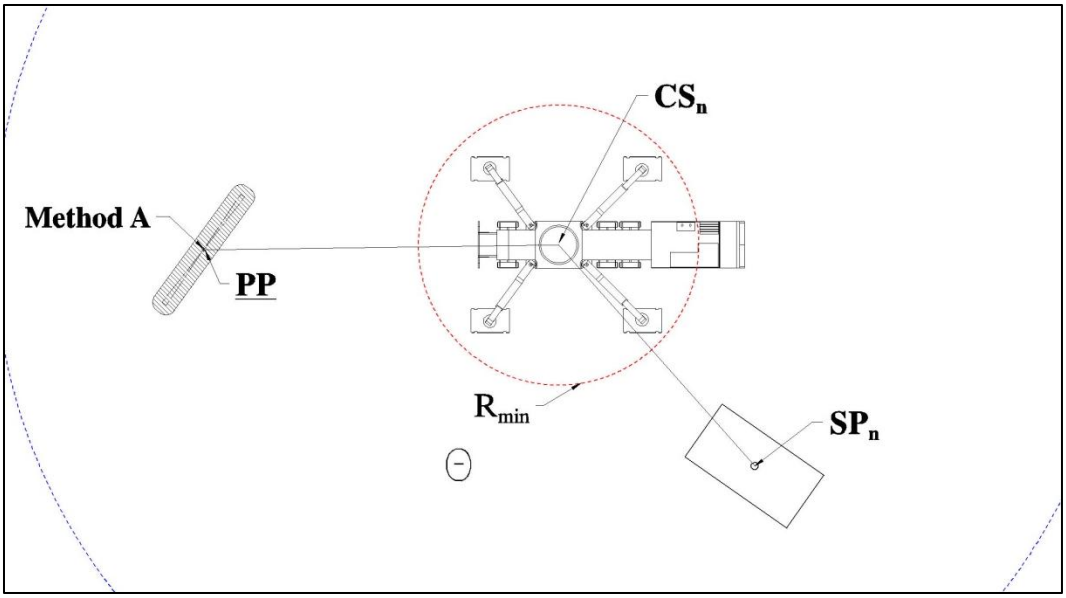

Figure 3.24 Method A - centroid area (10).

Method B of object pick-point analysis uses the shortest radius technique. It finds the closest point of a particular area to the crane set-point coordinates. Figure 3.25 shows a graphical interpretation (11) of the object pick-point shortest radius selection technique. The tangent arc (A_3) to the input area defines the intersection point (PP), which is stored in the database as the lifted object pick-point.

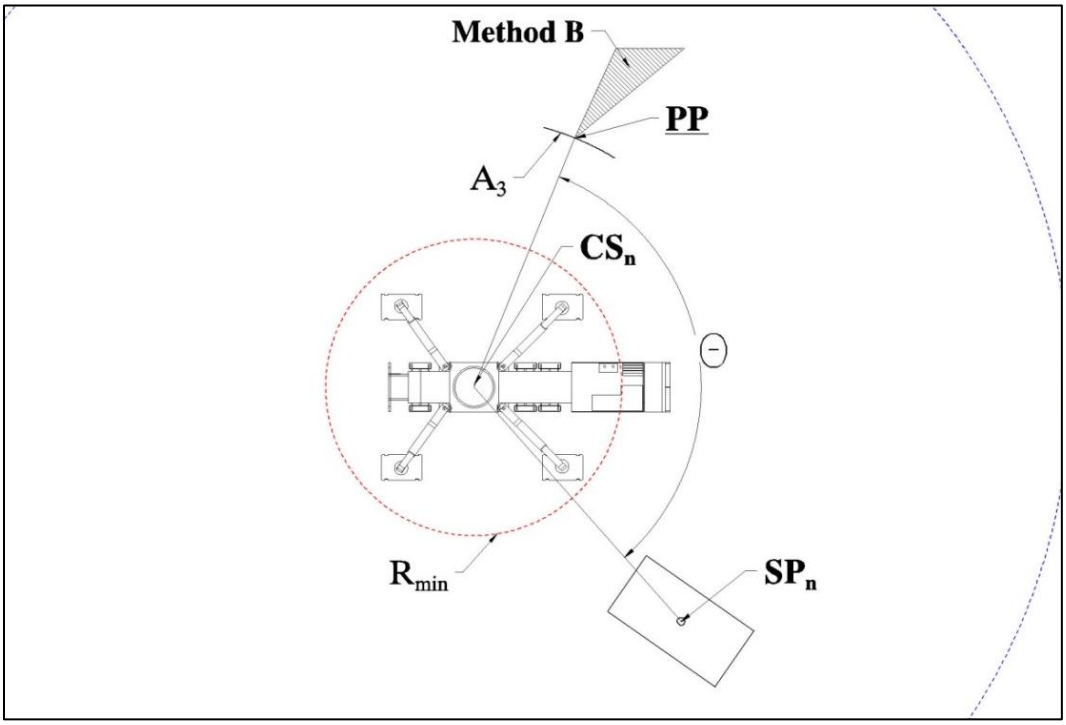

Figure 3.25 Method B - shortest radius (11).

Method C of the object pick-point analysis finds the shortest radius of the evaluated pick area to the object set-point coordinates. Figure 3.26 shows a graphical interpretation (12) of the shortest angle object pick-point method.

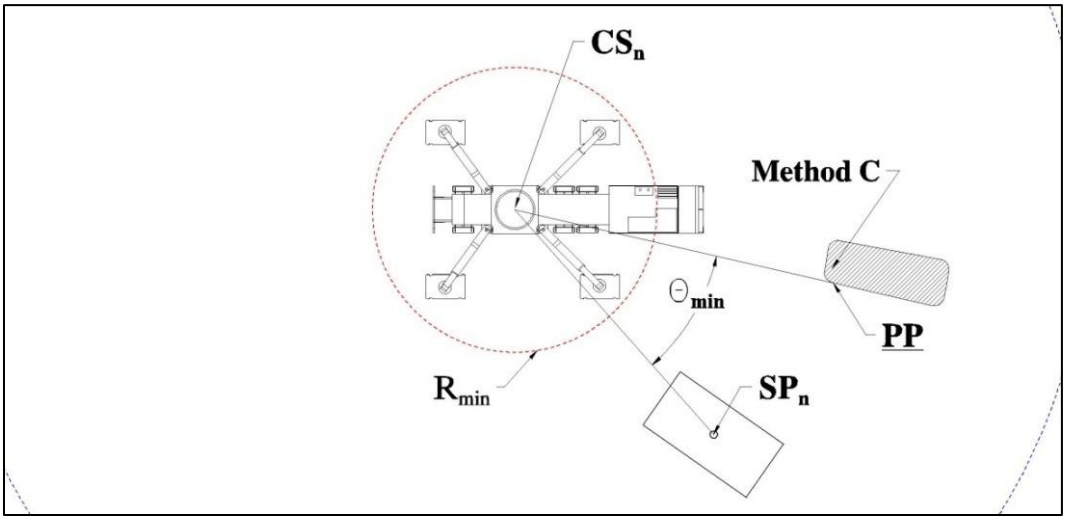

Figure 3.24 Method C - shortest angle (12).

The shortest angle from the input area to object set-point (SP) is defined by the area tangent line created from the crane center of rotation point (CS). In Figure 3.26, Θ_{min} angle is the shortest angle between the developed lines. However, the default method for the algorithm to select pick-point coordinates will be the centroid Method A. The user does have the option of selecting one of the other methods, however.

Phase 2;-Crane Boom Obstruction Region Analysis CRB): The objective is to develop a restricted crane boom region between R_{min} and R_{max} boundary radiuses of the particular crane configuration at the crane elevation plane. Figure 3.27 shows tasks involved in the analysis of the Phase 2 crane algorithm. The input box includes data related to the crane, such as boom offsets radiuses and set-point coordinates. Data of obstruction objects residing in the area defined by the crane configuration maximum radius must be available in this phase. The main process operation task starts with the creation of the crane boom maximum operation area, which is defined by the boom reach radius distance at 360° rotation and identified obstructions within that area. The second task calculates the identified obstruction's maximum radius (R_H). Next the decision diamond checks the calculated radius for its position in relation to crane R_{min} distance. If calculated R_H radius is smaller than the crane R_{min} value, the entire section between R_{min} and R_{max}, controlled by the obstruction shape offset, is eliminated. In case the calculated R_H radius is larger

than the crane R_{min} but smaller than the R_{max} value, the crane boom obstruction conflict region (CBR) is introduced. Such a recognized conflict area is stored in the database and the next obstruction start is analyzed (internal loop function). Once all obstructions are evaluated, those with a potential conflict area are separated, and critical restriction areas are unionized. The final output of this phase is stored in the database under the description CBR for utilization later in the algorithm.

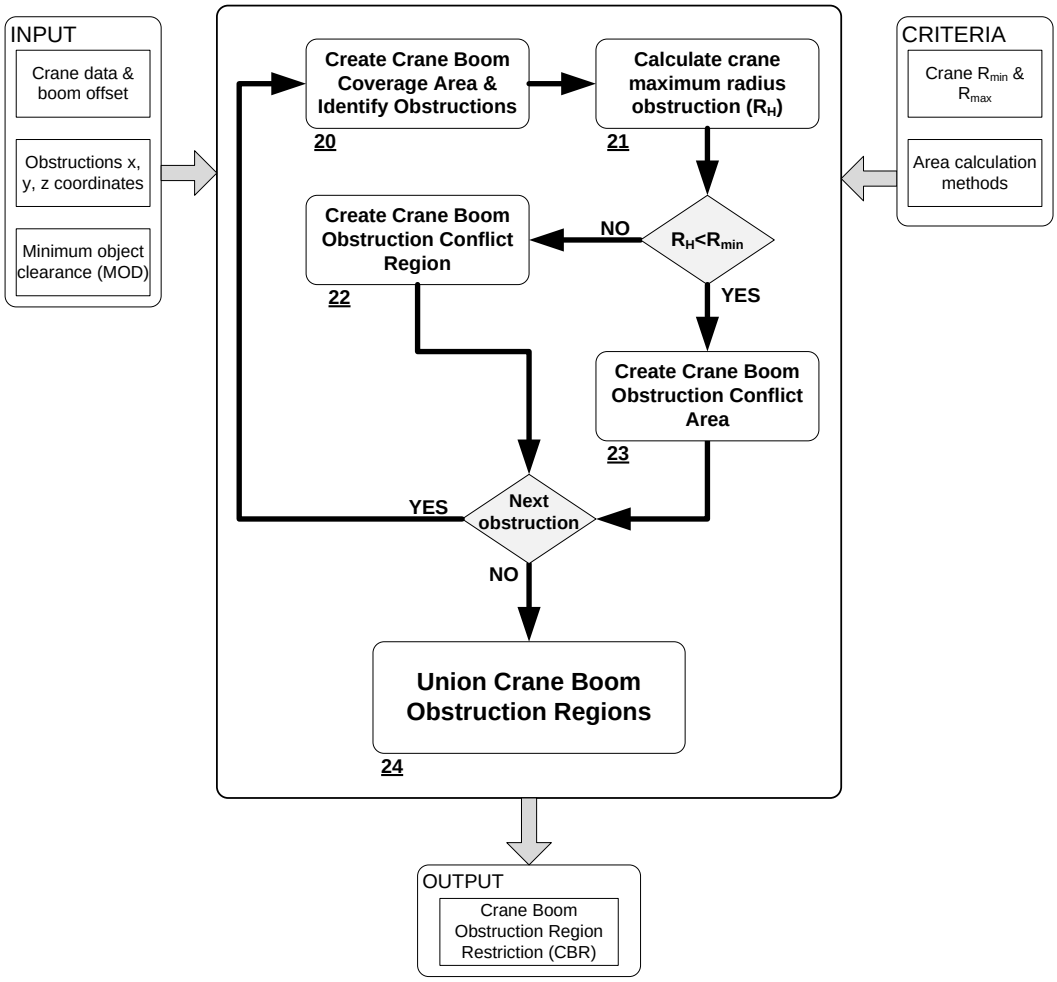

Figure 3.27 Crane boom obstruction region development flowchart (Ph-2).

Figure 3.28 shows the final results of the Phase 2 algorithm. Restricted areas are clearly identified and results stored in the database. But to get to the final task, a few small steps must be executed. First, the crane boom coverage area is designed (see Figure 3.29). The area is extended beyond the crane R_{max} distance for the value (*B'*), calculated in equation 3.37, to cover the boom additional attachment extension. Figure 3.29 presents steps assigned and executed in the first task. The elevation view explains the rationality behind the B' offset value. The covered area for the obstruction check must be offset by B'

outside the R_{max} circle. That additional distance creates a safety buffer around the boom perimeter where potential obstructions can be detected and marked for analysis.

$$B' = \frac{B}{2} + MOD \tag{3.37}$$

Where:

B - *Boom width dimension*

MOD - *Minimum object distance*

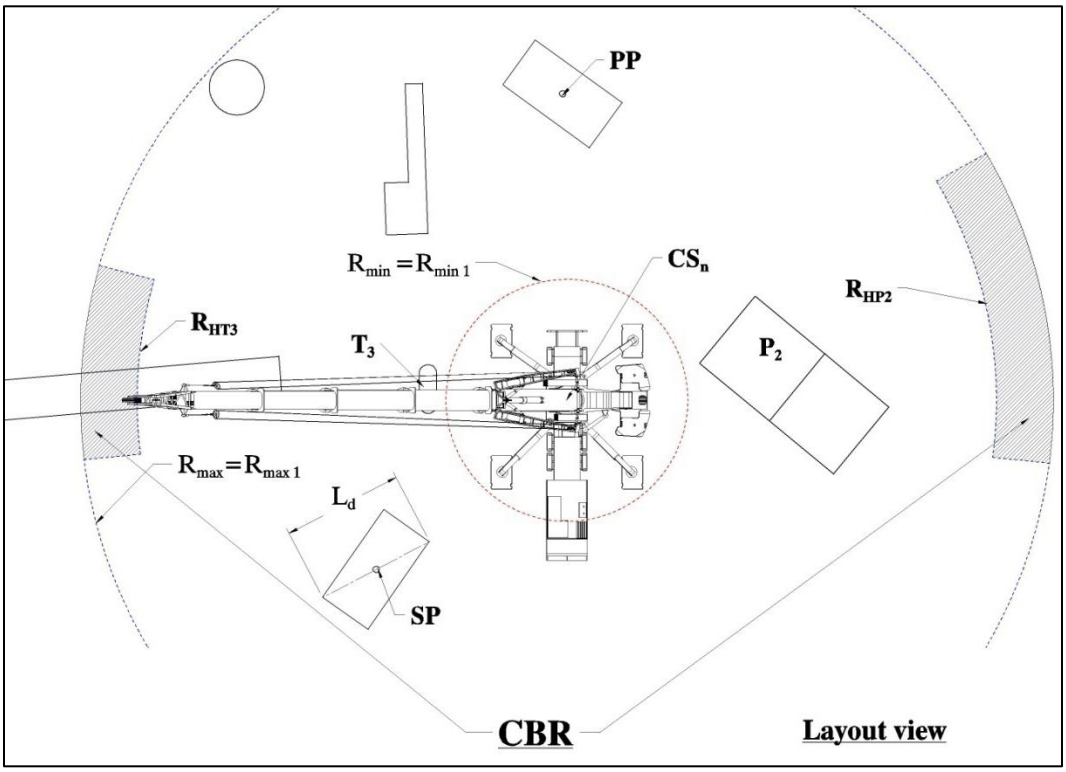

Figure 3.28 Crane boom restricted region development (24).

When all obstructions are recognized in the entire 360° region, their identity is recognized and maximum elevation values are retrieved for analysis. Crane elevation is the base elevation to analyze crane boom obstruction conflicts. R_{max} radius represents the crane configuration's maximum boom distance that can carry an assigned load and should not exceed 85% capacity due to discrepancies in object weight measurements. This information is collected and stored in the database from the crane manufacturer lift table (see Appendix A-14).

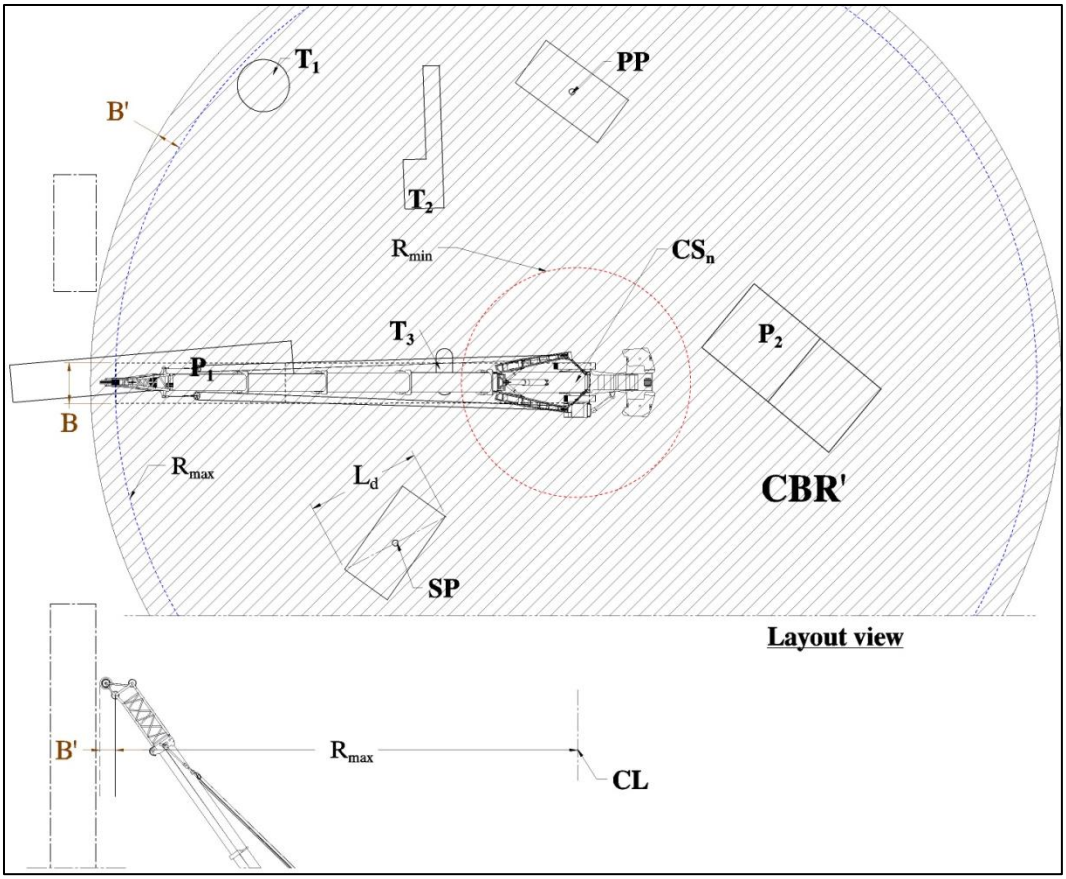

Figure 3.29 Region CBR' and obstructions (20).

The created area CBR' is checked for all obstructions. Each obstruction is analyzed separately by creating an internally developed obstruction loop. In the case of absence of obstructions in the analyzed area the algorithm flow is rerouted to a different path inside the task block and does not follow the route when obstructions are present. Such logic increases mathematical operations efficiency and significantly reduces the algorithm's operation process time. When an obstruction is recognized, it is checked for potential crane boom conflict. Figure 3.30 shows obstruction T_3 crane boom envelope conflict. The obstruction T_3 is height dimension limits the crane boom tip point inside the CBR' area circle boundary. In that instance a maximum obstruction crane boom radius R_{HT3} is created. On the opposite side the arc radius R_{HP2} represents limited reach due to obstruction P_2's height. Obstruction P_2 contains two different elevation heights and the tallest part is in conflict with the crane boom envelope.

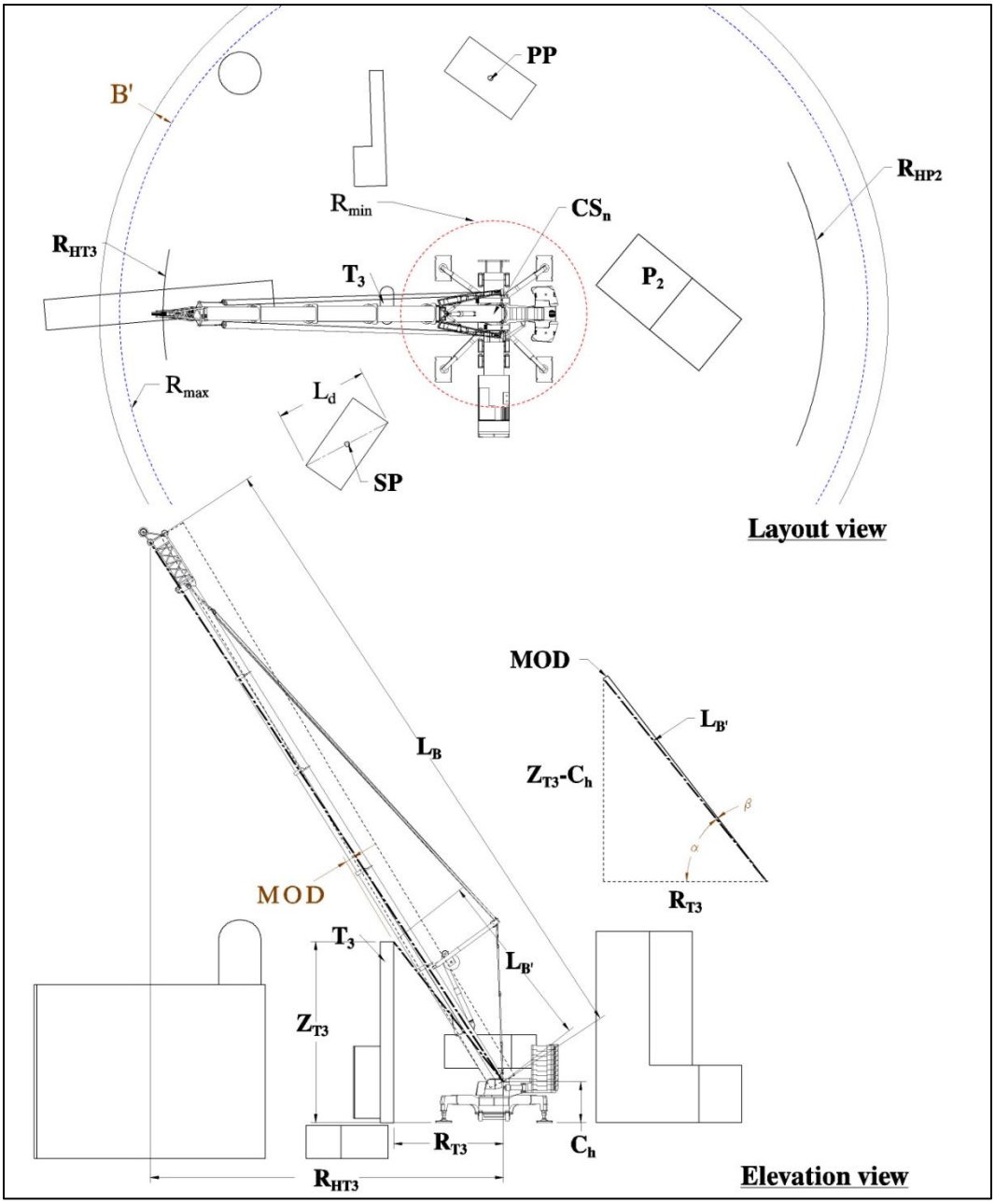

Figure 3.30 Maximum obstruction crane boom radius calculation (21).

Maximum obstruction crane boom radius R_{HT3} is calculated satisfying equation 3.38:

$$R_{HT3} = L_B \cos \alpha + \beta \tag{3.38}$$

Where:

$$\alpha = \tan^{-1} \frac{Z_{T3} - C_h}{R_{T3}}$$

$$\beta = sin^{-1} \frac{MOD}{L_{B'}}$$

$$L_{B'} = \sqrt{Z_{T3} - C_h\ ^2 + R_{T3}\ ^2}$$

Z_{T3} - *Obstruction vertical coordinate*

R_{T3} - *Obstruction radius to crane center of rotation*

C_h - *Boom rotation point offset distance*

L_B - *Boom length*

MOD - *Minimum object distance*

The next task evaluates the obstruction layout boundary. Figure 3.31 shows an obstruction offset area and tangent line creation. Analyzed obstruction shapes are offset by B' value distance to create safety buffer for crane boom operation.

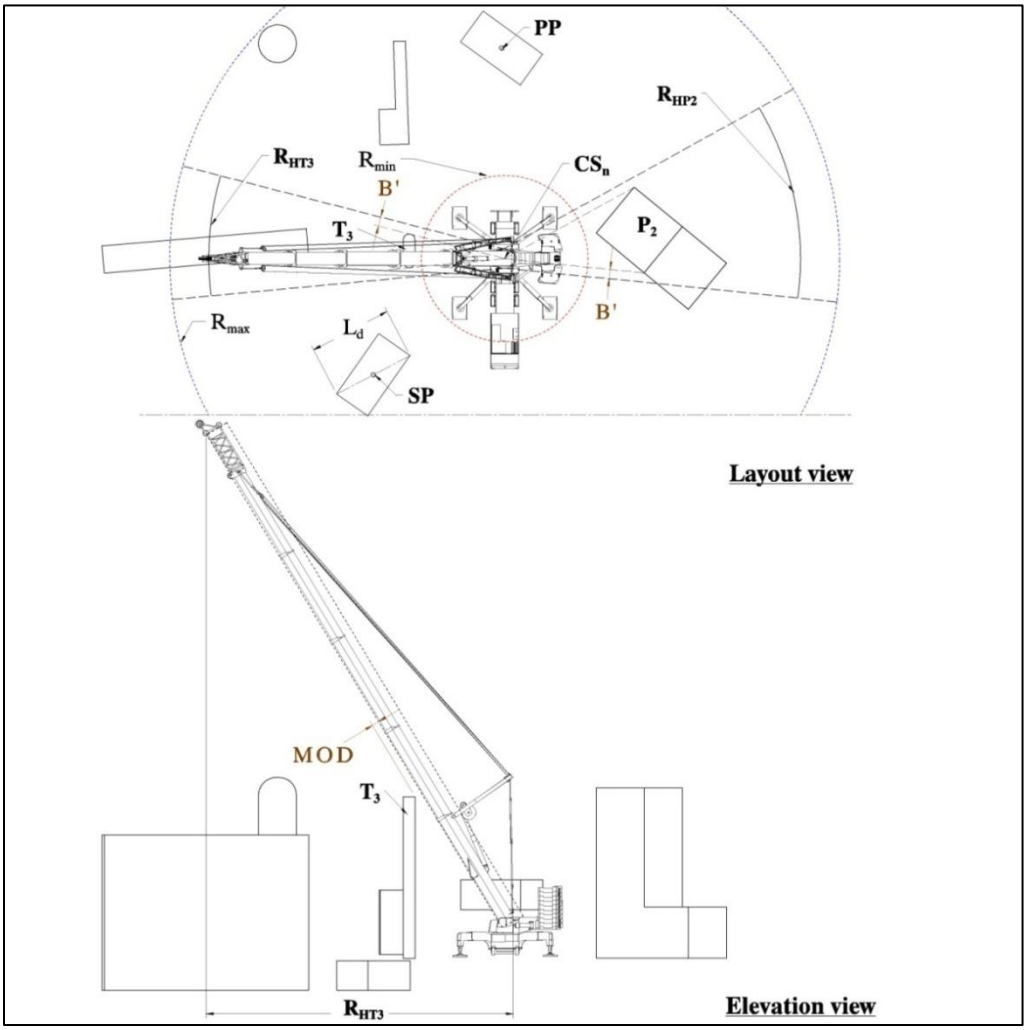

Figure 3.31 Obstruction tangents and offset lines (22).

From the crane CS point two tangent lines are created to an already recognized obstruction offset. Offset boundary B' value is calculated in equation 3.37. Depending on the obstruction shape, created lines are either tangent-to-curve or normal-to-tangent point. From the offset tangent points (see Figure 3.31), tangent lines are extended to the R_{max} circle boundary. The created area between R_{max} circle, R_{HT3} arc, and tangent lines identifies the restricted CBR area for a particular obstruction. Figure 3.32 shows a special case when $R_{Hn}<R_{min}$ and the proposed solution.

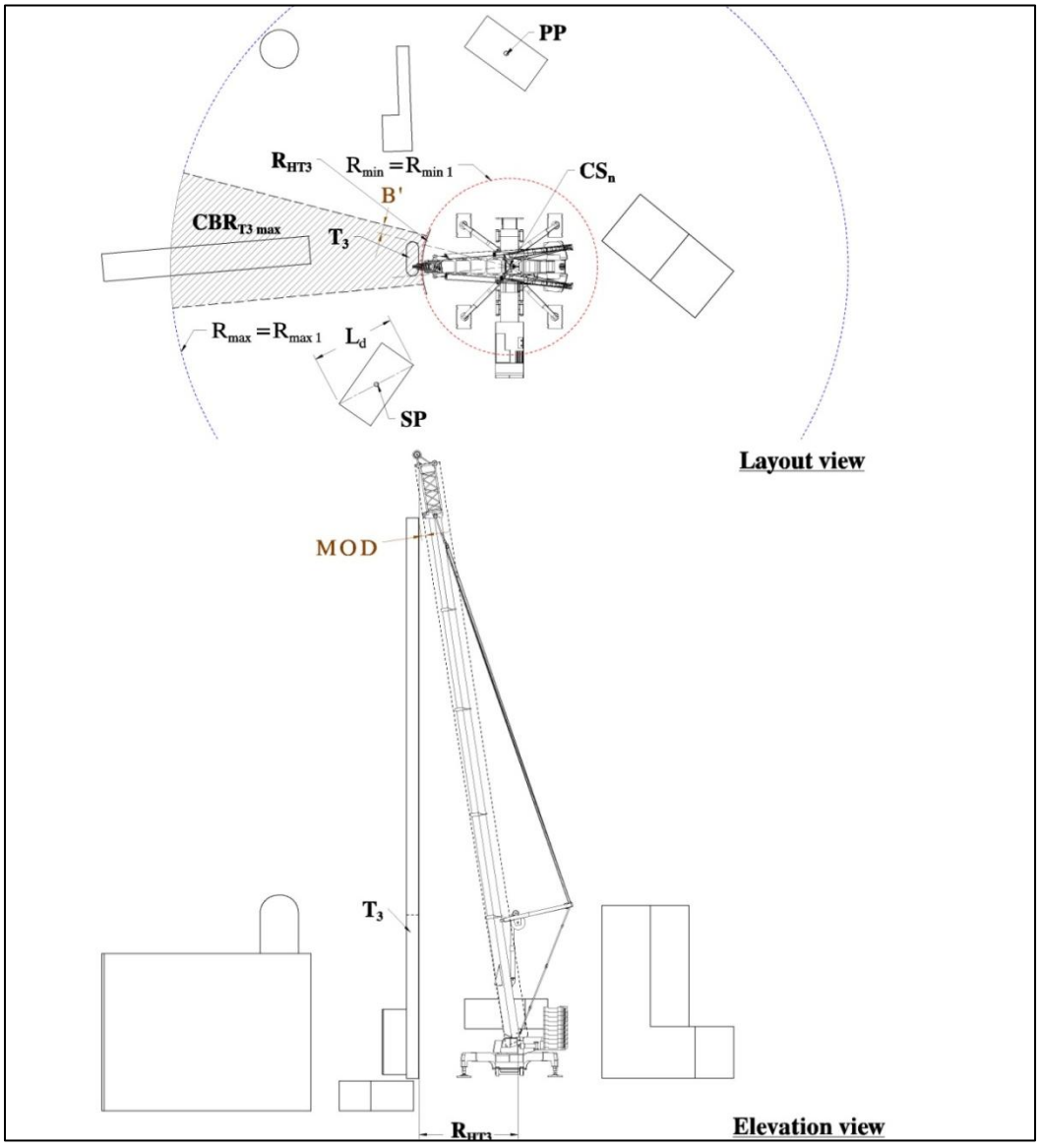

Figure 3.32 Crane boom obstruction critical position (23).

At the construction site, a specific situation may take place when the obstruction height position boom tip projection line is beyond the R_{min} radius value. In that situation tangent

lines are extended in both directions from the tangent points to meet R_{max} and R_{min} circles. The created restricted area takes a pie shape and eliminates any crane boom movement on this section between object pick-point and set-point.

There could be several smaller or larger CBR_n areas located around the perimeter of the positioned crane, but all must be analyzed individually and then stored. Figure 3.28 shows the union of two separate crane boom region areas. The joint area is called crane boom region (CBR) and stored for further analysis.

Phase 3;-Crane Superlift Region Development (CSR): The objective is to develop a restricted crane superlift area(s) for a crane with a wheeled superlift attachment. Figure 3.33 shows the phase flowchart.

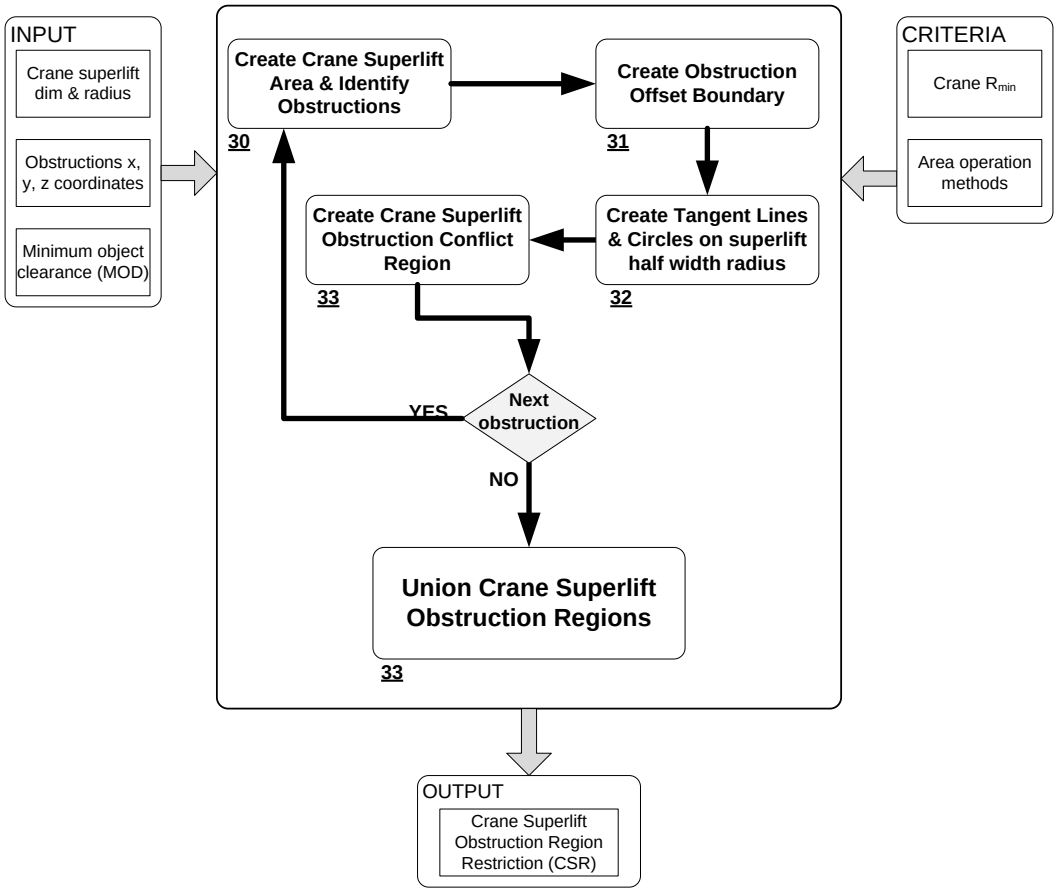

Figure 3.33 Crane supelift region development flowchart (Ph-3).

The phase flowchart follows the standard set-up arrangement with input, main process, criteria and output sections. The input section refers to the crane superlift dimensions, obstruction coordinates, and user defined clearances. The criteria section concentrates on

area operation methods and crane minimum radius values. A main process guides the phase's tasks from developing an area and finding obstructions, through analyzing and avoiding conflict. The CSR analysis phase is reserved only for a crane configuration with wheeled superlift attachment. The wheeled superlift section is attached to the crane carrier structure behind the counterweight section. Some all-terrain mobile crane superlift segments have two section masts attached to the main boom. Both types, either on the ground or boom attachment, increase crane lift capacity. Because only the wheeled type superlift may be in conflict with ground obstructions, that category will be the subject for analysis in this phase. The elevation analysis will be the crane body elevation. The final result of the CSR development phase can be seen on Figure 3.34

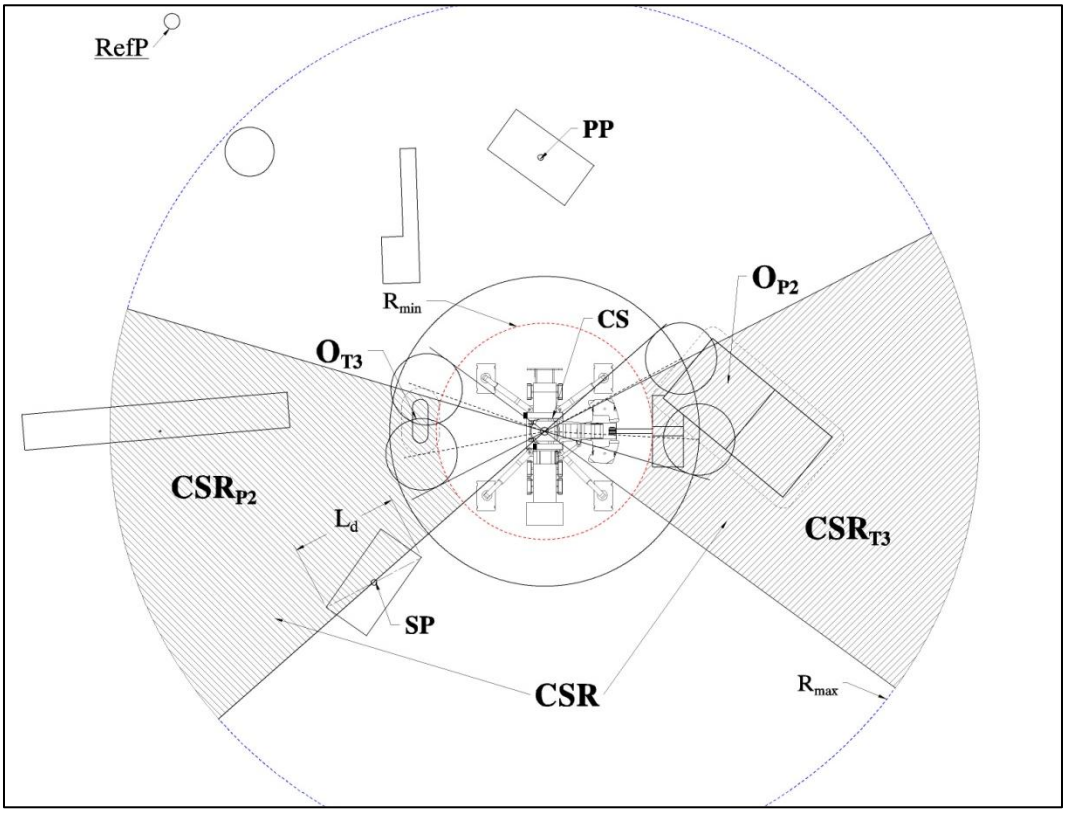

Figure 3.34 Crane superlift restriction area developments (33).

Two separate pie regions, CSR_{P2} and CSR_{T3} (hatched sections), are recognized and joined in one CSR region for further analysis. To get the results presented in Figure 3.34 first the wheeled superlift maximum radius is identified and the circle is offset by MOD value, creating a new CSR' region presented in a Figure 3.35. Implementing MOD offset to the crane superlift radius at this point simplifies the mathematical clearance calculation. The

created area between the crane's R_{min} circle and wheeled superlift maximum radius offset is checked for intersecting obstructions. Figure 3.35 displays identified the wheeled crane superlift region CSR' and two interfering obstructions: T_3 and P_2.

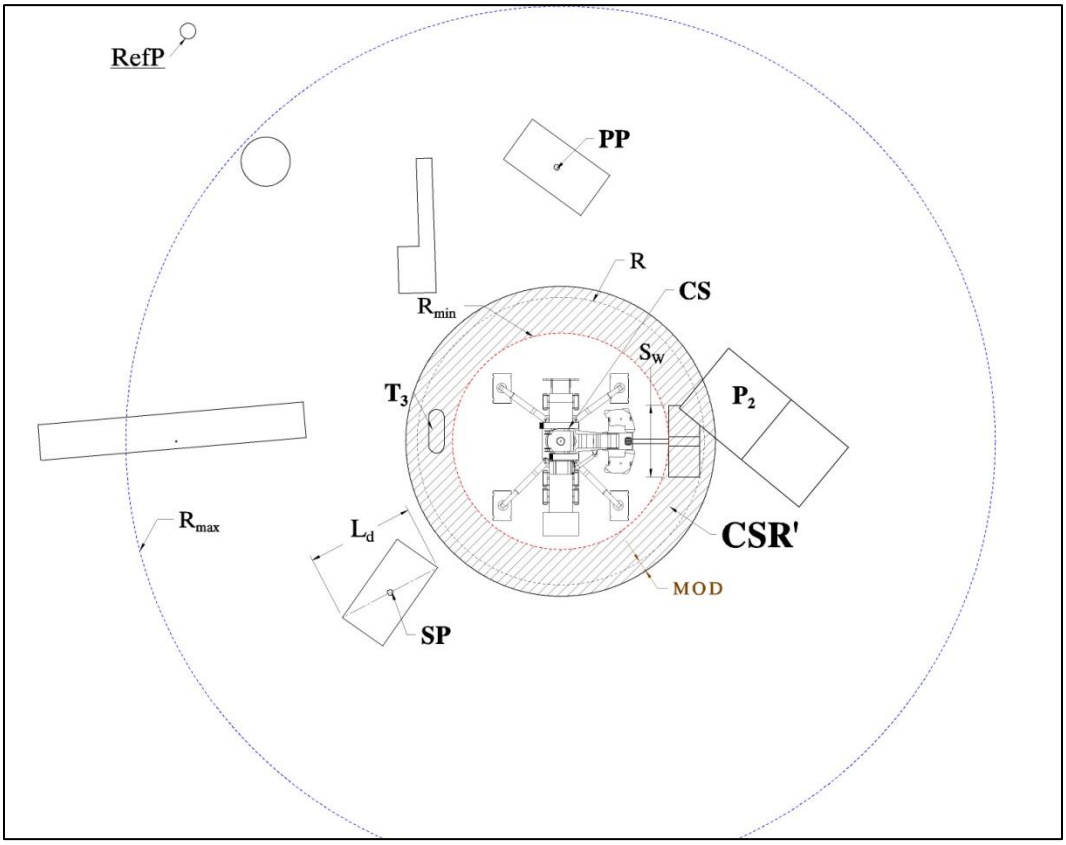

Figure 3.35 Crane carrier superlift area CSR'(30).

Identified obstructions may be entirely encompassed by the created area (T_3) or have a partial intersection zone (P_2). Regardless of obstruction intersection percentage, the next task offsets the obstructions' envelope boundary by the minimum clearance value (MOD). This operation immediately creates buffer zones around obstructions. Figure 3.36 shows the offset areas for intersected obstructions. After the obstruction offset is created, tangent lines are created between obstruction offsets' intersection points and center of crane rotation point (*CS*). Figure 3.37 explains tangent development operations. For obstruction T_3 the tangent-to-curve method is applied, and for obstruction P_2 a normal-to-tangent point is created. Calculated tangent points are the circle centers, where radius distance reflects half of the wheeled superlift carrier width (S_W). Two intersection

points between the created circles' perimeters and CSR' boundary are calculated. Only external intersections are issued in the analysis.

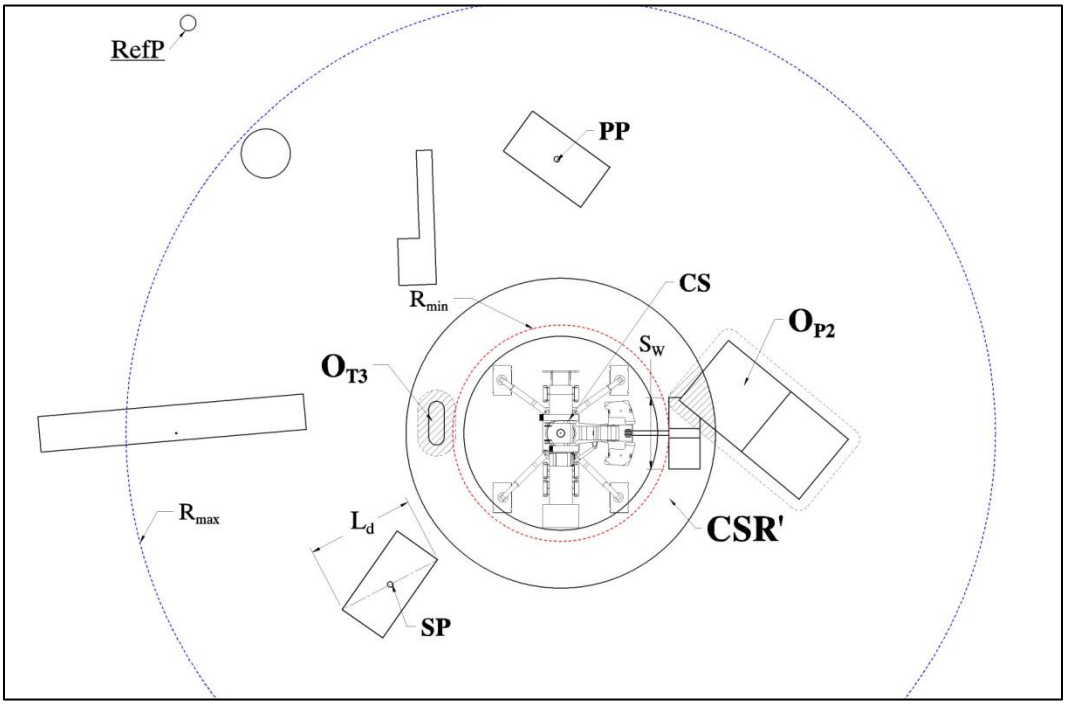

Figure 3.36 Obstruction offset boundary development (31).

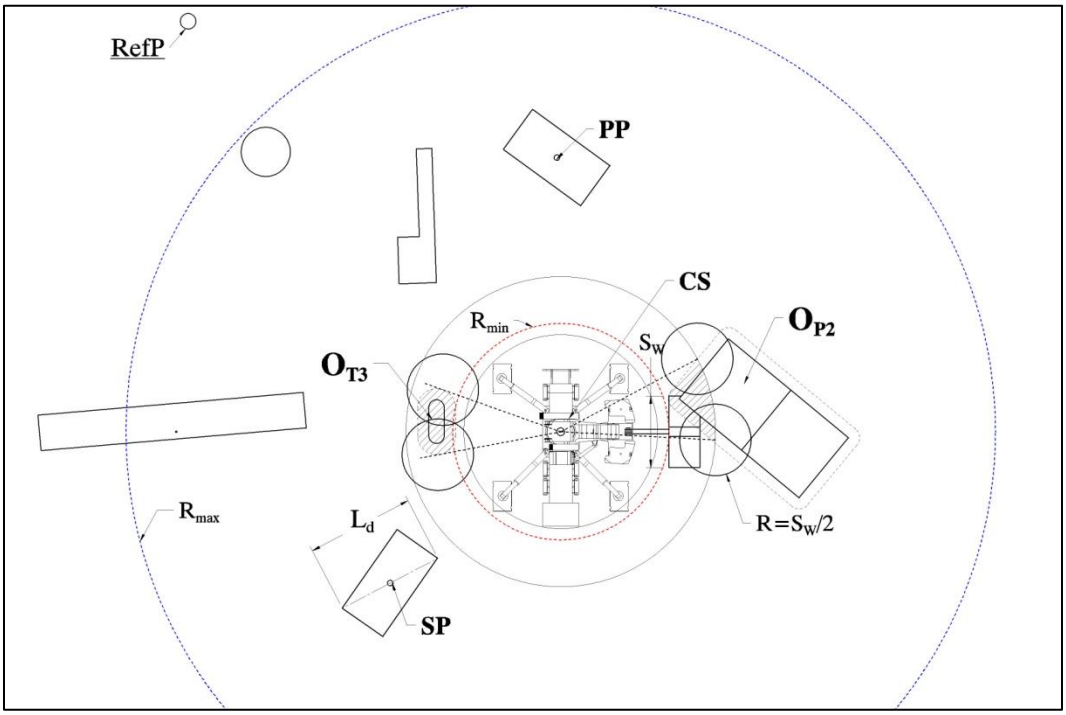

Figure 3.37 Tangent lines and circles development (32).

External intersections points together with the crane set (*CS*) point create boundary lines. These lines are extended to the opposite side of CS point (see Figure 3.34), with R_{max} - R_{min} circles creating a new region. This area is a restricted region where the crane cannot operate. Figure 3.34 shows the CSR restricted area. It contains areas marked CSR_{P2} and CSR_{T3}, which reflect zones defined by the respective obstructions.

Phase 4;-Object Crane Simplified Trajectory (CST) Path: The objective is to develop a crane simplified trajectory path (CST) for the lifted object. During lift operation the object's longest side (when object is rectangular) is constantly perpendicular to the crane boom plane. Also, the CST path is the shortest path between the pick-point and set-point. Figure 3.38 shows the phase algorithm flowchart.

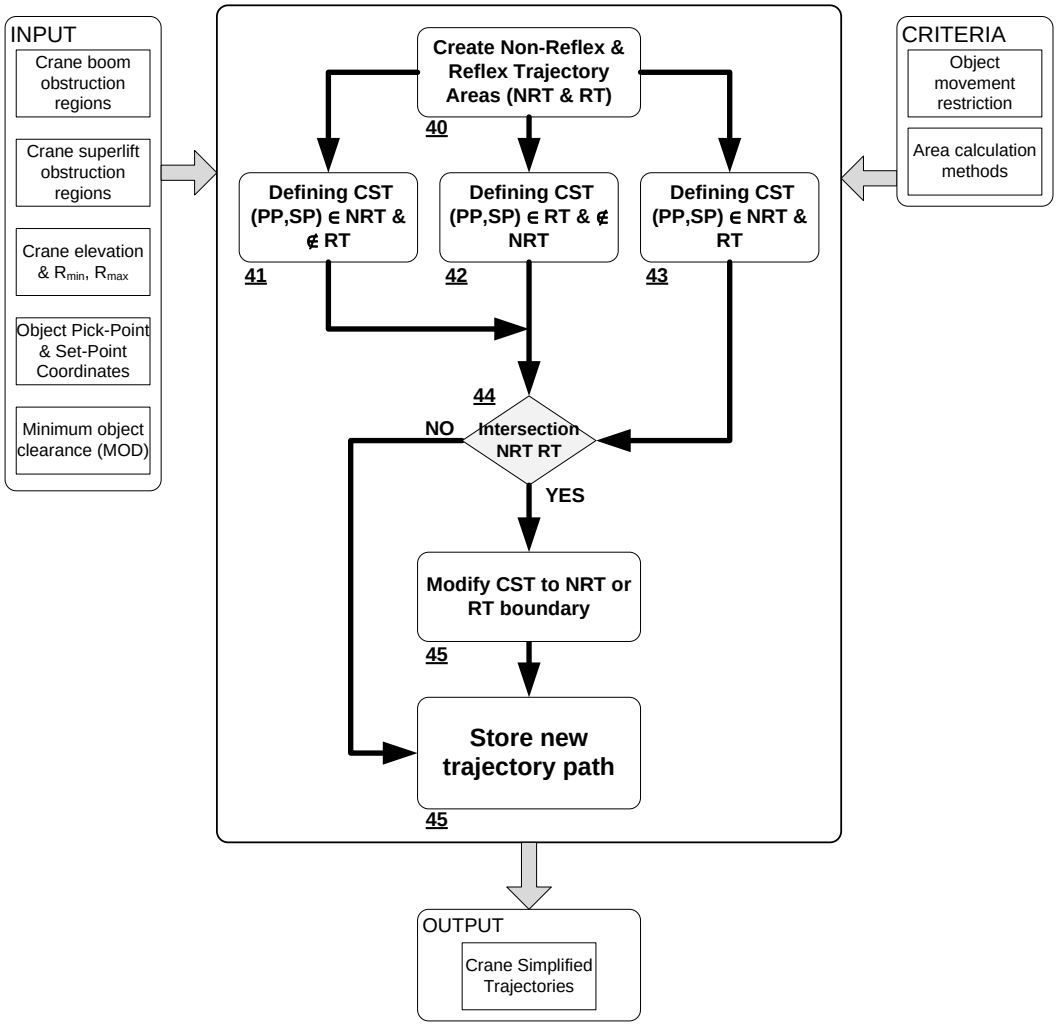

Figure 3.38 Object crane simplified trajectory (CST) path flowchart (Ph-4).

The input section covers crane elevation coordinates, crane R_{min} and R_{max} radiuses, and parameters already developed at the previous phases, like the CBR and CSR areas. It requires an object's pick-point and set-point as well as minimum object distance (*MOD*). Criteria refer only to object movement restrictions such as object position during the lifting operation and area calculation method. The main process's first task recognizes possible solutions based on crane boom region (*CBR*) and crane superlift region (*CSR*), if the superlift configuration is present. It analyzes region uniformity at the crane elevation of a full 360° angle. A positive result may exist either at a non-reflex or reflex angle between object pick-point (PP) and object set-point (*SP*). Figure 3.39 shows an example of such area analysis.

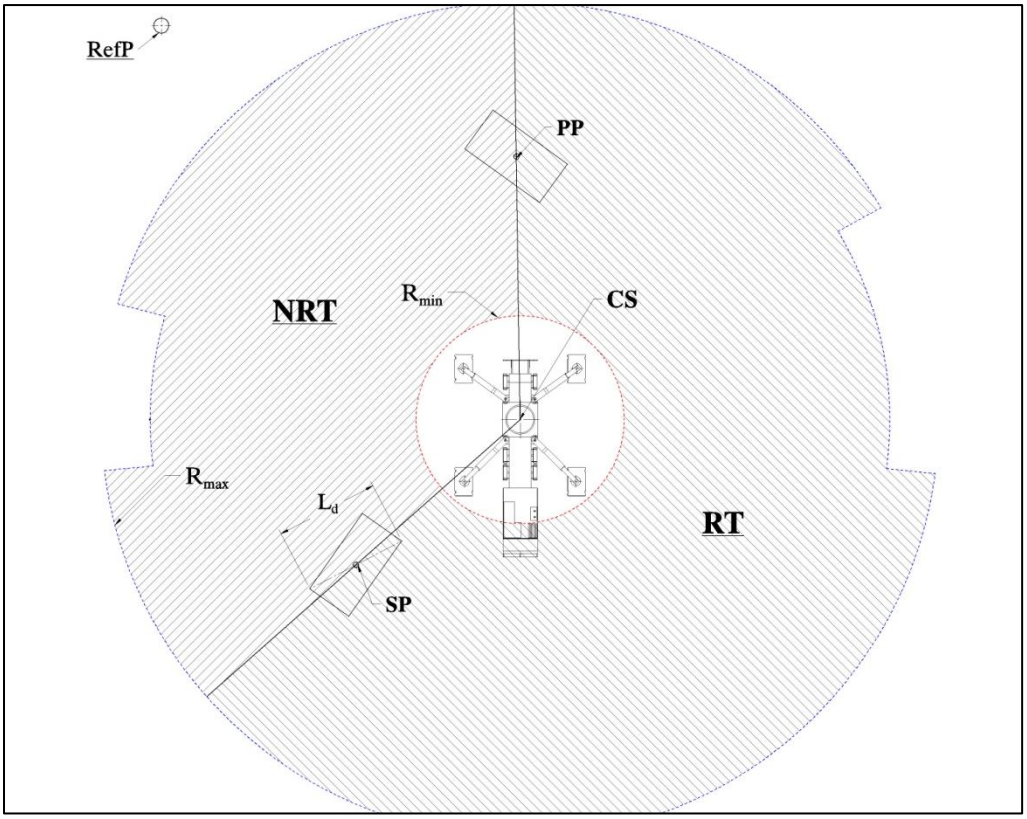

Figure 3.39 Non-reflex and reflex angle trajectory area development (40).

Non-reflex trajectory area (*NRT*) and reflex trajectory area (*RT*) are developed by subtracting crane boom region (*CBR*) and crane wheeled superlift region (*CSR*) from R_{min} - R_{max}. The area is then divided by two lines starting from the common crane set-point (CS) at object pick-point and set-point. From the input data rule, it is defined that the analyzed crane configuration set-up must have at least one solution, i.e. one polygon area that contains both object pick-point (*PP*) and object set-point (*SP*). Following this input

data rule one or two out of three different options may occur. Figure 3.40 shows the first possible solution for the CST path development in the non-reflex angle area. Because PP has a larger radial displacement than SP from the CS center, the first path portion is a straight line from PP point towards CS center to match the SP radial dimension.

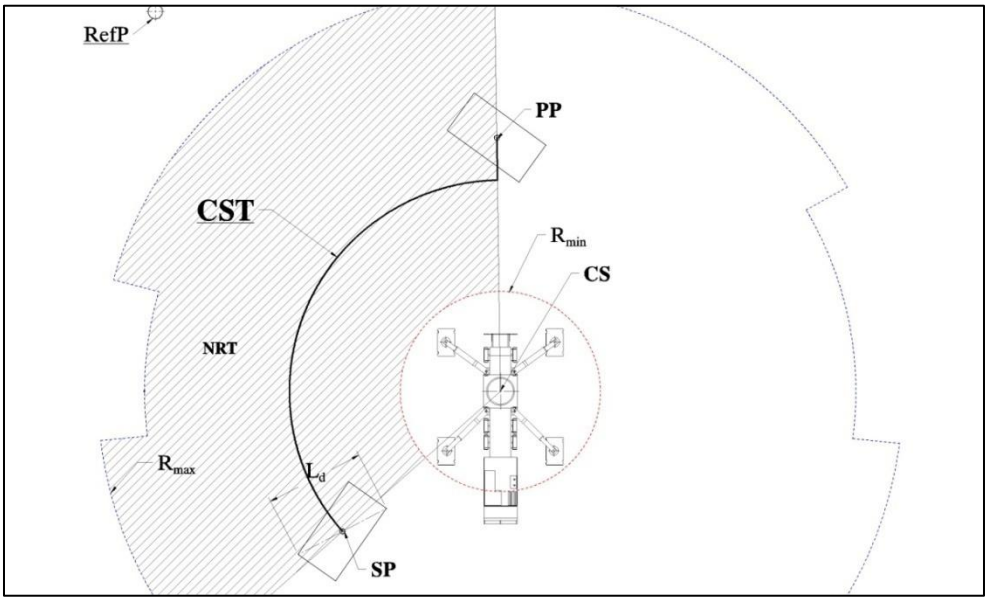

Figure 3.40 CST path development in NRT area (41).

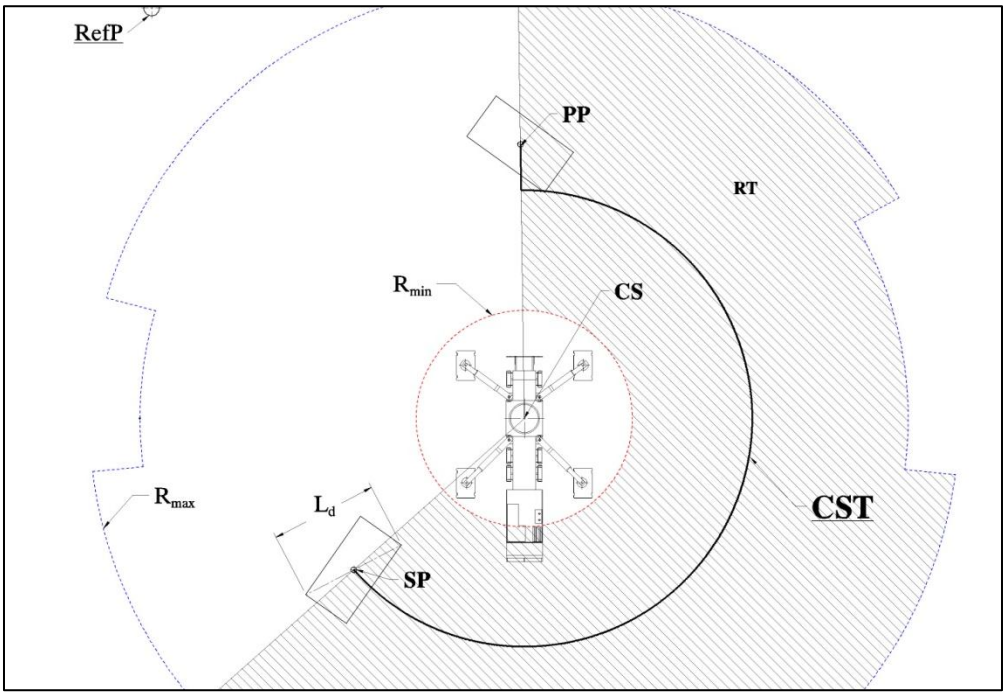

Figure 3.41 CST path development in RT area (42).

Once this is complete the arc, with center CS, connects and creates the end line with the object SP (follow Figure 3.40). Figure 3.41 shows a second possible solution to CST path development in the reflex angle quadrant. This scenario requires similar steps as CST path development in non-reflex angle area; the RT area is complementary to NRT area and corresponding CST arcs are complementary as well. These two scenarios cover situations where either area has a PP-SP connection (residing in the same polygon). The third alternative may occur when both sides are valid for analysis. Figure 3.42 shows development of two trajectory paths at the same time.

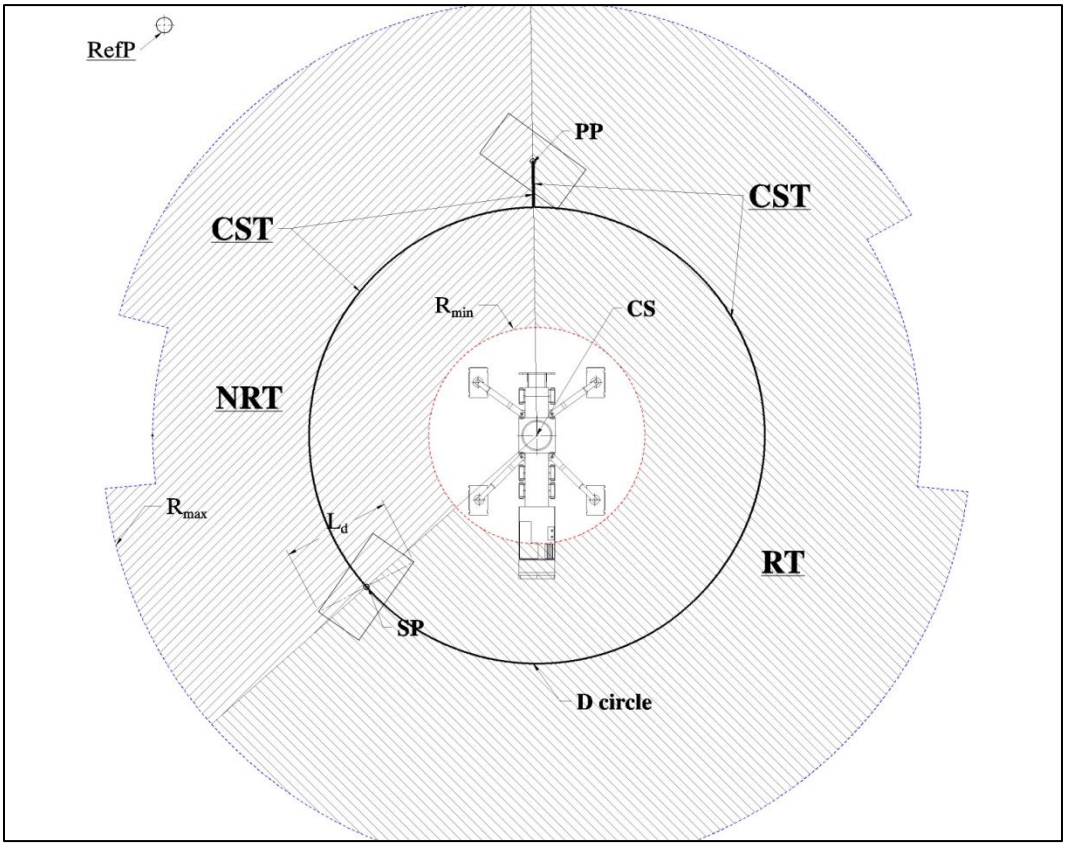

Figure 3.42 D circle path development (43).

The task for this alternative involves both NRT and RT available areas. It evaluates PP and SP for their closest distance to CS center, then creates D circle based on closest point radial displacement. The furthest point creates a radial line, which ends at intersection with D circle and divides D circle into two separate arcs, reflecting portions paths for non-reflex and reflex sections. Thus concludes the simultaneous development of CST paths in NRT and RT areas. The next task analyzes CST paths for their interference with NRT or RT boundaries. This action identifies already developed paths that must be

modified to reflect maximum allowance for the crane boom tip movement. Figure 3.43 displays a scenario where the NRT boundary intersects with a CST path, and Figure 3.44 displays the modified path.

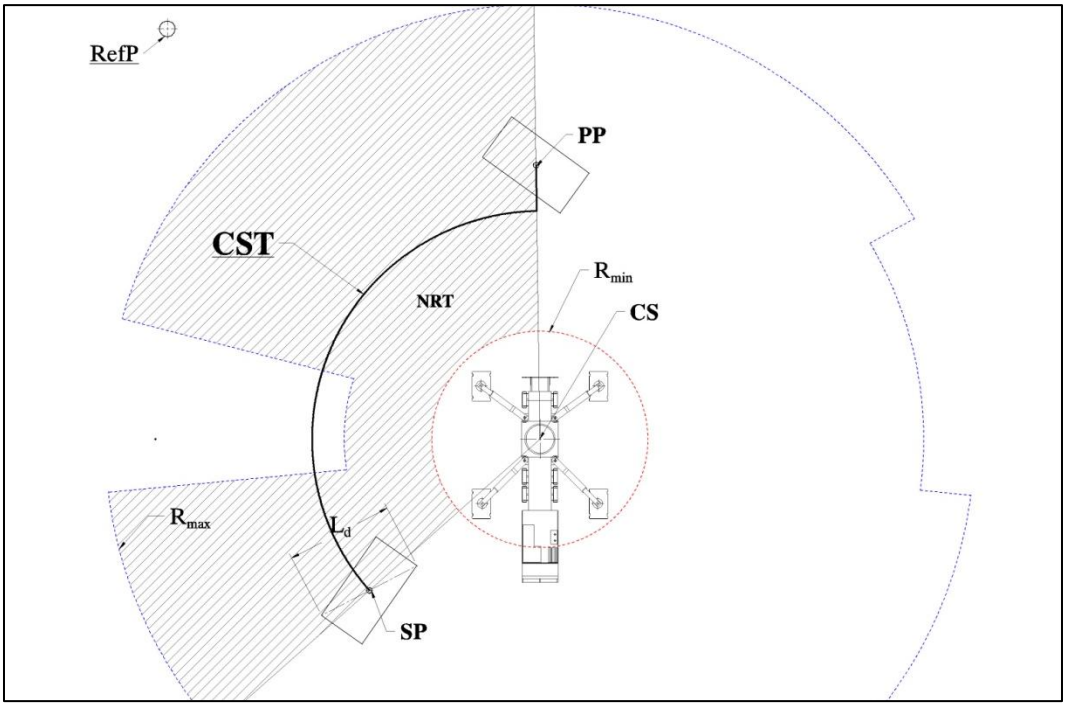

Figure 3.43 Intersection NRT boundary with CST path (44).

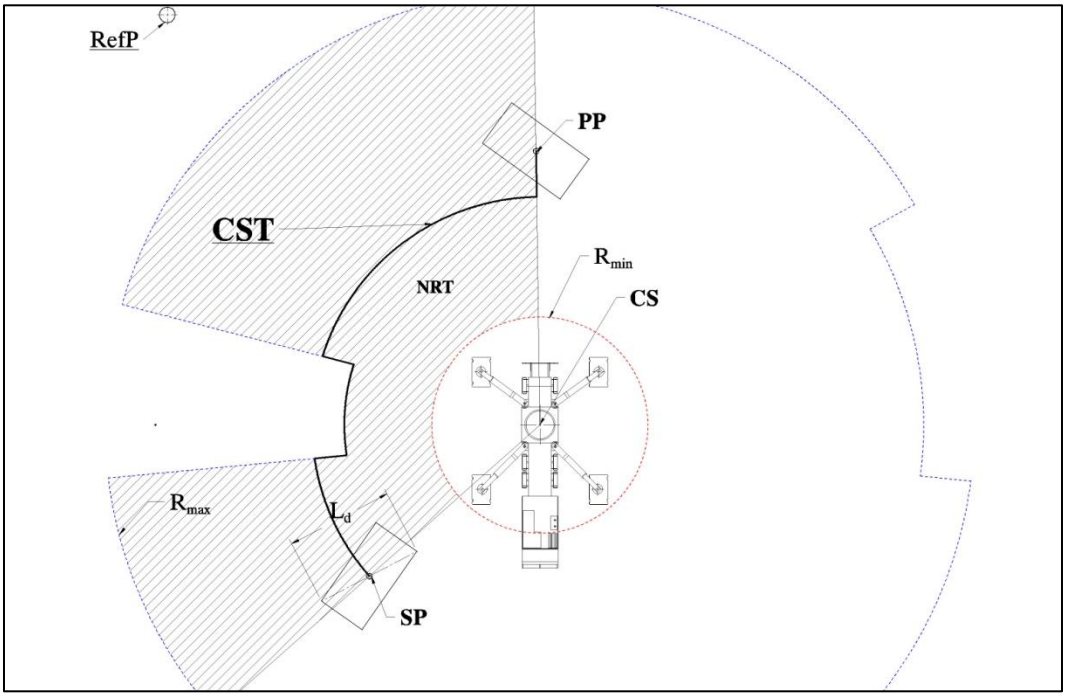

Figure 3.44 Modified CST path (45).

In such a situation the original CST path is cut at the point of intersection and instead follows boundary limit until interconnects with the original part direction. Developed and modified object trajectory paths are stored in the database for further analysis.

Phase 5;-Elevation Definition & Validation: The objectives are to validate vertical order (VO) elevation creation for crane set-point, object pick-point and set-point, as well as develop obstruction elevation analysis planes. Figure 3.45 shows a detailed phase flowchart. The input section includes crane boom tip elevation, crane rigging dimensions, obstructions elevations, and object pick-point and set-point elevations.

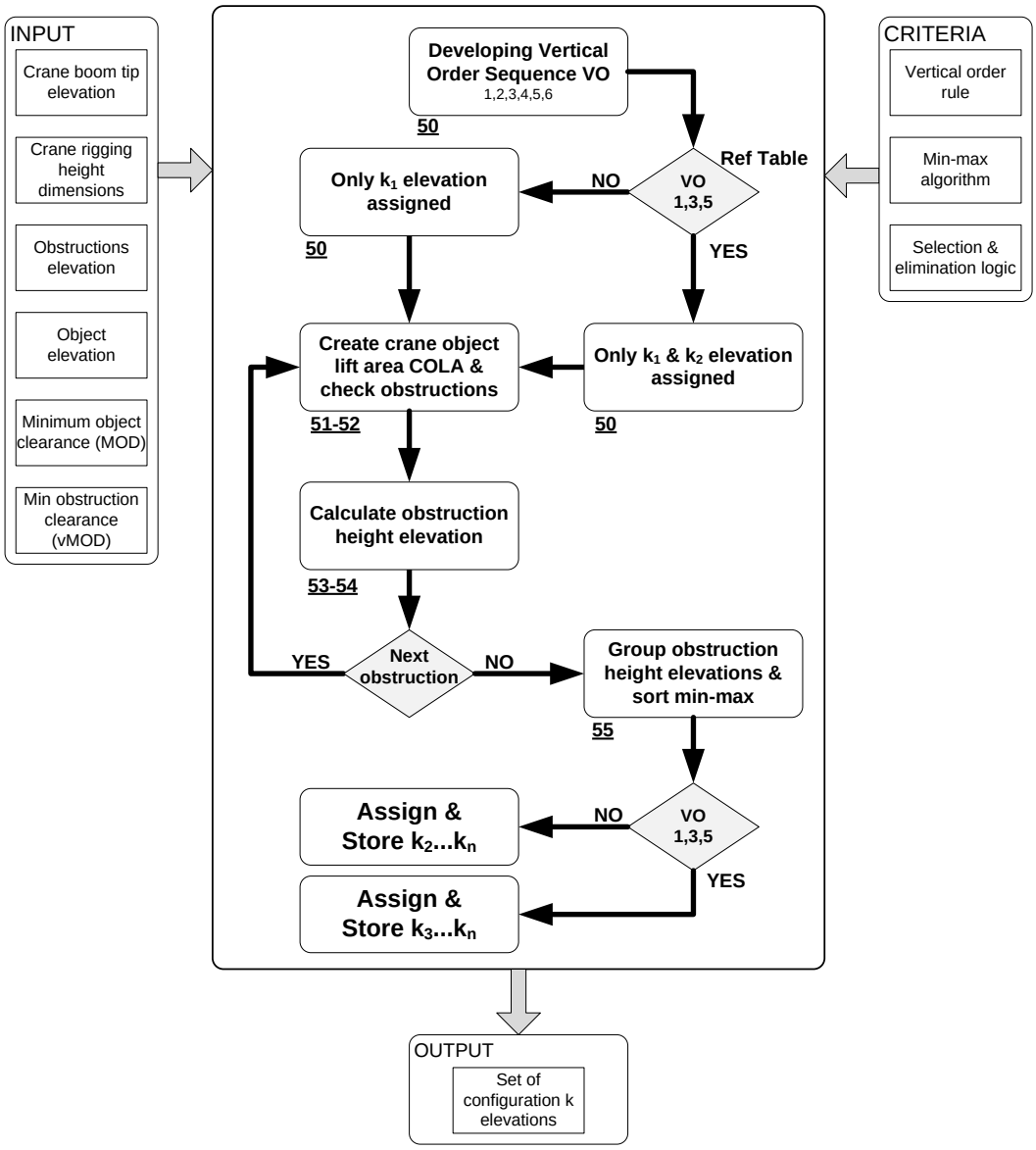

Figure 3.45 Elevation definition and validation flowchart (Ph-5).

The input box also contains default data for minimum object clearance (MOD) and minimum obstruction clearance (vMOD) that may differ from each other. The main operation process starts from developing the vertical order (VO) sequence for crane set-point and object pick-point and set-point. Six different configurations are predefined, where odd configuration numbers produce two elevations and even configuration numbers produce only one elevation. The next tasks create an area for identifying intersecting obstructions and then calculate obstruction height elevation. Grouping and sorting developed elevations are the tasks concluding the phase operation. Figure 3.46 shows the final output of the phase where only working elevations are recognized for further analysis.

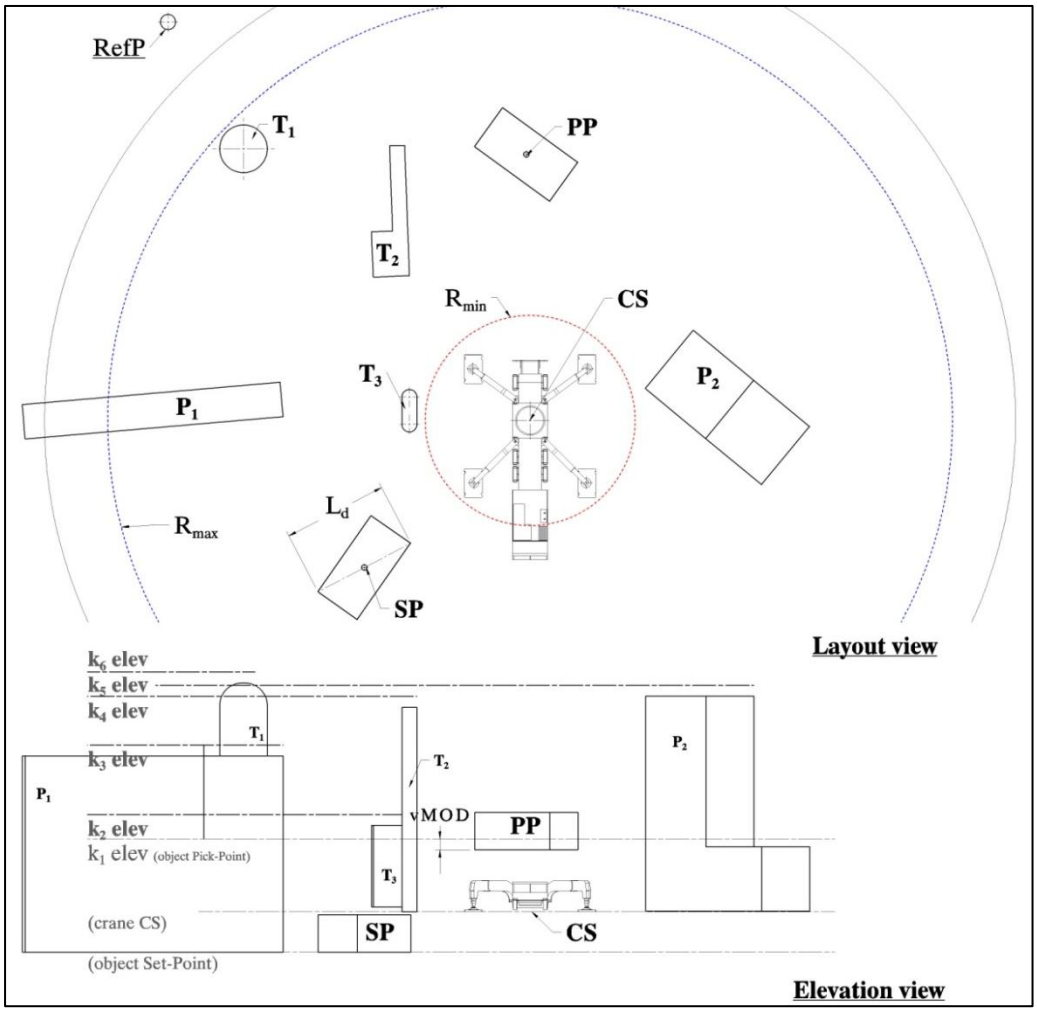

Figure 3.46 Crane configuration object trajectory elevations (55).

Either one or two created non-obstructed working elevations are based on developed trajectory vertical order (*VO*) rule. Table 3.2 shows the vertical order configuration set

up. In VO development strategy, only three elevations are involved: crane set-point (*CS*), lifted object pick-point (*PP*), and set-point (*SP*). These three elevations may have six different positions related to each other. Presented logic includes situations where the lift operation SP has a lower position than the PP. In this situation the lift must have a vertical up-motion from the PP so creation of the SP elevation is obsolete. An example of such situation is the VO 2 configuration that creates k_1 elevation at the PP. A setup rule forces the algorithm to add only the set point elevation.

Table 3.2 Trajectory vertical order.

		Vertical Order (VO)					
Elevation	Sym	1	2	3	4	5	6
CP (crane Set-Point)	C	x	y	z	x	y	z
SP (object Set-Point)	S	y	z	x	z	x	y
PP (object Pick-Point)	P	z	x	y	y	z	x
Developing	k1	C	P	P	C	C	P
Elevation Trajectory	k2	S		S		S	
Elevation Point (add)		P	S		P	P	S
					S		

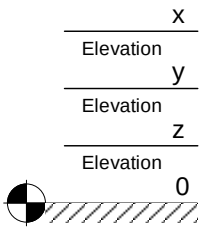

The situation shown at VO 3 configuration has a SP that is higher than the PP, so the algorithm creates two elevations at PP and SP. Figure 3.47 shows the VO 2 configuration where PP is higher, followed by CS and SP elevations.

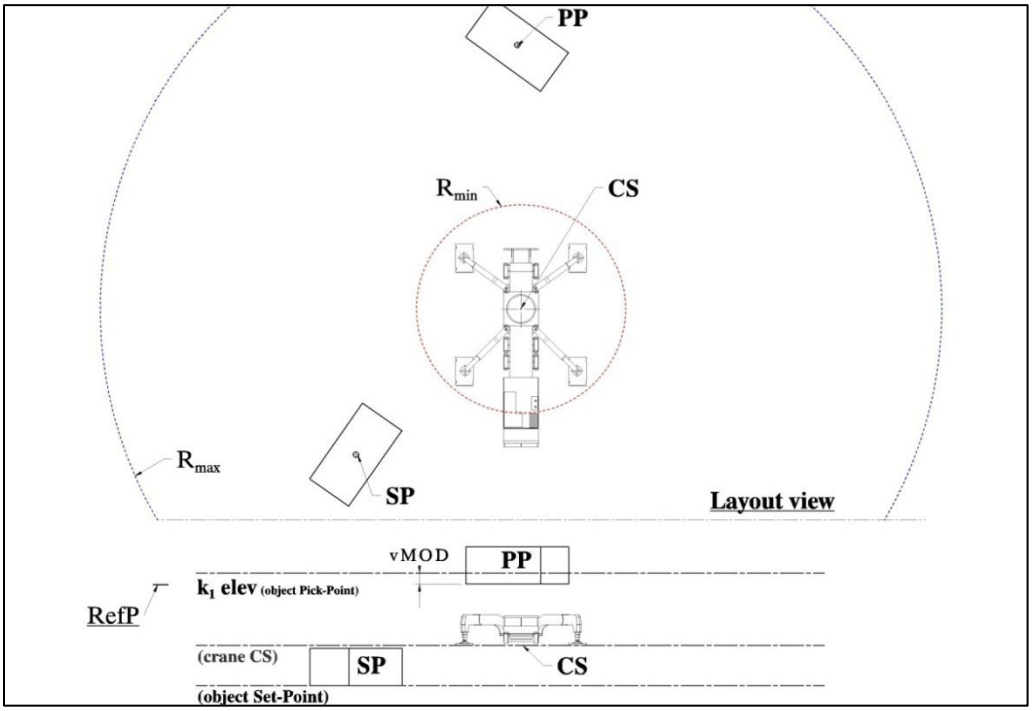

Figure 3.47 k_1 elevation identification (50).

This set-up allows the algorithm to create only the k_1 elevation. This elevation is offset from the PP elevation by vMOD distance (see Figure 3.48). Introducing the vMOD offset allows elimination of potential conflicts with a variety of different transportation platform heights that could be used for delivering objects at construction sites. The VO 2 configuration requires the algorithm to identify the object elevation set-point, which must be stored for the path connection operation. Figure 3.48 shows the task of crane object lift area (COLA) creation.

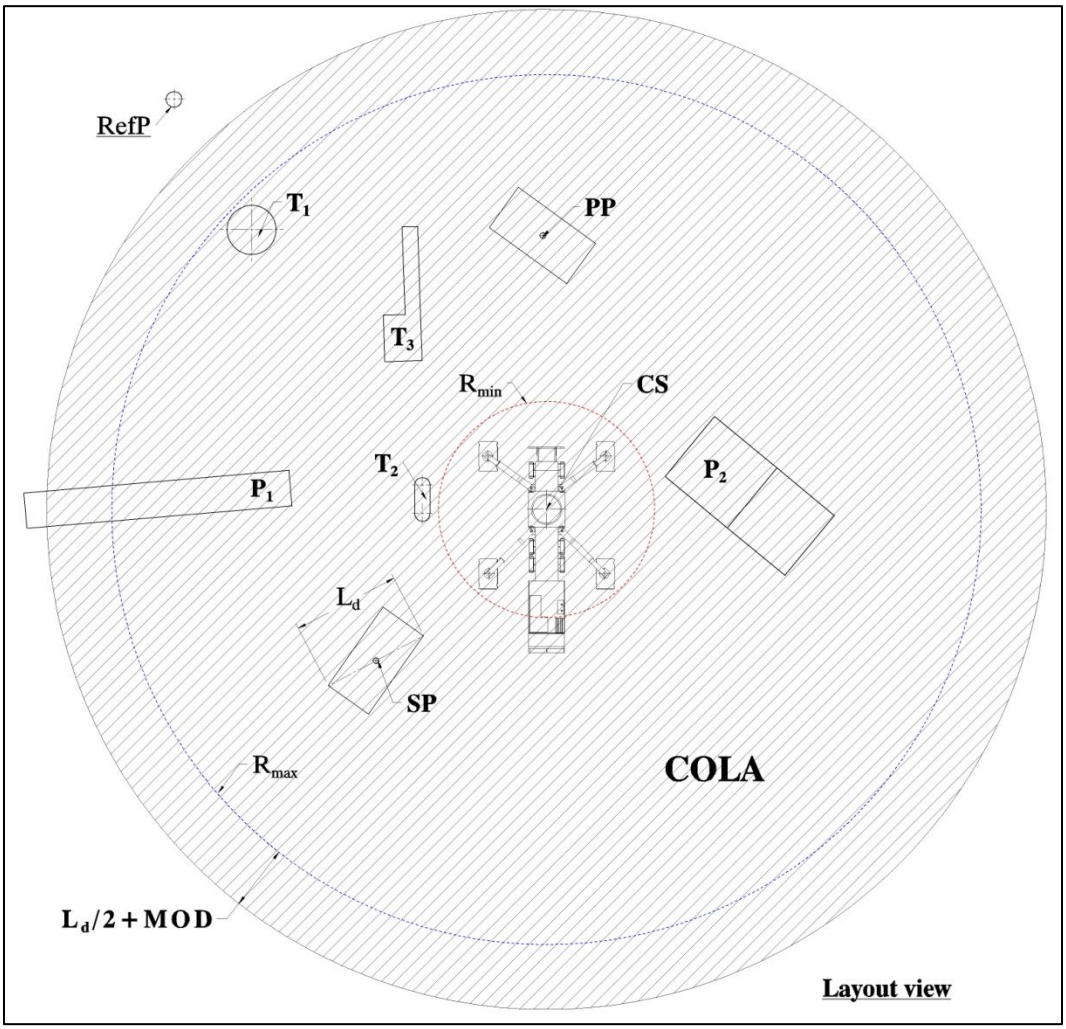

Figure 3.48 Crane object lift area creation (51).

At crane elevation, R_{max} circle is offset by distance $L_d/2$+MOD. L_d is the lifted object diagonal length. Created COLA is checked for obstructions. Obstructions recognized in the defined area are analyzed for their height. Figure 3.49 shows layout and elevation views of recognized obstructions. The already created k_1 elevation establishes a lower

limit for obstructions to be analyzed. This means that obstructions with height lower than k_1 elevation are ignored. Obstruction P_2s' lower portion resides below k_1 (minimum level) elevation and will not be analyzed for elevation development.

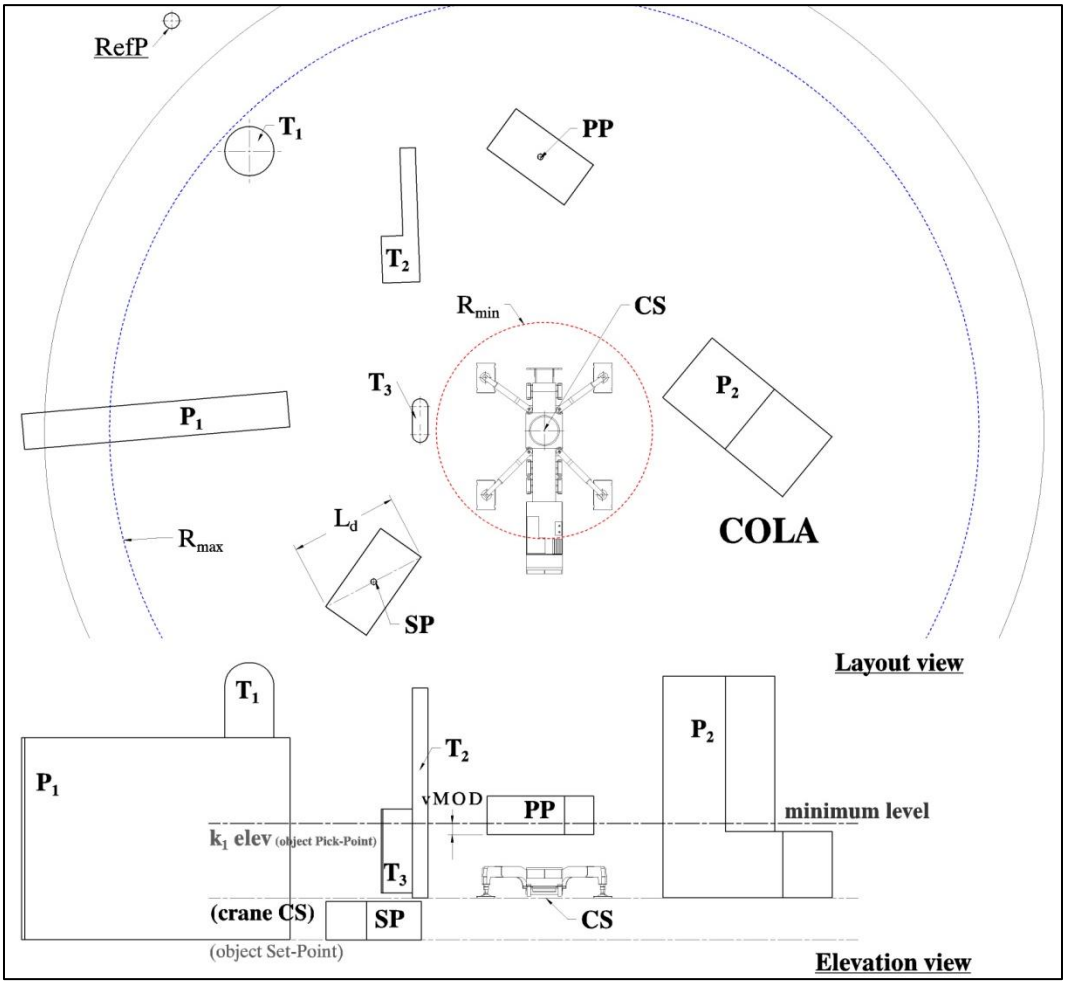

Figure 3.49 Minimum elevation obstructions check (52).

Establishing a minimum level boundary reduces the amount of operations due to the elimination of all obstructions whose height is lower than the minimum established level.

The next task is to focus on the crane configuration rigging arrangement. Evaluating rigging height allows defining the maximum level boundary for elevation calculation. Figure 3.50 shows the crane rigging height calculation and the maximum elevation boundary offset. Absolute crane boom tip height (H_B) is established at R_{min} value. This information is taken directly from the database, which refers to particular crane configuration.

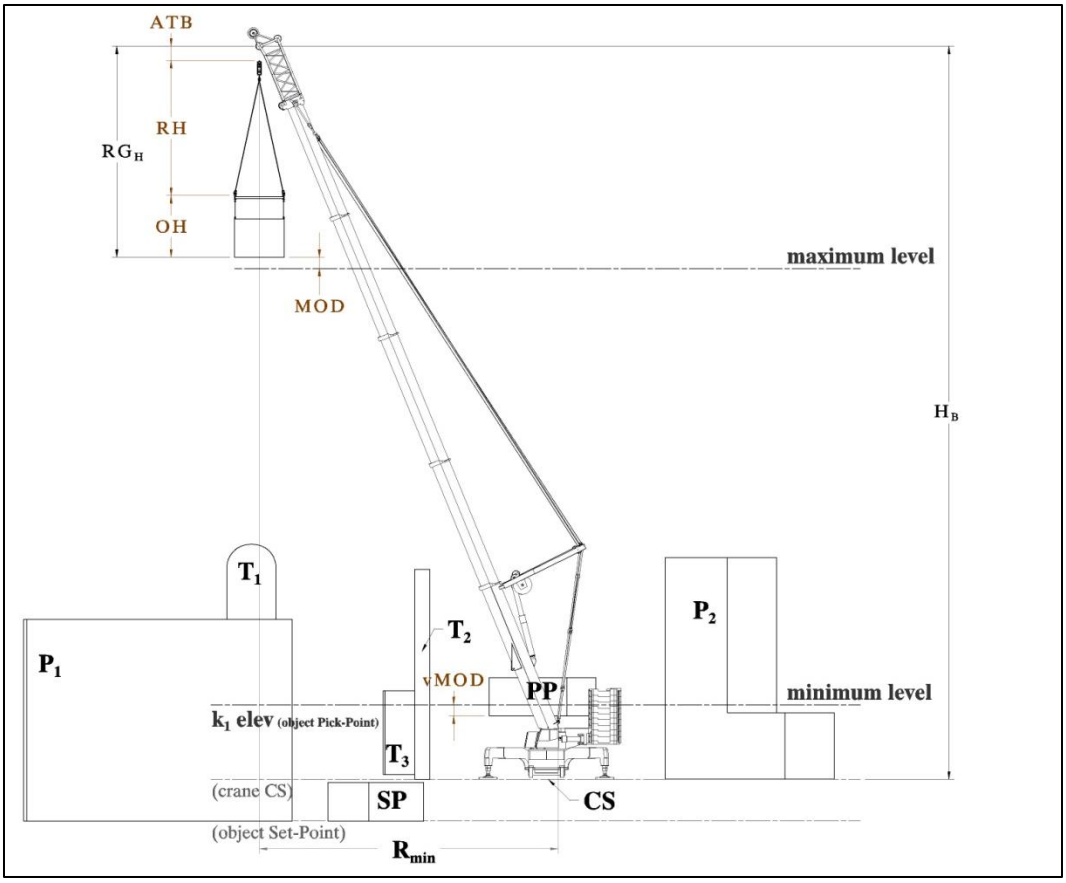

Figure 3.50 Obstruction maximum elevation boundary development (53).

Total rigging height (RG_H) consists of three dimensions: lifted object height (OH), rigging height (RH), and anti-two block (ATB) dimension, which is the minimum distance from the crane tip to crane boom block and is usually secured by an electronic device. This device switches off crane operation when the hook crosses minimum safe distance to the tip sheave. RH dimension depends on the (L) size of the lifted object, where rigging hook points could vary from four (4) to twelve (12) attachments that may have one, two, or three tier slings and bars arrangements. Such differences between rigging hook points is a result of evenly distributing heavy weight from the lifted object to the single main hook block. OH is the value of the lifted object height increased by the length of short slings, which transfer object load to the spreader bar vertically. The ATB dimension is specific for each crane and must be considered during maximum level calculation. Maximum level plane height must satisfy equation 3.39:

$$\boldsymbol{maximum\ level = H_B - RG_H - MOD} \qquad (\mathbf{3.39})$$

Where:

$$RG_H = ATB + RH + OH \quad (3.40)$$

H_B - *maximum boom tip height at R_{min} position*

RG_H - *Total rigging height*

ATB - *anti-two-block dimension*

RH - *rigging height*

OH - *object height*

MOD - *Minimum object distance*

The next task evaluates recognized obstructions by their maximum height (Z) value. Figure 3.51 shows dimensions (h) of each separate obstruction.

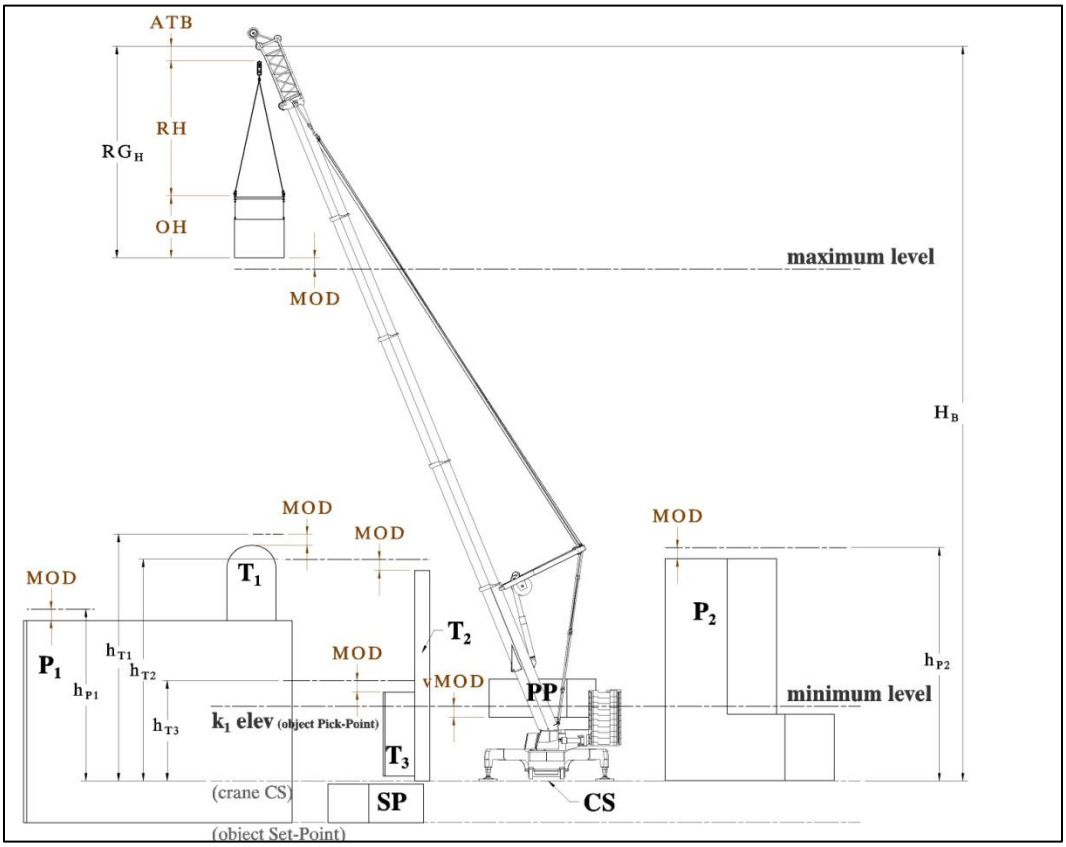

Figure 3.51 Obstruction elevations calculation (54).

Z dimensions are offset by MOD value, and establish obstruction specific elevation (h). All calculated obstruction elevations are subject to defined criteria.

$$k_1 < h_n < maximum\ level \quad (3.41)$$

Where:

k_1 - *minimum level boundary*

h_n - *developed elevation plane*

In this instance the accurate h_n elevation value is either stored if passed or rejected if failed. After the operation is finished the algorithm enters the loop to analyze the next obstruction elevation in a particular region. The final phase groups all elevations and sorts them in ascending order and renames them. Figure 3.46 shows all elevations in their final position.

Phase 6;-Anchored and Floating Obstruction Analysis: The objectives focus on the development of operational elevation areas by identifying involved elevation obstructions and segregating them for anchored (intersecting CST path) or floating (non-intersecting CST path) offset areas. The flowchart arrangement for this phase is shown in Figure 3.52.

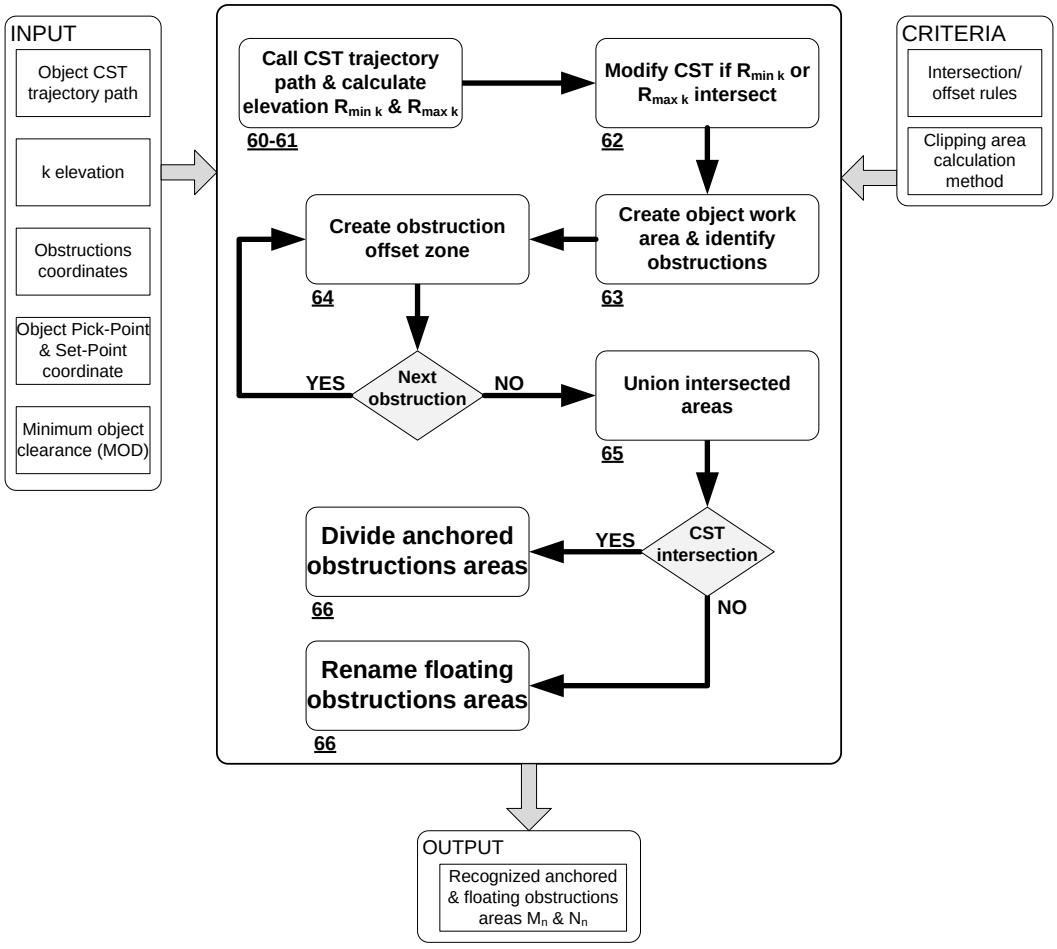

Figure 3.52 Anchored and floating obstruction definition (Ph-6).

The input module contains blocks that represent information needed in the phase. Some data, like obstruction coordinates, object pick-point and set-point x-y-z values, or user-defined MOD distance are taken from the database. But other information, such as object CST path or k elevations are used directly from the previous phases of the algorithm. The main process analysis starts from projecting the CST path at a specific elevation, then calculates elevation boundaries $R_{min\ k}$ and $R_{max\ k}$ and subtracts developed CBR and CSR restricted areas. As a result, a new area is recognized for obstruction interference analysis. Potential obstruction offset intersections are not only separated into anchored or floating areas, but also anchored obstruction offsets are divided into A and B parts that are analyzed separately. Phase criteria establish obstruction intersection offsets rules and the clipping area calculation method. Figure 3.53 shows the phase output result.

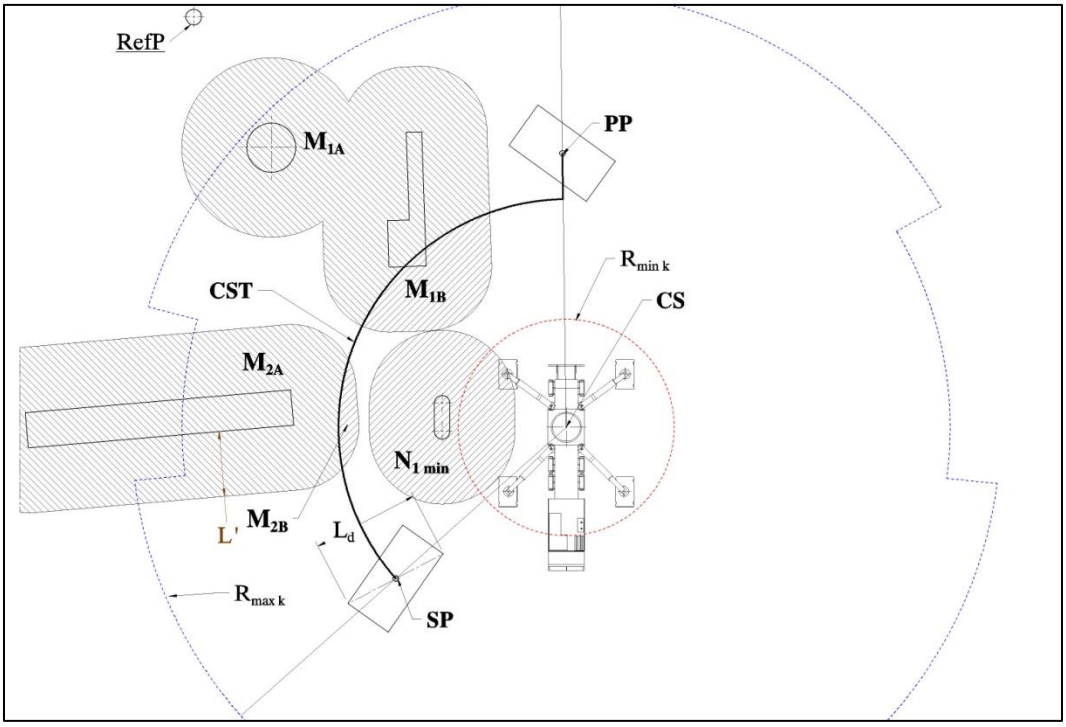

Figure 3.53 Obstruction offsets identification (66).

Intersecting M_1 and M_2 areas (anchored) are divided into A and B parts. The non-intersecting obstruction N_1 (floating) resides in B part area (inside CST path). The presented results cannot be achieved without the proceeding tasks. It starts from calculating elevation $R_{max\ k}$ and $R_{min\ k}$. This must be analyzed due to the different values of maximum and minimum crane boom radiuses at the crane elevation. Figure 3.54

shows the graphical method of elevation $R_{min\ k}$ and $R_{max\ k}$ analysis. The left side shows an elevation view recognizing $R_{min\ k}$ position and the right side evaluates $R_{max\ k}$ circles. The $R_{min\ k}$ value is driven by the load position in relation to the crane boom envelope. In the elevation view on the left (see Figure 3.54), dimension MOD clearance together with the k_n elevation plane defines horizontal object place. Such position establish minimum radius $R_{min\ k}$ dimension of the object. Equation 3.43 shows the calculation method of this parameter.

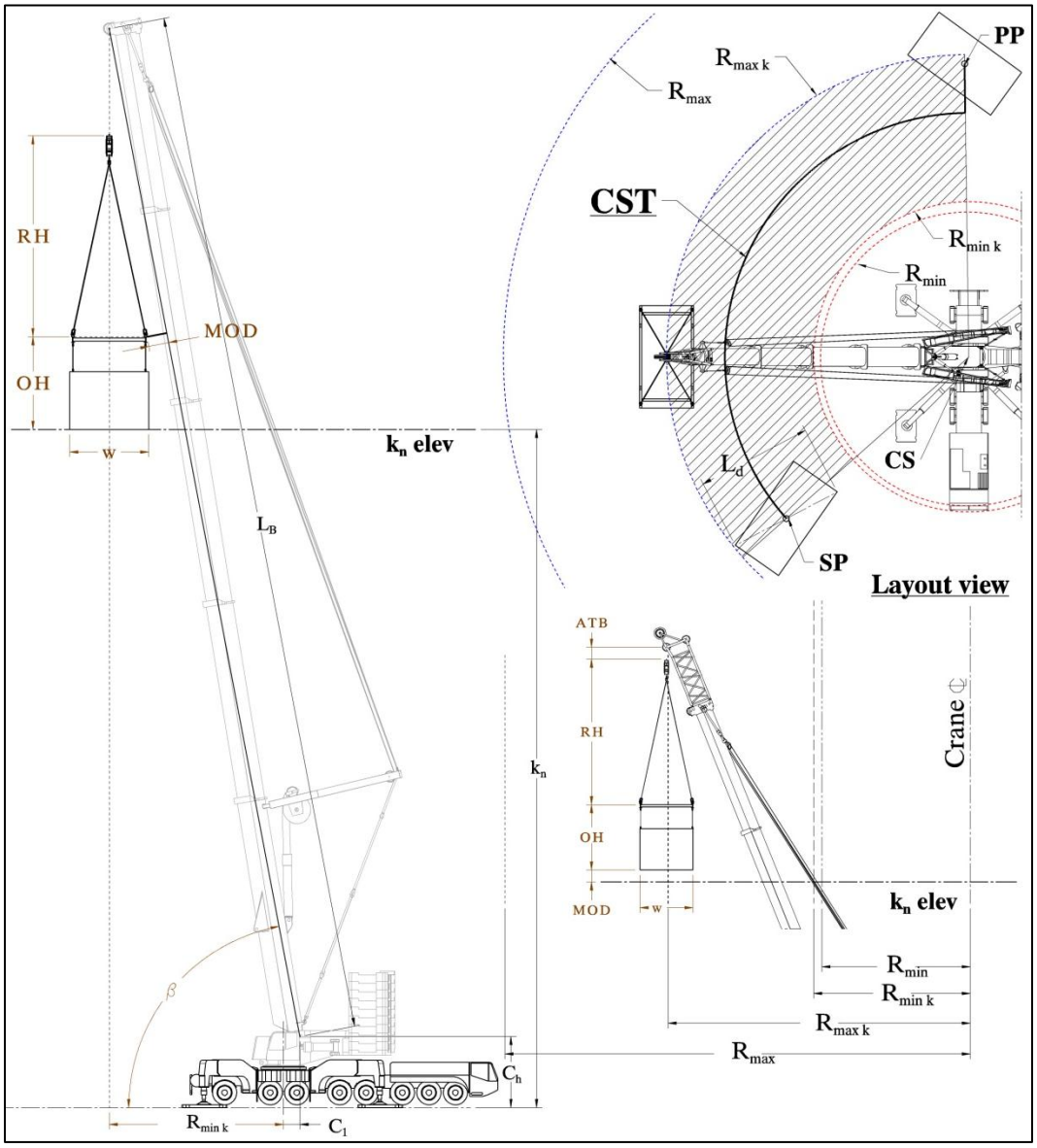

Figure 3.54 $R_{min\ k}$ and $R_{max\ k}$ calculation (60).

In the elevation view on the right side (see Figure 3.54), the $R_{max\ k}$ circle is defined by anchoring the lifted object with vertical bottom MOD offset to k_n elevation and placing boom tip point at ATB distance from the hook position. The resulting crane hook vertical line marks the $R_{max\ k}$ circle radius. Equation 3.42 shows the calculation method of this parameter. The $R_{max\ k}$ circle radius must satisfy equation 3.42:

$$R_{max\,k} = \sqrt{L_B^{\,2} - \left(RG_H + k_n - C_h\right)^2} \qquad (3.42)$$

Where:

L_B - *Boom length (see Figure 3.30)*

RG_H - *Under-the-hook items (see Equation 3.40)*

C_h - *Boom rotation point offset distance (see Figure 3.30)*

k_n - *Elevation vertical dimension (see Figure 3.46)*

$R_{min\ k}$ circle radius must also satisfy equation 3.43:

$$R_{min\,k} = L_1 \cos\beta - C_1 \qquad (3.43)$$

Where:

β - *angle is calculated from polynomial equation*

$$\left(k_n - C_h - MOD\right)\tan\frac{\beta}{2}^{4} - \left(2L_B + w\right)\tan\frac{\beta}{2}^{3} - \left(2MOD\right)\tan\frac{\beta}{2}^{2} + \left(2L_B - w\right)\tan\frac{\beta}{2} - \left(k_n - C_h + w\right) = 0$$

L_B - *Boom length (see Figure 3.30)*

C_1 - *Boom rotation axis offset (see Figure 3.54)*

C_h - *Boom rotation point offset distance (see Figure 3.30)*

k_n - *Elevation vertical dimension (see Figure 3.46)*

OH - *Object height dimension*

w - *Object width dimension*

After both elevation radiuses are defined, CBR and CSR restricted areas are subtracted from the $R_{max\ k}$- $R_{min\ k}$ donut, resulting in a new zone suitable for crane movement. CBR and CSR areas are independent of the elevation restriction and must be subtracted from any developed elevation.

The next task projects the CST path onto the analyzed elevation. Figure 3.55 shows the modified elevation of maximum and minimum boundaries with projected CST path.

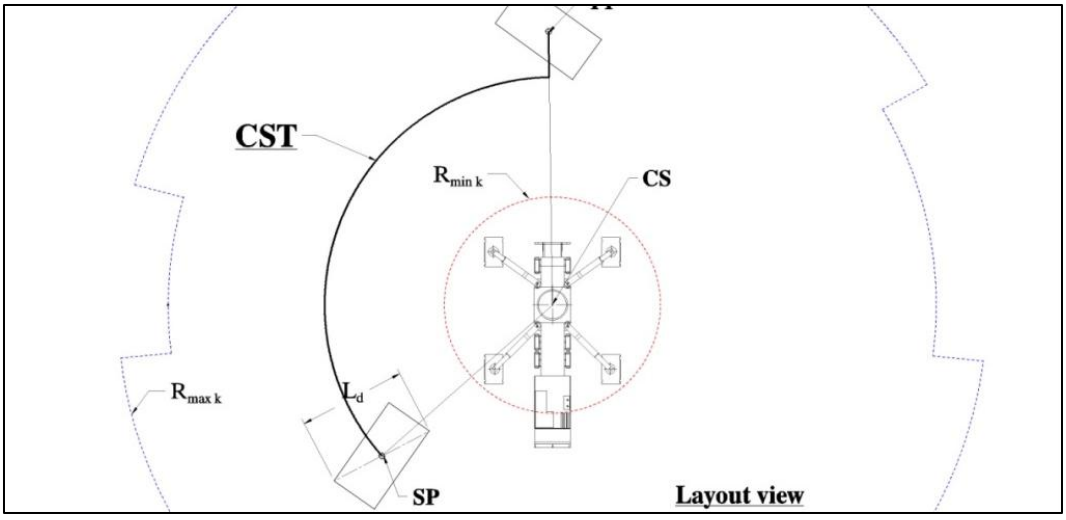

Figure 3.55 CST path elevation projection (61).

Projected CST path is checked for its continuity in the new area between minimum and maximum elevation boundaries. If the calculated boundaries intersect with the projected CST path, the path must be modified to meet maximum or minimum elevation boundary requirements. Figure 3.56 shows a sample when the modified elevation CST path follows inside boundary limits at the section where its continuity is interrupted.

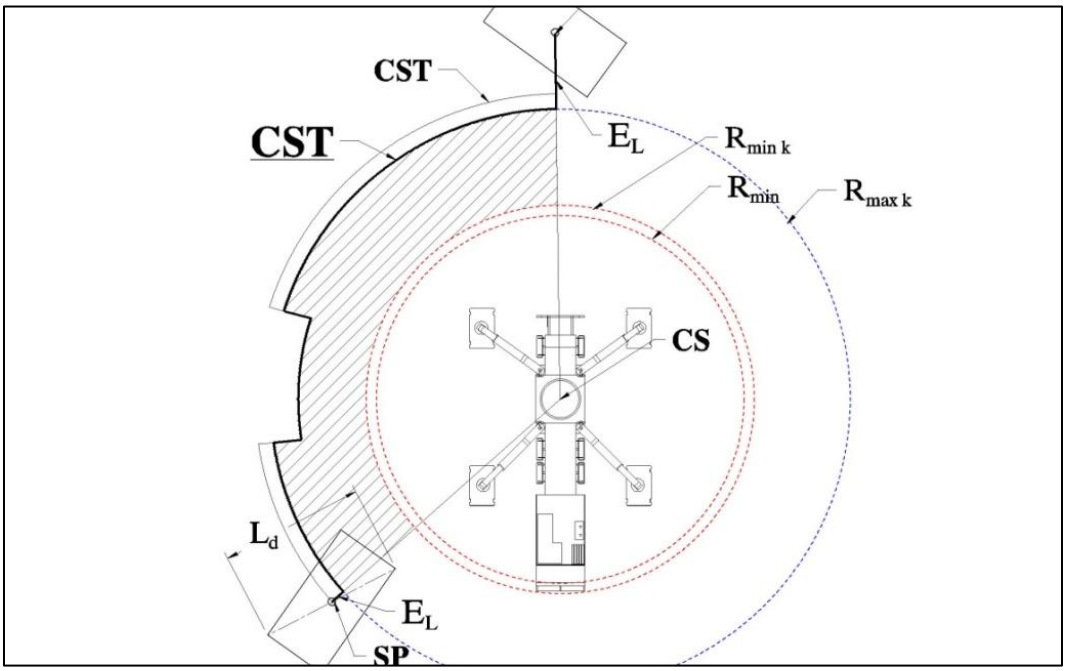

Figure 3.56 Elevation boundary and trajectory path intersection (62).

Usually, the presented scenario in Figure 3.56 will take place at the highest elevation level. However, when the path is offset from its original position, the elevation lines (E_L) are introduced to make continuity from PP to SP points. E_L lines, shown in Figure 3.56, belong to the lower calculated elevations and must be connected to projected end points of the offset path.

The projected path defines an angle direction for the lifted object. It may be of non-reflex or reflex direction. Figure 3.57 show a non-reflex angle CST path and outline an elevation boundary that is enlarged by the offset L' distance. As a result, object work area (Q_k) was created. Calculation of offset L' distance satisfies equation 3.44:

$$L' = \frac{L_d}{2} + MOD \qquad (3.44)$$

Where;

L_d – *Object diagonal distance*

MOD – *Minimum clearance distance (user define)*

In the developed Q_k area, the algorithm checks for elevation obstructions, and when it finds one creates obstruction offsets on the L' dimension.

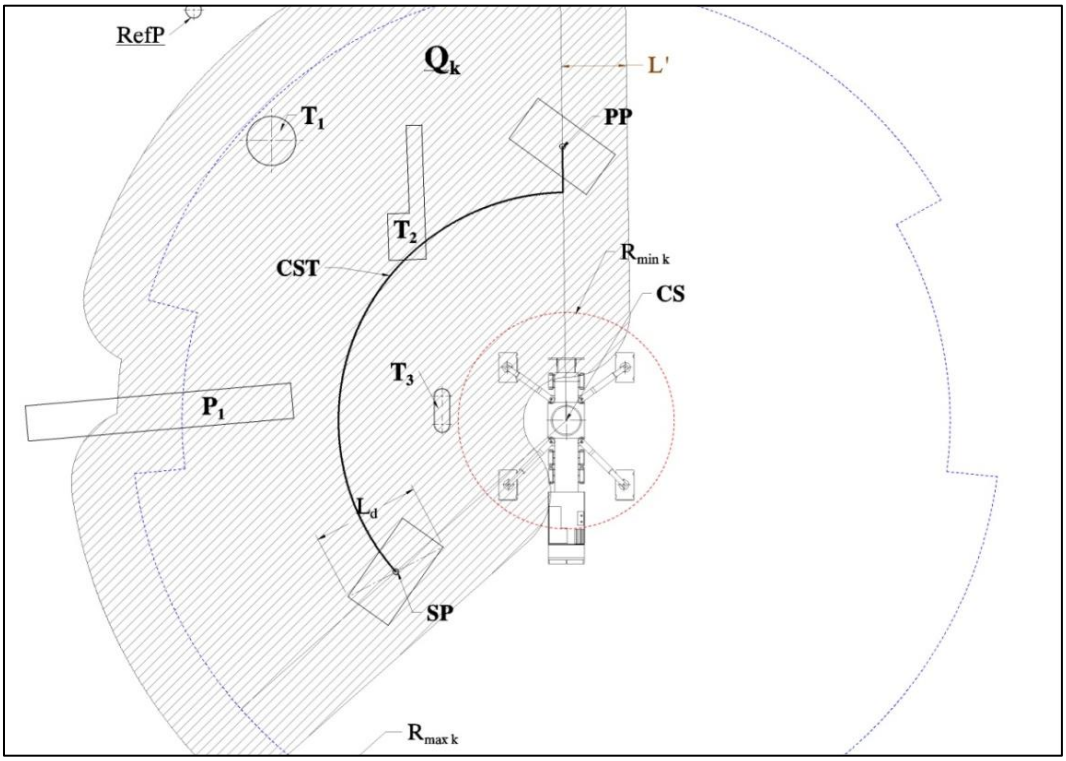

Figure 3.57 Object work area Q_k and obstructions definition (63).

The obstruction's boundaries are offset by the L' value, in order to create maximum clearance for lifted object. Figure 3.58 shows the located obstructions' offset zones (OZ_n) in Q_k area.

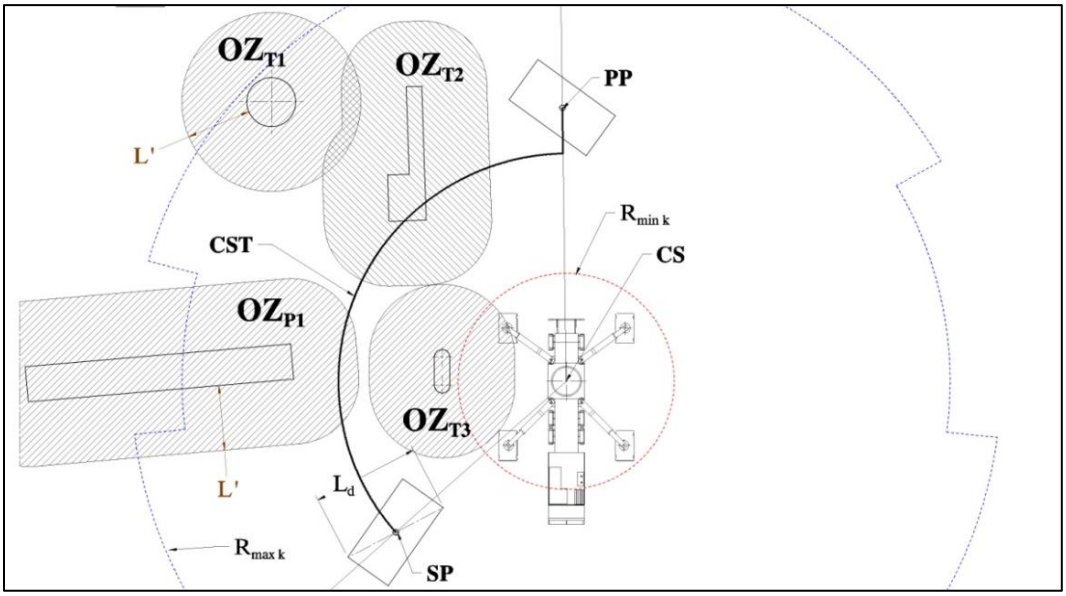

Figure 3.58 Obstruction offset zones (64).

After all obstruction offsets are created, the algorithm recognizes obstructions that are intersecting and joins them. Figure 3.59 shows the joined area of OU_1 for obstructions OZ_{T1} and OZ_{T2}.

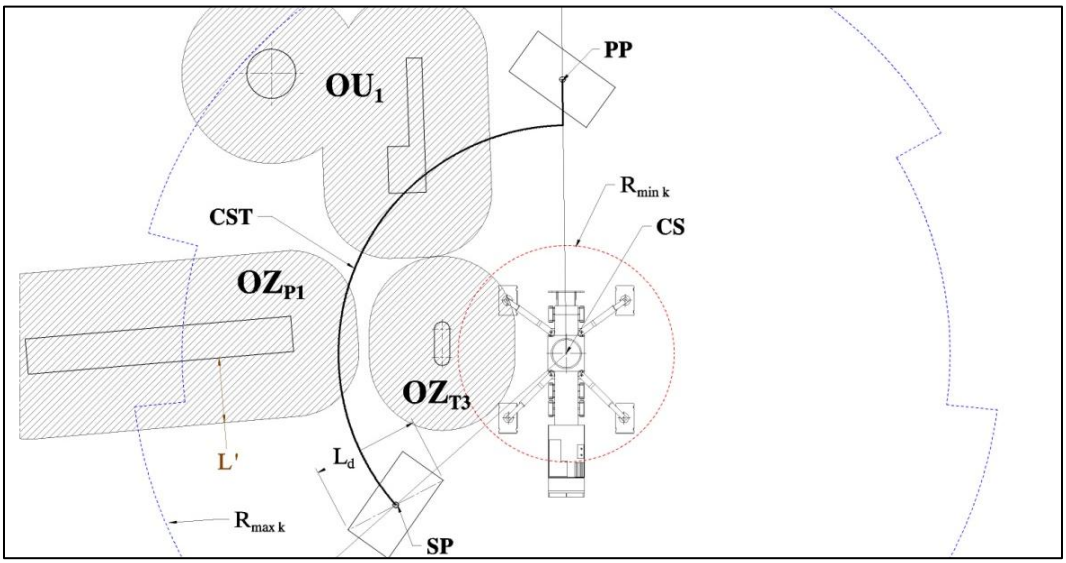

Figure 3.59 Obstruction offsets' intersection union (65)

The last task recognizes offset obstructions that are intersecting the CST path, divides them into A and B sections, and renames them as M_{nA} and M_{nB} (anchored obstructions). Obstruction offsets that are not in contact with the CST path are renamed to N_{nA} and N_{nB} (floating obstruction). Figure 3.53 shows the anchored and floating obstruction offsets development.

Phase 7;-Elevation Trajectory Path Development: The objective is to modify the CST path in reference to recognized obstructions and record full or partial object trajectory paths for further analysis. Figure 3.60 shows a detailed phase flowchart.

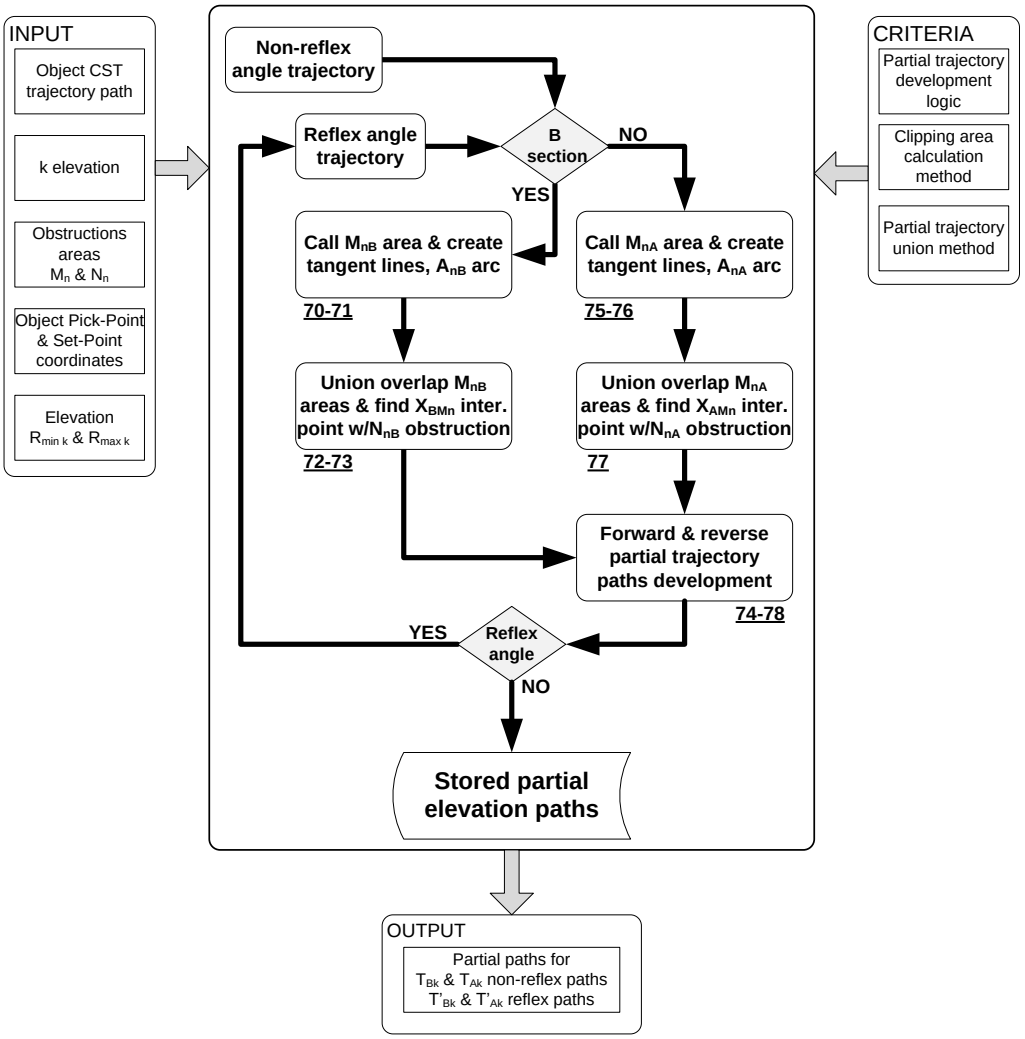

Figure 3.60 Elevation trajectory path development flowchart (Ph 7).

Input data, which is necessary in the phase's main process, requires information processed from the previous phases. CST object trajectory modified path, anchored and

floating obstruction offsets, elevation boundaries, and object pick-point (PP) and set-point (SP) coordinates are examples of information required for the main process. The main process starts with the identification of the non-reflex angle CST path and the analysis of its trajectory at the section B. It requires M_{nB} areas for creating tangent lines AT_{BMn} and tangent circles A_{nB}. If the algorithm analyzes section A of the non-reflex angle CST path, operations similar to section B follow, but the algorithm creates tangent lines and circles on the opposite side of the CST path. Created tangent circles and lines specify boundaries for the area that may overlap and, in this situation; the union areas operation take place. Next, tangent point X_{BMn} between M_{nB} area and A_{nB} circle is recognized and stored. If floating obstruction N_{nB} interferes with modified M_{nB} area at A_{nB} arc, intersection point Y_{BMn} is created either on the left or right side from tangent point X_{BMn}. From the intersection Y_{BMn} point, a set of radial-line and tangent-arc is designed to meet AT_{BMn} lines. If Y_{BMn} point is closer to the object SP than the X_{BMn} point, the designed set of radial-line and tangent-arc is called forward trajectory path FA_{nB}. If it is opposite of the radial-line and tangent-arc, it is called reverse trajectory path RA_{nB}. Such recognition is critical since the RA_{nB} path requires additional operations of reverse point orders implementation after meeting AT_{BMn} line. Once the algorithm finishes checking elevations, T_{Bk}, T_{Ak}, T'_{Bk} and T'_{Ak} paths are stored. They represent the possible object movement in two sections from the non-reflex angle and the two sections in reflex angle analysis. Figure 3.61 shows the area M_{nB} tangent point development operation.

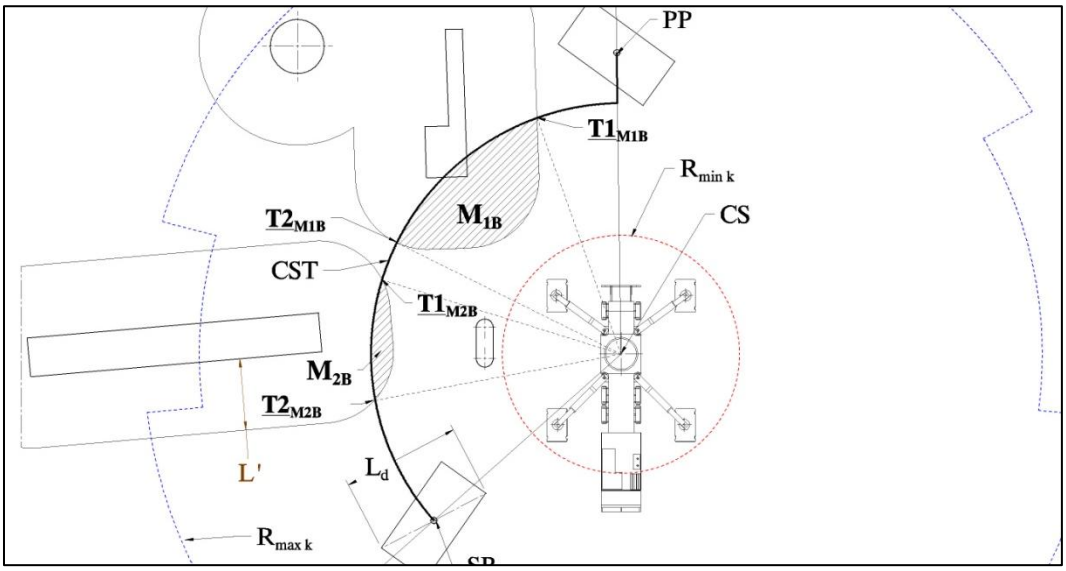

Figure 3.61 Area M_{nB} tangent point development (70).

Tangent points for area M_{1B} are identified as $T1_{M1B}$ and $T2_{M1B}$. The points' sequence allows placing first intersection point of modifying path always closer to object PP point. Then creating tangent arc A_{1B} omits the obstruction in direction B. Figure 3.62 shows the modified CST path in relation to anchored obstruction offset.

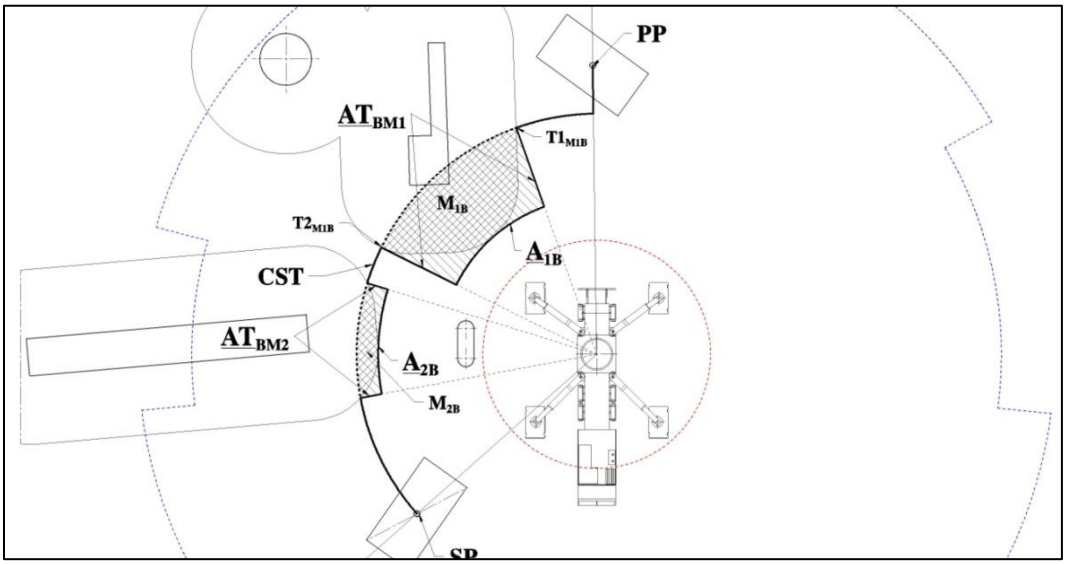

Figure 3.62 Anchored obstructions and modified CST path (71).

Developed CST path intersection points serve as breaks to the original CST path, as well as the start and end points for the modified trajectory. The tandem of tangent arc A_{1B} and two radial lines, AT_{BM1}, diverts paths in the analyzed section around the identified obstruction. The tandem also creates an area that is helpful in the situation, presented in Figure 3.63, where two separate tandems intersect.

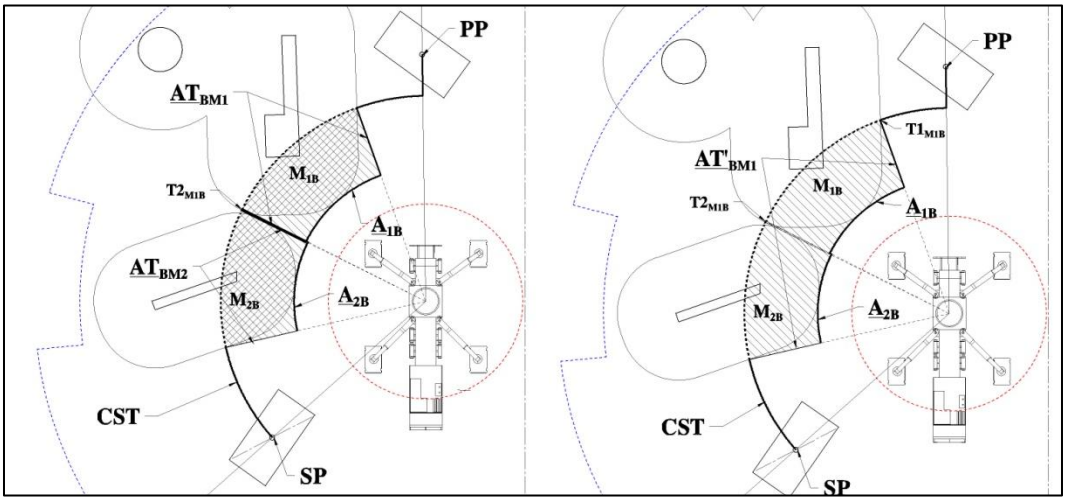

Figure 3.63 M_{nB} areas intersection union (72).

In such a situation a joint operation is introduced and two separate arcs, A_{1B} and A_{2B}, of a joint area are stored for further operations. Such a solution eliminates the problem when two arcs have different radiuses. Figure 3.64 shows tangent points X_{BM1} and X_{BM2} development for A_{1B} and A_{2B} arcs, respectively. Also it shows the floating obstruction offset interference.

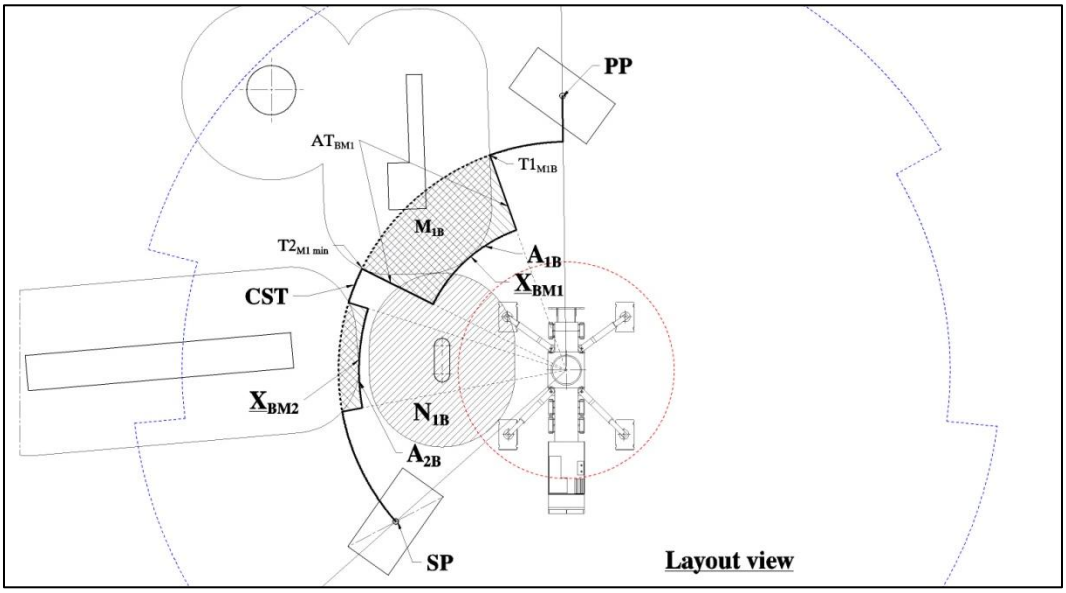

Figure 3.64 Floating obstruction offset intersection and A_{nB} tangent points (73).

The next task of the algorithm analyzes a situation where the floating obstruction offset intersects a diverted path. Two possible intersections will be analyzed in the following paragraphs. Figure 3.64 shows a situation of opposite corners of X_{BMn} point analysis. Figure 3.65 shows a detailed view of the intersection. The intersection area creates point Y_{BM1} within arc A_{1B}. This point is the starting point of the sequential line-arc path creation. Figure 3.65 shows a zoomed spot area of the sequential path. Point Y_{BM1} is used to create a line to the CS center and this line extends to intersect the original M_{1B} offset boundary. From that creation the intersection arc, with the center of the CS point, intersects the floating obstruction N_{1B} boundary. Then the line to the CS point is extended to the original M_{1B} offset. Such oscillating movements finally reach the AT_{BM1} line to end the repetitive operation. Because intersection point Y_{BM1} is located between X_{BM1} and object SP, the developed sequential path is called forward partial trajectory FA_{1B} and is stored for further calculation. The FA_{nB} path can be simple, only requiring a few oscillating movements to reach the AT_{BMn} line, if a floating obstruction offset N_{nB} is at a

larger distance from M_{nB} but still intersects arc A_{1B}. A complicated situation is presented in Figure 3.65 which displays a close position of a floating obstruction offset N_{nB} to the anchored obstruction offset M_{nB}.

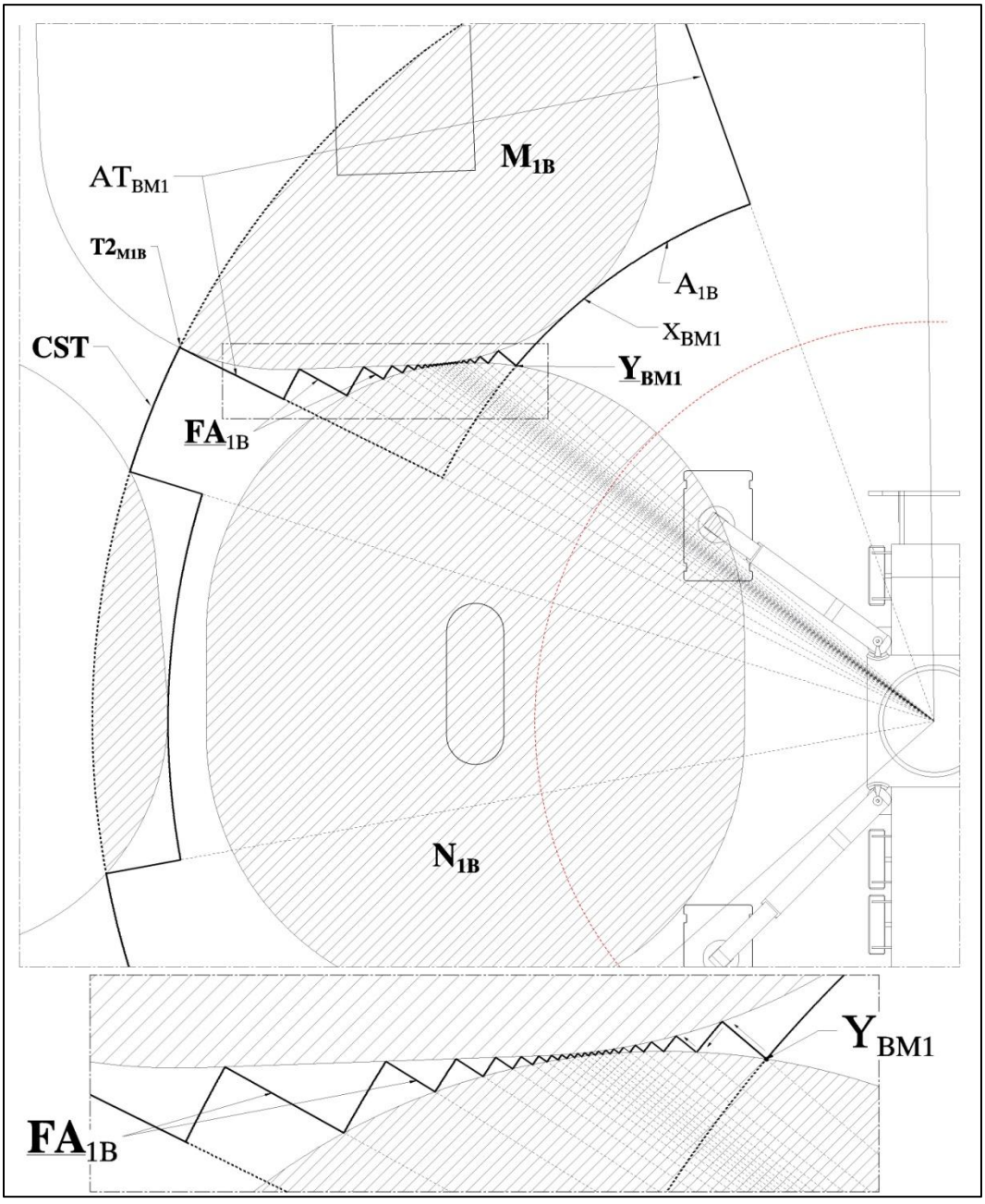

Figure 3.65 Forward path development operation (74.1)

When a floating obstruction offset intersects a developed diverted path between X_{BMn} and PP, the operation step is similar as presented above. However, an additional task must be

introduced. Figure 3.66 shows reverse trajectory path development. As point Y_{BM1} is recognized, a line to the CS point is created and extended to intersect with the M_{1B} obstruction offset. Then an arc with the CS center point is created to intersect the AT_{BM1} line or N_{2B} floating obstruction offset boundary. This represents a reverse sequential trajectory path RA_{1B} development.

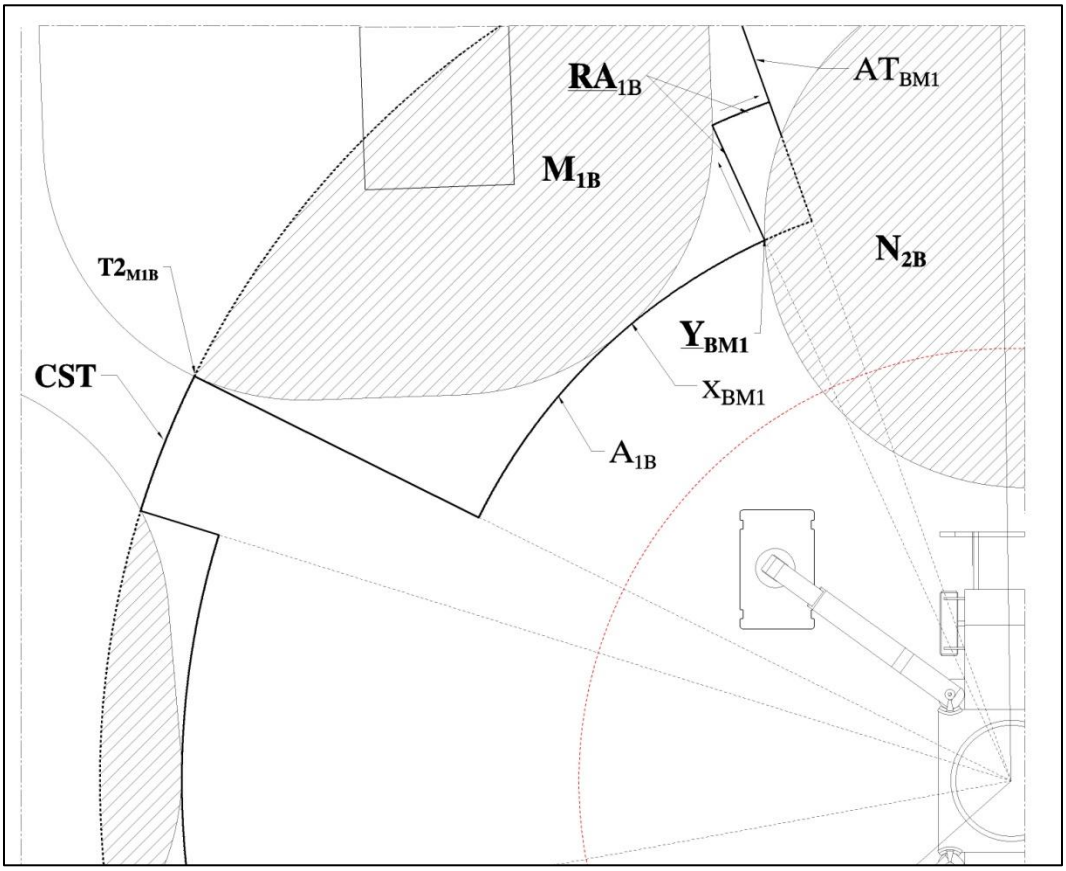

Figure 3.66 Reverse path development operation (74.2).

Before the reverse sequential trajectory path is stored for further operation, a reverse action must be implemented to induce the right direction point sequence from PP to SP. Figure 3.67 shows a preparation operation of a modified non-reflex angle CST path toward outside (A) direction. Obstruction offset M_{1A} is used to create tangent lines from the CS point and intersection points $T1_{M1A}$ and $T2_{M1A}$. The operation of creating a path occurs in a similar fashion as to section B (inside). Created arc A_{1A} is tangent to the area as shown in Figure 3.67. Connected and extended tangent lines AT_{AM1} remodel the area M_{1A} for further analysis. Because created arc A_{1A} and partial AT_{AM1} tangent lines are outside the developed $R_{max\ k}$ elevation boundary, the entire outside section is cut out from

created trajectory path. In this situation a partial trajectory is created, where its ends are located at the $R_{max\,k}$ elevation boundary (see Figure 3.67).

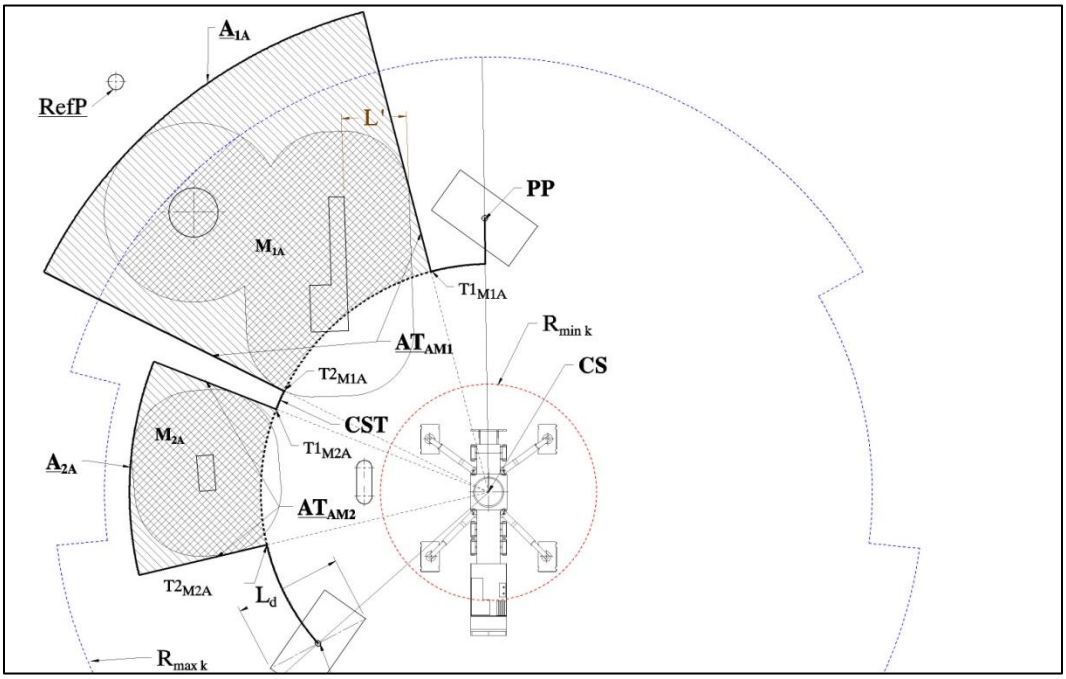

Figure 3.67 Area M_{nA} tangent points and path development (75).

Figure 3.68 shows the modified CST trajectory path.

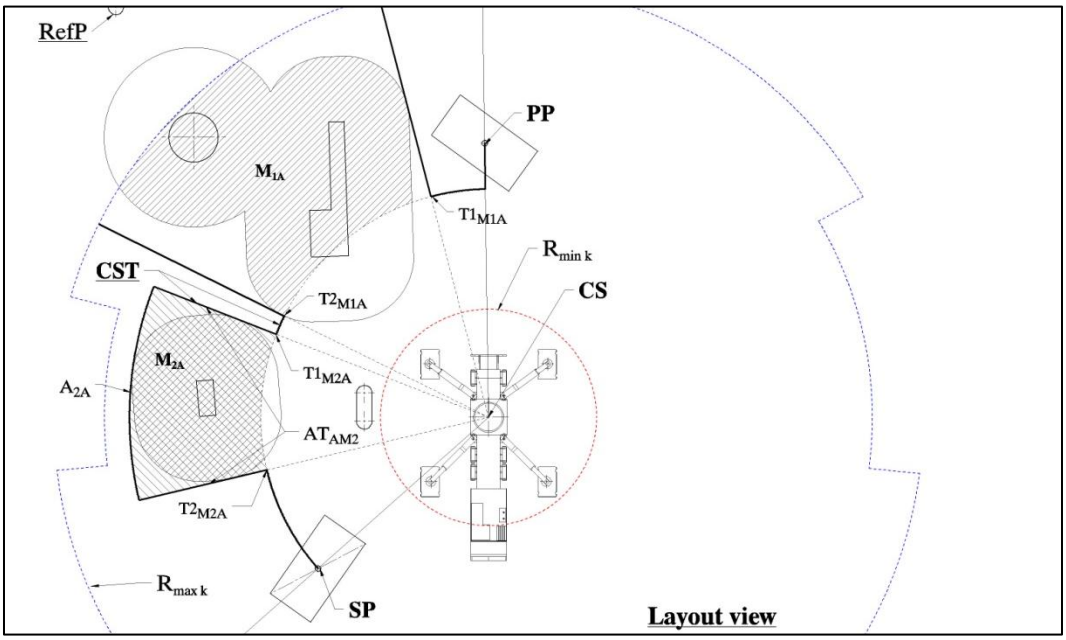

Figure 3.68 Modified CST path by M_{nA} area (76).

The CST path between two tangent lines does not have continuity but is still stored in the algorithm database and is called CST partial trajectory path. Figure 3.69 shows a scenario where a developed M_{2A} area is intersected by floating obstruction offset N_{4A}.

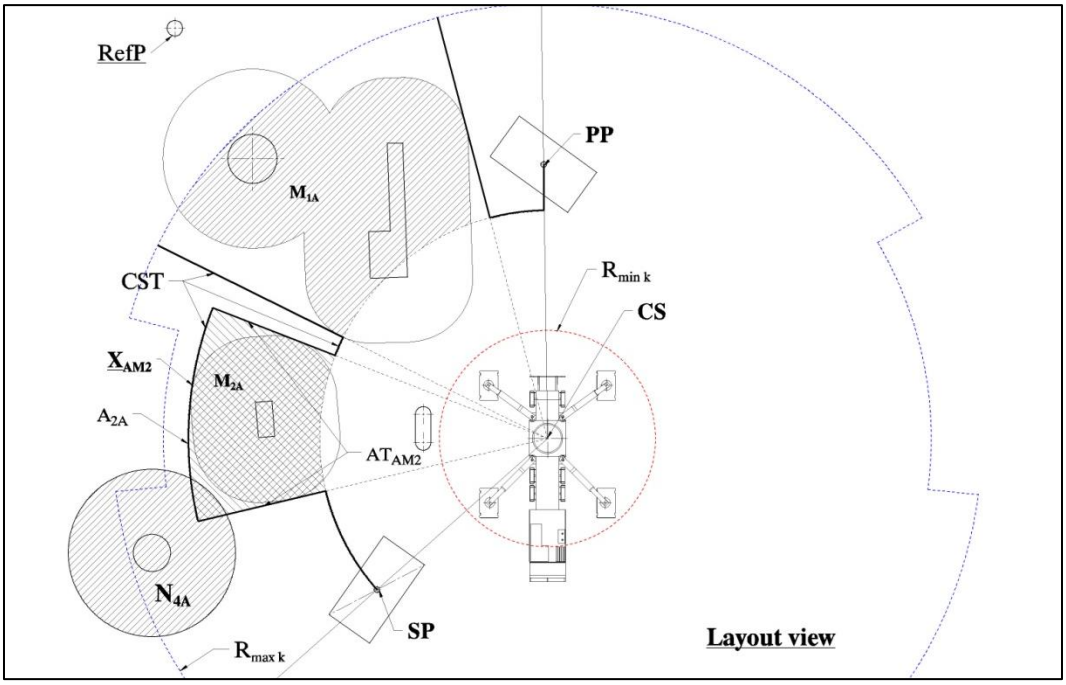

Figure 3.69 N_{4A} boundary and M_{1A} area intersection (77).

Procedures for developing forward or reverse trajectory are similarly presented for section B. Created tangent point X_{AM2} defines the site of the involved intersection area and identifies either reverse or forward partial trajectory. Figure 3.70 shows such a case.

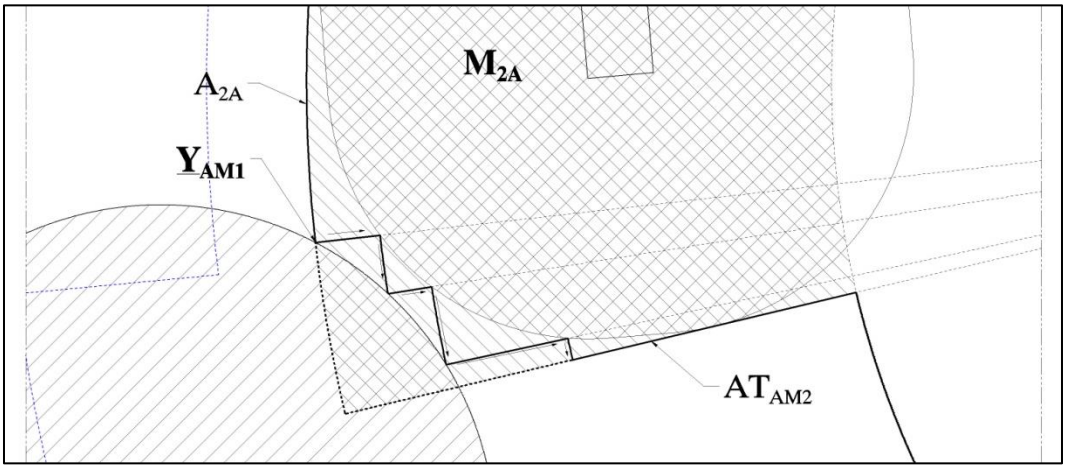

Figure 3.70 Forward path development zoomed area (78.1).

Phase six and phase seven operations are performed on the same elevation. After the last task of phase seven is complete, the algorithm enters a loop to check another recognized elevation. Table 3.3 shows a sample of a developed trajectory path matrix.

Table 3.3 Possible path identification.

	Non-reflex angle		Reflex angle	
elev	A-sec	B-sec	A-sec	B-sec
k1	P	F	P	F
k2	P	F	P	F
k3	F	F	P	F
k4	F	F	P	F
k5	F	F	F	F
k6	F	F	F	F

P-partial trajectory
F-full (connected) trajectory

Phase 8;-Object Trajectory Path Optimization: The objectives are to develop connection elevation lines, including object pick-point or/and set-point connection, assign weight values connections, and develop a routine to optimize trajectory path. Figure 3.71 shows the phase flowchart. The input box includes object full and partial trajectory paths for each analyzed elevation, and object pick-point and set-point coordinates. The main process starts from recognizing each path at its specific elevation and direction points. Direction points are projected up and down from each elevation except first (when projected up) and last (when projected only down). After the point is projected onto a lower or higher elevation, it is checked for intersection with residing elevation path. If the point intersects the path, it acts as a breaking spot and divides the path line or path curve into two separate pieces. Where the projected point lands in an empty space it is immediately rejected and deleted. An accepted projected point is then connected to its source point creating an elevation path connection line. After all elevation connection lines are recognized, the algorithm checks the vertical order (VO) rule to identify if both PP and SP are connected to the elevation trajectory web. Having a web of different connections between the partial or full elevation trajectories, the next task recognizes the variety of line segments and their connections to assign weight values. After lines and web connections are weighted, the algorithm routine checks the least weight path between PP and SP. The optimized object trajectory final path is stored for other purposes such as creating animation in the visualization section. Process operations are subject to criteria rules, which define weight classification (different values for different connections) and optimization method routine. The output box contains the optimized

final path, which may include several different lines, curves, and points connected sequentially from pick-point to set-point.

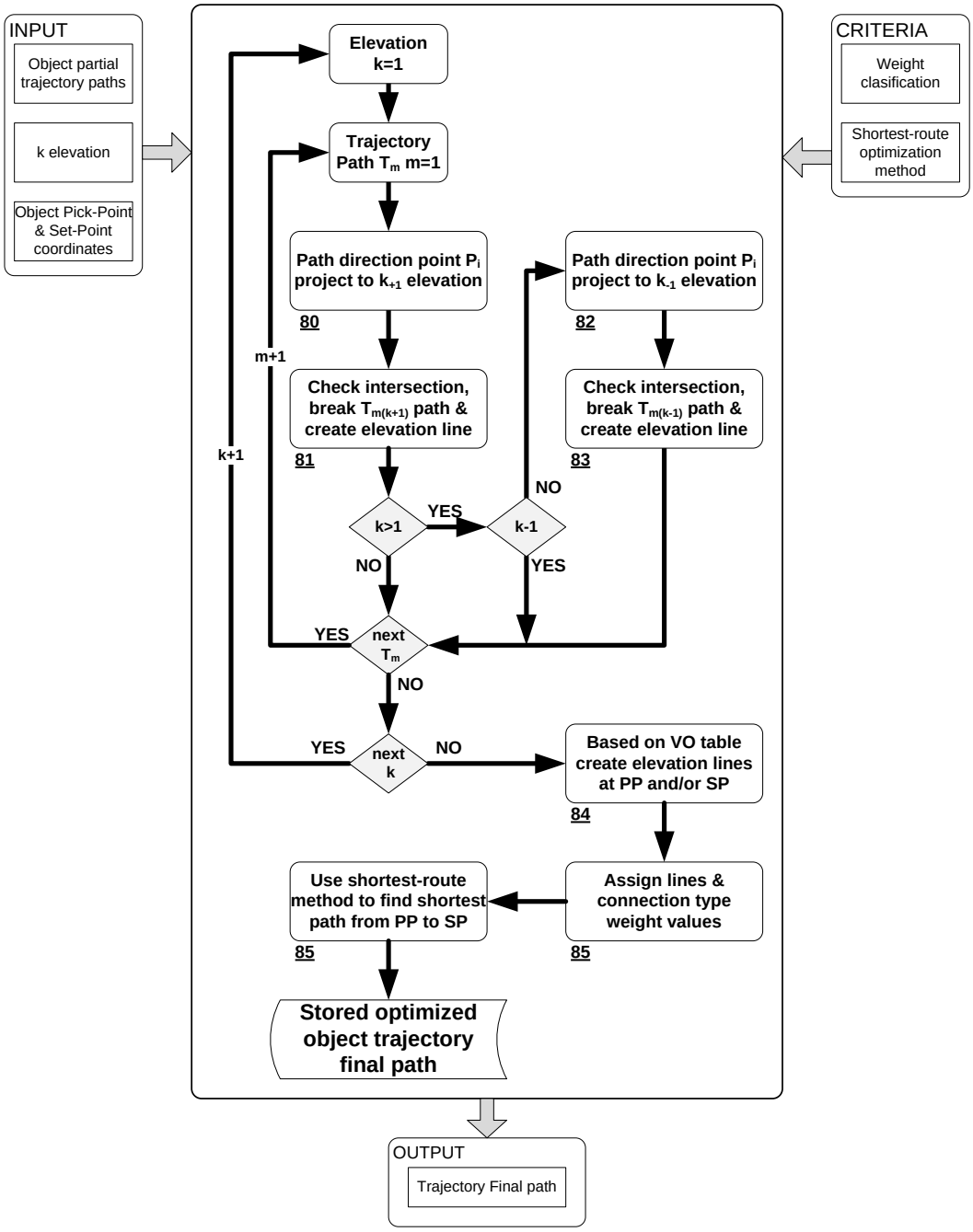

Figure 3.71 Object trajectory path optimization flowchart (Ph-8).

The first task of the phase recognizes the elevation and trajectory path for direction point analysis. Figure 3.72 show the direction point projection operation. From the lower

elevation the direction point is projected onto a higher elevation to recognize its membership with the upper trajectory path.

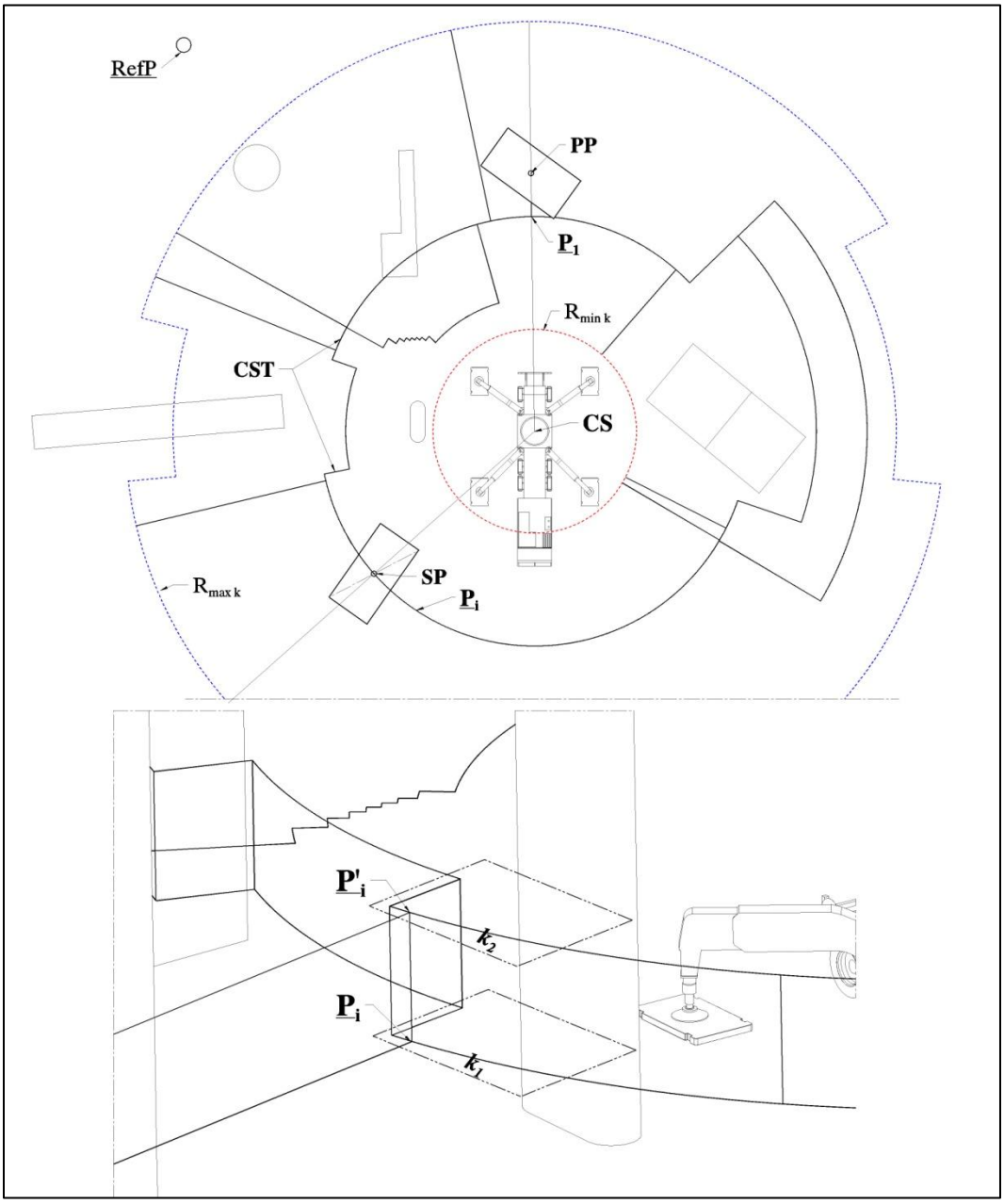

Figure 3.72 Direction points vertical-up projection (80).

If membership is confirmed, the projection point P'_i is checked to make sure that the upper path does not have a direction point at that position. If the projection point confirms membership and there is no point duplicity, it acts as a breaking point and divides the path at its projected coordinates. Immediately after that operation, the

direction point sequence of the upper path is updated to include the next projected point to maintain elevation line continuity, and vertical elevation is created. In the case when duplicity is confirmed (projected point has the same coordinates as existing point at projected elevation), the projected point is not created but a vertical elevation line is generated. When a projected point does not confirm membership with the upper path, the projected point is deleted and a vertical elevation line is not created. This operation is performed until all direction points of the lower elevation are analyzed. The next task evaluates operations in the opposite direction. Figure 3.73 shows elevation direction points with projection down operation.

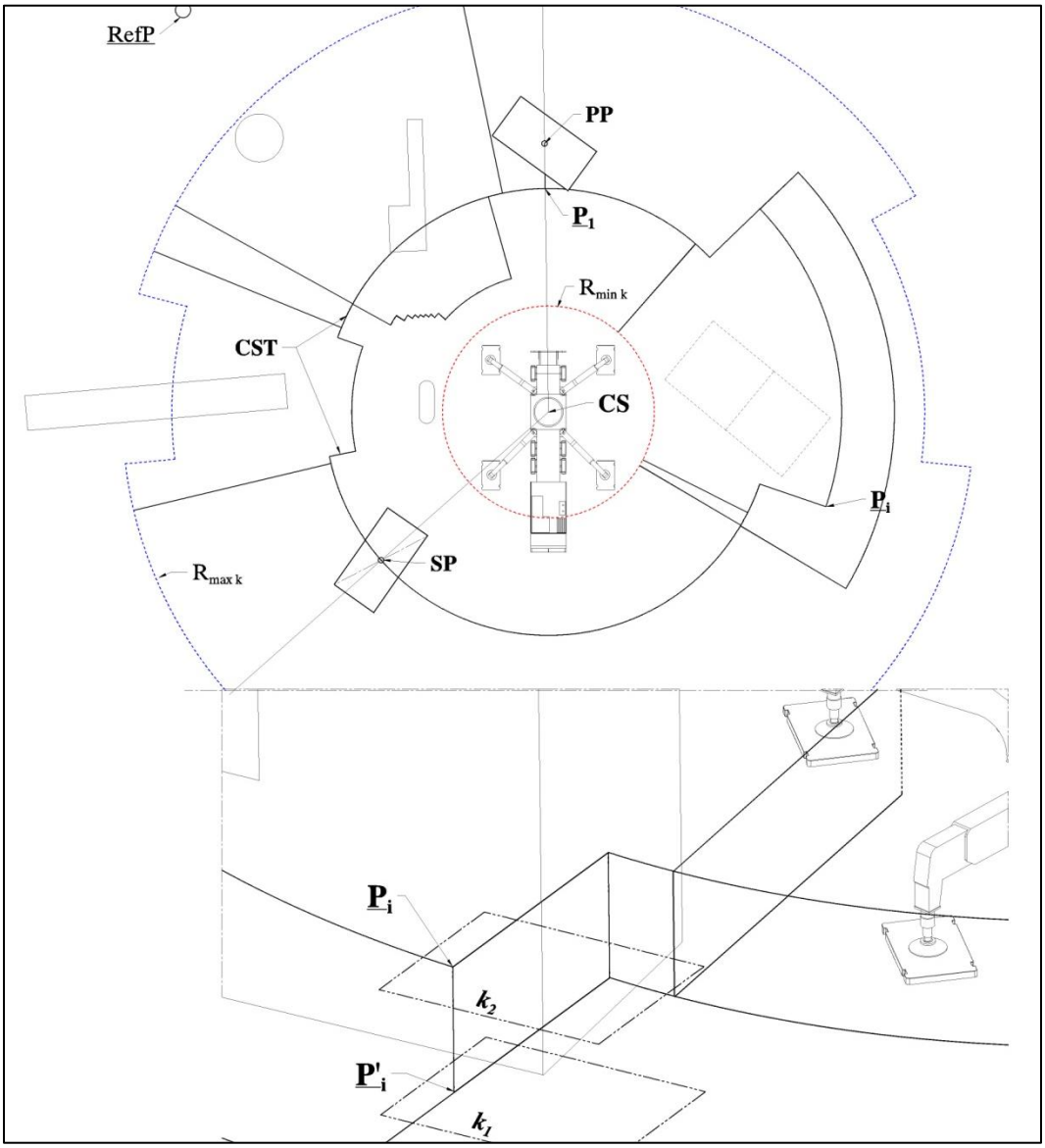

Figure 3.73 Direction points vertical-down projection (81).

Projection down direction is similar to translation and procedures follow the same pattern with divisions of elevation paths. Also, when points are duplicated they are erased and eliminated from further operations. The next task of the algorithm checks vertical order (VO) rule to establish web points connections (PP and SP). In the presented sample SP must be connected vertically to the web. Figure 3.74 shows creation of elevation lines between object set-point and web grid.

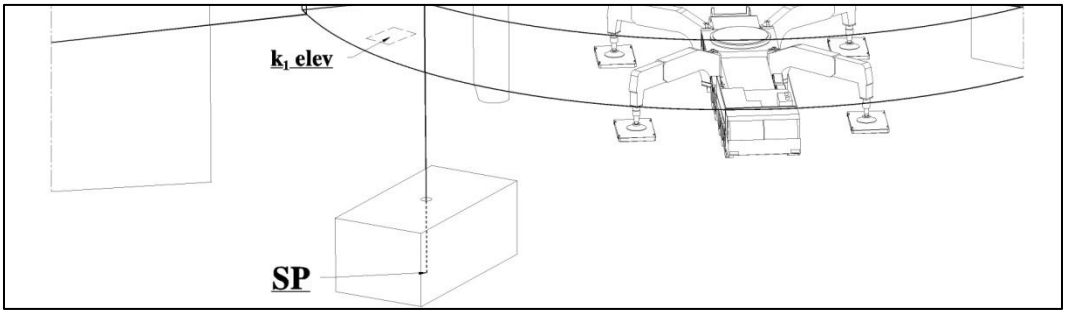

Figure 3.74 Object set-point to web grid connection (82).

Now, when object PP and SP are connected with the 3D grid, the next task assigns weight values to lines and connections to grade preferable movements. Figure 3.75 shows weight values assigned to lines and elevations connections.

Speed	Code				
straight - horizontal	S	55	ft/min	660.00	in/min
curve - horizontal	C	164	ft/min	1968.00	in/min
vertical up	Vu	100	ft/min	1200.00	in/min
vertical down	Vd	100	ft/min	1200.00	in/min

Movement Change Time Penalty

S-C	0.25	min
C-S	0.25	min
S-Vu	0.25	min
Vu-S	0.25	min
S-Vu	0.25	min
Vd-S	0.25	min
C-Vu	0.25	min
Vu-C	0.25	min
C-Vd	0.25	min
Vd-C	0.25	min

Height Penalty

k_1-elevation	no penalty
k-elevations	add 10% to each elevation

Figure 3.75 Algorithm lines and connections weight criteria.

At each elevation points are in sequence of ascending order from projected PP to projected SP. Elevation lines and curves are one directional vectors, but vertical elevation connection lines are bi-directional vectors. This clarifies algorithm moving restrictions. A penalty weight system was developed based on expert knowledge. Figure 3.76 shows full trajectory paths web.

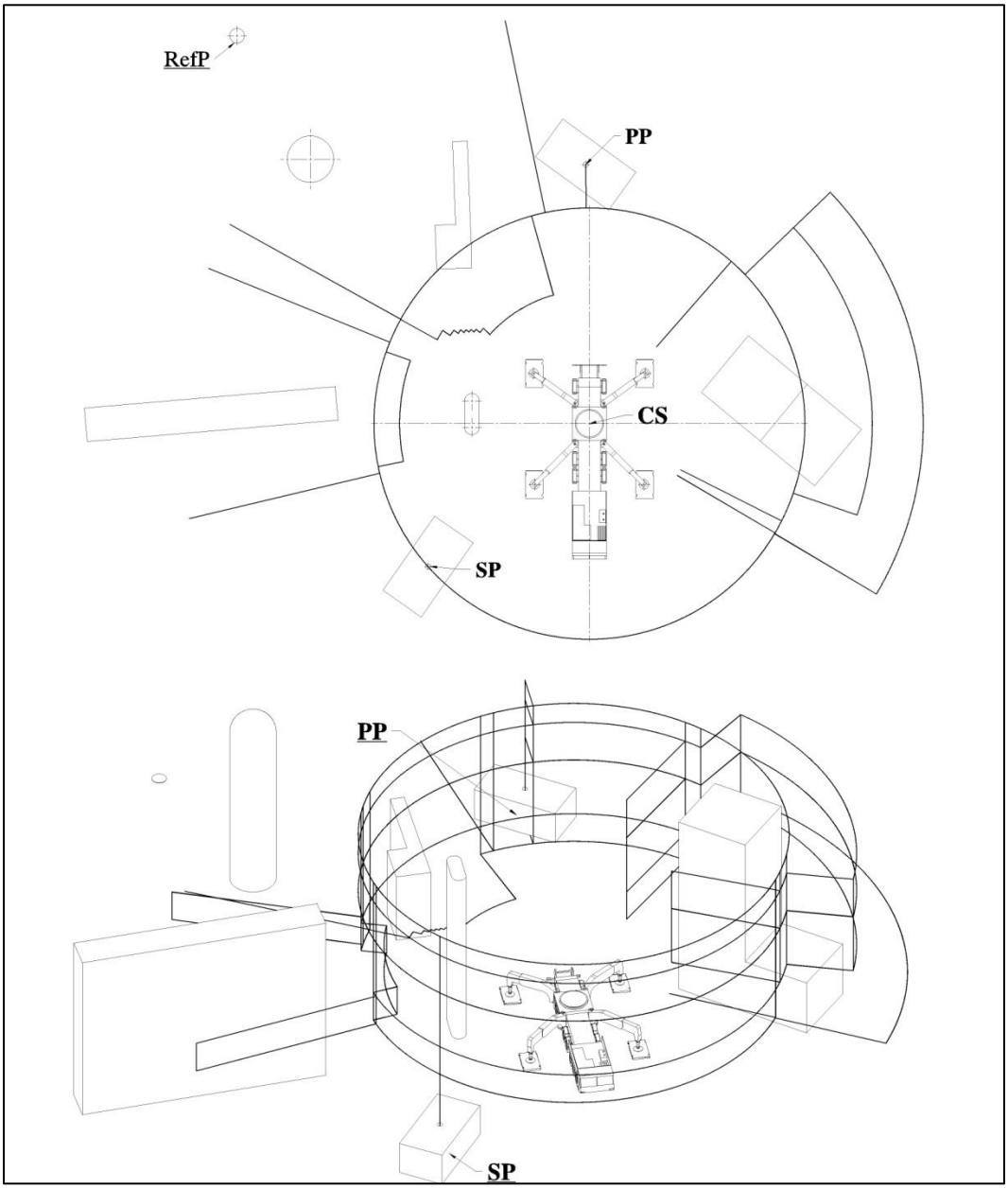

Figure 3.76 Object trajectory paths web (83).

Spatial point coordinates, shown in Appendix A-07, are numbered in a three digit sequence where the first digit represents the residing elevation and next two sequence order. Also, they are listed from projected PP to coordinate SP. Appendix A-08 shows all layout and elevation vector collections that have assigned calculated distances between direction points. The last task optimizes the trajectory by finding the shortest path between PP and SP. It applies a simple graph search algorithm and stores solutions for analysis. A large amount of connections have created great amounts of data. Evaluating the logic of the graph search algorithm established an additional limit criterion. The recursive method was then implemented in programming algorithm, following established rules at each node individually. Figure 3.77 shows a sample node graph flowchart with connections and weight values. The algorithm routine must find the shortest path between two nodes (01-80) with one-directional flow criterion (the path cannot pass the same node twice). One directional flow criterion at specific elevation is the optimization algorithm's main criterion.

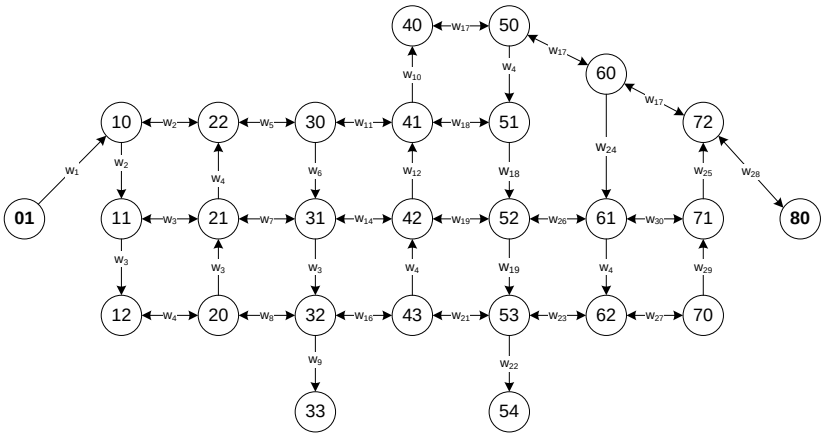

Con	W-t	Con	W-t
w_1	5	w_{13}	4
w_2	4	w_{14}	4
w_3	6	w_{15}	3
w_4	3	w_{16}	4
w_5	6	w_{17}	5
w_6	4	w_{18}	7
w_7	4	w_{19}	4
w_8	4	w_{20}	6
w_9	6	w_{21}	5
w_{10}	5	w_{22}	5
w_{11}	6	w_{23}	3
w_{12}	4	w_{24}	2

Figure 3.77 Node graph flowchart and connections weight values.

Figure 3.79 shows a run table of the optimization algorithm. The algorithm recognizes all available paths and stores only those with a solution that reaches the end. Description nodes simulate original case study scenario numbering, and the first digit identifies elevation and the second sequence. At the elevation level, nodes are one-directional, and connections between elevations are bi-directional. Also, there are four different penalties introduced in the sample. They are valued by favoring easiest and simplest connections that mimic crane movement's difficulties. Figure 3.78 shows a penalty matrix.

	1	2	3	4
1	0	3	4	2
2	3	0	5	3
3	3	4	0	0
4	2	3	0	0

1 Straigth
2 Arc
3 Vertical-up
4 Vertical-down

Figure 3.78 Move penalty matrix.

In the presented sample, the algorithm has 219 valid runs. Run '215' is recognized as the optimum path. The optimum path has a total distance, weight between nodes, and a connection penalty summarized to 50 with a weight 39 and a penalty 11. Figure 3.80 shows highlighted numbers, which are marked for paths within 10% of the lowest value. A general logic optimization concept displayed in this sample had 27 nodes and 24 different connections. This set-up allowed a manual test of the implemented algorithm. The methodology study contains 144 nodes and 340 connections. To find feasible solutions among that many nodes and connections, a visual basic (VB) routine was developed and a recursive method was used to simplify operations and reduce computational time. The total run time using the recursive method was 35 seconds.

	Weight	Penalty	Total	Path Route
1	99	61	160	1 10 11 12 20 21 22 30 31 32 43 42 41 40 50 51 52 53 62 70 71 72 80 0
2	100	66	166	1 10 11 12 20 21 22 30 31 32 43 42 41 40 50 51 52 61 62 70 71 72 80 0
3	89	53	142	1 10 11 12 20 21 22 30 31 32 43 42 41 40 50 51 52 61 71 72 80 0 0 0
10	82	53	135	1 10 11 12 20 21 22 30 31 32 43 42 41 51 52 61 71 72 80 0 0 0 0 0
11	84	57	141	1 10 11 12 20 21 22 30 31 32 43 42 52 53 62 70 71 72 80 0 0 0 0 0
12	85	57	142	1 10 11 12 20 21 22 30 31 32 43 42 52 61 62 70 71 72 80 0 0 0 0 0
13	74	44	118	1 10 11 12 20 21 22 30 31 32 43 42 52 61 71 72 80 0 0 0 0 0 0 0
97	77	45	122	1 10 11 21 22 30 31 32 43 42 41 40 50 51 52 61 71 72 80 0 0 0 0 0
98	98	55	153	1 10 11 21 22 30 31 32 43 42 41 40 50 60 61 52 53 62 70 71 72 80 0 0
99	85	53	138	1 10 11 21 22 30 31 32 43 42 41 40 50 60 61 62 70 71 72 80 0 0 0 0
100	74	45	119	1 10 11 21 22 30 31 32 43 42 41 40 50 60 61 71 72 80 0 0 0 0 0 0
101	67	33	100	1 10 11 21 22 30 31 32 43 42 41 40 50 60 72 80 0 0 0 0 0 0 0 0
102	80	53	133	1 10 11 21 22 30 31 32 43 42 41 51 52 53 62 70 71 72 80 0 0 0 0 0
103	81	58	139	1 10 11 21 22 30 31 32 43 42 41 51 52 61 62 70 71 72 80 0 0 0 0 0
104	70	45	115	1 10 11 21 22 30 31 32 43 42 41 51 52 61 71 72 80 0 0 0 0 0 0 0
105	72	49	121	1 10 11 21 22 30 31 32 43 42 52 53 62 70 71 72 80 0 0 0 0 0 0 0
206	42	16	58	1 10 22 30 31 42 52 61 71 72 80 0 0 0 0 0 0 0 0 0 0 0 0 0
207	78	33	111	1 10 22 30 41 40 50 51 52 42 31 32 43 53 62 70 71 72 80 0 0 0 0 0
208	59	31	90	1 10 22 30 41 40 50 51 52 53 62 70 71 72 80 0 0 0 0 0 0 0 0 0
209	60	36	96	1 10 22 30 41 40 50 51 52 61 62 70 71 72 80 0 0 0 0 0 0 0 0 0
210	49	23	72	1 10 22 30 41 40 50 51 52 61 71 72 80 0 0 0 0 0 0 0 0 0 0 0
211	89	33	122	1 10 22 30 41 40 50 60 61 52 42 31 32 43 53 62 70 71 72 80 0 0 0 0
212	70	33	103	1 10 22 30 41 40 50 60 61 52 53 62 70 71 72 80 0 0 0 0 0 0 0 0
213	57	31	88	1 10 22 30 41 40 50 60 61 62 70 71 72 80 0 0 0 0 0 0 0 0 0 0
214	46	23	69	1 10 22 30 41 40 50 60 61 71 72 80 0 0 0 0 0 0 0 0 0 0 0 0
215	39	11	50	1 10 22 30 41 40 50 60 72 80 0 0 0 0 0 0 0 0 0 0 0 0 0 0
216	71	26	97	1 10 22 30 41 51 52 42 31 32 43 53 62 70 71 72 80 0 0 0 0 0 0 0
217	52	24	76	1 10 22 30 41 51 52 53 62 70 71 72 80 0 0 0 0 0 0 0 0 0 0 0
218	53	29	82	1 10 22 30 41 51 52 61 62 70 71 72 80 0 0 0 0 0 0 0 0 0 0 0
219	42	16	58	1 10 22 30 41 51 52 61 71 72 80 0 0 0 0 0 0 0 0 0 0 0 0 0

Figure 3.79 Optimization algorithm paths – sample.

Figure 3.80 shows run ‘215’ sample optimized path with highlighted nodes. The full node graph can be seen in Appendix A-09, where the first digit of the node number represents elevation, except the SP node, which poses as the first elevation value.

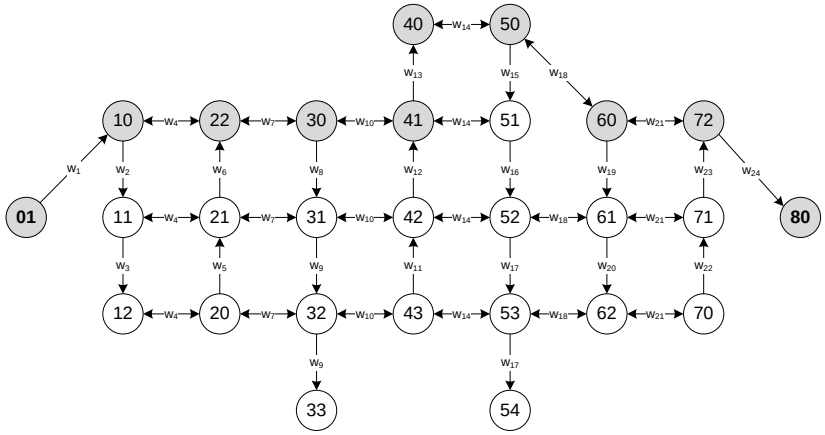

Figure 3.80 Optimized path ‘215’ – sample.

This state-of-the-art methodology approach recognizes, analyzes, and optimizes the crane lifted object spatial trajectory. It is divided into concise phases, which act as independent problem solving methods, but are connected into a smooth flowing process. Each phase structure starts from objective description then shows and discusses proposed phase flowcharts. This technique creates a feeling of full descent into the problem and clearly explains the solution in the form of graphical pictures, which are supported by mathematical equations. The reader is guided from one task of the phase to another until the phase objectives are met. Logical transitions between phases create an explanation of equipment behavior and development of simplified trajectory, which is modified by elevation obstructions and final optimizations of adjusted trajectories. The proposed methodology proves to be effective, and in particular it serves to eliminate guess-work. The entire logical concept is based on solid groundwork and expert knowledge that involves professionals from several different academic fields, such as construction and mechanical engineering faculty, mathematics faculty, and computer science and engineering management department scientists. But the most critical field expert knowledge, which must be recognized, came from individuals who on a daily basis are involved in the real situation and must deal with and solve critical and complicated crane-object-obstruction relations. The methodology was tested in a number of challenging case studies, two of which are presented in this paper. Users of this methodology include owners, designers, practitioners, and contractors; in addition, the proposed method lends

itself to becoming a useful tool for teaching at universities. This research captures both academic and construction field expert knowledge in the form of predefined logic and decisions.

CHAPTER 4 – METHODOLOGY IMPLEMENTATION

This chapter will discuss methodology implementation and validation of proposed solutions. It begins with project description, crane position calculation, and evaluation of boom clearances to a sloped angle roof surface. The project was commenced by Kullman Building Corp. in Allentown Pennsylvania. Also, it will discuss modular assembly operation in specific and describe the lifted object spatial trajectory analysis of the same project.

4.1 Crane Boom Clearance - Top Surface Slope Area

Problem Definition

Fully finished modules were delivered to Muhlenberg College in Allentown, Pennsylvania, for assembly into five new buildings. These three-story dormitory units were to house 145 students each, replacing seven single-level units built in 1981 to accommodate 56 students each. Each floor in the new unit was divided into 6 different modules, with the entire building structure consisting of 18 modules. Unwrapped at the staging area, the modules were trucked to the lifting spot for the crane lifting operation. Figure 4.1 shows an exploded view of a sample dormitory in which each module is clearly visible. Figure 4.2 shows a typical floor layout. Modules ranged from 39,000 lb (17.7 tonnes) to 72,000 lb (32.7 tonnes) in weight and from 22’ (6.7 m) x 14’ (4.3 m) to 51’ (15.5 m) x 14’ (4.3 m) in length and width. Due to the nature of typical academic activities, the college established a main time constraint at the beginning of the contract.

Figure 4.1 Building exploded view.

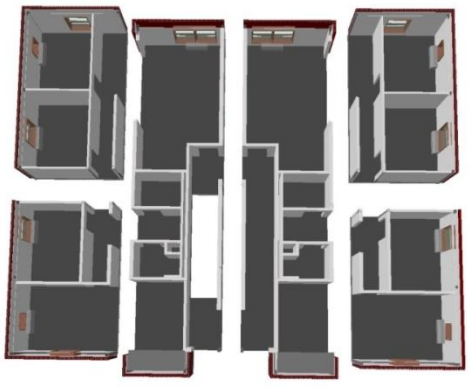

Figure 4.2 Typical floor layout.

Summer break months and early student dismissal from the college created a time window of only 10 weeks for the construction management team to deliver the first three units for student occupancy (August 15). The fourth and fifth units were to be completed by the end of September. The time constraint factor eliminated the stick-building construction option, along with the architectural requirement that the dormitories be built with brick exterior walls. Based on the module construction we proposed to assemble the 5 buildings onsite in three weeks. To manage the tight delivery deadline, a detailed schedule (minute-by-minute) of each operation was created (see Figure 4.4 and Appendix A-02). Figure 4.3 shows an operational flow chart of the assembly operation (Appendix 03). In the highlighted area, spatial coordinates are automatically calculated.

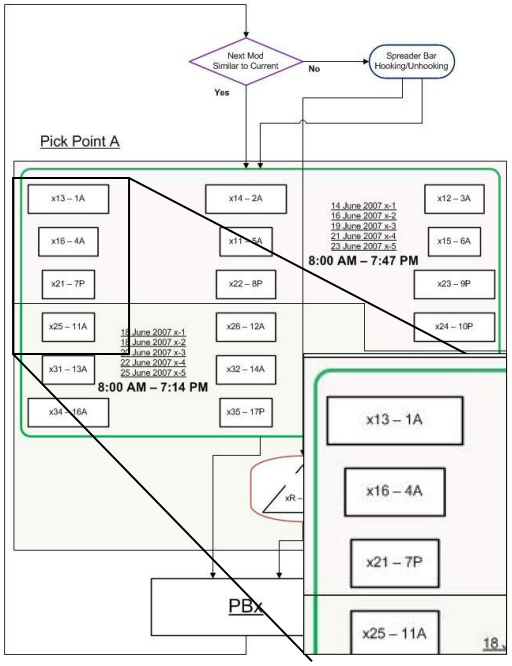

Figure 4.3 Operation flow chart.

	oper code	activity/operation	module	start zone	crew	workers time p (m)	workers time ml (m)	workers time o (m)	crane time p (m)	crane time ml (m)	crane time o (m)	finish zone
	21-Jun-07											
901	C	Extend Crane HydBoom		C					8	6	5	C
902	K1	Hooking spreader bar		C	2	12	10	8				C
903	C-sb	Crane next position		C					4	2	1	A
904	T1	Placing Module Trailer	413	-	1	25	20	15				A
905	K2	Hooking Module	413	A	2	20	17	15				A
906	T1	Removing Empty Trailer		A	1	25	20	15				-
907	C-sb	load hoisting up	413	A					3	2	1	
908	C-sb	load booming up	413						2	1.5	1	
909	C-sb	load swing	413						3.3	2.7	2	
910	C-sb	load hoisting down	413						4.2	2.8	2	PB4-1
911	K2	Securing-lining up	413	PB4-1	2	30	20	15				PB4-1
912	K1	Securing-bolting together	413	PB4-1	2	30	22	15				PB4-1
913	K2	Unhooking	413	PB4-1	2	12	9	8				PB4-1
914	K1	Removing lifting lugs	413	PB4-1	2	16	13	11				PB4-1
915	K3	Welding bottom - one side	413	PB4-1	1	30	20	15				PB4-1
916	K3	Welding bottom - other side	413	PB4-1	1	30	20	15				PB4-1
917	C-sb	Crane next position		PB4-1					3	2	1	A
918	T1	Placing Module Trailer	414	-	1	25	20	15				A
919	K2	Hooking Module	414	A	2	20	17	15				A
920	T1	Removing Empty Trailer		A	1	25	20	15				-
921	C-sb	load hoisting up	414	A					3	2	1	
922	C-sb	load booming up	414						2	1.5	1	
923	C-sb	load swing	414						3.3	2.7	2	
924	C-sb	load hoisting down	414						4.2	2.8	2	PB4-1
925	K2	Securing-lining up	414	PB4-1	2	30	20	15				PB4-1
926	K1	Securing-bolting together	414	PB4-1	2	25	17	10				PB4-1
927	K2	Unhooking	414	PB4-1	2	12	9	8				PB4-1
928	K1	Removing lifting lugs	414	PB4-1	2	16	13	11				PB4-1
929	K3	Welding bottom - one side	414	PB4-1	1	40	25	20				PB4-1
930	K3	Welding top - mod together	414	PB4-1	1	42	35	30				PB4-1
931	C-sb	Crane next position		PB4-1					3	2	1	C
932	K1	Unhooking spreader bar		C	2	12	10	8				C
933	C	Crane next position		C					3	2	1	A
934	T1	Placing Module Trailer	411	-	1	20	15	10				A
935	K2	Hooking Module	411	A	2	20	17	15				A
936	T1	Removing Empty Trailer		A	1	25	20	15				-
937	C	load hoisting up	411	A					3	2	1	
938	C	load booming up	411						2	1.5	1	
939	C	load swing	411						2.8	2	1.7	
940	C	load hoisting down	411						4	2.5	1.9	PB4-1
941	K2	Securing-lining up	411	PB4-1	2	25	18	12				PB4-1
942	K1	Securing-bolting together	411	PB4-1	2	20	15	8				PB4-1
943	K2	Unhooking	411	PB4-1	2	9	7	5				PB4-1
944	K1	Removing lifting lugs	411	PB4-1	2	15	11	10				PB4-1
945	K3	Welding top	411	PB4-1	1	25	20	17				PB4-1
946	K3	Welding bottom	411	PB4-1	1	25	20	17				PB4-1
947	C	Crane next position		PB4-1					3	2	1	A
948	T1	Placing Module Trailer	412	-	1	20	15	10				A

Figure 4.4 Schedule (minute-by-minute).

In this figure, the divided shaded square area represents two different days (top and bottom sections, respectively). Modules placed in the top section were to be lifted on the first day while modules in the bottom were to be lifted on the second day. Module descriptions ending with the letter A were lifted from the staging area delivery batch (having arrived onsite a day before), and modules ending with the letter P were delivered to the site the same day as the lift. This way, an entire building was assembled in just two days. Appendix A-04 shows the proposed and actual timetables. Underlined and bold fonts show a sample time record of the site operations. Developed geometric center of each lifted object set-point allowed for automatic calculation of each object's envelope points with a general position of objects pick-point coordinates (Appendix A-05).

Capacity Check

A significant factor that was carefully analyzed had to do with the selection of a crane to lift all modules and place them at their desired locations.

Not only lift capacity was considered in the selection, but also assembly flexibility and site accessibility, especially with regard to ground configuration. From Equation 3.1 total lift weight with spreader bar was calculated:

$$\boldsymbol{T_W = L_{W1} + SL_W + SB_W = 72,080 + 500 + 5,600 = 78,180\ lb}$$

And without spreader bar lift weight:

$$\boldsymbol{T_W = L_{W2} + SL_W = 42,460 + 500 = 42,960\ lb}$$

Where:

T_w	*- Total lift weight*
L_{w1}	*- Lift weight$_1$ max (72,080 lb)*
L_{w2}	*- Lift weight$_2$ max (42,460 lb)*
SL_w	*- Total weight of slings (500 lb)*
SB_w	*- Total weight of spreader bar (5,600 lb)*

Figure 4.5 shows typical under hook configuration with spreader bar and Figure 4.6 load without spreader bar.

Figure 4.5 Large units under hook configuration.

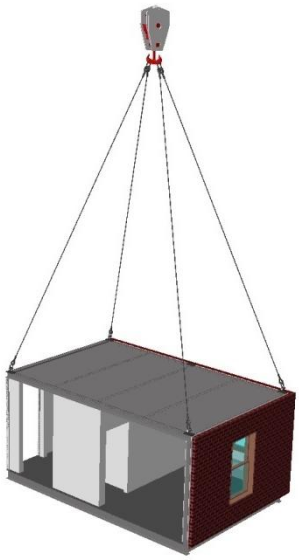

Figure 4.6 Load without spreader bar.

Crane Placement Location and Selection

To properly define the crane position at the construction site, lifted objects' radiuses must be analyzed and optimized. As stated in the methodology section, all the modules' centroids are analyzed to establish the site centroid position. Modules' centroids are evaluated only based on one elevation layout since all building floors are identical. Therefore, for this exercise there are only 30 modules located on the construction site. Figure 4.7 shows part of modules' geometric center coordinate dimensions and site geometric center calculation. For full size drawings refer to Appendix A-12.

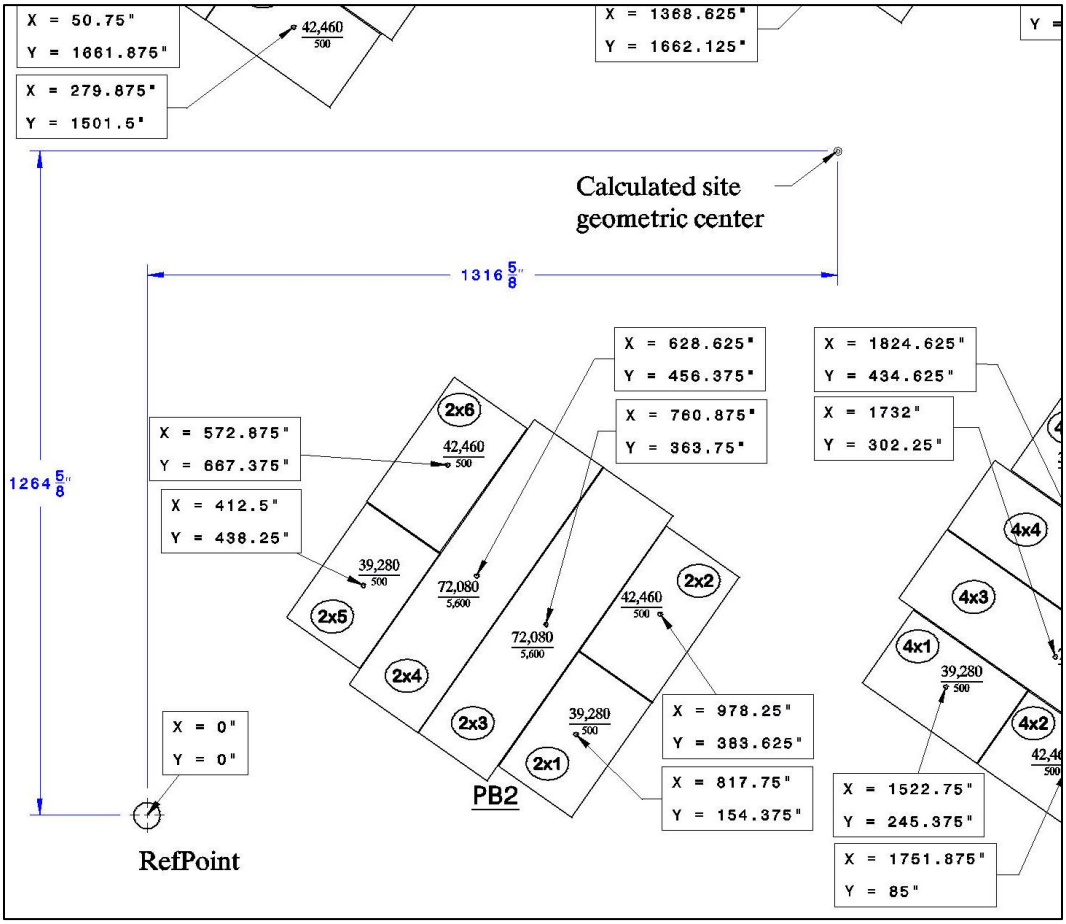

Figure 4.7 Modules geometric center dimensions.

The established reference point is a base for all lifted objects' geometric center position. Each set of three rectangular modules' number are shown in an ellipse, where the first number represents building unit, second (x) elevation, and third module type. There are also two other numbers close to each module's geometric center, the top number being the unit weight and bottom the rigging weight. The smaller units' rigging weight includes slings, but the larger modules' rigging contains spreader bar and slings' weight. Figure

4.8 shows the spreadsheet table where all data for this task is collected. The first column includes the module number (see Figure 4.7), second and third columns show module and spreader bar/slings' weight, and fourth and fifth columns parameters of reference point values. Data related to lifting radiuses will be discussed later.

Module		**Spreaderbar /Slings**	**Reference Point Coordinate**	
Module	Weight	Weight	x	y
	[lb]	*[lb]*	*[in]*	*[in]*
1x1	39,280	500	50.750	1661.875
1x2	42,460	500	279.875	1501.500
1x3	72,080	5,600	260.000	1718.750
1x4	72,080	5,600	352.625	1851.125
1x5	39,280	500	334.500	2067.250
1x6	42,460	500	563.750	1906.750
2x1	39,280	500	817.750	154.375
2x2	42,460	500	978.250	383.625
2x3	72,080	5,600	760.875	363.750
2x4	72,080	5,600	628.625	456.375
2x5	39,280	500	412.500	438.250
2x6	42,460	500	572.875	667.375
3x1	39,280	500	1139.500	1822.625
3x2	42,460	500	1368.625	1662.125
3x3	72,080	5,600	1348.750	1879.500
3x4	72,080	5,600	1441.375	2011.750
3x5	39,280	500	1423.250	2227.875
3x6	42,460	500	1652.375	2067.375
4x1	39,280	500	1522.750	245.375
4x2	42,460	500	1751.875	85.000
4x3	72,080	5,600	1732.000	302.250
4x4	72,080	5,600	1824.625	434.625
4x5	39,280	500	1806.500	650.750
4x6	42,460	500	2035.750	490.250
5x1	39,280	500	2277.750	2075.125
5x2	42,460	500	2117.250	1846.000
5x3	72,080	5,600	2334.625	1865.875
5x4	72,080	5,600	2466.875	1773.250
5x5	39,280	500	2683.000	1794.375
5x6	42,460	500	2522.625	1562.125

Figure 4.8 Geometric center calculation data.

The centroid of a set of *30* point masses m_i *(i=1-6)* located at position x_i is:

$$x = \frac{\sum_{i=1}^{n} m_i x_i}{\sum_{i=1}^{n} m_i} = \frac{2,112,214,135}{1,604,200} = 1,316\ \frac{5}{8}" \qquad (4.1)$$

The centroid of a set of *30* point masses m_i located at position y_i is:

$$y = \frac{\sum_{i=1}^{n} m_i y_i}{\sum_{i=1}^{n} m_i} = \frac{2,028,754,338}{1,604,200} = 1,264\ \frac{5}{8}" \qquad (4.2)$$

The reference point can be established at any position on the construction site. However all analyzed components should be referred to from such a point. After the geometrical center is identified, the next step analyzes the maximum radius for each type of lifted object. Figure 4.9 shows a partial layout of the objects' set-point radiuses. Appendix A-13 shows entire site layout with radiuses calculated from the developed geometric center.

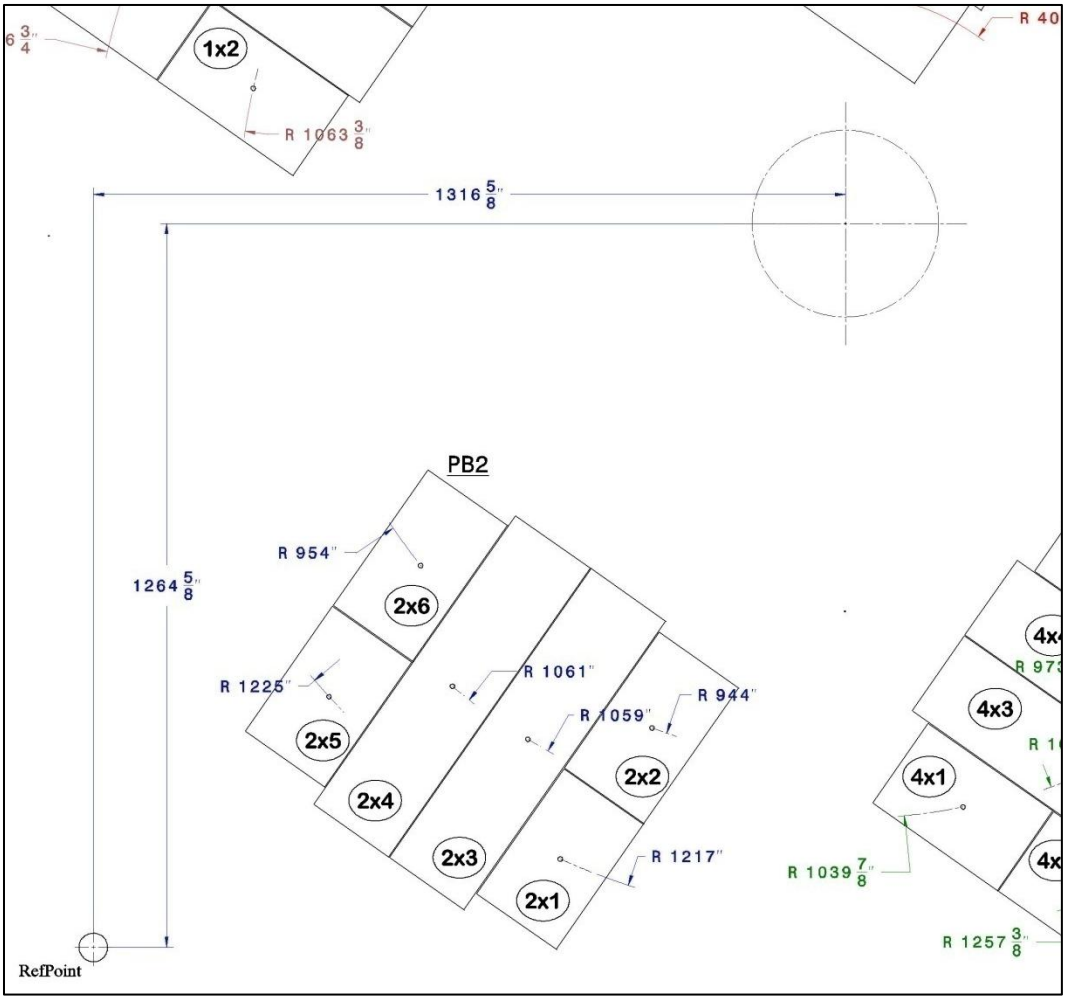

Figure 4.9 Object set-point radiuses.

Module radius analysis establishes critical modules' positions, which influence crane selection. It is helpful to choose the most economical crane configuration that allows lifting of all units at initial set up, without reconfiguring and relocating the unit. Figure 4.10 shows expanded spreadsheet data for each module's maximum lift radius.

	Module		Spreaderbar /Slings	Reference Point Coordinate		Radiuses	
						Pick	Set
	Module	Weight	Weight	x	y	-Point	-Point
		[lb]	*[lb]*	*[in]*	*[in]*	*[ft-in]*	*[ft-in]*
1	**1x1**	39,280	500	50.750	1661.875	74'-7"	110'-7"
2	**1x2**	42,460	500	279.875	1501.500	74'-7"	88'-8"
3	**1x3**	72,080	5,600	260.000	1718.750	74'-7"	95'-10"
4	**1x4**	72,080	5,600	352.625	1851.125	74'-7"	94'
5	**1x5**	39,280	500	334.500	2067.250	74'-7"	104'-11"
6	**1x6**	42,460	500	563.750	1906.750	74'-7"	82'-6"
19	**2x1**	39,280	500	817.750	154.375	74'-7"	101'-5"
20	**2x2**	42,460	500	978.250	383.625	74'-7"	78'-8"
21	**2x3**	72,080	5,600	760.875	363.750	74'-7"	88'-3"
22	**2x4**	72,080	5,600	628.625	456.375	74'-7"	88'-6"
23	**2x5**	39,280	500	412.500	438.250	74'-7"	102'-1"
24	**2x6**	42,460	500	572.875	667.375	74'-7"	79'-6"
37	**3x1**	39,280	500	1139.500	1822.625	74'-7"	48'-9"
38	**3x2**	42,460	500	1368.625	1662.125	74'-7"	38'-5"
39	**3x3**	72,080	5,600	1348.750	1879.500	74'-7"	51'-4"
40	**3x4**	72,080	5,600	1441.375	2011.750	74'-7"	63'-2"
41	**3x5**	39,280	500	1423.250	2227.875	74'-7"	80'-9"
42	**3x6**	42,460	500	1652.375	2067.375	74'-7"	72'-6"
55	**4x1**	39,280	500	1522.750	245.375	74'-7"	86'-8"
56	**4x2**	42,460	500	1751.875	85.000	74'-7"	104'-9"
57	**4x3**	72,080	5,600	1732.000	302.250	74'-7"	87'-4"
58	**4x4**	72,080	5,600	1824.625	434.625	74'-7"	81'-1"
59	**4x5**	39,280	500	1806.500	650.750	74'-7"	65'-5"
60	**4x6**	42,460	500	2035.750	490.250	74'-7"	88'-1"
73	**5x1**	39,280	500	2277.750	2075.125	74'-7"	104'-9"
74	**5x2**	42,460	500	2117.250	1846.000	74'-7"	82'-5"
75	**5x3**	72,080	5,600	2334.625	1865.875	74'-7"	98'-6"
76	**5x4**	72,080	5,600	2466.875	1773.250	74'-7"	104'-10"
77	**5x5**	39,280	500	2683.000	1794.375	74'-7"	122'
78	**5x6**	42,460	500	2522.625	1562.125	74'-7"	103'-6"

Figure 4.10 Modules coordinate and radiuses data

A crane may be selected based on lifted objects' weight and their final position, but there are other factors, such as price or availability, that may influence which unit should be

employed. Nevertheless, whichever crane will be used it must be able to lift and place specified objects. As the data presented in Figure 4.10 shows, there are three different types of modules that must be assembled. The first type of module is (xx1) and (xx5) with each weighting 39,280 lb plus an additional 500 lb for slings; the second type is (xx2) and (xx6) with each weighing 42,460 lb plus an additional 500 lb for slings; the third type is (xx3) and (xx4) with each weighing 72,080 lb plus an additional 5,600 lb for spreader bars and slings. Each type must be analyzed separately for its lift capacity and a champion unit, with the largest radius selected. These three units will define the minimum radius within which the selected crane must operate. Figure 4.10 shows shaded units 4x2, 5x4 and 5x5 that have radiuses 104'-9", 104'-10" and 122', respectively. Now, activating a crane selection algorithm [Al-Hussein at al. 2001] allows defining the minimum crane configuration for lifted objects. Evaluating all the factors and units' availability, the Demag AC 500-1 mobile hydraulic telescopic boom crane with a lifting capacity of 600 tonnes (500,000 kg) was selected. Figure 4.11 shows a CAD model of employed unit.

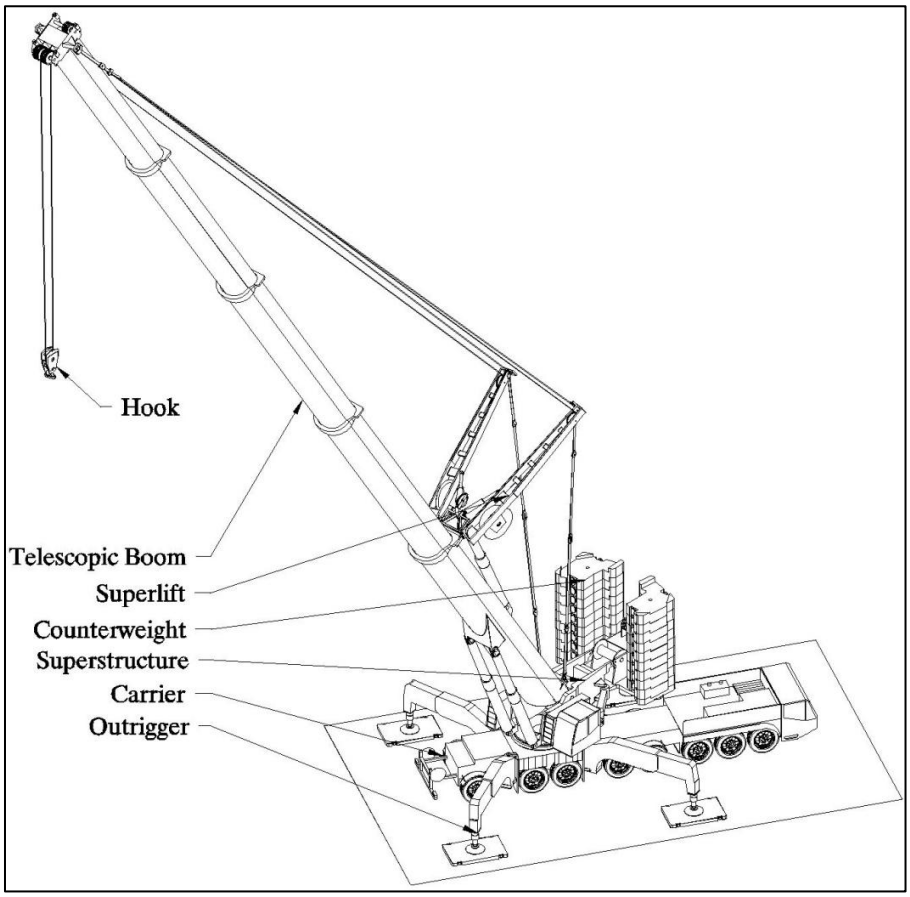

Figure 4.11 Demag AC 500-1 all-terrain hydraulic crane.

The crane may have several different configurations. The chosen configuration has a full extended and pinned boom (183.7'), a superlift that will be attached to the boom, and a superstructure that will carry maximum counterweight balance of 396,900 lb. The manufacturers' lifting capacity chart for the chosen configuration can be seen in Appendix A-14. Figure 4.12 shows an extended spreadsheet from the previous coordinates radiuses analysis and presents selected AC 500-1 crane capacity with calculated lift percentage.

	Module		Spreaderbar /Slings	Reference Point Coordinate		C-weight - 396,900 lb		
						Crane Radius m. boom		
						Set	Capacity	Lift
	Module	Weight	Weight	x	y	-Point	at 183.7'	
		[lb]	*[lb]*	*[in]*	*[in]*	*[ft-in]*	*[lb]*	%
1	**1x1**	39,280	500	50.750	1661.875	110'-7"	84,100	47%
2	**1x2**	42,460	500	279.875	1501.500	88'-8"	109,100	39%
3	**1x3**	72,080	5,600	260.000	1718.750	95'-10"	100,200	78%
4	**1x4**	72,080	5,600	352.625	1851.125	94'	100,200	78%
5	**1x5**	39,280	500	334.500	2067.250	104'-11"	91,000	44%
6	**1x6**	42,460	500	563.750	1906.750	82'-6"	119,500	36%
19	**2x1**	39,280	500	817.750	154.375	101'-5"	91,000	43%
20	**2x2**	42,460	500	978.250	383.625	78'-8"	129,600	33%
21	**2x3**	72,080	5,600	760.875	363.750	88'-3"	109,100	71%
22	**2x4**	72,080	5,600	628.625	456.375	88'-6"	109,100	71%
23	**2x5**	39,280	500	412.500	438.250	102'-1"	91,000	43%
24	**2x6**	42,460	500	572.875	667.375	79'-6"	119,500	36%
37	**3x1**	39,280	500	1139.500	1822.625	48'-9"	157,100	25%
38	**3x2**	42,460	500	1368.625	1662.125	38'-5"	172,400	25%
39	**3x3**	72,080	5,600	1348.750	1879.500	51'-4"	157,100	49%
40	**3x4**	72,080	5,600	1441.375	2011.750	63'-2"	143,900	54%
41	**3x5**	39,280	500	1423.250	2227.875	80'-9"	119,500	33%
42	**3x6**	42,460	500	1652.375	2067.375	72'-6"	129,600	33%
55	**4x1**	39,280	500	1522.750	245.375	86'-8"	109,100	36%
56	**4x2**	42,460	500	1751.875	85.000	104'-9"	91,000	47%
57	**4x3**	72,080	5,600	1732.000	302.250	87'-4"	109,100	71%
58	**4x4**	72,080	5,600	1824.625	434.625	81'-1"	119,500	65%
59	**4x5**	39,280	500	1806.500	650.750	65'-5"	136,800	29%
60	**4x6**	42,460	500	2035.750	490.250	88'-1"	109,100	39%
73	**5x1**	39,280	500	2277.750	2075.125	104'-9"	91,000	43%
74	**5x2**	42,460	500	2117.250	1846.000	82'-5"	119,500	36%
75	**5x3**	72,080	5,600	2334.625	1865.875	98'-6"	91,000	85%
76	**5x4**	72,080	5,600	2466.875	1773.250	104'-10"	91,000	85%
77	**5x5**	39,280	500	2683.000	1794.375	122'	71,800	55%
78	**5x6**	42,460	500	2522.625	1562.125	103'-6"	91,000	47%

Figure 4.12 Modules' lifting parameters data.

$$MAX \quad R_{xxx}\ m_{xxx} \quad < R_{max}\ W$$

$$MAX \quad R_{4x2} \ < R_{max}\ W \qquad 104' - 9" < 164' \qquad (4.3)$$

$$MAX \quad R_{5x4} < R_{max} \; W \qquad 104' - 10" < 118' \qquad (4.4)$$

$$MAX \quad R_{5x5} < R_{max} \; W \qquad 122' < 170' \qquad (4.5)$$

Equations 4.3, 4.4 and 4.5 show that each module type champion's radius is below crane maximum reach for chosen module capacity. Figure 4.13 shows part of layout top site view with circles of calculated radiuses. For a full drawing with marked maximum radius for each type of selected module refer to Appendix A-15.

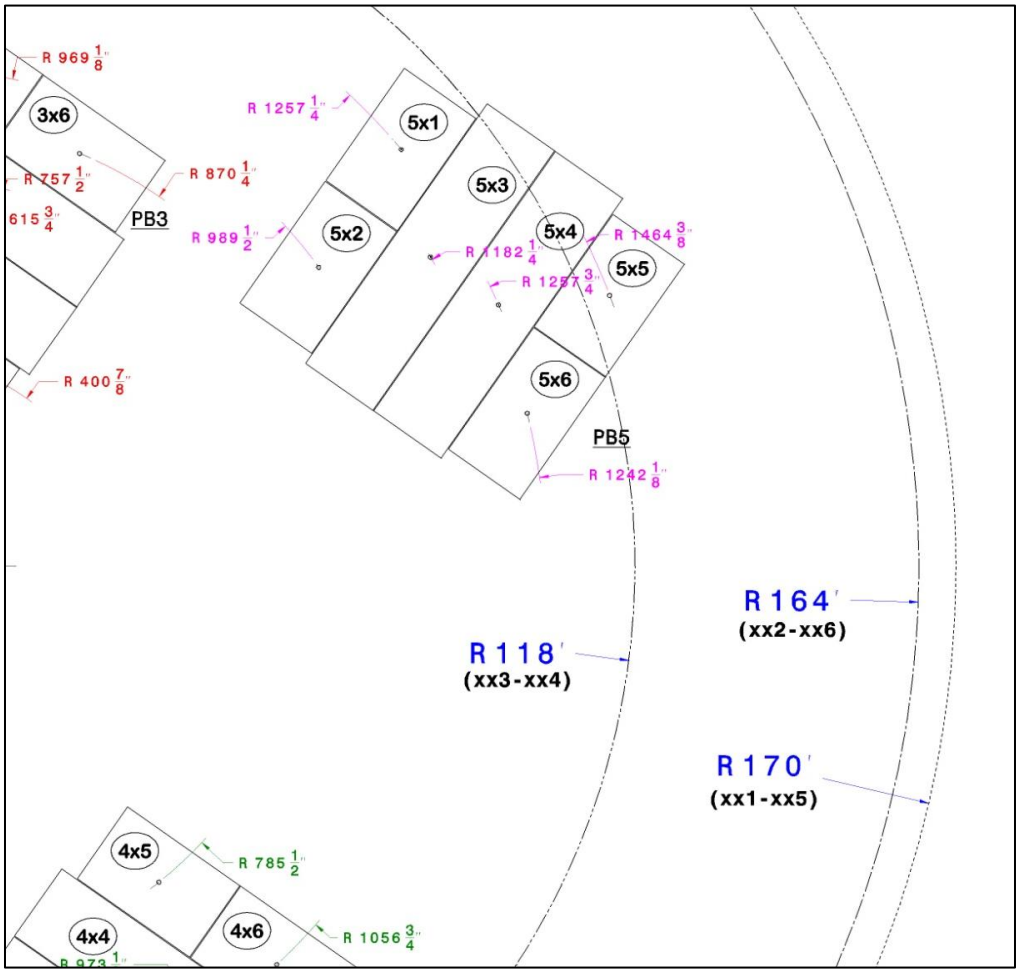

Figure 4.13 Maximum radiuses for each module type.

Confirming the capability of the selected crane is the last task of the crane position and selection section.

Crane Carrier Clearance

This section will calculate the shortest distance of the crane carrier to the site obstructions. Obstructions are defined as independent not lifted objects that reside in the

critical crane working zone. They can also refer to already placed objects. Figure 4.14 shows the selected crane carrier positioned at the site's calculated geometric center with dimensions that are critical for a clearance distance calculation.

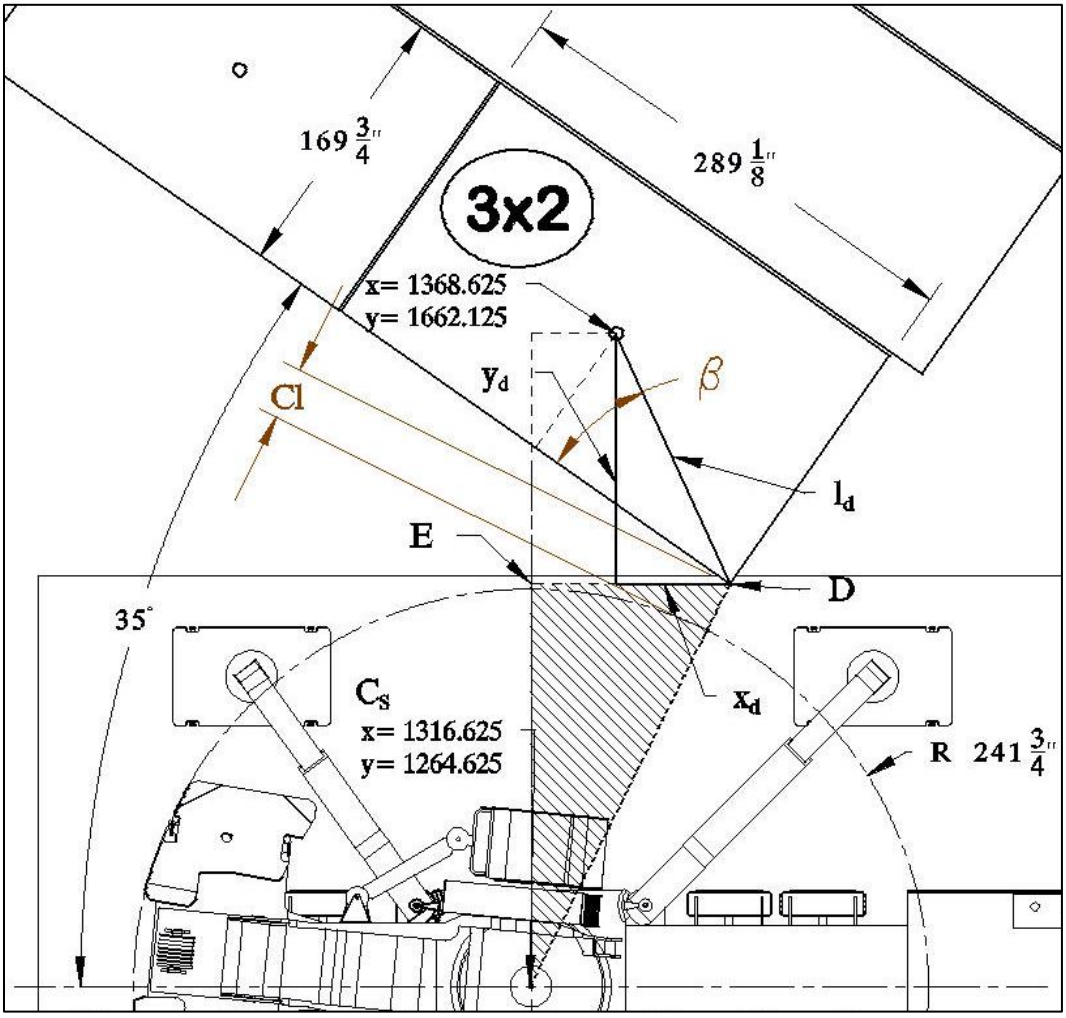

Figure 4.14 Crane carrier clearance calculation.

Lifted object diagonal length equal:

$$l_d = \sqrt{\left(\frac{l}{2}\right)^2 + \left(\frac{w}{2}\right)^2} = \sqrt{\left(\frac{289.125}{2}\right)^2 + \left(\frac{169.75}{2}\right)^2} = 167.375" \quad (4.6)$$

Diagonal (l_d) length angle (β) to object boundary equal:

$$\beta = arctg\ \frac{w}{2 * l_d} = arctg\ \frac{169.75}{2 * 167.375} = 26.89° \quad (4.7)$$

Top triangle sides (x_d) and (y_d) equal:

$$y_d = l_d * sin\ \varepsilon + \beta = 167.375 * sin\ 35 + 26.89 = 147.625" \quad (4.8)$$

$$x_d = l_d * cos\ \varepsilon + \beta\ = 167.375 * cos(35 + 26.89) = 78.875" \quad (4.9)$$

Bottom triangle sides (C_s, E) and (E, D):

$$C_s, E = y_{3x2} - y - y_d = 1662.125 - 1264.625 - 147.625 = 250.125" \quad (4.10)$$

$$E, D = x_{3x2} - x + x_d = 1368.625 - 1316.625 + 78.875 = 130.875" \quad (4.11)$$

Crane carrier clearance (*Cl*):

$$Cl = \sqrt{y_{3x2} - y - y_d\ ^2 + \ x_{3x2} - x + x_d\ ^2} - R_{CW}$$

$$Cl = \sqrt{250.125\ ^2 + \ 130.875\ ^2} - 241.75 = 40.54" \quad (4.12)$$

Total clearance value 40.5" is a sufficient distance to accept final crane position at calculated geometric center point. Minimum value for such clearance should not be less than 3'.

Boom Clearance

Boom radius and tip height calculation. Crane selection allows for confirmation of crane carrier position and all necessary clearances to obstructions, and at the same time allows for a second look at the schedule time frame. The original assembly schedule was designed to build roofs for each building in a traditional way by lifting separate pieces of roof trusses and assembling them on top of each erected building. After evaluating several options, pre-assembly of the roof at a nearby tennis court was opted for, followed by lifting each of the roof units from the assembly location to the desired building. However, while this decision reduced total assembly time, it created additional challenges related to handling very large lifts in the air. An object with a large surface area lifted above the ground behaves like a sail where even an imperceptible wind speed can pose problems. It was also found that the predetermined lift sequences created a difficult situation with the last roof lift. The lift was carefully analyzed and in this particular situation, lift operation had to be performed at the end of the assembly process. In order to accomplish this final lift, the crane had to be equipped with an additional boom extension. This came up after the crane boom clearance calculation was already performed. First, to calculate the boom angle and tip height, scenario 3 of boom clearance analysis was deployed. Parameters were known for crane length, added extension length, and lift radius. The closest tennis court area to the crane set-point position was considered for assembling the building roof. It was difficult to predict what can or cannot be

assembled on the roof, before calculations were performed. The confirmed roof lift radius and boom clearance to adjusted building would drive roof maximum weight. Figure 4.15 shows parameters for crane lift radius calculation.

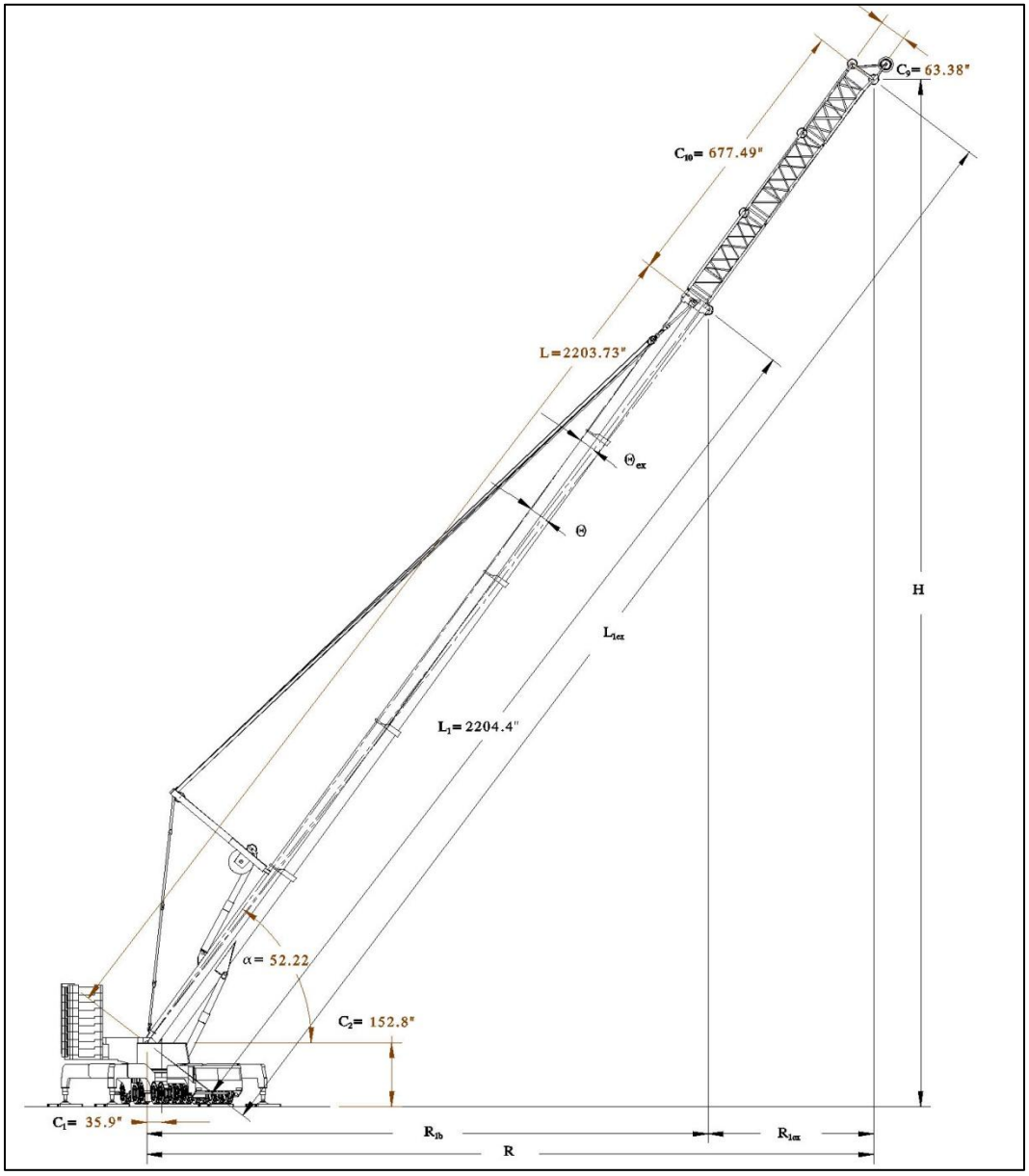

Figure 4.15 Scenario 3 method analysis

Extension sheave center to boom line angle:

$$\theta_{ex} = tan^{-1} \frac{C_9}{L + C_{10}} = tan^{-1} \frac{63.379}{2203.728 + 677.468} = 1.26° \qquad (4.13)$$

Main boom sheave center to boom line angle:

$$\theta = cos^{-1}\ \frac{L}{L_1}\ = cos^{-1}\ \frac{2203.728}{2204.398}\ = 1.41° \quad (4.14)$$

Main boom radius at boom angle (α):

$$R_{1b} + C_1 = L_1 * cos\ \alpha - \theta\ = 2204.398 * cos\ 52.22 - 1.41\ = 1392.9" \quad (4.15)$$

Then extension length (L_{1ex}):

$$L_{1ex} = \sqrt{L + C_{10}\ ^2 + C_9^2} = \sqrt{2203.728 + 677.468\ ^2 + 63.379^2}$$

$$L_{1ex} = 2881.893" \quad (4.16)$$

Extension radius projection (L_{1ex}):

$$R_{1ex} = L_{1ex} * cos\ \alpha - \theta_{1ex}\ - R_{1b} = 2881.893 * cos\ 52.22 - 1.26\ - 1392.9$$

$$R_{1ex} = 422.3" \quad (4.17)$$

Lift radius (R) at boom angle (α):

$$R = R_{1ex} + R_{1b} - C_1 = 422.3 + 1392.9 - 115.2 = 1700" \quad (4.18)$$

Total boom height (H) at boom angle (α):

$$H = L_{1ex} * cos\ \alpha - \theta_{1ex}\ + C_2 = 2881.893 * cos\ 52.22 - 1.26\ + 152.8$$

$$H = 1968" \quad (4.19)$$

After evaluating the configuration crane lift table for maximum radius 1700" [141'-8"], the maximum load that can be used is 56,900 lb.

Boom clearance to slope surface analysis. When crane configurations are checked for crane radiuses, with and without boom extension, the next step evaluates boom clearance distance to obstruction. Figure 4.16 shows a top layout of crane boom position in relation to close obstruction. Fist, the boom offset angle (α_B) calculation is used:

$$\alpha_B = \alpha - \theta_{1ex}\ = 52.22 - 1.26\ = 50.96°$$

Then the true length angle (λ) is calculated (see Figure 3.18):

$$\lambda = tan^{-1}\ \frac{h + j\ tan\delta}{R\ tan\alpha_B}\ = tan^{-1}\ \frac{251 + 1454.8\ * tan 45°}{1700 * tan 51°}$$

$$\lambda = 39° \qquad (4.20)$$

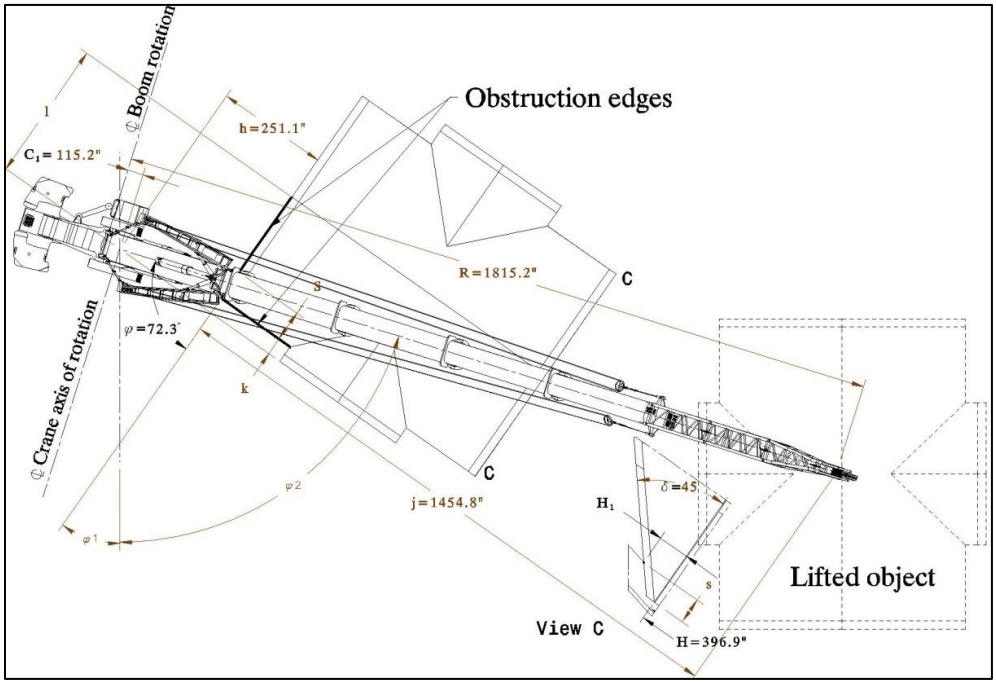

Figure 4.16 Boom obstruction plan view – numerical.

The clearance (*K*) value is the closest crane boom distance to the obstruction edge. In Figure 4.16 the boom section is just above the closest distance to obstruction. Figure 4.17 shows a computer generated picture of CAD model of boom proximity to sloped roof. Figure 4.18 shows the picture of the actual crane boom position.

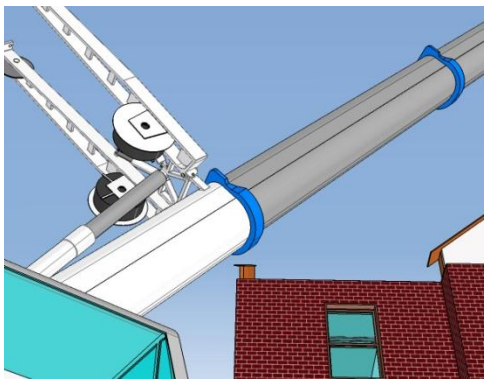

Figure 4.17 Computer image of clearance.

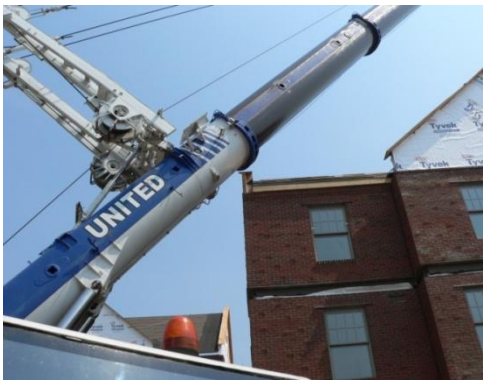

Figure 4.18 Actual picture of clearance.

Based on final equation 3.34 clearance (*K*) value is calculated:

$$K = \frac{1}{W} \quad R - \frac{H - C_2}{\tan \alpha_B} - \frac{D}{2 \sin \alpha_B} \quad \sin \varphi - \frac{B}{2} \cos \varphi - j$$

But first the parameter (*W*) must be calculated:

$$W = \frac{1 + sin^2 \lambda \ cos \delta}{cos \lambda} = \frac{1 + sin^2 39 \, cos 45}{cos 39} = 2.06 \qquad (4.21)$$

Final clearance distance (*K*) where D=50" and B=72":

$$K = \frac{1}{2.06} \quad 1700 - \frac{396.9 - 152.8}{tan 51^\circ} - \frac{50}{2 \ sin 51^\circ} \ sin 72.3^\circ - \frac{72}{2} cos 72.3^\circ - 1454.8 \ = \ 8.75" \qquad (4.22)$$

Calculated clearance (*K*) is less than one foot, and to increase this dimension to the MOD value, an additional extension is required. This created another problem due to increased lift radius and at the same time reduced lifting weight capacity. The lifted roof was already "stripped" from shingles layer to keep its maximum weight just below 56,900 lb. The lift was performed at defined boom radius 1700" (141'-8") but additional safety precautions were implemented. It was observed that clearance (*K*) was reduced to approximately three inches during the initial lift due to boom spring deflection under the load.

Early discoveries of potential difficulties with roof placement, along with the relocation of the roof construction process to the nearby tennis court, allowed planners to remove the entire operation from the main critical-path schedule. Dealing with last-minute changes of object pick-point did not halt the construction assembly, but instead affected site managers' decisions by making them rely on computer-simulated results. Being aware of troubled tasks allows managers to properly redirect resources, create time safety buffers, or simply relax the schedule. Each decision depends on particular circumstances and individual interpretation, but was optimized in the present situation. The succesful CAD assemblies of simulation, animation, interference checks with trajectory, and crane movements made decision makers more confident that downstream operations would succeed.

4.2 Spatial Trajectory Analysis for Crane Lifting Operation

Problem Definition

The Muhlenberg College in Allentown, Pennsylvania construction site had a ground slope of about 7°. The site was classified as too difficult to operate in the traditional way

of the stick-building method. However, assembling entire buildings from large modular units meant that specific crane lifting expert knowledge and detailed lift analyses were required. The modular components were manufactured several miles from the site and delivered to the construction site. Each piece was covered for transportation, delivered, and hooked to the crane and placed at the desired location. The objectives were to optimize lifting activities, predefine potential problems before, during, and after each lift, and assist rigging and site management to coordinate crane operations.

During the lift assembly operation, the crane operator was unable to control the rotation of the hanging object even though he had assistance from two rigging workers holding tag-lines. The heavy load slowly responded to the pulling action and, during this time, rotation of the crane boom's load swung toward an obstruction. Further analyses of swing load behavior and trajectory paths were recommended on the eve of the final day of the project.

Algorithm Evaluation

Analysis of the lifted object trajectory is critical, and the presented algorithm in this section is based on the assumptions that; each crane action is assigned as a single operation, for example, rotation is represented as an arc, booming up, down, and radial displacement are represented as line. No combination movements, such as booming and rotating at the same time are assessed. A numerical example validates presented analysis in the methodology chapter.

Phase 1;-Object Pick-Point Optimization: The phase uses Method A to analyze centroid point for provided area. The centroid method calculation was presented in the methodology section with equations 3.2 and 3.3. Calculation of the area centroid point does not account for mass and that factor has 1 value for all x and y parameters. Coordinate x for pick area geometric center calculation:

$$x = \frac{\sum_{i=1}^{n} x_4}{4} = \frac{218.83 + 430.43 + 624.6 + 413}{1,604,200} = 421.21" \quad (4.23)$$

And coordinate y for input pick area:

$$y = \frac{\sum_{i=1}^{n} y_4}{4} = \frac{1177.04 + 1468.28 + 1327.2 + 1036}{4} = 1,252.13" \quad (4.24)$$

Figure 4.19 shows the input pick area and calculation of lifted object pick-point. Coordinate values for x and y parameters define the maximum pick radius (R 74’8”), which must be between crane R_{min} (R-348”) and R_{max} (R-2040”).

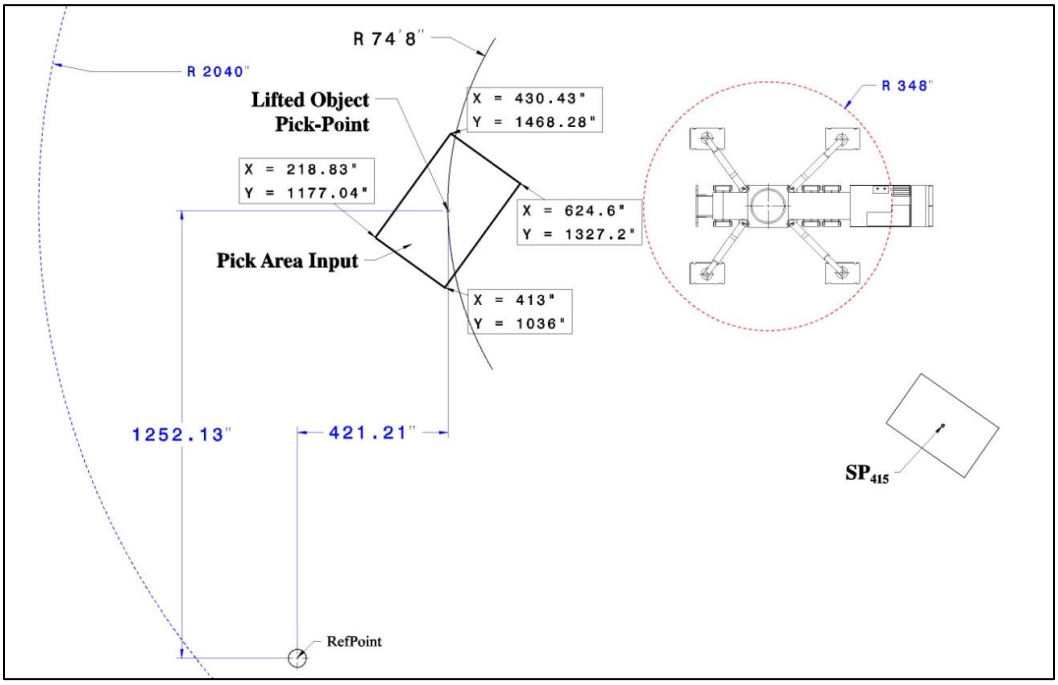

Figure 4.19 Object pick-point calculation.

Pick-point coordinate values are x=421.21” and y=1252.13”. Placing the lifted object in the calculated spot required additional information about lifted object orientation, which was provided as an input parameter.

Phase 2;-Crane Boom Obstruction Region Analysis (CBR): The phase will identify the restricted area for boom operation. Figure 4.20 shows crane boom section dimension values.

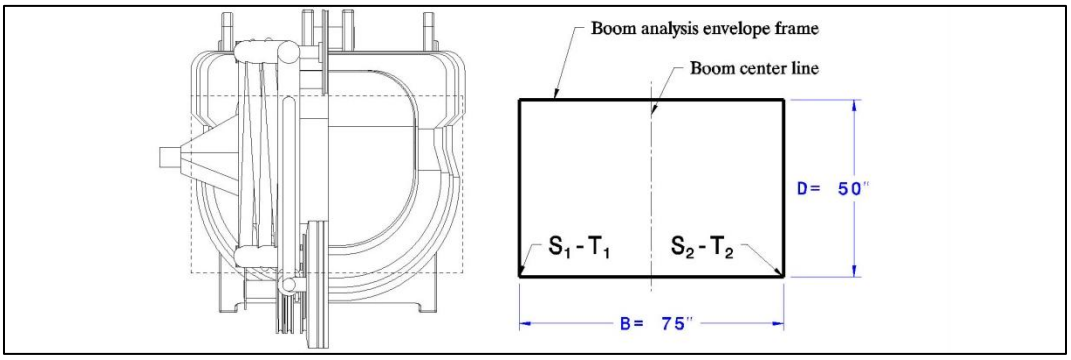

Figure 4.20 Boom section dimension value.

The boom section dimension is the average section distance of the entire boom length. The maximum crane boom radius area must be increased to cover the boom tip sheave dimension offset. Additional area offset distance B':

$$B' = \frac{B}{2} + MOD = \frac{75}{2} + 36 = 72.5" \qquad (4.25)$$

The minimum object distance value (MOD) is the input parameter, and its value can be from 2-4 feet depending on project complexity. In the created extended area all obstructions are identified and their closest point 3D coordinate values recorded. Figure 4.21 shows created analysis area and recognized obstructions.

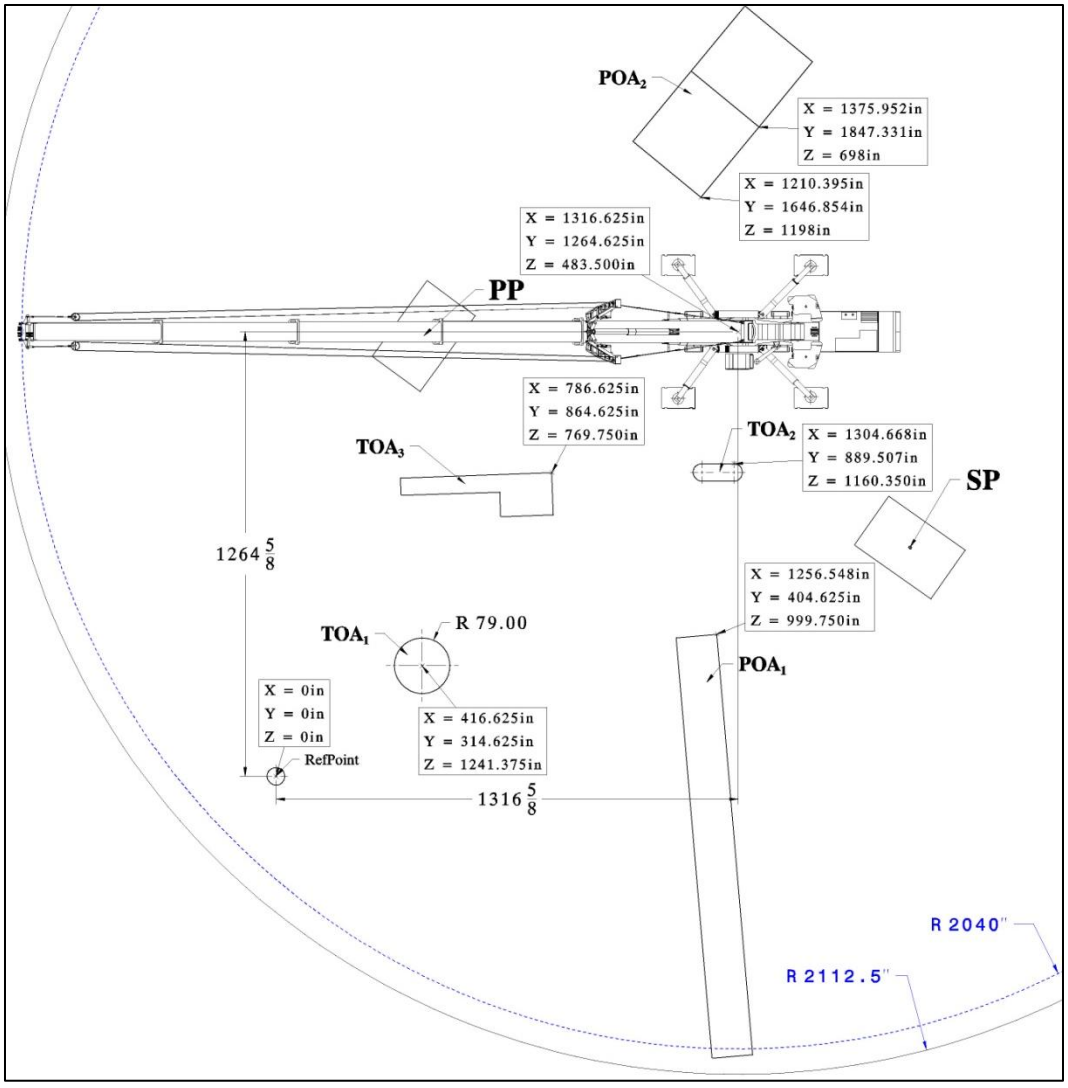

Figure 4.21 Analysis area and recognized obstructions.

Using only the closest point of an analyzed obstruction simplifies calculation and speeds the operation to recognize which obstruction is in conflict with the crane boom envelope. The mathematical calculation of the closest obstruction point's radius, vertical displacement overlays the crane boom envelope position at radius R-2040" and identifies intersections. Conflict obstructions are identified. Figure 4.22 shows graphically projected results of this analysis. It shows that the crane boom intersects only four obstructions (TOA_1, POA_1, POA_{21} and TOA_3), and these obstructions' restricted area will be calculated.

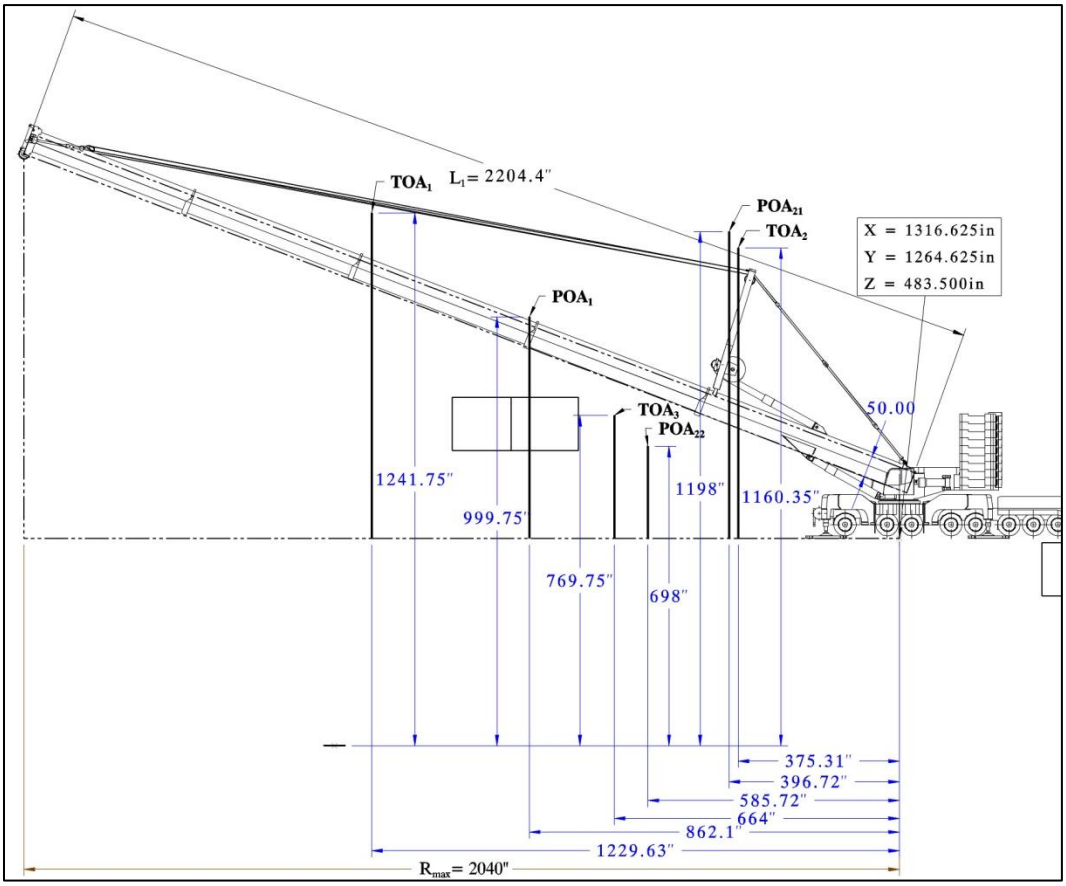

Figure 4.22 Obstruction conflict analysis result.

To clear the intersecting obstructions the crane must be lifted to above the highest point at MOD distance. At that position, the crane boom tip point projection establishes the maximum radius for the particular obstruction area. Figure 4.23 shows calculated maximum radiuses for the closest point of intersecting obstructions. Closest points have a clearance distance 36", which is the established input value for MOD. Rectangular shapes represent crane boom envelopes and the length of the maximum boom tip position.

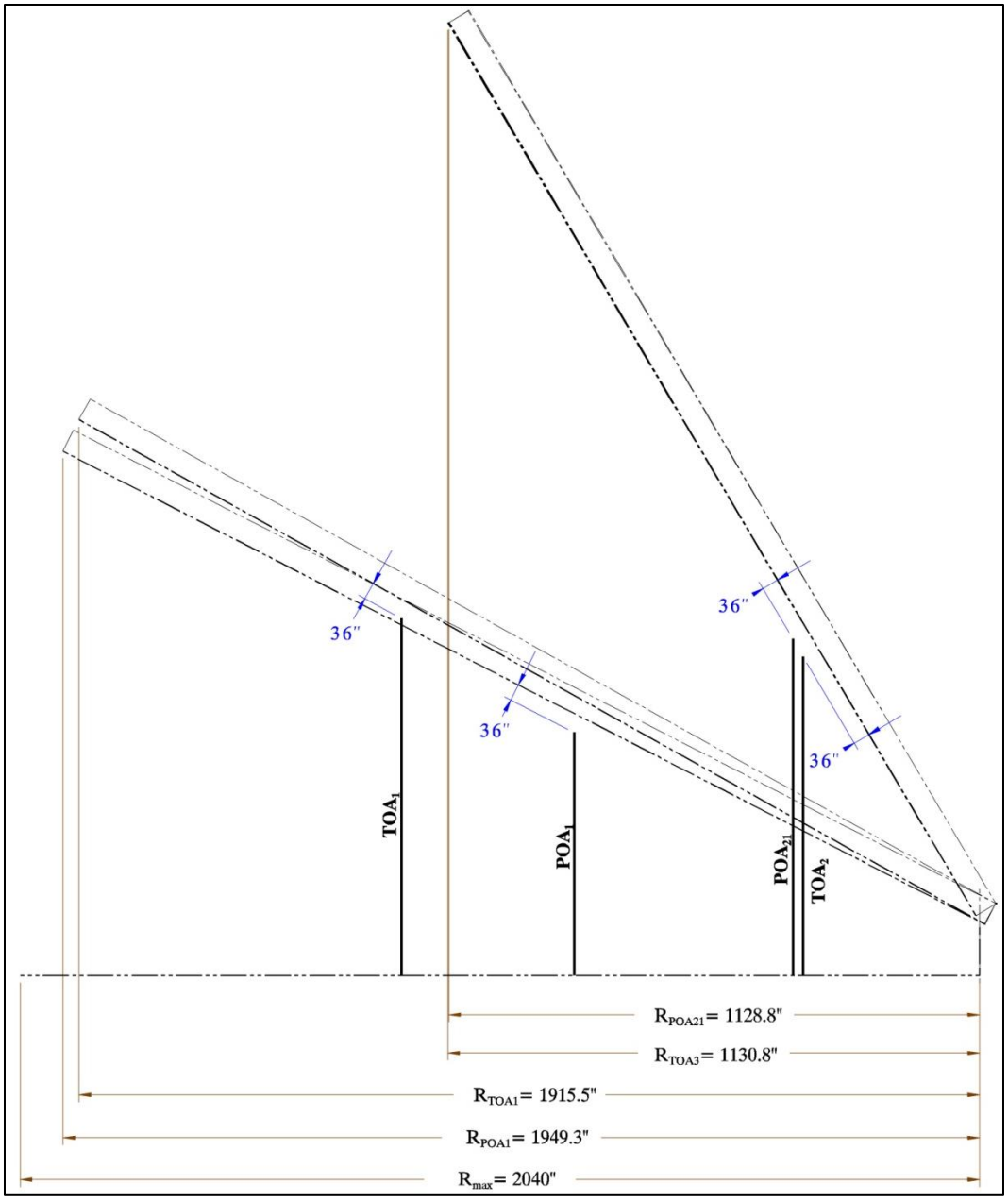

Figure 4.23 Crane boom obstruction maximum radiuses.

The calculated maximum radius for each intersecting obstruction required additional layout boundary offsets radial lines to conclude the area development. They will secure only that portion of the maximum outside radius that directly refers to a particular object. The layout boundary is developed by offsetting obstruction shape by dimension value B' (see equation 4.24). As a result the safety buffer around obstructions is secured. Figure 4.24 shows obstruction offsets, tangent lines, and the imported maximum radius. It shows a shaded area that represents crane boom regions (CBRs). The CBR secures a restricted

area for crane boom movement and is created by a joint operation for all individual obstructions. The CBR area is stored and will be used later in the analysis.

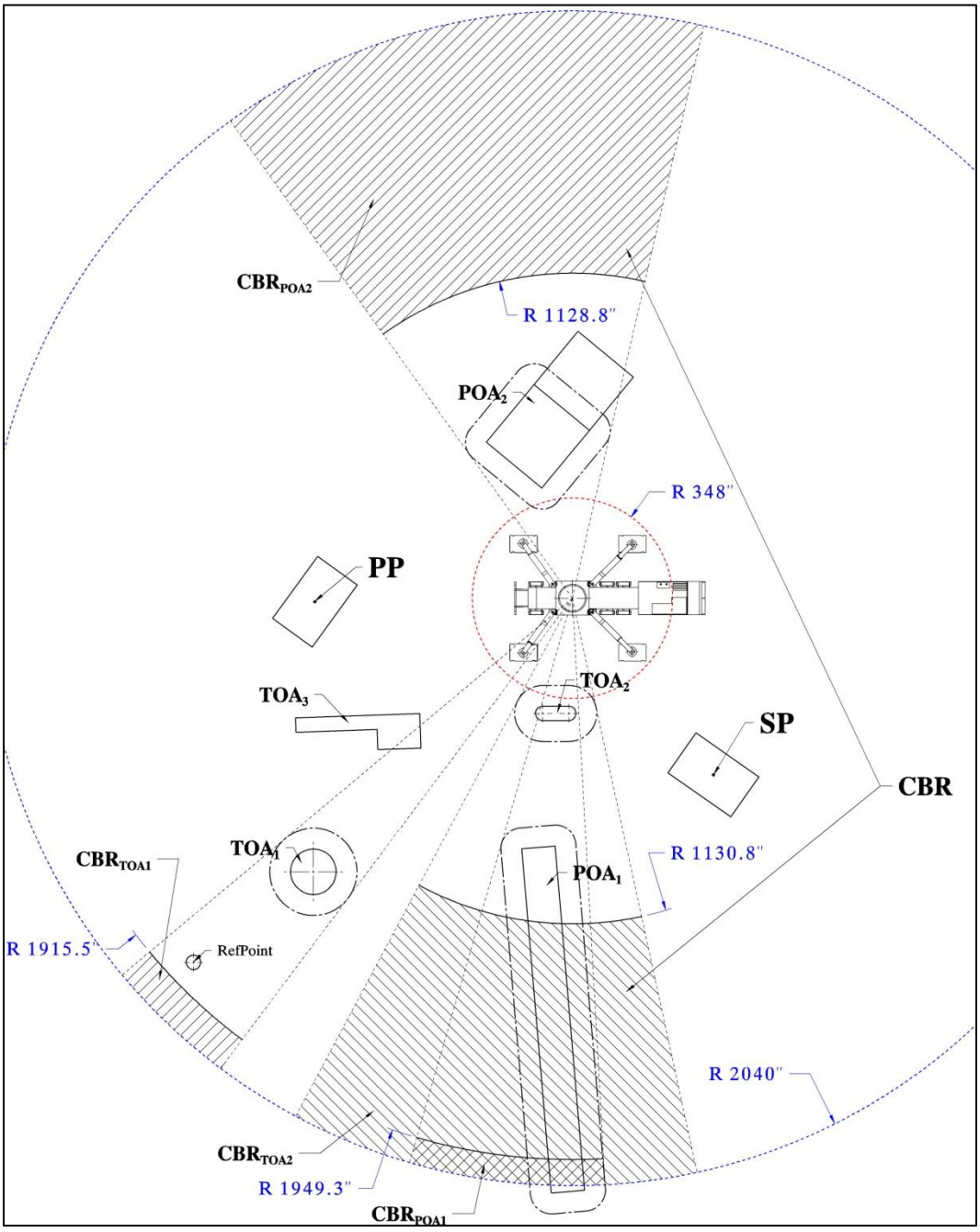

Figure 4.24 Crane boom region calculation.

Phase 3;-Crane Superlift Obstruction Region Analysis (CSR): This phase is not activated because the analyzed crane configuration does not have a wheeled superlift attachment section.

Phase 4;-Object Crane Simplified Trajectory (CST) Path: This phase creates simplified trails in both directions for the lifted object from pick-point (PP) to set-point (SP). The CST path is created at crane elevation. Figure 4.25 shows CST paths for non-reflex trajectory (NRT) angle and reflex trajectory angle (RT).

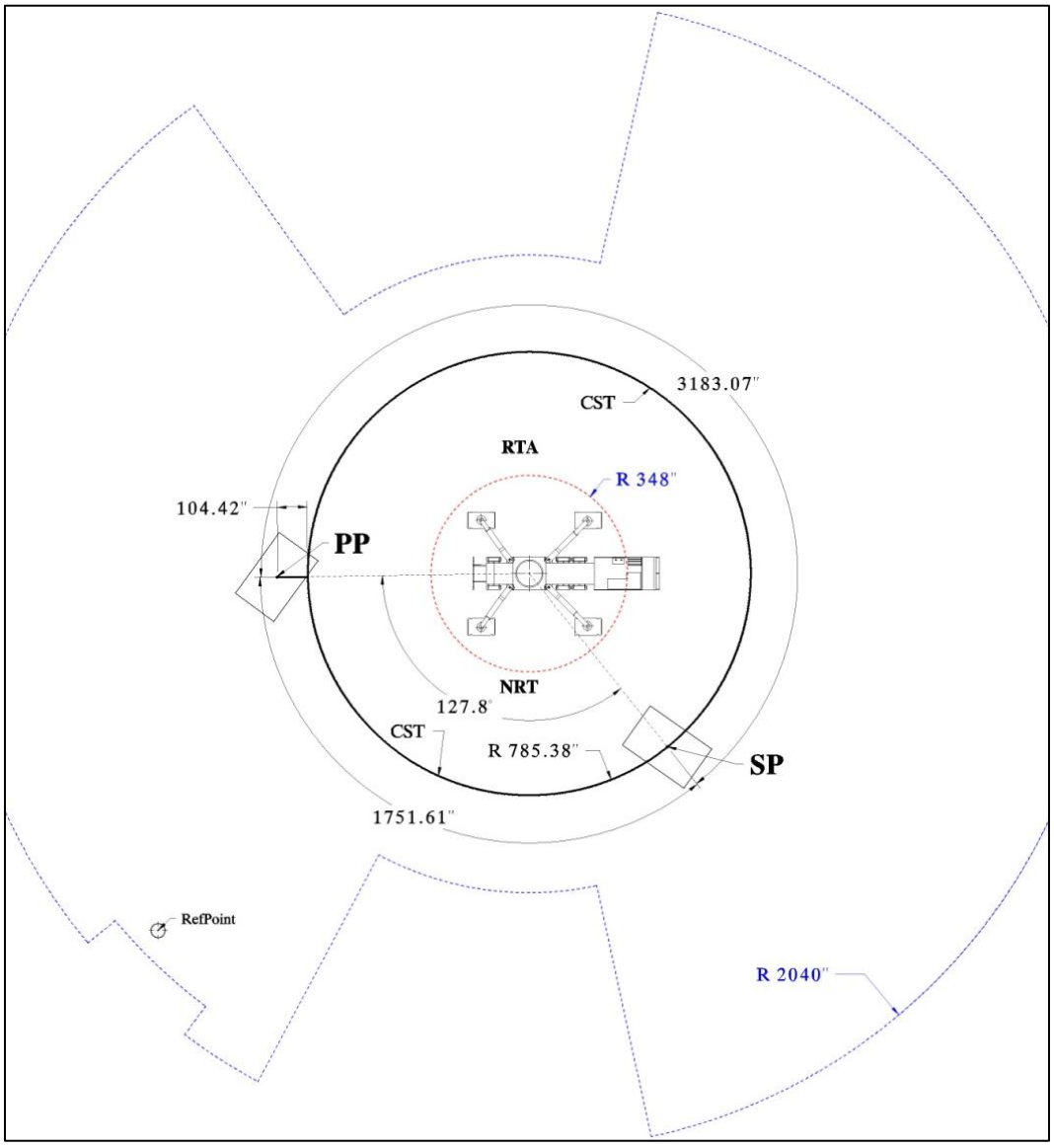

Figure 4.25 Crane simplified trajectory paths.

The CST path starts as a radial line (due to an SP radius -785.38" smaller than PP radius -889.8") from PP to meet the arc created at the SP maximum radius. The path can continue in NRT or RT sections. The NRT section total length equals 1856.03", while the RT section path total length equals 3287.5". The CST path is the basis for developing elevation paths. To create both directions' trajectory possibilities, all available solutions

for a particular crane-object tandem configuration are evaluated. Developed CST paths are stored for further analysis.

Phase 5;-Elevations Definition and Validation: This phase helps identify working elevations. The vertical order (VO-2) rule (see Table 3.2) creates k_1 elevation plane at PP base offset surface called the minimum level. Figure 4.26 shows final results of implementing the VO-2 rule.

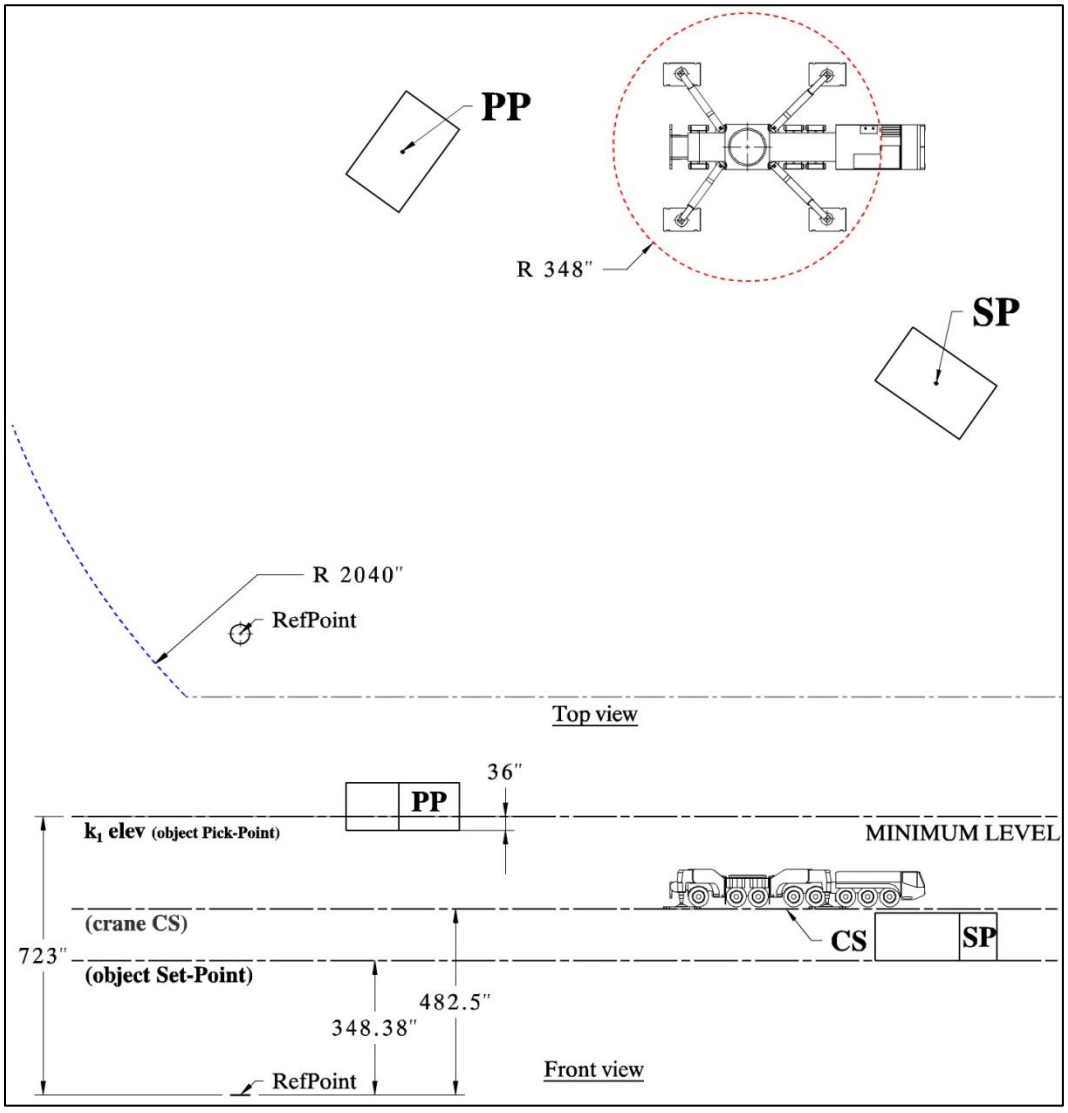

Figure 4.26 Vertical Order and minimum elevation.

The minimum elevation level creates a plane bottom boundary for elevation development. At this lift configuration the SP requires vertical connection only. The next task creates the maximum level boundary limit. The maximum elevation boundary does

not create a working elevation plane but establishes the maximum limit for elevation to be accepted. There are two separate checks that must be performed to establish the maximum limit: one that places the boom tip with full rigged load at R_{min} radius and one that checks the hanging object clearance to the boom envelope. The clearance must not exceed the defined MOD value. Figure 4.27 shows the maximum elevation boundary calculation.

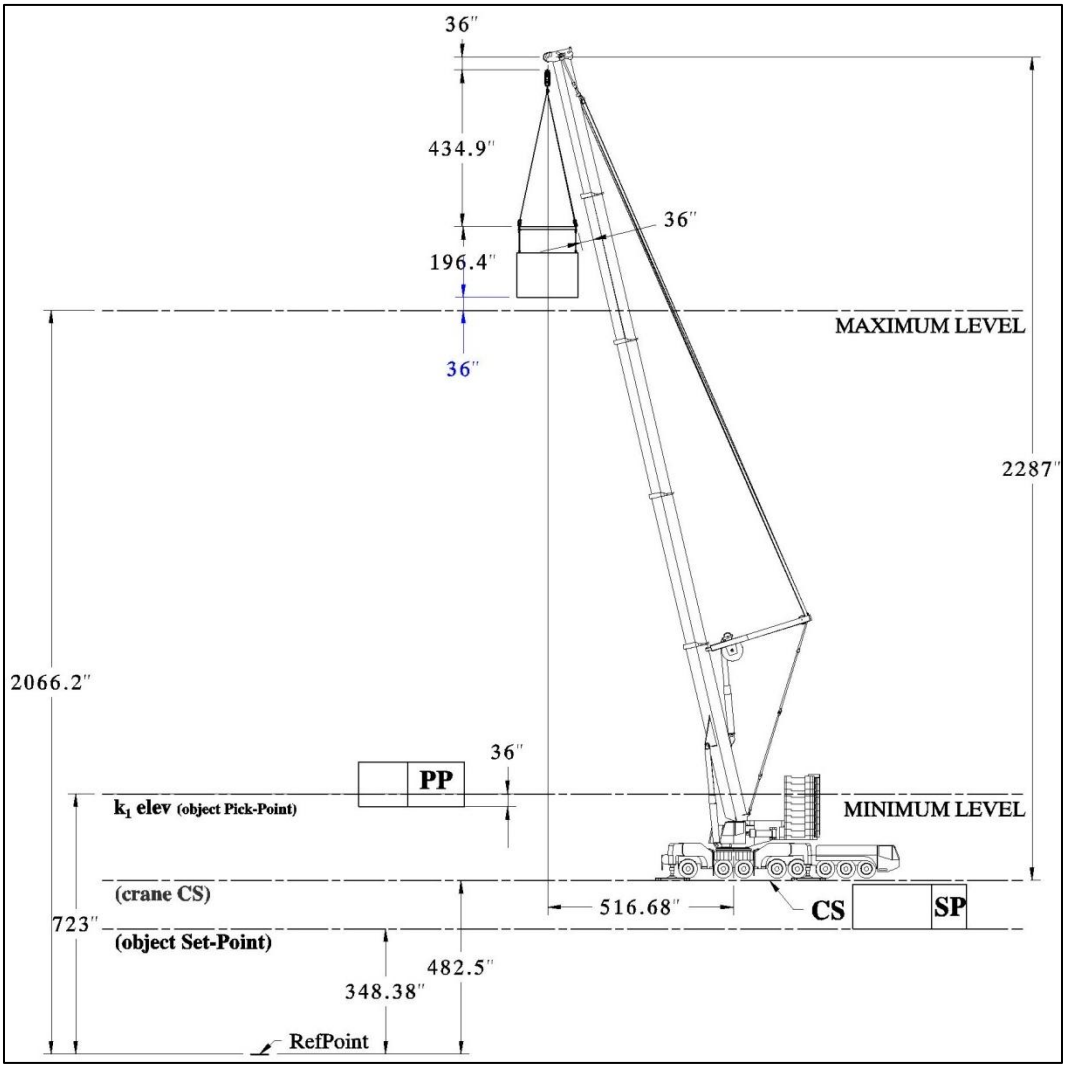

Figure 4.27 Maximum elevation boundary calculation.

Rigging height (RG_H) calculation:

$$RG_H = ATB + RH + OH = 36 + 434.9 + 196.4 = 667.3" \qquad (4.26)$$

Followed by the maximum boundary elevation calculation:

$$M.LEVEL = H_B - RG_H - MOD = 2287 - 667.3 - 36 + 482.5 = 2066.2"(4.27)$$

Object width, rigging height (RG_H), and MOD clearance must be maintained from the crane's tip point. This establishes the new minimum radius R_{MLmin} for the maximum boundary level, which is as follows:

$$R_{MLmin} \geq R_{min} \quad 516.7" > 348" \qquad (4.28)$$

The analyzed obstructions may create working elevations k only between the minimum and maximum boundaries. Obstruction elevations analysis requires recognition of the crane object lift area (COLA), which covers the maximum area where an object may come into contact with possible obstructions. In this case the R_{max} circle is offset by the diagonal object length with an added MOD distance. Figure 4.28 shows the COLA layout area of recognized obstructions.

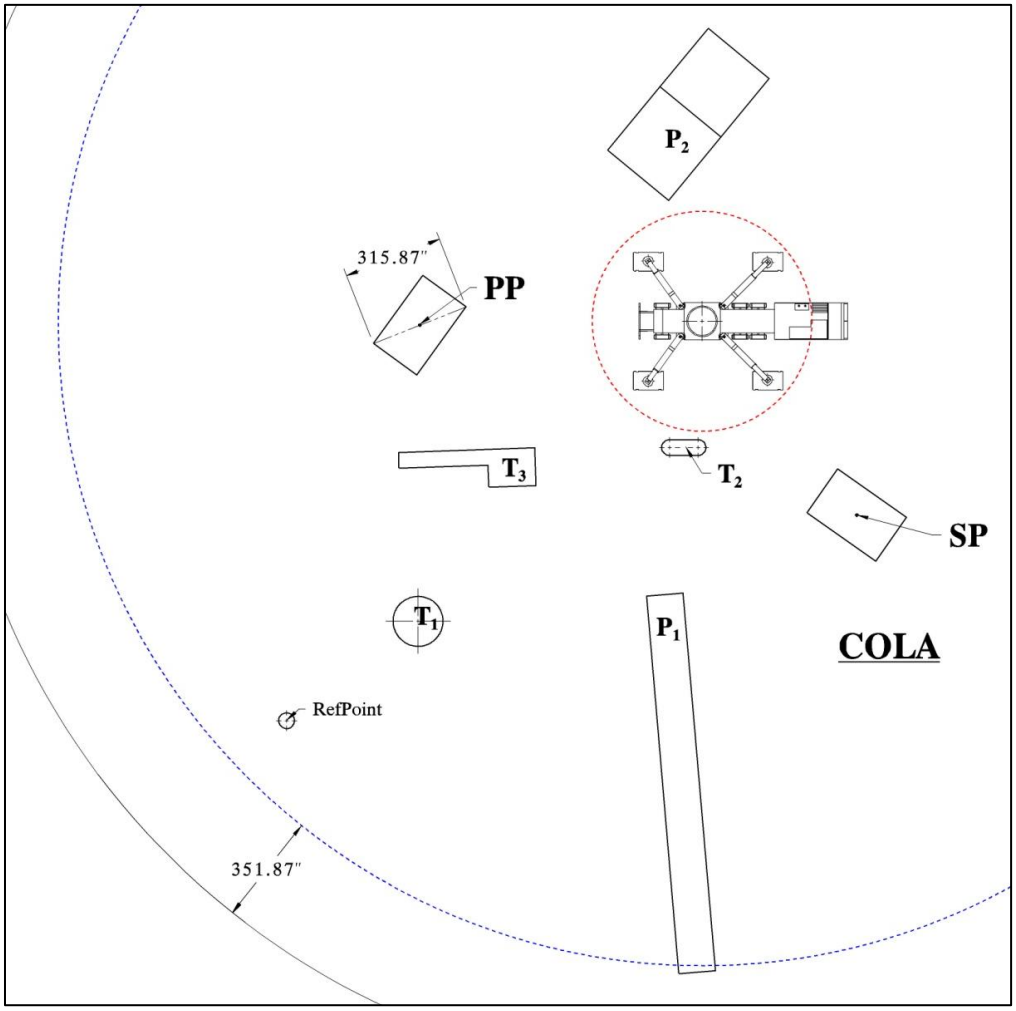

Figure 4.28 COLA development area and obstructions.

There are five obstructions in the COLA area. Each obstruction height will be analyzed for possibility of creating an elevation working plane. Figure 4.29 shows the elevation view and assigned elevation working planes.

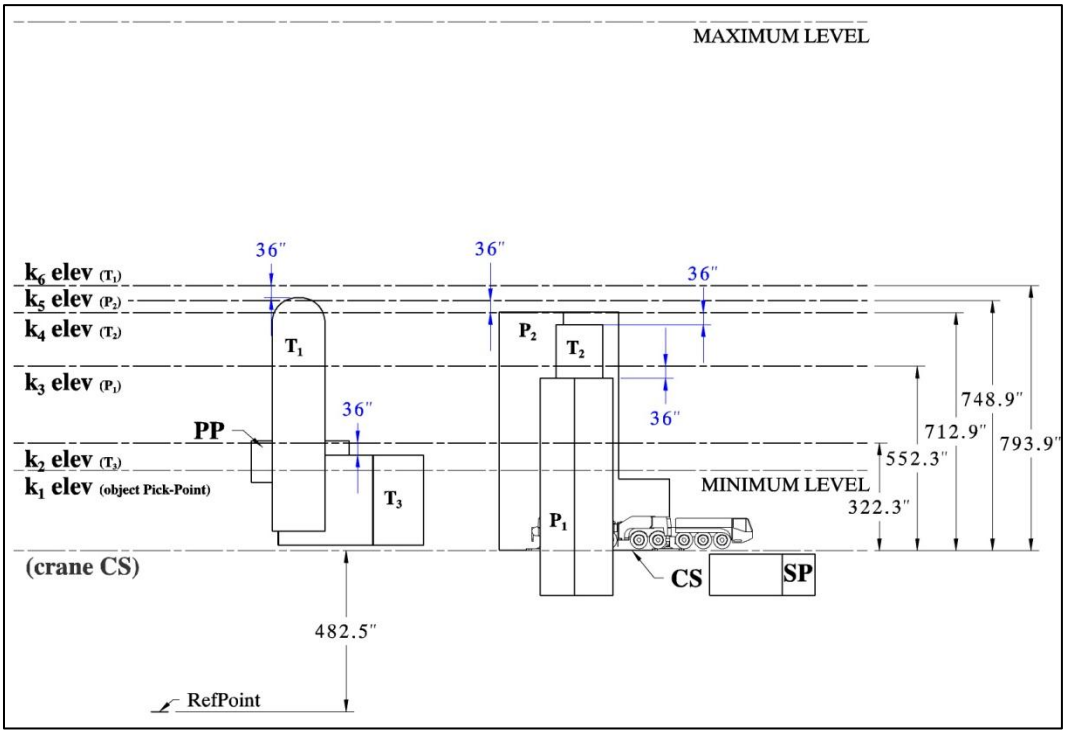

Figure 4.29 Working elevation definition.

Obstruction T_2 has two different heights, but only the tallest creates the elevation working plane due to the lower height residing below the minimum boundary level. There are six elevation working planes created for trajectory analysis. They are referenced from the crane CS point elevation.

Phase 6;-Anchored and Floating Obstructions Analysis: This phase completes its tasks on each elevation separately. It starts with validation and if necessary calculation of the minimum and maximum elevation radiuses. Because elevation radiuses deviate at the highest elevation, the validation procedure starts from the k_6 elevation working plane.

$$R_{max\,k} = \sqrt{L_B^{\,2} - RG_H + k_n - C_h\ ^2} \qquad (4.29)$$

$$L_B^{\,2} = L_1^{\,2} + D^2 = 2204.4^2 + 50^2 = 4861879.4$$

$$R_{max\,6} = \sqrt{4861879.4 - 667.3 + 793.9 - 152.8\ ^2} = 1774.82"$$

$$R_{max\,6} < R_{max} \quad 1774.82 < 2040 \qquad (4.30)$$

$$R_{max\,5} = \sqrt{4861879.4 - 667.3 + 748.9 - 152.8^{\,2}} = 1807.13"$$

$$R_{max\,5} < R_{max} \quad 1807.13 < 2040 \qquad (4.31)$$

$$R_{max\,4} = \sqrt{4861879.4 - 667.3 + 712.9 - 152.8^{\,2}} = 1831.77"$$

$$R_{max\,4} < R_{max} \quad 1831.77 < 2040 \qquad (4.32)$$

$$R_{max\,3} = \sqrt{4861879.4 - 667.3 + 552.3 - 152.8^{\,2}} = 1929.72"$$

$$R_{max\,3} < R_{max} \quad 1929.72 < 2040 \qquad (4.33)$$

$$R_{max\,2} = \sqrt{4861879.4 - 667.3 + 322.3 - 152.8^{\,2}} = 2040.01"$$

$$R_{max\,2} > R_{max} \quad 2040.01 > 2040 \qquad (4.34)$$

The calculated results show that the left side of equations 4.30, 4.31, 4.32 and 4.33 were smaller than the right side; meaning that the maximum elevations radiuses were smaller than the crane maximum R_{max} for this load. Only the calculated maximum radius at elevation k_2 was larger than crane R_{max}, and in this situation R_{max} creates the elevation outside the boundary.

The next step checks the position of elevation $R_{min\,k}$, which must satisfy equation 4.35:

$$R_{min\,k} = L_1 \cos\beta_k - C_1 \qquad (4.35)$$

$$\beta_6 = 83.62°$$

$$R_{min\,6} = L_1 \cos\beta - C_1 = 2204,04 * \cos 83.62 - 35.44 = 209.54"$$

$$R_{min\,6} < R_{min} \quad 209.54 < 348 \qquad (4.36)$$

It is not necessary to calculate lower elevations $R_{min\,k}$ since $R_{min\,6}$ is already lower than R_{min} (see equation 4.36). For analysis R_{min} is transferred to each elevation and acts as elevation $R_{min\,k}$.

Once $R_{max\,k}$ and $R_{min\,k}$ are calculated, the next step projects the CST path onto each elevation plane and recognizes anchored and floating obstructions. Figure 4.30 shows the elevation k_1 projected CST path, analyzed area, and recognized obstructions offsets.

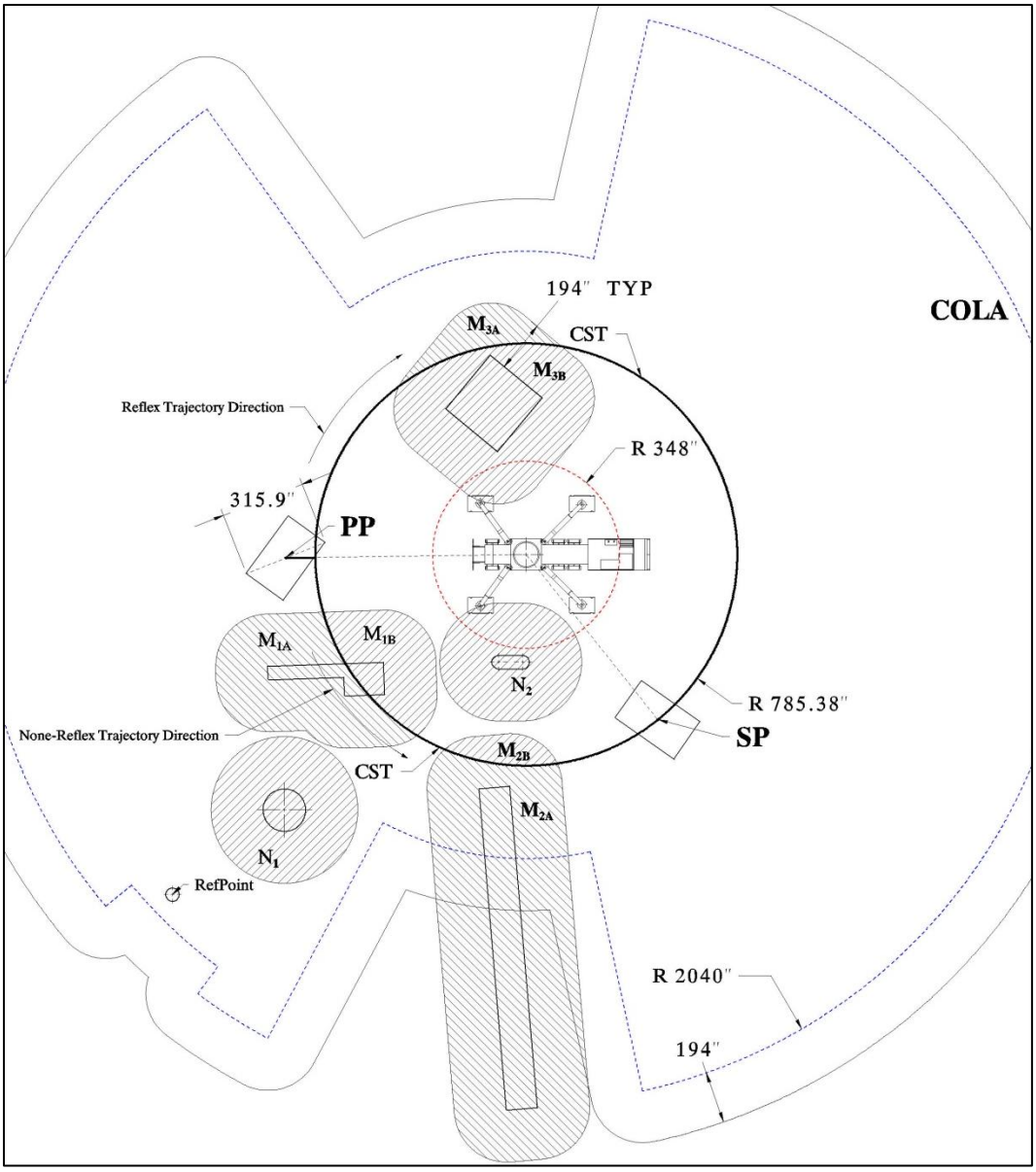

Figure 4.30 Elevation k_1 path and obstruction recognition.

The analyzed area is offset (*L'*) value, which creates elevation COLA.

$$L' = \frac{L_d}{2} + MOD = \frac{315.9}{2} + 36 = 194" \qquad (4.37)$$

In created COLA obstructions are recognized and the offset is applied to obstruction boundaries. Convex corners are automatically rounded to (*L'*) radius value. Obstruction offset areas, which intersect the CST paths, are renamed to anchored "M" obstruction offsets, and those which do not intersect the CST path are renamed to floating "N" obstruction offsets. Anchored obstruction offsets are divided into A and B parts by the

CST path. Parts A resides outside the CST path, parts B inside. Figure 4.30 shows the anchored obstruction offsets divided by CST paths. At elevation k_1, $R_{min\ 1}$ and $R_{max\ 1}$ are the same as crane R_{min} and R_{max}, respectively. For the next five elevation paths and obstruction recognition refer to Appendix A-16 through Appendix A-20, respectively.

Phase 7;-Elevation Trajectory Path Development: This phase creates complete or partial paths at each recognized elevation. Already calculated CST paths are modified depending on identified elevation obstruction offsets. Figure 4.31 shows the developed trajectory path for elevation k_1.

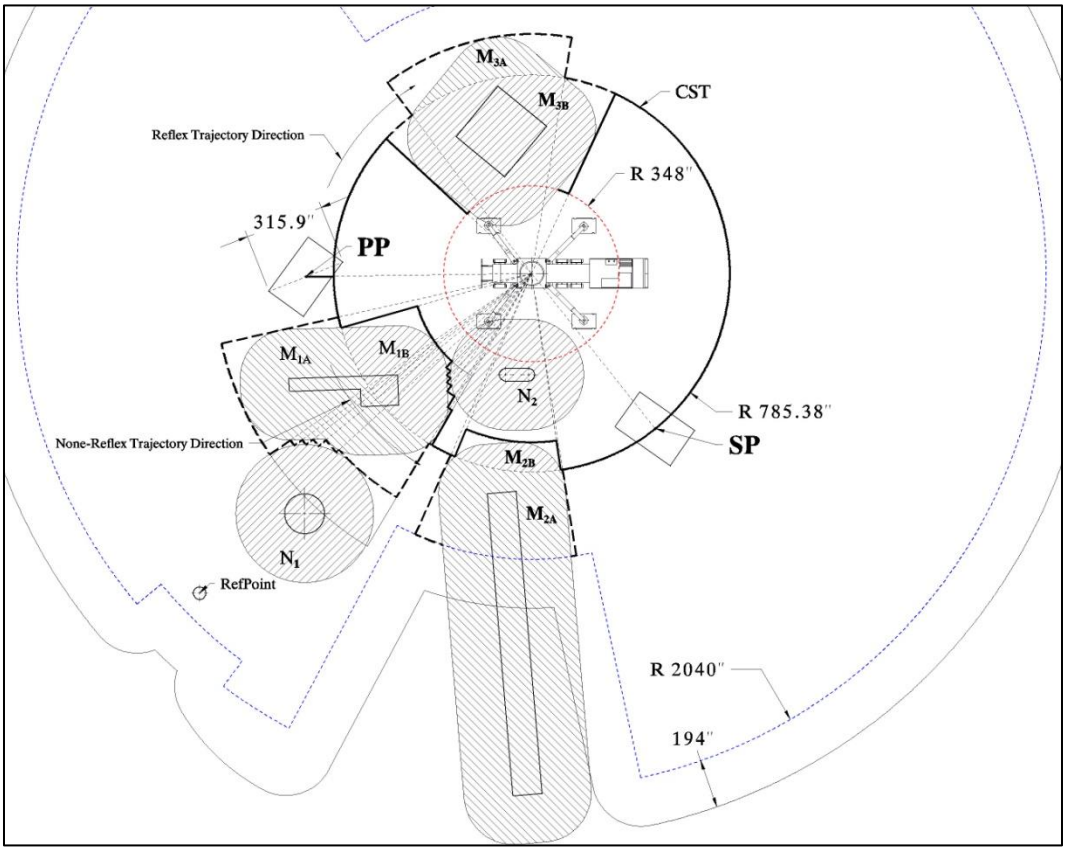

Figure 4.31 Developed object path trajectory for k1 elevation.

The Figure shows attached tangent lines to anchored obstruction offset in both directions A (outside dotted) and B (inside solid) and an oscillating step for passing nearby floating obstructions. Developing path around M_{2A} offset obstruction at direction A shows a partial trajectory path creation (dotted lines). The operation of creating either a full or partial trajectory path in non-reflex and reflex directions ends at the SP point. Because Phase 6 and Phase 7 are on an elevation loop, the trajectory elevation path

operation ends when all elevations are checked. For the next five elevation paths' trajectory development refer to Appendix A-21 through Appendix A-25, respectively.

Phase 8;-Object Trajectory Path Optimization: This phase starts by recognizing all critical points, curves, and lines at each elevation and dividing them if necessary. It takes each line's end points and checks that the below and above curves are not in the projected crossing conflict that means there will be line continuity. If the line does cross, it divides such line into two separate pieces, recording coordinate of the intersecting gate point "GP". GP points allow the algorithm to cross between elevations. When all elevations paths are prepared, vertical connections join elevations at GP points in both directions. Table 4.1 includes all recognized points, with the shaded area representing non-gate points. Appendix A-26 shows all recognized directional points.

Table 4.1 Elevation path direction points.

Point	X	Y	Z	Point	X	Y	Z
102	421.71	1252.13	688.00	152	740.47	1798.34	723.00
701	1806.50	650.75	349.38	153	1061.33	1501.12	723.00
103	421.71	1252.13	723.00	154	1070.57	1510.72	723.00
104	531.33	1253.66	723.00	201	531.33	1253.66	804.80
105	550.38	1092.35	723.00	202	550.38	1092.35	804.80
106	560.90	1050.86	723.00	203	560.90	1050.86	804.80
107	864.37	1136.70	723.00	204	910.78	592.24	804.80
108	1000.75	916.60	723.00	205	922.60	585.24	804.80
109	978.65	892.25	723.00	206	996.65	547.39	804.80
110	994.90	878.12	723.00	207	856.21	232.59	804.80
111	980.86	861.25	723.00	208	963.70	191.07	804.80
112	994.98	849.91	723.00	209	1012.83	540.39	804.80
113	981.85	832.97	723.00	210	1058.20	648.54	804.80
114	999.05	820.16	723.00	211	1414.63	603.76	804.80
115	983.08	797.81	723.00	212	1431.84	487.75	804.80
116	1012.23	778.30	723.00	213	1439.60	488.94	804.80
117	984.52	734.03	723.00	214	1493.58	148.49	804.80

When trajectories' points are identified, connections between them are recognized and adequate parameters assigned. For example a curve will have a start and end point as well as radius value. Table 4.2 shows connections' data and calculated length. Full connection points' data is available in Appendix A-27.

Table 4.2 Connection points' data.

ID	Start	End	Type	Dist	ID	Start	End	Type	Dist
87	204	131	Vd	81.80	130	147	219	Vu	81.80
88	132	205	Vu	81.80	131	219	147	Vd	81.80
89	205	132	Vd	81.80	132	301	302	C	162.72
90	133	206	Vu	81.80	133	302	303	C	42.80
91	206	133	Vd	81.80	134	303	304	C	590.67
92	134	207	Vu	81.80	135	304	305	C	13.73
93	207	134	Vd	81.80	136	305	306	C	83.20
94	135	208	Vu	81.80	137	306	307	C	17.64
95	208	135	Vd	81.80	138	307	308	C	427.56
96	136	209	Vu	81.80	139	308	309	C	7.86
97	209	136	Vd	81.80	140	309	310	C	405.48
98	137	210	Vu	81.80	141	301	318	C	597.78
99	210	137	Vd	81.80	142	318	319	L	437.37
100	138	211	Vu	81.80	143	319	320	C	13.33
101	211	138	Vd	81.80	144	318	317	C	139.01
102	139	212	Vu	81.80	145	317	316	L	162.42
103	212	139	Vd	81.80	146	316	315	C	773.09
104	140	213	Vu	81.80	147	315	314	L	162.42
105	213	140	Vd	81.80	148	314	311	C	212.06
106	141	214	Vu	81.80	149	311	312	L	437.38

Each connection type is assigned a penalty value. Switching from a vertical up (*Vu*) to a curve (*C*) connection has a different penalty value than switching from a vertical down (*Vd*) to line (*L*) connection. Table 4.3 shows crane speed definition.

Table 4.3 Crane speed definition.

straight - horizontal	S	150	ft/min
curve - horizontal	C	300	ft/min
vertical up	Vu	50	ft/min
vertical down	Vd	50	ft/min

Depending on the crane movement, crane speed values can change and new parameters assigned. Table 4.4 shows elevation change penalties, which favor lower elevation for operations.

Table 4.4 Elevation penalties.

k_1-elevation	no penalty
k_2-elevation	add 10%
k_3-elevation	add 10%
k_4-elevation	add 10%
k_5-elevation	add 10%
k_6-elevation	add 10%

Changing directions horizontally and/or vertically is also penalized, and values may be modified accordingly. Table 4.5 shows changing direction penalties.

Table 4.5 Changing direction penalties.

Straight - Curve	S-C	0.25	min
Curve - Straight	C-S	0.25	min
Straight - Vertical Up	S-Vu	0.25	min
Vertical Up - Straight	Vu-S	0.25	min
Straight - Vertical Down	S-Vd	0.25	min
Vertical Down - Straight	Vd-S	0.25	min
Curve - Vertical Up	C-Vu	0.25	min
Vertical Up - Curve	Vu-C	0.25	min
Curve - Vertical Down	C-Vd	0.25	min
Vertical Down - Curve	Vd-C	0.25	min

With all points' data coordinates, connection identifications, and speed movement and penalties assigned, simple database queries can provide information about minimum weight path from PP to SP. Figure 4.32 shows the form created to run the optimization algorithm.

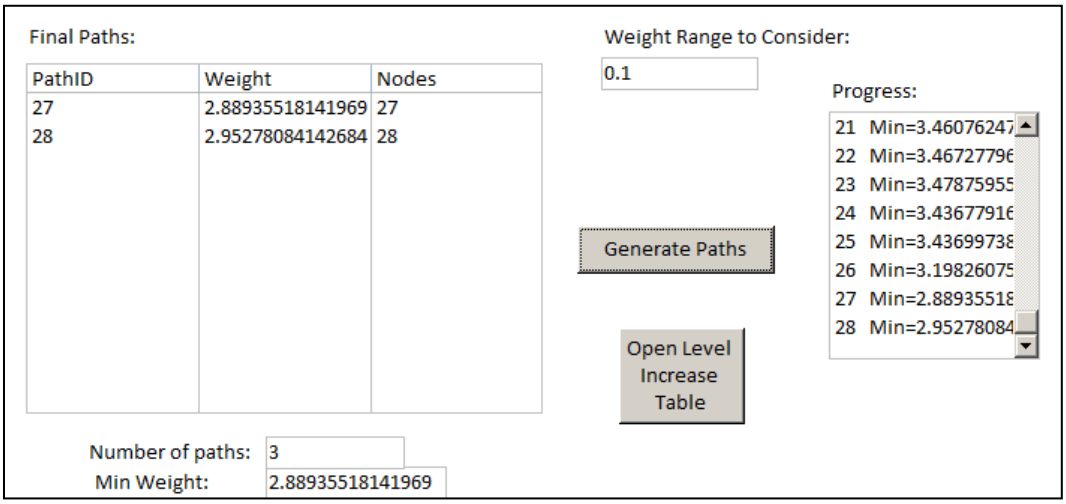

Figure 4.32 Optimization program form interface.

The form presents path ID, total path weight, and number of path nodes. Changing the weight range allows evaluating other paths that are within such values. Figure 4.32 shows path ID 27 with minimum weight of 2.8893 minutes. Lifted object must change direction 12 times during placing operation (see Table 4.6). There is no restriction about object position through the lifting operation, since assigned obstruction offsets cover the maximum diagonal object measurement. Table 4.6 shows object path points' sequence, starting from pick-point (102) and finishing at set-point (701).

Table 4.6 Path point sequence

ConnID	Start	End	Dist
1	**102**	103	35.00
2	103	104	109.63
43	104	152	597.78
46	152	151	139.01
47	151	150	162.42
48	150	149	773.09
49	149	148	162.42
50	148	145	212.06
53	145	144	1593.54
42	144	**701**	373.63
		Sum	**4158.58**

The table also indicates a total length of 4158.58 inches, and dividing that amount by 2.8893 minutes gives an average speed of 119.9 ft/min, which is acceptable movement of the crane. Figure 4.33 shows lifted object available paths web and the minimum path between two points.

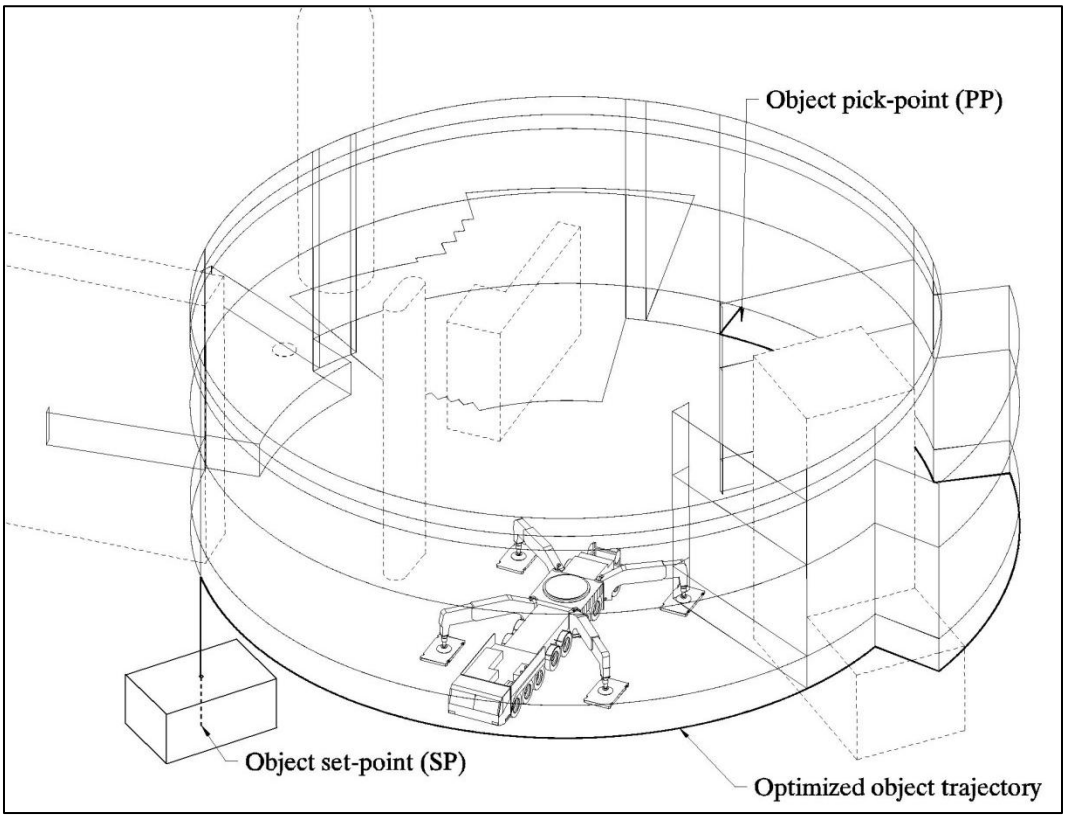

Figure 4.33 Minimum weight lifted object trajectory path.

The algorithm stores the minimum weight path and then starts analysis for the next lifted object.

CHAPTER 5 – CONCLUSION

5.1 General Conclusion

It is expected that the crane lifting analysis in presented lifting cases will generate sufficient information, such that the results may be applied to any specific critical lift within the construction industry. Analyses of potential interferences and clashes have provided very useful information when performed in advance. With increasing advancement in crane capacity and functionality, supported by computerized control movements, the risk of mishandling heavy loads rises exponentially and its consequences can be tragic. Independent consulting firms evaluating crane-related accidents determined that the human factor is the weakest link. Their reports strongly encourage using the crane manufacturer's implemented algorithms to control or help operators safely evaluate lifting situations. At the same time, implementing a crane automation process increases the lifetime of already expensive equipment. Finding the right balance between crane automation and safest operation is a difficult task, and the results may not be impartial. This research is a tool for professionals to harness many variables related to safer and economical lift analysis, especially unknown lifted object trajectory paths.

5.2 Research Contribution

Space management on construction sites for industrial projects is essential. Planners and engineers on typical project sites face constant changes and equipment allocation. Cranes, the most expensive equipment on construction sites, require proper location planning in advance to avoid costly relocations. Currently, practitioners analyze heavy lifts manually based on individual experiences using spreadsheets to simplify repetitive calculations. However, this method does not solve complicated problems with satisfactory results, but instead is slow and prone to errors. Although this method produces results, it is not the optimal solution since an individual approach has a subjective outcome. Generations of engineers have based their techniques of lifts analysis on CAD systems. Although they do not have a problem operating programs, they are deficient in lift expert knowledge. The algorithm presented in this research has embedded the expert knowledge in the form of tasks and best decision practices. The algorithm will help engineers confirm findings or influence their opinions. Experienced engineers may analyze lifted object trajectory by drawing circles or lines around obstructions to mimic crane movements, but the solution

may not be the right one, and a stepped algorithm would help find the most economical result. The algorithm structure is based on the simplification of complicated crane movement. It focuses on three major transformations: radial movement, plane rotation, and vertical up or down displacement. In practice, crane operators activate in one direction movement at the time and are rarely able to observe a combination of movements at the same time. Thus, it's difficult to envision all possible lifted object paths from pick-point to set-point. In fact, a simplification developed in 2D layout was expanded to a 3D environment. By focusing only on significant obstructions' height elevation, the vertical constant grid offset operation is eliminated, further simplifying the developed algorithm. In previous work, some researchers evaluate elevation conflict by creating vertical planes at specific intersections [Al-Hussein et al. 2005] and analyzing clearance distances. This algorithm analyzes all elevation planes for possible clashes and not just at the intersected spot. When several elevation paths are created, custom routines are introduced which allow full or partial trajectory connections. Such methods have not been presented in any publication related to crane lifting operations. When all paths are collected, distances are calculated and speed for radial movement or angular rotation is assigned. In that moment each displacement is weighted. In real lift operations changing direction requires slowing down the crane boom movement and accelerating again. In the algorithm, this operation is penalized depending on the direction the lifted object is displaced. When all weights and penalties are assigned to the spatial trajectories web, the graph finding algorithm presents results as the optimized trajectory path.

5.3 Limitation of Research

As no research endeavor has unlimited resources, this one also experienced its limitation constraints. Even though detailed planning at the beginning set major milestone days for specific accomplishments, as the research progressed the plan had to be rewritten and new milestones set. During research advancement many interesting topics were dropped due to time constraints. However, although the publication evaluation covered in the literature review presented current trends and partial solutions, it did not provide a united method for manual crane lifts and location optimization, not to mention automation of such operations. The publication resources' limitations promote innovation and development of new ideas, but they must be realistic and practical. Expertise knowledge limitation, which could propel such inventions, was the next challenge on the road of research. Developing complex algorithms for trajectory optimization required intensive

programming knowledge, and the skill of converting years of crane lifting operation expertise into computer code language. The limits of experienced engineers in crane lifting operation knowledge did not allow for objective solutions to specific lifts. Also, the presented data, case study, and validation suggestion give an impression of research generality and uniqueness, but are based only on a program code sample. In depth program code development and full real complex scenario assessment is required.

5.4 Recommendation for Future Research

As mentioned in the previous section, many aspects of the research which are significant to proper algorithm function had to be dropped, due to research constraints,. In this thesis the obstruction offset area was calculated based on maximum diagonal shape distance and the result was provided. Future work requires full minimum diagonal shape distance analysis evaluation. The method of this analysis must be developed, and it may cover already analyzed maximum diagonal distance. The assigned lift change direction, and elevation displacement weight and penalties were basic for the reason of simplifying an already complex method. Future research should concentrate on full development of weight and penalties matrix, and this activity may be expanded as an independent research topic. Full exploitation, validation, and confirmation of the functionality of the developed algorithm can be properly tested only in a 3D digital environment. As such, 3D animation and visualization of lifted object path, crane position, and repercussion of conflict with passing obstructions are the next steps for future research. Rapidly changing computer technology and advancement in programming code simplification opens the door for the next impartial research subject. Presented research discussed a single crane and lift analysis, but when multi-crane lift operations are performed, the algorithm cannot be utilized. It compels the development of a new process that can be based on a single operation, which must consider a number of crane lift operations at the same time. New constraints, rules, and codes must be developed and the complexities of such operations need to be considered in future research.

Research Publications

Journal Article:

- Olearczyk, J., Al-Hussein, M., Bouferguene, A. and Telyas, A. (2009). "Industrialization of the Construction Process." Published in Canadian Civil Engineer, winter 2009-2010, 26.5, 10-12.

Conference Papers:

- J. Olearczyk, Ulrich (Rick) Hermann, M. Al-Hussein, A. Bouferguene (2010). "Spatial trajectory analysis for cranes operations on construction sites." Published in the Proceedings of the 2010 Construction Research Congress, Banff, Canada, May 8-11, 2010, 359-368.
- U. (Rick) Hermann, A. Hendi, J. Olearczyk, M. Al-Hussein (2010). "An integrated system to select, position, and simulate mobile cranes for complex industrial projects." Published in the Proceedings of the 2010 Construction Research Congress, Banff, Canada, May 8-11, 2010, 267-276.
- Olearczyk, J., Al-Hussein, M., Bouferguene, A. and Telyas, A. (2009). "Construction automation for modular assembly." Published in the Proceedings of 1st International conference on improving construction and use trough Integrated Design Solutions, Espoo, Finland, June 10-12, 2009.
- Olearczyk, J., Al-Hussein, M., Bouferguene, A. and Telyas, A. (2009). "Virtual construction automation for modular assembly operation." Published in the Proceedings of the 2009 Construction Research Congress, Seattle, WA, April 5-7, 2009. 406-415.
- Olearczyk, J., Al-Hussein, M., Bouferguene, A. and Telyas, A. (2008). "Interactive 4D Modeling for Modular Building Construction." Published in the Proceedings of the 2008 CSCE Annual Conference, Quebec City, Canada, June 10-13, 2008.
- Olearczyk, J., Al-Hussein, M., Bouferguene, A. and Telyas, A. (2007). "Crane layout optimization for five new student residence buildings at Muhlenberg, MacGregor Village in Allentown, Pennsylvania." Project Final Report for Kullman Building Corp. Lebanon, NJ, USA, September 2007.

Bibliography

Ahuja, R.K., Orlin, J.B., Pallottino, S., and Scuttela, M.G. (2002). "Dynamic Shortest Paths Minimizing Travel Times and Costs." *Massachusetts Institute of Technology* (MIT), Sloan School of Management, Working Paper 4390-02, August 9, 2002.

Alexandrov, N., and Dennis, J.E. (1994). "Algorithms for Bi-level Optimization." ICASE *Universities Space Research Association*, NASA, Langley Research Center, 1994.

Al-Hussein, M., Alkass, S. and Moselhi, O. (2000). "D-Crane: a database system for utilization of cranes." *Canadian Journal of Civil Engineering*, 27 (6), 1130-1138.

Al-Hussein, M., Alkass, S., and Moselhi, O. (2001). **"**An algorithm for mobile crane selection and location on construction sites." *Construction Innovation Journal*, UK, 1-91–105.

Al-Hussein, M., Alkass, S. and Moselhi, O. (2005). "Optimization Algorithm for Selection and on Site Location of Mobile Cranes". *Journal of Construction Engineering and Management*, ASCE 131(5), 579-590.

Amato, F., Basile. F. and Chiaccho. P. (2002). "Crane and Shuttle Optimization in Warehousing Systems." Published in the Proceedings of the *2002 IEEE International Conference on Robotics & Automation*, Washington, DC.

Ascheuer, N., Grotschel, M., and Abdel-Aziz Abdel-Hamid, A. (1999). "Order Picking in an Automatic Warehouse: Solving Online Asymmetric TSPs." *Mathematical Methods of Operations Research*, Springer-Verlag.

Atkinson, A., Payling, J., Lucas, B. and Gray, K. (2001). "Affordable Housing Adaptation Using Modular Construction - A Case Study in Applied Project Management." CIB World Building Congress, Wellington, New Zealand.

Azimov, D. (2005). "Active Rocket Trajectory Arcs: A Review." *Automation and Remote Control*, Vol. 66, No.11, 1715-1732.

Bergounioux, M., and Haddou, M. (2006). "A regularization method for ill-posed bi-level optimization problems." MAPMO-UMR 6628 *Universite d'orleans* – BP 6759 March 31, 2006.

Bernold, L. (2002). "Spatial Integration in Construction." *Journal of Construction Engineering and Management*, ASCE 128 (5), 400-408.

Bialas, W., and Karwan, M. (1984). "Two-level Linear Programming." *Management Science*, 30(8), 1004-1020.

Bock, T. (2007). "Construction Robotics." *Autonomous Robotics* 22, 201-209.

Booth, W. (2007). "House Proud." *Smithsonian Magazine. Science and Technology.*

Boussedjra, M., Bloch, C., and El Moudni, A. (2004). "An Exact Method to Find the Intermodal Shortest Path (ISP)." Proceedings of the 2004 IEEE International Conference on Networking, Sensing & Control, Taipei, Taiwan, March 21-23, 2004, 1075-1080.

Cardenas, A. and Domenech, F. (2005). "Assembly Required." *American School & University*, 74(4), 39-41.

Cartz, J.P. and Crosby, M. (2007). "Building High-Rise Modular Homes." *The Structural Engineer*, 9, 20-21.

Chanron V., Lewis, K., Murase, Y., Izui, K., Nishiwaki, S., and Yoshimura, M. (2005). "Handling Multi Objectives in Decentralized Design." Published in the Proceedings of the IDETC/CIE 2005 ASME International Design Engineering Technical Conferences & Computers and Information in Engineering, September 24-28, 2005, Long Beach, California, USA.

Chehayeb, N. and AbouRizk, S. (1998). "Simulation-Based Scheduling with Continuous Activity Relationships." *Journal of Construction Engineering and Management*, ASCE, 124, 107-115.

Da Cunha C., Agard, B., and Kusiak, A. (2007). "Design for Cost: Module-Based Mass Customization." *IEEE Transaction on Automation Science and Engineering*, 4(3), 107-121.

Deen, Ali M.S.A., Babu, N.R. and Varghese, K. (2005). "Collision Free path Planning of Cooperative Crane Manipulators Using Genetic Algorithm." *Journal of Computing in Civil Engineering*, ACSE/ April 2005 19(2), 182-193.

Del Rio-Cidoncha, M.G., Iglesias, J.E., and Martinez-Palacios, J. (2007). "A Comparison of Floor plan Design Strategies in Architecture and Engineering." *Automation in Construction*, 16, 559-568.

Dempe, S., and Richter, K. (2000). "Bi-level programming with knapsack constraints." *Central European Journal of Operations Research*, 8(93) 107.

Dempe, S. (2001). "Discrete Bi-level Optimization Problems." Institut fur Wirtschaftsinformatic, Universitat Leipzig, D-04109, Leipzig, Germany, Oct. 15, 2001.

Dolan T.C. (2006). "Instant classrooms." Construction, *School Planning and Management*, 4(1).

Editorial Hospital (2006). "Modular technique builds new hospital wing." News, *Hospital Development* (HD). July 20, 2006, Published by Wilmington Media Ltd, 3.

Editorial Health (2007). "Building Systems: Modular mission." *Hospital Development* (HD). April, 2007, 29.

Editorial Leonard (2007). "RAIC Award – Innovation in Architecture: "Leonard Avenue Modular Housing." *Canadian Architect*, 05, 28-29.

Editorial Off-Site (2006). "Off-site construction guide goes online." News, *Hospital Development* (HD). September 21, 2006, Published by Wilmington Media Ltd., 3.

Editorial Operating (2007). "Modular operating theatres for Cannock Chase Hospital." News, *Hospital Development* (HD). May 03, 2007, Published by Wilmington Media Ltd., 3.

Editorial Pharmacy (2008). "Modular build for hospital pharmacy." News, *Hospital Development* (HD). August 28, 2007, Published by Wilmington Media Ltd. 4.

Ehrsson H. (2007). "The Experimental Induction of Out-of-Body Experiences." Brevia, *Science*, 317, 1048.

El Beltagi, E. and Hegazy, T. (2001). "Hybrid Al-Based System for Site Layout Planning In Construction." *Computer Aided Civil and Infrastructure Engineering*, Blackwell Publishers, 16, 79-93.

El Ganainy, A., Olearczyk, J. and Al-Hussein, M. (2007). "Space optimization for panelized prefabricated wood structure for residential construction." Published in the Proceedings of the 4th International Structural Engineering & Construction Conference (ISEC-4), Melbourne, Australia, September 26-28, 2007.

Guang-Min, W., Zhong-Ping, W., and Xian-Jia, W. (2002). "Genetic Algorithm for Solving Convex Quadratic Bi-level Programming Problem." School of Mathematics and Statistics, Wuhan University, Wuhan 430072.

Hajjar, D., and AbouRizk, S. (2002). "Unified Modeling Methodology for Construction Simulation." *Journal of Construction Engineering and Management*, ASCE, 128(2), 174-185.

Jang H., Lee, S., and Choi, S. (2007). "Optimization of floor-level construction material layout using Genetic Algorithms." *Automation in Construction*, 16, 531–545.

Klamroth, K., Tind, J., and Zust, S. (2004). "Integer Programming Duality in Multiple Objective Programming." *Journal of Global Optimization*, 29(1), 1-8.

Korhonen, A. (2003). "Visual Algorithm Simulation." Dissertation for the degree of Doctor of Science in Technology, Helsinki University of Technology, Espoo, Finland.

Lenggenhager B., Tadi, T., Metzinger, T., and Blanke, O. (2007). "Video Ergo Sum: Manipulating Bodily Self-Consciousness." Reports, *Science*, 317, 1096.

Leonov M. and Nikitin A. (1997). "A closed set of algorithms for performing set operations on polygonal regions in the plane". Academic paper translation of A.P.Ershov Institute of Information Systems, Siberian Branch of Russian Academy of Sciences.

Lin K-L (1995). "Planning for critical construction operations involving large semi-stationary equipment.". Dissertation for the degree of Doctor of Philosophy, University of Texas at Austin, December, 1995.

Makhanov, S. (2007). "Optimization and correction of the tool path of the five-axis milling machine Part 1. Spatial optimization." *Mathematics and Computers in Simulation*, 75, 210-230.

Manrique, J.D., Al-Hussein, M., Telyas, A., and Funston, G. (2007). "Constructing a Complex Precast Tilt-Up-Panel Structure Utilizing an Optimization Model, 3D CAD and Animation." *Journal of Construction Engineering and Management*, ASCE, 133(3), 199-207.

Mashood, P.K., Krishnamoorthy, C.S., and Ramamurthy, K. (2007). "KB GA Based Hybrid System for layout planning of Multistory Buildings." *Journal of Computing in Civil Engineering*, ACSE, 21(4), 229-237.

Matsuo, H., Shang, J.S., and Sullivan, R.S. (1991). "A Crane Scheduling Problem in Computer Integrated Manufacturing Environment." *Management Science*, 37(5), 587-605.

Messner, J., Riley, D., and Moeck, M. (2006). "Virtual Facility Prototyping for Sustainable Project Delivery." *Journal of Information Technology in Construction*, 11, 723-738.

Moselhi, O., Alkass, S., and Al-Hussein, M. (2004). "Innovative 3D-Modeling for Selecting and Locating Mobile Cranes." *Engineering Construction and Architectural Management*, 11(5), 373-380.

Murdock, J. (2005). "The Modular Squad." *Architecture*, 94(6), 25-28.

Nasereddin, M., Mullens, M.A., and Cope, D. (2007). "Automated Simulator Development: A Strategy for Modeling Modular Housing Production." *Automation in Construction*, 16, 212-223.

Okyere, M. K. (2004), "Virtual City: A Heterogeneous System Model of an Intelligent Road Navigation System Incorporating Data Mining Concepts." Published in the Proceedings of the National Conference on Undergraduate Research (NCUR), Indianapolis, Indiana, April 16, 2004.

Olearczyk, J. and Al-Hussein, M. (2006). "Oil Sands Construction Automation 3D Solid Modeling and Animation." Published in the Proceedings of the International Conference on Computing and Decision Making in Civil and Building Engineering, Montreal, Canada, June 14-16, 2006.

Olearczyk, J., Al-Hussein, M., Bouferguene, A., and Telyas, A. (2007). "Crane Layout Optimization for Five New Student Residence Buildings at Muhlenberg,

MacGregor Village in Allentown, Pennsylvania *Muhlenberg College, Final report (August 2007).*

Otto, G., Messner, J. and Kalisperis, L. (2005). "Expanding the Boundaries of Virtual Reality for Building Design and Construction." *Computing in Civil Engineering*, 79(12) 1061-1071.

Rehfeld, B. (2006). "Even Some Contractors are Choosing Modular Homes." *The New York Times (East Coast)*, New York, NY, Sept. 30, 2006.

Riley, P. (2007). "A justifiable objective? Analysis: Nuclear Energy" *Power Engineer*, 21(1), 10-11,.

Shapiro, H., Shapiro, J., and Shapiro, L. (1999). "Cranes and Derricks." Chapter in Professional Engineering, 3rd Edition, McGraw-Hill, ISBN 0-07-057889-3.

Sivakumar, P.L., Varghese, K., and Babu, N.R. (2003). "Automated Path Planning of Cooperative Crane Lifts Using Heuristic Search." *Journal of Computing in Civil Engineering*, ACSE, 17(3), 197-207.

Smith, K. (2006). "Advantages of Modularity and Commonality in a Spacecraft Architecture." Published in the Proceedings of the 10th Biannual International Conference on Engineering, Construction, and Operations in Challenging Environments (Earth & Space 2006) and the 2nd NASA/ARO/ASCE Workshop on Granular Materials in Lunar and Martian Exploration, League City/Houston, TX, March 5-8, 2006.

Staub-French, S. and Khanzode, A. (2007). "3D and 4D Modeling for Design and Construction Coordination: Issues and Lessons Learned." *Journal of Information Technology in Construction*, 12, 381-407.

Tam, C.M., Tong, T.K.L., and Chan, W.K.W. (2001). "Genetic Algorithm for Optimizing Supply Locations Around Tower Crane." *Journal of Construction Engineering and Management*, ASCE, 127(4), 315-321.

Tam, C.M. and Tong, T.K.L. (2003). "GA-ANN Model for Optimizing the Location of Tower Crane and Supply Points for High-Rise Public Housing Construction." *Construction Management and Economics*, 21 257-266.

Weise, T. (2008). "Global Optimization Algorithms – Theory and Application." http://www.it-weise.de/projects/book.pdf April 16, 2008

Williams, E. J. and Narayanaswamy, R. (1997). "Application of Simulation to Scheduling, Sequencing and Material Handling." Published in the Proceedings of the 29th Conference on Winter Simulation, Atlanta, USA, December 7-10, 861-865.

Vatti B. (1992). "A generic solution to polygon clipping". *Communication of the ACM* July 1992. Vol.35, No.7.

Veale, J. and Postawa, L. (2007). "Preparing for take-off, – designing the New Terminal Building at Madrid Barajas Airport, Spain." Evening Meeting, *The Structural Engineer*, 3, 39-44.

Vincent, T. (1983). "Game Theory as a Design Tool." *Journal of Mechanisms, Transmissions, and Automation in Design*, 105(165-170).

Xu, J., (2001). "CAD-Based Integrated Simulation Environment (CAD-ISE)." Dissertation for the degree of Doctor of Science in Construction Engineering and Management, University of Alberta, Edmonton, Canada, January, 2001.

Yoders, J. (2005). "Reinventing Modular Construction." *Building Design and Construction*, 8(5), 2.

Yoshimura, M., Murase, Y., Yamauchi, M., Izui, K., Nishiwaki, S., Ohba, H., Moriya, S., and Hishimoto, H. (2004). "Development of an Integrated Design Environment for Space Satellite Structures." Published in the Proceedings of the 10th AIAA/ISSMO Multidisciplinary Analysis and Optimization Conference, August 30 – September 1, 2004, Albany, New York.

jYu, H., Al-Hussein, M., and Nasseri, R. (2007). "Process Flowcharting And Simulation Of House Structure Components Production Process." *Proceedings of the 2007 Winter Simulation Conference*, ed S. G. Henderson, B. Biller, M.-H. Hsieh, J. Shortle, J. D. Tew, and R. R. Barton, 2066-2072.

Zhang, P., Harris, F.C., Olomolalye, P.O., and Holt, G.D. (1999). "Location Optimization for a Group of Tower Cranes." *Journal of Construction Engineering and Management*, ASCE, 125(2), 115-122.

Appendices

Appendix A-01, Inter-Phase Output Parameters

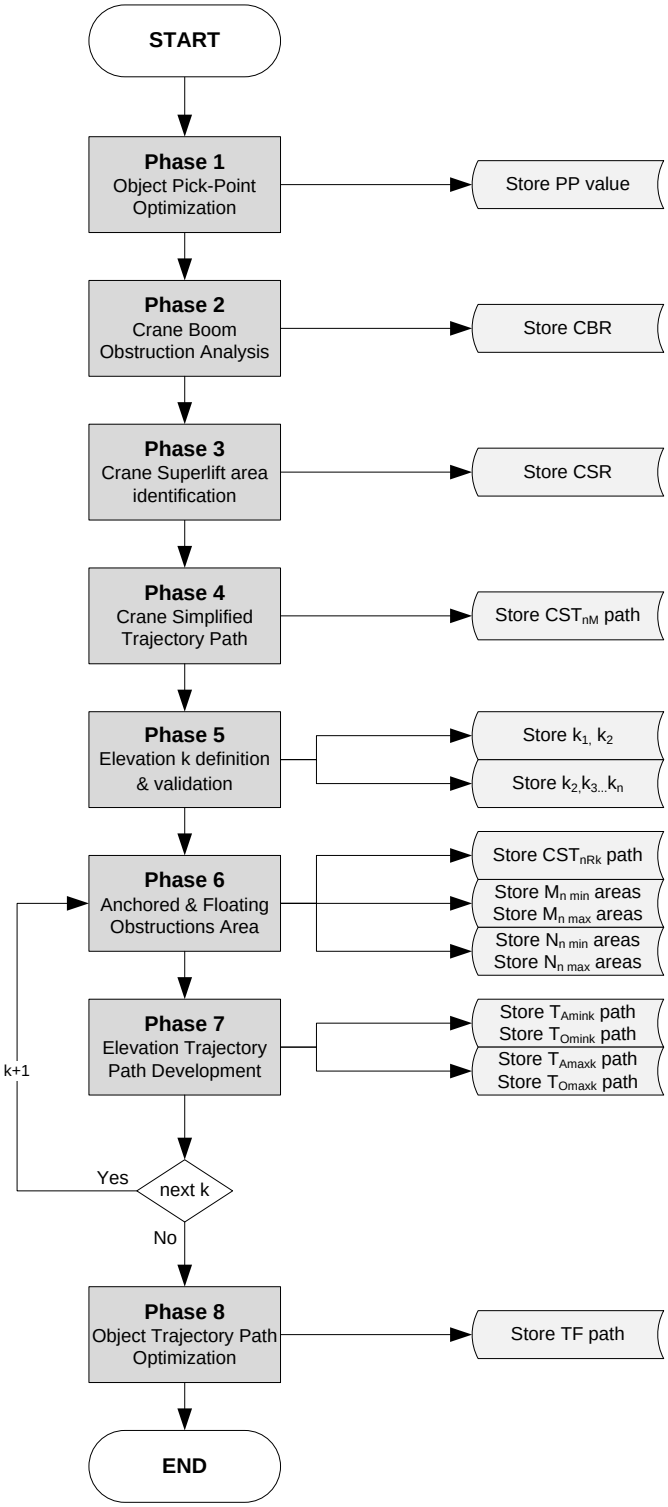

Appendix A-02, PB3 Minute-By-Minute Schedule

	oper code	activity/operation	module	start zone	crew	workers time p (m)	workers time ml (m)	workers time o (m)	crane time p (m)	crane time ml (m)	crane time o (m)	finish zone
	19-Jun-07											
601	C	Extend Crane HydBoom		C					8	6	5	C
602	K1	Hooking spreader bar		C	2	12	10	8				C
603	C-sb	Crane next position		C					4	2	1	A
604	T1	Placing Module Trailer	313	-	1	25	20	15				A
605	K2	Hooking Module	313	A	2	20	17	15				A
606	T1	Removing Empty Trailer		A	1	25	20	15				-
607	C-sb	load hoisting up	313	A					3	2	1	
608	C-sb	load booming up	313						2	1.5	1	
609	C-sb	load swing	313						3	2	1.7	
610	C-sb	load hoisting down	313						4	2.5	1.5	PB3-1
611	K2	Securing-lining up	313	PB3-1	2	30	20	15				PB3-1
612	K1	Securing-bolting together	313	PB3-1	2	30	22	15				PB3-1
613	K2	Unhooking	313	PB3-1	2	12	9	8				PB3-1
614	K1	Removing lifting lugs	313	PB3-1	2	16	13	11				PB3-1
615	K3	Welding bottom - one side	313	PB3-1	1	30	20	15				PB3-1
616	K3	Welding bottom - other side	313	PB3-1	1	30	20	15				PB3-1
617	C-sb	Crane next position		PB3-1					3	2	1	A
618	T1	Placing Module Trailer	314	-	1	25	20	15				A
619	K2	Hooking Module	314	A	2	20	17	15				A
620	T1	Removing Empty Trailer		A	1	25	20	15				-
621	C-sb	load hoisting up	314	A					3	2	1	
622	C-sb	load booming up	314						2	1.5	1	
623	C-sb	load swing	314						3	2	1.7	
624	C-sb	load hoisting down	314						4	2.5	1.5	PB3-1
625	K2	Securing-lining up	314	PB3-1	2	30	20	15				PB3-1
626	K1	Securing-bolting together	314	PB3-1	2	25	17	10				PB3-1
627	K2	Unhooking	314	PB3-1	2	12	9	8				PB3-1
628	K1	Removing lifting lugs	314	PB3-1	2	16	13	11				PB3-1
629	K3	Welding bottom - one side	314	PB3-1	1	40	25	20				PB3-1
630	K3	Welding top - mod together	314	PB3-1	1	42	35	30				PB3-1
631	C-sb	Crane next position		PB3-1					3	2	1	C
632	K1	Unhooking spreader bar		C	2	12	10	8				C
633	C	Crane next position		C					3	2	1	A
634	T1	Placing Module Trailer	311	-	1	20	15	10				A
635	K2	Hooking Module	311	A	2	20	17	15				A
636	T1	Removing Empty Trailer		A	1	25	20	15				-
637	C	load hoisting up	311	A					3	2	1	
638	C	load booming up	311						2	1.5	1	
639	C	load swing	311						2	1.5	1	
640	C	load hoisting down	311						3.5	3	1.5	PB3-1
641	K2	Securing-lining up	311	PB3-1	2	25	18	12				PB3-1
642	K1	Securing-bolting together	311	PB3-1	2	20	15	8				PB3-1
643	K2	Unhooking	311	PB3-1	2	9	7	5				PB3-1
644	K1	Removing lifting lugs	311	PB3-1	2	15	11	10				PB3-1
645	K3	Welding top	311	PB3-1	1	25	20	17				PB3-1
646	K3	Welding bottom	311	PB3-1	1	25	20	17				PB3-1
647	C	Crane next position		PB3-1					3	2	1	A
648	T1	Placing Module Trailer	312	-	1	20	15	10				A
649	K2	Hooking Module	312	A	2	20	17	15				A
650	T1	Removing Empty Trailer		A	1	25	20	15				-
651	C	load hoisting up	312	A					3	2	1	
652	C	load booming up	312						2	1.5	1	
653	C	load swing	312						2	1.5	1	
654	C	load hoisting down	312						3.2	3	1.5	PB3-1
655	K2	Securing-lining up	312	PB3-1	2	25	18	12				PB3-1
656	K1	Securing-bolting together	312	PB3-1	2	20	15	8				PB3-1

657	K2	Unhooking	312	PB3-1	2	9	7	5				PB3-1
658	K1	Removing lifting lugs	312	PB3-1	2	15	11	10				PB3-1
659	K3	Welding top only	312	PB3-1	1	25	20	17				PB3-1
660	C	Crane next position		PB3-1					3	2	1	A
661	T1	Placing Module Trailer	315	-	1	20	15	10				A
662	K2	Hooking Module	315	A	2	20	17	15				A
663	T1	Removing Empty Trailer		A	1	25	20	15				-
664	C	load hoisting up	315	A					3	2	1	
665	C	load booming up	315						2	1.5	1	
666	C	load swing	315						2	2	1.5	
667	C	load hoisting down	315						4	3.5	2.8	PB3-1
668	K2	Securing-lining up	315	PB3-1	2	25	18	12				PB3-1
669	K1	Securing-bolting together	315	PB3-1	2	20	15	8				PB3-1
670	K2	Unhooking	315	PB3-1	2	9	7	5				PB3-1
671	K1	Removing lifting lugs	315	PB3-1	2	15	11	10				PB3-1
672	K3	Welding top	315	PB3-1	1	25	20	17				PB3-1
673	K3	Welding bottom	315	PB3-1	1	25	20	17				PB3-1
674	C	Crane next position		PB3-1					3	2	1	A
675	T1	Placing Module Trailer	316	-	1	20	15	10				A
676	K2	Hooking Module	316	A	2	20	17	15				A
677	T1	Removing Empty Trailer		A	1	25	20	15				-
678	C	load hoisting up	316	A					3	2	1	
679	C	load booming up	316						1.5	1	0.5	
680	C	load swing	316						2	1.5	1	
681	C	load hoisting down	316						3.5	2.5	1.8	PB3-1
682	K2	Securing-lining up	316	PB3-1	2	25	18	12				PB3-1
683	K1	Securing-bolting together	316	PB3-1	2	20	15	8				PB3-1
684	K2	Unhooking	316	PB3-1	2	9	7	5				PB3-1
685	K1	Removing lifting lugs	316	PB3-1	2	15	11	10				PB3-1
686	K3	Welding top only	316	PB3-1	1	25	20	17				PB3-1
687	C	Crane next position		PB3-1					3	2	1	C
688	K1	Hooking spreader bar		C	2	12	10	8				C
689	C-sb	Crane next position		C					3	2	1	A
690	T1	Placing Module Trailer	323	-	1	25	20	15				A
691	K2	Hooking Module	323	A	2	20	17	15				A
692	T1	Removing Empty Trailer		A	1	25	20	15				-
693	C-sb	load hoisting up	323	A					3	2	1	
694	C-sb	load booming up	323						2	1.7	1.4	
695	C-sb	load swing	323						3.3	2.5	2	
696	C-sb	load hoisting down	323						4	2.8	1.5	PB3-2
697	K2	Securing-lining up	323	PB3-2	2	30	20	15				PB3-2
698	K1	Securing-bolting together	323	PB3-2	2	30	22	15				PB3-2
699	K2	Unhooking	323	PB3-2	2	12	9	8				PB3-2
700	K1	Removing lifting lugs	323	PB3-2	2	16	13	11				PB3-2
701	K3	Welding bottom - one side	323	PB3-2	1	30	20	15				PB3-2
702	K3	Welding bottom - other side	323	PB3-2	1	30	20	15				PB3-2
703	C-sb	Crane next position		PB3-1					3	2	1	A
704	T1	Placing Module Trailer	324	-	1	25	20	15				A
705	K2	Hooking Module	324	A	2	20	17	15				A
706	T1	Removing Empty Trailer		A	1	25	20	15				-
707	C-sb	load hoisting up	324	A					3	2	1	
708	C-sb	load booming up	324						2	1	0.7	
709	C-sb	load swing	324						3	2.1	1.7	
710	C-sb	load hoisting down	324						4.2	2.9	2	PB3-2
711	K2	Securing-lining up	324	PB3-2	2	30	20	15				PB3-2
712	K1	Securing-bolting together	324	PB3-2	2	25	17	10				PB3-2
713	K2	Unhooking	324	PB3-2	2	12	9	8				PB3-2
714	K1	Removing lifting lugs	324	PB3-2	2	16	13	11				PB3-2
715	K3	Welding bottom - one side	324	PB3-2	1	40	25	20				PB3-2
716	K3	Welding top - mod together	324	PB3-2	1	42	35	30				PB3-2
717	C-sb	Crane next position		PB3-2					3	2	1	C
718	K1	Unhooking spreader bar		C	2	30	20	15				C
719	C	Crane next position		C					3	2	1	A
720	T1	Placing Module Trailer	321	-	1	20	15	10				A
721	K2	Hooking Module	321	A	2	20	17	15				A
722	T1	Removing Empty Trailer		A	1	25	20	15				-
723	C	load hoisting up	321	A					3	2	1	

724	C	load booming up	321						2	1.5	1	
725	C	load swing	321						2	1.5	1	
726	C	load hoisting down	321						3	2	1	PB3-2
727	K2	Securing-lining up	321	PB3-2	2	25	18	12				PB3-2
728	K1	Securing-bolting together	321	PB3-2	2	20	15	8				PB3-2
729	K2	Unhooking	321	PB3-2	2	9	7	5				PB3-2
730	K1	Removing lifting lugs	321	PB3-2	2	15	11	10				PB3-2
731	K3	Welding top	321	PB3-2	1	25	20	17				PB3-2
732	K3	Welding bottom	321	PB3-2	1	25	20	17				PB3-2
733	C	Crane next position		PB3-2					3	2	1	A
734	T1	Placing Module Trailer	322	-	1	20	15	10				A
735	K2	Hooking Module	322	A	2	20	17	15				A
736	T1	Removing Empty Trailer		A	1	25	20	15				-
737	C	load hoisting up	322	A					3	2	1	
738	C	load booming up	322						2	1.5	1	
739	C	load swing	322						2	1.5	1	
740	C	load hoisting down	322						3	2	1	PB3-2
741	K2	Securing-lining up	322	PB3-2	2	25	18	12				PB3-2
742	K1	Securing-bolting together	322	PB3-2	2	20	15	8				PB3-2
743	K2	Unhooking	322	PB3-2	2	9	7	5				PB3-2
744	K1	Removing lifting lugs	322	PB3-2	2	15	11	10				PB3-2
745	K3	Welding top only	322	PB3-2	1	25	20	17				PB3-2
746	C	Crane next position		PB3-2					3	2	1	D
747	K1	Hooking cover wrap		D	2	7	5	4				D
748	C	load hoisting up	Cover	D					3	2	1	
749	C	load booming up	Cover						3	1.5	1	
750	C	load swing	Cover						3.5	2.5	1.2	
751	C	load hoisting down	Cover						3	2	1	PB3-2
752	K	Cover modules	Cover	PB3-2	6	12	10	8				PB3-2
753	C	Crane next position	Cover	PB3-2					3	2	1	C
754	C	Retract Crane HydBoom		C					8	6	5	C
	20-Jun-07											
755	C	Extend Crane HydBoom		C					8	6	5	C
756	C	Crane next position		C					3	2	1	PB3-2
757	K1	Hooking cover wrap		PB3-2	2	7	5	4				PB3-2
758	C	load hoisting up	Cover	PB3-2					3	2	1	
759	C	load booming up	Cover						3	2	1	
760	C	load swing	Cover						3.5	2.5	1.2	
761	C	load hoisting down	Cover						3	2.5	1	D
762	K1	Unhooking cover wrap	Cover	D	2	7	5	4				D
763	C	Crane next position	Cover	D					3	2	1	A
764	T1	Placing Module Trailer	325	-	1	20	15	10				A
765	K2	Hooking Module	325	A	2	20	17	15				A
766	T1	Removing Empty Trailer		A	1	25	20	15				-
767	C	load hoisting up	325	A					3	2	1	
768	C	load booming up	325						2	1.7	1	
769	C	load swing	325						3.2	2.5	1.9	
770	C	load hoisting down	325						4	2.8	2	PB3-2
771	K2	Securing-lining up	325	PB3-2	2	25	18	12				PB3-2
772	K1	Securing-bolting together	325	PB3-2	2	20	15	8				PB3-2
773	K2	Unhooking	325	PB3-2	2	9	7	5				PB3-2
774	K1	Removing lifting lugs	325	PB3-2	2	15	11	10				PB3-2
775	K3	Welding top	325	PB3-2	1	25	20	17				PB3-2
776	K3	Welding bottom	325	PB3-2	1	25	20	17				PB3-2
777	C	Crane next position		PB3-2					3	2	1	A
778	T1	Placing Module Trailer	326	-	1	20	15	10				A
779	K2	Hooking Module	326	A	2	20	17	15				A
780	T1	Removing Empty Trailer		A	1	25	20	15				-
781	C	load hoisting up	326	A					3	2	1	
782	C	load booming up	326						2	1.7	1	
783	C	load swing	326						3.2	2.5	1.9	
784	C	load hoisting down	326						4	2.8	2	PB3-2
785	K2	Securing-lining up	326	PB3-2	2	25	18	12				PB3-2
786	K1	Securing-bolting together	326	PB3-2	2	20	15	8				PB3-2
787	K2	Unhooking	326	PB3-2	2	9	7	5				PB3-2
788	K1	Removing lifting lugs	326	PB3-2	2	15	11	10				PB3-2
789	K3	Welding top	326	PB3-2	1	25	20	17				PB3-2

790	C	Crane next position		PB3-2					3	2	1	C
791	K1	Hooking spreader bar		C	2	12	10	8				C
792	C-sb	Crane next position		C					3	2	1	A
793	T1	Placing Module Trailer	333	-	1	25	20	15				A
794	K2	Hooking Module	333	A	2	20	17	15				A
795	T1	Removing Empty Trailer		A	1	25	20	15				-
796	C-sb	load hoisting up	333	A					3	2	1	
797	C-sb	load booming up	333						2	1.5	1	
798	C-sb	load swing	333						3	2	1.7	
799	C-sb	load hoisting down	333						4	2.5	1.5	PB3-3
800	K2	Securing-lining up	333	PB3-3	2	30	20	15				PB3-3
801	K1	Securing-bolting together	333	PB3-3	2	30	22	15				PB3-3
802	K2	Unhooking	333	PB3-3	2	12	9	8				PB3-3
803	K1	Removing lifting lugs	333	PB3-3	2	16	13	11				PB3-3
804	K3	Welding bottom - one side	333	PB3-3	1	30	20	15				PB3-3
805	K3	Welding bottom - other side	333	PB3-3	1	30	20	15				PB3-3
806	C-sb	Crane next position		PB3-3					3	2	1	A
807	T1	Placing Module Trailer	334	-	1	25	20	15				A
808	K2	Hooking Module	334	A	2	20	17	15				A
809	T1	Removing Empty Trailer		A	1	25	20	15				-
810	C-sb	load hoisting up	334	A					3	2	1	
811	C-sb	load booming up	334						2	1.5	1	
812	C-sb	load swing	334						3	2	1.7	
813	C-sb	load hoisting down	334						4	2.5	1.5	PB3-3
814	K2	Securing-lining up	334	PB3-3	2	30	20	15				PB3-3
815	K1	Securing-bolting together	334	PB3-3	2	25	17	10				PB3-3
816	K2	Unhooking	334	PB3-3	2	12	9	8				PB3-3
817	K1	Removing lifting lugs	334	PB3-3	2	16	13	11				PB3-3
818	K3	Welding bottom - one side	334	PB3-3	1	40	25	20				PB3-3
819	K3	Welding top - mod together	334	PB3-3	1	42	35	30				PB3-3
820	C-sb	Crane next position		PB3-3					3	2	1	C
821	K1	Unhooking spreader bar		C	2	30	20	15				C
822	C	Crane next position		C					3	2	1	A
823	T1	Placing Module Trailer	331	-	1	20	15	10				A
824	K2	Hooking Module	331	A	2	20	17	15				A
825	T1	Removing Empty Trailer		A	1	25	20	15				-
826	C	load hoisting up	331	A					3	2	1	
827	C	load booming up	331						2	1.5	1	
828	C	load swing	331						2	1.7	1	
829	C	load hoisting down	331						3.5	2.8	1.8	PB3-3
830	K2	Securing-lining up	331	PB3-3	2	25	18	12				PB3-3
831	K1	Securing-bolting together	331	PB3-3	2	20	15	8				PB3-3
832	K2	Unhooking	331	PB3-3	2	9	7	5				PB3-3
833	K1	Removing lifting lugs	331	PB3-3	2	15	11	10				PB3-3
834	K3	Welding top	331	PB3-3	1	25	20	17				PB3-3
835	K3	Welding bottom	331	PB3-3	1	25	20	17				PB3-3
836	C	Crane next position		PB3-3					3	2	1	A
837	T1	Placing Module Trailer	332	-	1	20	15	10				A
838	K2	Hooking Module	332	A	2	20	17	15				A
839	T1	Removing Empty Trailer		A	1	25	20	15				-
840	C	load hoisting up	332	A					3	2	1	
841	C	load booming up	332						2	1.5	1	
842	C	load swing	332						2	1.5	1	
843	C	load hoisting down	332						3.2	2	1.8	PB3-3
844	K2	Securing-lining up	332	PB3-3	2	25	18	12				PB3-3
845	K1	Securing-bolting together	332	PB3-3	2	20	15	8				PB3-3
846	K2	Unhooking	332	PB3-3	2	9	7	5				PB3-3
847	K1	Removing lifting lugs	332	PB3-3	2	15	11	10				PB3-3
848	K3	Welding top only	332	PB3-3	1	25	20	17				PB3-3
849	C	Crane next position		PB3-3					3	2	1	A
850	T1	Placing Module Trailer	335	-	1	20	15	10				A
851	K2	Hooking Module	335	A	2	20	17	15				A
852	T1	Removing Empty Trailer		A	1	25	20	15				-
853	C	load hoisting up	335	A					3	2	1	
854	C	load booming up	335						2	1.5	1	
855	C	load swing	335						3.2	2.7	1.9	
856	C	load hoisting down	335						4	2.8	2	PB3-3

857	K2	Securing-lining up	335	PB3-3	2	25	18	12				PB3-3
858	K1	Securing-bolting together	335	PB3-3	2	20	15	8				PB3-3
859	K2	Unhooking	335	PB3-3	2	9	7	5				PB3-3
860	K1	Removing lifting lugs	335	PB3-3	2	15	11	10				PB3-3
861	K3	Welding top	335	PB3-3	1	25	20	17				PB3-3
862	K3	Welding bottom	335	PB3-3	1	25	20	17				PB3-3
863	C	Crane next position		PB3-3					3	2	1	A
864	T1	Placing Module Trailer	336	-	1	20	15	10				A
865	K2	Hooking Module	336	A	2	20	17	15				A
866	T1	Removing Empty Trailer		A	1	25	20	15				-
867	C	load hoisting up	336	A					3	2	1	
868	C	load booming up	336						2	1.5	1	
869	C	load swing	336						3.2	2.7	1.9	
870	C	load hoisting down	336						4	2.8	2	PB3-3
871	K2	Securing-lining up	336	PB3-3	2	25	18	12				PB3-3
872	K1	Securing-bolting together	336	PB3-3	2	20	15	8				PB3-3
873	K2	Unhooking	336	PB3-3	2	9	7	5				PB3-3
874	K1	Removing lifting lugs	336	PB3-3	2	15	11	10				PB3-3
875	K3	Welding top	336	PB3-3	1	25	20	17				PB3-3
876	C	Crane next position		PB3-3					3	2	1	A
877	T1	Placing Walkway Trailer	3B	-	1	20	15	10				A
878	K2	Hooking Walkway	3B	A	2	20	17	15				A
879	T1	Removing Empty Trailer		A	1	25	20	15				-
880	C	load hoisting up	3B	A					3	2	1	
881	C	load booming up	3B						2	1.5	1	
882	C	load swing	3B						2	1.5	1	
883	C	load hoisting down	3B						4	3	2	PB3
884	K2	Securing-lining up	3B	PB3	2	13	10	8				PB3
885	K2	Unhooking	3B	PB3	2	4	3	2				PB3
886	K3	Welding bottom	3B	PB3	1	17	15	12				PB3
887	C	Crane next position		PB3					3	2	1	C
888	K1	Hooking spreader bar-R		C	2	12	10	8				C
889	C-sb	Crane next position		C					3	2	1	PB4
890	K2	Hooking Roof	3R	PB4	2	25	20	15				PB4
891	C-sb	load hoisting up	3R	PB4					6	4	3	
892	C-sb	load booming up	3R						2	1.5	1	
893	C-sb	load swing	3R						4	3	2	
894	C-sb	load hoisting down	3R						4.5	3.5	2.8	PB3
895	K2	Securing-lining up	3R	PB3	2	30	24	20				PB3
896	K2	Unhooking	3R	PB3	2	9	7	5				PB3
897	K3	Welding bottom	3R	PB3	2	17	15	12				PB3
898	C-sb	Crane next position		PB3					3	2	1	C
899	K1	Unhooking spreader bar		C	2	30	20	15				C
900	C	Retract Crane HydBoom		C					8	6	5	C

Appendix A-03, Operation Flowcharts

Preliminary Operation Flowchart.

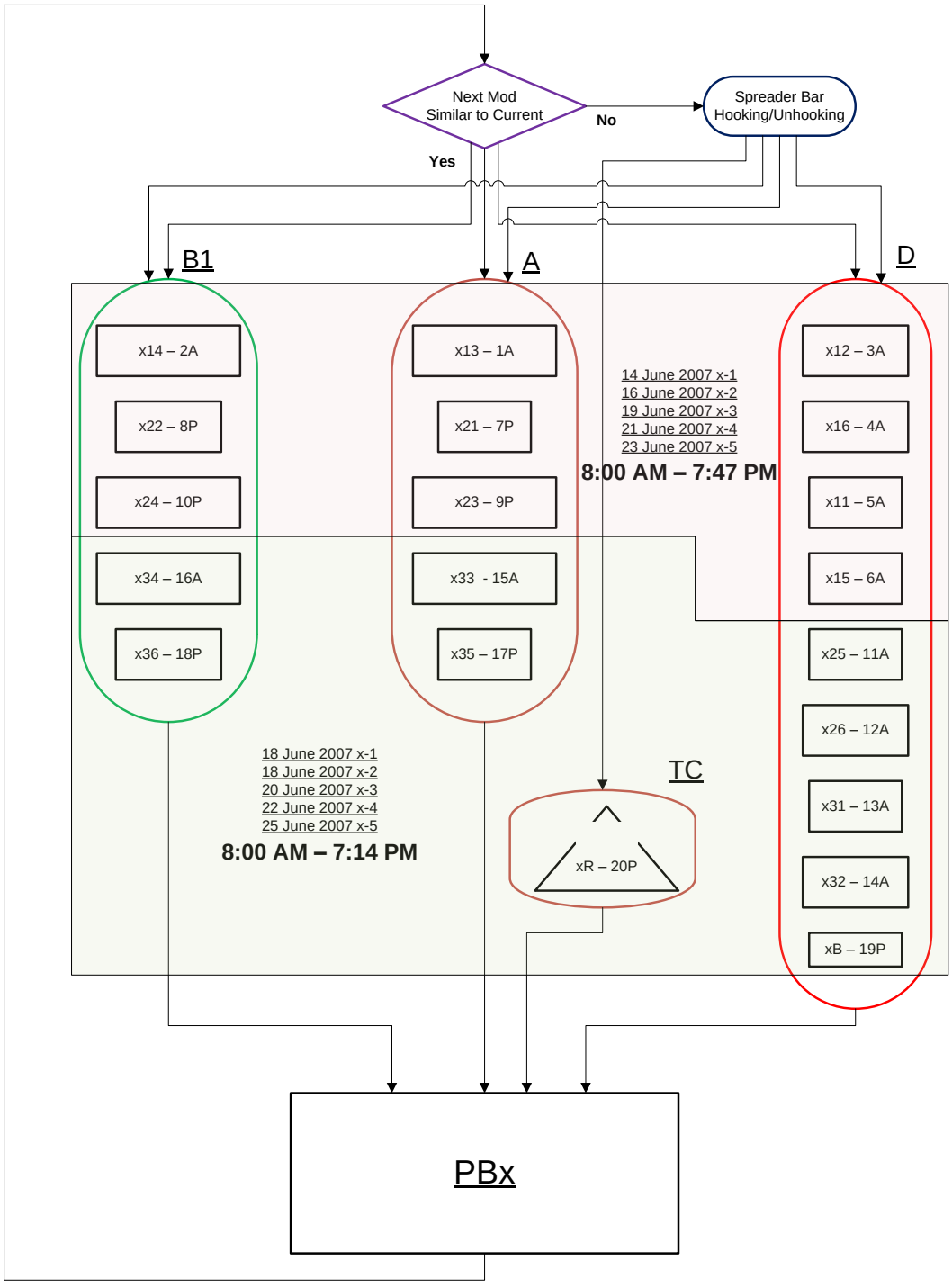

Final Operation Flowchart.

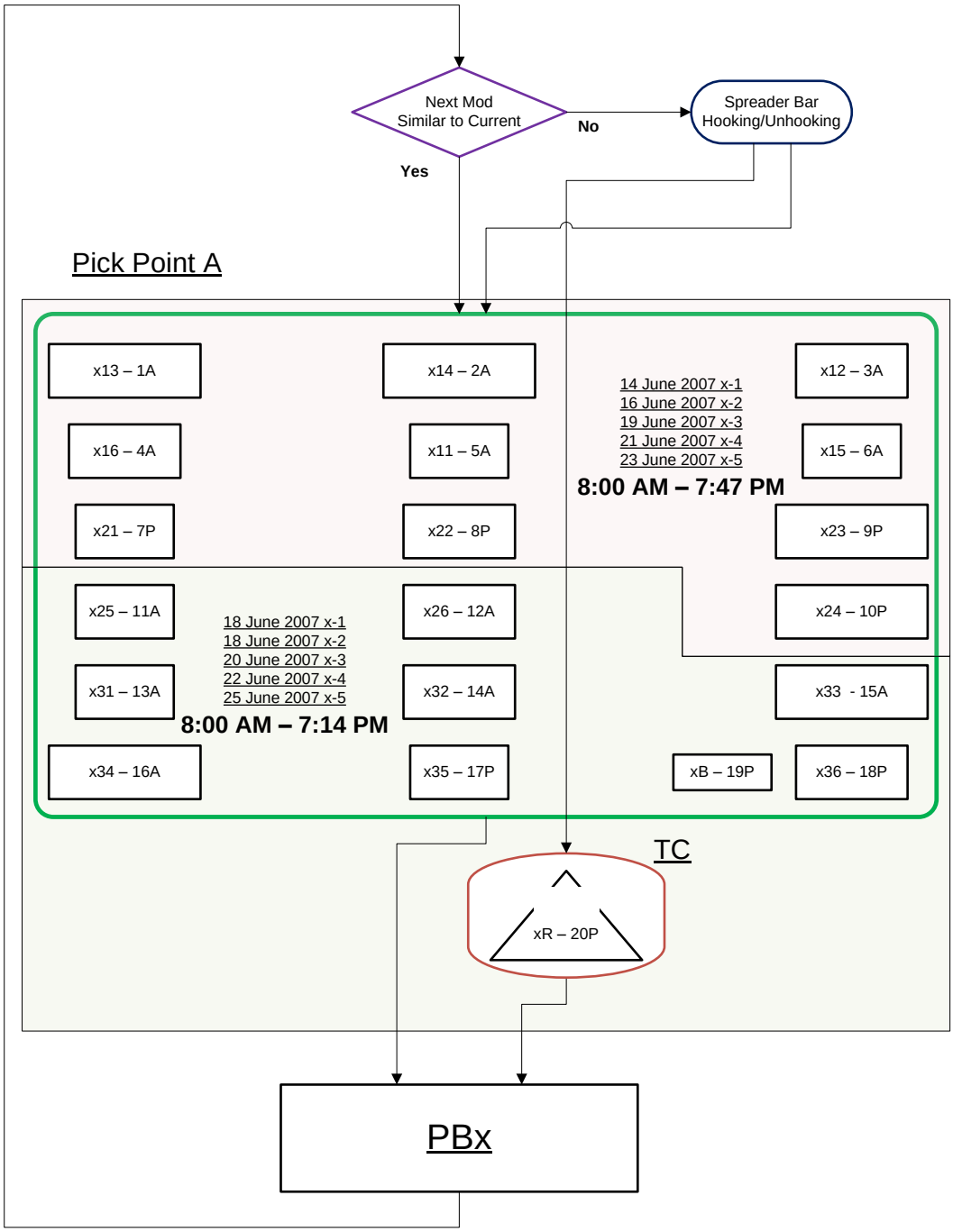

Appendix A-04, PB3 Planned vs. Actual Schedule

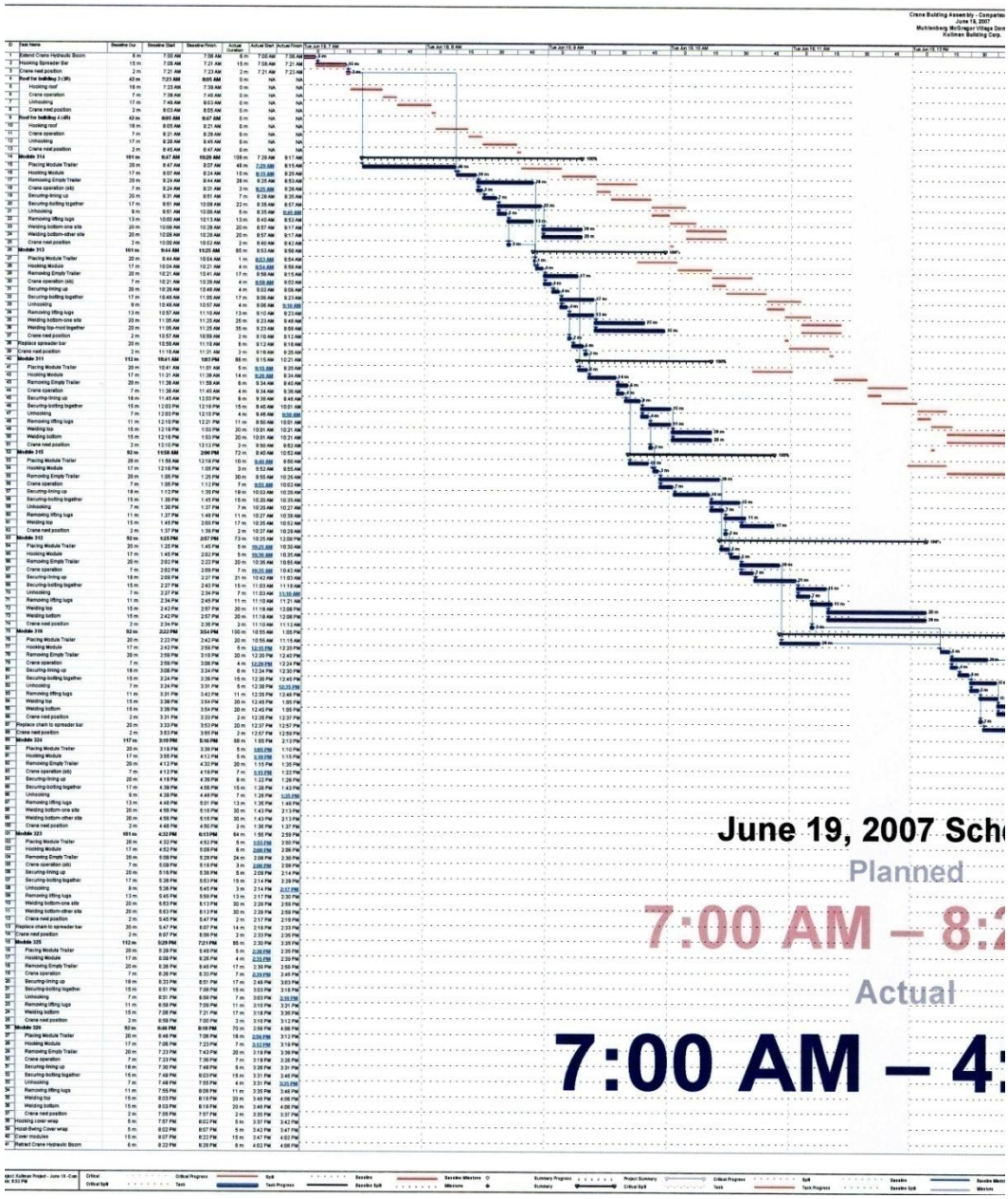

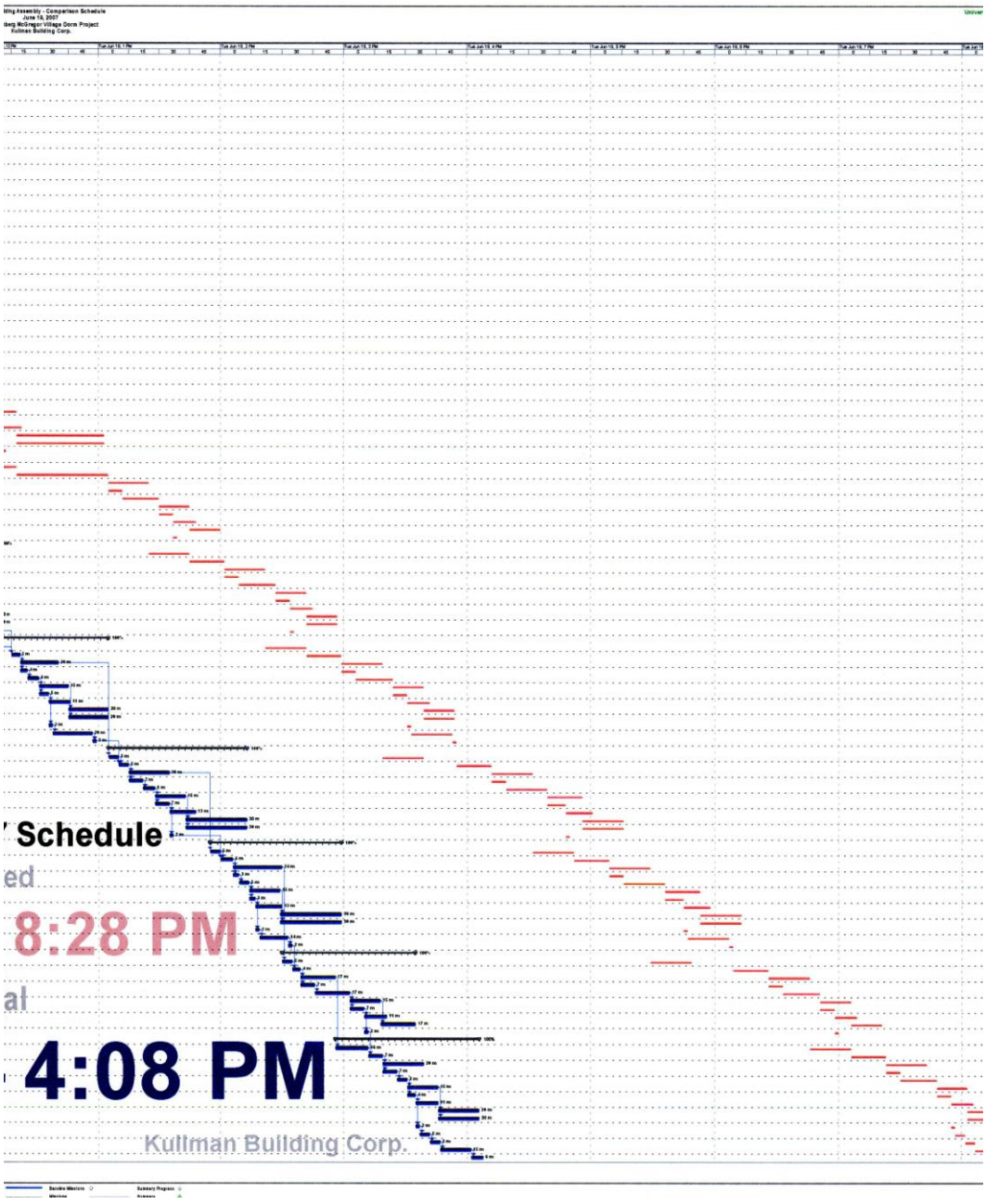
Schedule
ed
8:28 PM
al
4:08 PM
Kullman Building Corp.

Appendix A-05, Object Pick-Point and Set-Point Coordinates

Module	OBJECT						Crane Hook			PICK-POSITION (Z
	Parameters					Rigging				Object Top Points ($T_X pp_x$)
										T_A
	l	w	h	Θ_1	Θ_2	H	x	y	z	x	y	z
111	266.375	169.750	124.000	54.000	35.000	354.709	438.411	1187.700	481.750	448.031	1345.339	127.041
112	289.125	169.750	124.000	54.000	35.000	354.709	438.411	1187.700	481.750	454.717	1354.542	127.041
113	616.000	159.500	124.000	54.000	35.000	450.709	438.411	1187.700	577.750	554.930	1483.753	127.041
114	616.000	159.500	124.000	54.000	35.000	450.709	438.411	1187.700	577.750	554.930	1483.753	127.041
115	266.375	169.750	124.000	54.000	35.000	354.709	438.411	1187.700	481.750	448.031	1345.339	127.041
116	289.125	169.750	124.000	54.000	35.000	354.709	438.411	1187.700	481.750	454.717	1354.542	127.041
121	266.375	169.750	124.000	54.000	35.000	354.709	438.411	1187.700	481.750	448.031	1345.339	127.041
122	289.125	169.750	124.000	54.000	35.000	354.709	438.411	1187.700	481.750	454.717	1354.542	127.041
123	616.000	159.500	124.000	54.000	35.000	450.709	438.411	1187.700	577.750	554.930	1483.753	127.041
124	616.000	159.500	124.000	54.000	35.000	450.709	438.411	1187.700	577.750	554.930	1483.753	127.041
125	266.375	169.750	124.000	54.000	35.000	354.709	438.411	1187.700	481.750	448.031	1345.339	127.041
126	289.125	169.750	124.000	54.000	35.000	354.709	438.411	1187.700	481.750	454.717	1354.542	127.041
131	266.375	169.750	116.500	54.000	35.000	354.709	438.411	1187.700	474.250	448.031	1345.339	119.541
132	289.125	169.750	116.500	54.000	35.000	354.709	438.411	1187.700	474.250	454.717	1354.542	119.541
133	616.000	159.500	116.500	54.000	35.000	450.709	438.411	1187.700	570.250	554.930	1483.753	119.541
134	616.000	159.500	116.500	54.000	35.000	450.709	438.411	1187.700	570.250	554.930	1483.753	119.541
135	266.375	169.750	116.500	54.000	35.000	354.709	438.411	1187.700	474.250	448.031	1345.339	119.541
136	289.125	169.750	116.500	54.000	35.000	354.709	438.411	1187.700	474.250	454.717	1354.542	119.541
1R												
211	266.375	169.750	124.000	54.000	55.000	354.709	438.411	1187.700	481.750	448.031	1345.339	127.041
212	289.125	169.750	124.000	54.000	55.000	354.709	438.411	1187.700	481.750	454.717	1354.542	127.041
213	616.000	159.500	124.000	54.000	55.000	450.709	438.411	1187.700	577.750	554.930	1483.753	127.041
214	616.000	159.500	124.000	54.000	55.000	450.709	438.411	1187.700	577.750	554.930	1483.753	127.041
215	266.375	169.750	124.000	54.000	55.000	354.709	438.411	1187.700	481.750	448.031	1345.339	127.041
216	289.125	169.750	124.000	54.000	55.000	354.709	438.411	1187.700	481.750	454.717	1354.542	127.041
221	266.375	169.750	124.000	54.000	55.000	354.709	438.411	1187.700	481.750	448.031	1345.339	127.041
222	289.125	169.750	124.000	54.000	55.000	354.709	438.411	1187.700	481.750	454.717	1354.542	127.041
223	616.000	159.500	124.000	54.000	55.000	450.709	438.411	1187.700	577.750	554.930	1483.753	127.041
224	616.000	159.500	124.000	54.000	55.000	450.709	438.411	1187.700	577.750	554.930	1483.753	127.041
225	266.375	169.750	124.000	54.000	55.000	354.709	438.411	1187.700	481.750	448.031	1345.339	127.041
226	289.125	169.750	124.000	54.000	55.000	354.709	438.411	1187.700	481.750	454.717	1354.542	127.041
231	266.375	169.750	116.500	54.000	55.000	354.709	438.411	1187.700	474.250	448.031	1345.339	119.541
232	289.125	169.750	116.500	54.000	55.000	354.709	438.411	1187.700	474.250	454.717	1354.542	119.541
233	616.000	159.500	116.500	54.000	55.000	450.709	438.411	1187.700	570.250	554.930	1483.753	119.541
234	616.000	159.500	116.500	54.000	55.000	450.709	438.411	1187.700	570.250	554.930	1483.753	119.541
235	266.375	169.750	116.500	54.000	55.000	354.709	438.411	1187.700	474.250	448.031	1345.339	119.541
236	289.125	169.750	116.500	54.000	55.000	354.709	438.411	1187.700	474.250	454.717	1354.542	119.541
2R												
311	266.375	169.750	124.000	54.000	35.000	354.709	438.411	1187.700	481.750	448.031	1345.339	127.041
312	289.125	169.750	124.000	54.000	35.000	354.709	438.411	1187.700	481.750	454.717	1354.542	127.041
313	616.000	159.500	124.000	54.000	35.000	450.709	438.411	1187.700	577.750	554.930	1483.753	127.041
314	616.000	159.500	124.000	54.000	35.000	450.709	438.411	1187.700	577.750	554.930	1483.753	127.041
315	266.375	169.750	124.000	54.000	35.000	354.709	438.411	1187.700	481.750	448.031	1345.339	127.041
316	289.125	169.750	124.000	54.000	35.000	354.709	438.411	1187.700	481.750	454.717	1354.542	127.041
321	266.375	169.750	124.000	54.000	35.000	354.709	438.411	1187.700	481.750	448.031	1345.339	127.041
322	289.125	169.750	124.000	54.000	35.000	354.709	438.411	1187.700	481.750	454.717	1354.542	127.041
323	616.000	159.500	124.000	54.000	35.000	450.709	438.411	1187.700	577.750	554.930	1483.753	127.041
324	616.000	159.500	124.000	54.000	35.000	450.709	438.411	1187.700	577.750	554.930	1483.753	127.041
325	266.375	169.750	124.000	54.000	35.000	354.709	438.411	1187.700	481.750	448.031	1345.339	127.041
326	289.125	169.750	124.000	54.000	35.000	354.709	438.411	1187.700	481.750	454.717	1354.542	127.041
331	266.375	169.750	116.500	54.000	35.000	354.709	438.411	1187.700	474.250	448.031	1345.339	119.541
332	289.125	169.750	116.500	54.000	35.000	354.709	438.411	1187.700	474.250	454.717	1354.542	119.541
333	616.000	159.500	116.500	54.000	35.000	450.709	438.411	1187.700	570.250	554.930	1483.753	119.541
334	616.000	159.500	116.500	54.000	35.000	450.709	438.411	1187.700	570.250	554.930	1483.753	119.541
335	266.375	169.750	116.500	54.000	35.000	354.709	438.411	1187.700	474.250	448.031	1345.339	119.541
336	289.125	169.750	116.500	54.000	35.000	354.709	438.411	1187.700	474.250	454.717	1354.542	119.541
3R												
411	266.375	169.750	124.000	54.000	35.000	354.709	438.411	1187.700	481.750	448.031	1345.339	127.041
412	289.125	169.750	124.000	54.000	35.000	354.709	438.411	1187.700	481.750	454.717	1354.542	127.041
413	616.000	159.500	124.000	54.000	35.000	450.709	438.411	1187.700	577.750	554.930	1483.753	127.041
414	616.000	159.500	124.000	54.000	35.000	450.709	438.411	1187.700	577.750	554.930	1483.753	127.041
415	266.375	169.750	124.000	54.000	35.000	354.709	438.411	1187.700	481.750	448.031	1345.339	127.041
416	289.125	169.750	124.000	54.000	35.000	354.709	438.411	1187.700	481.750	454.717	1354.542	127.041
421	266.375	169.750	124.000	54.000	35.000	354.709	438.411	1187.700	481.750	448.031	1345.339	127.041
422	289.125	169.750	124.000	54.000	35.000	354.709	438.411	1187.700	481.750	454.717	1354.542	127.041
423	616.000	159.500	124.000	54.000	35.000	450.709	438.411	1187.700	577.750	554.930	1483.753	127.041
424	616.000	159.500	124.000	54.000	35.000	450.709	438.411	1187.700	577.750	554.930	1483.753	127.041
425	266.375	169.750	124.000	54.000	35.000	354.709	438.411	1187.700	481.750	448.031	1345.339	127.041
426	289.125	169.750	124.000	54.000	35.000	354.709	438.411	1187.700	481.750	454.717	1354.542	127.041
431	266.375	169.750	116.500	54.000	35.000	354.709	438.411	1187.700	474.250	448.031	1345.339	119.541
432	289.125	169.750	116.500	54.000	35.000	354.709	438.411	1187.700	474.250	454.717	1354.542	119.541
433	616.000	159.500	116.500	54.000	35.000	450.709	438.411	1187.700	570.250	554.930	1483.753	119.541
434	616.000	159.500	116.500	54.000	35.000	450.709	438.411	1187.700	570.250	554.930	1483.753	119.541
435	266.375	169.750	116.500	54.000	35.000	354.709	438.411	1187.700	474.250	448.031	1345.339	119.541
436	289.125	169.750	116.500	54.000	35.000	354.709	438.411	1187.700	474.250	454.717	1354.542	119.541
4R												
511	266.375	169.750	124.000	54.000	55.000	354.709	438.411	1187.700	481.750	448.031	1345.339	127.041
512	289.125	169.750	124.000	54.000	55.000	354.709	438.411	1187.700	481.750	454.717	1354.542	127.041
513	616.000	159.500	124.000	54.000	55.000	450.709	438.411	1187.700	577.750	554.930	1483.753	127.041
514	616.000	159.500	124.000	54.000	55.000	450.709	438.411	1187.700	577.750	554.930	1483.753	127.041
515	266.375	169.750	124.000	54.000	55.000	354.709	438.411	1187.700	481.750	448.031	1345.339	127.041
516	289.125	169.750	124.000	54.000	55.000	354.709	438.411	1187.700	481.750	454.717	1354.542	127.041
521	266.375	169.750	124.000	54.000	55.000	354.709	438.411	1187.700	481.750	448.031	1345.339	127.041
522	289.125	169.750	124.000	54.000	55.000	354.709	438.411	1187.700	481.750	454.717	1354.542	127.041
523	616.000	159.500	124.000	54.000	55.000	450.709	438.411	1187.700	577.750	554.930	1483.753	127.041
524	616.000	159.500	124.000	54.000	55.000	450.709	438.411	1187.700	577.750	554.930	1483.753	127.041
525	266.375	169.750	124.000	54.000	55.000	354.709	438.411	1187.700	481.750	448.031	1345.339	127.041
526	289.125	169.750	124.000	54.000	55.000	354.709	438.411	1187.700	481.750	454.717	1354.542	127.041
531	266.375	169.750	116.500	54.000	55.000	354.709	438.411	1187.700	474.250	448.031	1345.339	119.541
532	289.125	169.750	116.500	54.000	55.000	354.709	438.411	1187.700	474.250	454.717	1354.542	119.541
533	616.000	159.500	116.500	54.000	55.000	450.709	438.411	1187.700	570.250	554.930	1483.753	119.541
534	616.000	159.500	116.500	54.000	55.000	450.709	438.411	1187.700	570.250	554.930	1483.753	119.541
535	266.375	169.750	116.500	54.000	55.000	354.709	438.411	1187.700	474.250	448.031	1345.339	119.541
536	289.125	169.750	116.500	54.000	55.000	354.709	438.411	1187.700	474.250	454.717	1354.542	119.541

Module	Object Top Points ($T_X pp_x$)								
	T_B			T_C			T_D		
	x	y	z	x	y	z	x	y	
111	291.460	1129.837	127.041	428.791	1030.061	127.041	585.362	1245.563	
112	284.774	1120.635	127.041	422.105	1020.858	127.041	592.048	1254.765	
113	192.854	985.399	127.041	321.892	891.647	127.041	683.968	1390.001	
114	192.854	985.399	127.041	321.892	891.647	127.041	683.968	1390.001	
115	291.460	1129.837	127.041	428.791	1030.061	127.041	585.362	1245.563	
116	284.774	1120.635	127.041	422.105	1020.858	127.041	592.048	1254.765	
121	291.460	1129.837	127.041	428.791	1030.061	127.041	585.362	1245.563	
122	284.774	1120.635	127.041	422.105	1020.858	127.041	592.048	1254.765	
123	192.854	985.399	127.041	321.892	891.647	127.041	683.968	1390.001	
124	192.854	985.399	127.041	321.892	891.647	127.041	683.968	1390.001	
125	291.460	1129.837	127.041	428.791	1030.061	127.041	585.362	1245.563	
126	284.774	1120.635	127.041	422.105	1020.858	127.041	592.048	1254.765	
131	291.460	1129.837	119.541	428.791	1030.061	119.541	585.362	1245.563	
132	284.774	1120.635	119.541	422.105	1020.858	119.541	592.048	1254.765	
133	192.854	985.399	119.541	321.892	891.647	119.541	683.968	1390.001	
134	192.854	985.399	119.541	321.892	891.647	119.541	683.968	1390.001	
135	291.460	1129.837	119.541	428.791	1030.061	119.541	585.362	1245.563	
136	284.774	1120.635	119.541	422.105	1020.858	119.541	592.048	1254.765	
1R									
211	291.460	1129.837	127.041	428.791	1030.061	127.041	585.362	1245.563	
212	284.774	1120.635	127.041	422.105	1020.858	127.041	592.048	1254.765	
213	192.854	985.399	127.041	321.892	891.647	127.041	683.968	1390.001	
214	192.854	985.399	127.041	321.892	891.647	127.041	683.968	1390.001	
215	291.460	1129.837	127.041	428.791	1030.061	127.041	585.362	1245.563	
216	284.774	1120.635	127.041	422.105	1020.858	127.041	592.048	1254.765	
221	291.460	1129.837	127.041	428.791	1030.061	127.041	585.362	1245.563	
222	284.774	1120.635	127.041	422.105	1020.858	127.041	592.048	1254.765	
223	192.854	985.399	127.041	321.892	891.647	127.041	683.968	1390.001	
224	192.854	985.399	127.041	321.892	891.647	127.041	683.968	1390.001	
225	291.460	1129.837	127.041	428.791	1030.061	127.041	585.362	1245.563	
226	284.774	1120.635	127.041	422.105	1020.858	127.041	592.048	1254.765	
231	291.460	1129.837	119.541	428.791	1030.061	119.541	585.362	1245.563	
232	284.774	1120.635	119.541	422.105	1020.858	119.541	592.048	1254.765	
233	192.854	985.399	119.541	321.892	891.647	119.541	683.968	1390.001	
234	192.854	985.399	119.541	321.892	891.647	119.541	683.968	1390.001	
235	291.460	1129.837	119.541	428.791	1030.061	119.541	585.362	1245.563	
236	284.774	1120.635	119.541	422.105	1020.858	119.541	592.048	1254.765	
2R									
311	291.460	1129.837	127.041	428.791	1030.061	127.041	585.362	1245.563	
312	284.774	1120.635	127.041	422.105	1020.858	127.041	592.048	1254.765	
313	192.854	985.399	127.041	321.892	891.647	127.041	683.968	1390.001	
314	192.854	985.399	127.041	321.892	891.647	127.041	683.968	1390.001	
315	291.460	1129.837	127.041	428.791	1030.061	127.041	585.362	1245.563	
316	284.774	1120.635	127.041	422.105	1020.858	127.041	592.048	1254.765	
321	291.460	1129.837	127.041	428.791	1030.061	127.041	585.362	1245.563	
322	284.774	1120.635	127.041	422.105	1020.858	127.041	592.048	1254.765	
323	192.854	985.399	127.041	321.892	891.647	127.041	683.968	1390.001	
324	192.854	985.399	127.041	321.892	891.647	127.041	683.968	1390.001	
325	291.460	1129.837	127.041	428.791	1030.061	127.041	585.362	1245.563	
326	284.774	1120.635	127.041	422.105	1020.858	127.041	592.048	1254.765	
331	291.460	1129.837	119.541	428.791	1030.061	119.541	585.362	1245.563	
332	284.774	1120.635	119.541	422.105	1020.858	119.541	592.048	1254.765	
333	192.854	985.399	119.541	321.892	891.647	119.541	683.968	1390.001	
334	192.854	985.399	119.541	321.892	891.647	119.541	683.968	1390.001	
335	291.460	1129.837	119.541	428.791	1030.061	119.541	585.362	1245.563	
336	284.774	1120.635	119.541	422.105	1020.858	119.541	592.048	1254.765	
3R									
411	291.460	1129.837	127.041	428.791	1030.061	127.041	585.362	1245.563	
412	284.774	1120.635	127.041	422.105	1020.858	127.041	592.048	1254.765	
413	192.854	985.399	127.041	321.892	891.647	127.041	683.968	1390.001	
414	192.854	985.399	127.041	321.892	891.647	127.041	683.968	1390.001	
415	291.460	1129.837	127.041	428.791	1030.061	127.041	585.362	1245.563	
416	284.774	1120.635	127.041	422.105	1020.858	127.041	592.048	1254.765	
421	291.460	1129.837	127.041	428.791	1030.061	127.041	585.362	1245.563	
422	284.774	1120.635	127.041	422.105	1020.858	127.041	592.048	1254.765	
423	192.854	985.399	127.041	321.892	891.647	127.041	683.968	1390.001	
424	192.854	985.399	127.041	321.892	891.647	127.041	683.968	1390.001	
425	291.460	1129.837	127.041	428.791	1030.061	127.041	585.362	1245.563	
426	284.774	1120.635	127.041	422.105	1020.858	127.041	592.048	1254.765	
431	291.460	1129.837	119.541	428.791	1030.061	119.541	585.362	1245.563	
432	284.774	1120.635	119.541	422.105	1020.858	119.541	592.048	1254.765	
433	192.854	985.399	119.541	321.892	891.647	119.541	683.968	1390.001	
434	192.854	985.399	119.541	321.892	891.647	119.541	683.968	1390.001	
435	291.460	1129.837	119.541	428.791	1030.061	119.541	585.362	1245.563	
436	284.774	1120.635	119.541	422.105	1020.858	119.541	592.048	1254.765	
4R									
511	291.460	1129.837	127.041	428.791	1030.061	127.041	585.362	1245.563	
512	284.774	1120.635	127.041	422.105	1020.858	127.041	592.048	1254.765	
513	192.854	985.399	127.041	321.892	891.647	127.041	683.968	1390.001	
514	192.854	985.399	127.041	321.892	891.647	127.041	683.968	1390.001	
515	291.460	1129.837	127.041	428.791	1030.061	127.041	585.362	1245.563	
516	284.774	1120.635	127.041	422.105	1020.858	127.041	592.048	1254.765	
521	291.460	1129.837	127.041	428.791	1030.061	127.041	585.362	1245.563	
522	284.774	1120.635	127.041	422.105	1020.858	127.041	592.048	1254.765	
523	192.854	985.399	127.041	321.892	891.647	127.041	683.968	1390.001	
524	192.854	985.399	127.041	321.892	891.647	127.041	683.968	1390.001	
525	291.460	1129.837	127.041	428.791	1030.061	127.041	585.362	1245.563	
526	284.774	1120.635	127.041	422.105	1020.858	127.041	592.048	1254.765	
531	291.460	1129.837	119.541	428.791	1030.061	119.541	585.362	1245.563	
532	284.774	1120.635	119.541	422.105	1020.858	119.541	592.048	1254.765	
533	192.854	985.399	119.541	321.892	891.647	119.541	683.968	1390.001	
534	192.854	985.399	119.541	321.892	891.647	119.541	683.968	1390.001	
535	291.460	1129.837	119.541	428.791	1030.061	119.541	585.362	1245.563	
536	284.774	1120.635	119.541	422.105	1020.858	119.541	592.048	1254.765	

XX**pp**$_x$)																				
	Object Bottom Points (BXpp_x)												Crane Hook			T_A			T_B	
	B_A			B_B			B_C			B_D										
z	x	y	z	x	y	z	x	y	z	x	y	z	x	y	z	x	y	z	x	y
127.041	448.031	1345.339	3.041	291.460	1129.837	3.041	428.791	1030.061	3.041	585.362	1245.563	3.041	50.771	1661.925	441.125	-107.012	1668.793	86.416	111.190	1516.006
127.041	454.717	1354.542	3.041	284.774	1120.635	3.041	422.105	1020.858	3.041	592.048	1254.765	3.041	279.929	1501.467	441.125	112.828	1514.859	86.416	349.665	1349.024
127.041	554.930	1483.753	3.041	192.854	985.399	3.041	321.892	891.647	3.041	683.968	1390.001	3.041	260.052	1718.797	537.125	-37.990	1830.131	86.416	466.608	1476.808
127.041	554.930	1483.753	3.041	192.854	985.399	3.041	321.892	891.647	3.041	683.968	1390.001	3.041	352.684	1851.090	537.125	54.642	1962.424	86.416	559.240	1609.101
127.041	448.031	1345.339	3.041	291.460	1129.837	3.041	428.791	1030.061	3.041	585.362	1245.563	3.041	334.548	2067.201	441.125	176.765	2074.069	86.416	394.967	1921.282
127.041	454.717	1354.542	3.041	284.774	1120.635	3.041	422.105	1020.858	3.041	592.048	1254.765	3.041	563.706	1906.743	441.125	396.605	1920.135	86.416	633.442	1754.300
127.041	448.031	1345.339	3.041	291.460	1129.837	3.041	428.791	1030.061	3.041	585.362	1245.563	3.041	50.771	1661.925	565.125	-107.012	1668.793	210.416	111.190	1516.006
127.041	454.717	1354.542	3.041	284.774	1120.635	3.041	422.105	1020.858	3.041	592.048	1254.765	3.041	279.929	1501.467	565.125	112.828	1514.859	210.416	349.665	1349.024
127.041	554.930	1483.753	3.041	192.854	985.399	3.041	321.892	891.647	3.041	683.968	1390.001	3.041	260.052	1718.797	661.125	-37.990	1830.131	210.416	466.608	1476.808
127.041	554.930	1483.753	3.041	192.854	985.399	3.041	321.892	891.647	3.041	683.968	1390.001	3.041	352.684	1851.090	661.125	54.642	1962.424	210.416	559.240	1609.101
127.041	448.031	1345.339	3.041	291.460	1129.837	3.041	428.791	1030.061	3.041	585.362	1245.563	3.041	334.548	2067.201	565.125	176.765	2074.069	210.416	394.967	1921.282
127.041	454.717	1354.542	3.041	284.774	1120.635	3.041	422.105	1020.858	3.041	592.048	1254.765	3.041	563.706	1906.743	565.125	396.605	1920.135	210.416	633.442	1754.300
119.541	448.031	1345.339	3.041	291.460	1129.837	3.041	428.791	1030.061	3.041	585.362	1245.563	3.041	50.771	1661.925	913.125	-107.012	1668.793	558.416	111.190	1516.006
119.541	454.717	1354.542	3.041	284.774	1120.635	3.041	422.105	1020.858	3.041	592.048	1254.765	3.041	279.929	1501.467	913.125	112.828	1514.859	558.416	349.665	1349.024
119.541	554.930	1483.753	3.041	192.854	985.399	3.041	321.892	891.647	3.041	683.968	1390.001	3.041	260.052	1718.797	1009.125	-37.990	1830.131	558.416	466.608	1476.808
119.541	554.930	1483.753	3.041	192.854	985.399	3.041	321.892	891.647	3.041	683.968	1390.001	3.041	352.684	1851.090	1009.125	54.642	1962.424	558.416	559.240	1609.101
119.541	448.031	1345.339	3.041	291.460	1129.837	3.041	428.791	1030.061	3.041	585.362	1245.563	3.041	334.548	2067.201	913.125	176.765	2074.069	558.416	394.967	1921.282
119.541	454.717	1354.542	3.041	284.774	1120.635	3.041	422.105	1020.858	3.041	592.048	1254.765	3.041	563.706	1906.743	913.125	396.605	1920.135	558.416	633.442	1754.300
127.041	448.031	1345.339	3.041	291.460	1129.837	3.041	428.791	1030.061	3.041	585.362	1245.563	3.041	817.744	154.424	335.125	810.876	-3.359	-19.584	963.663	214.843
127.041	454.717	1354.542	3.041	284.774	1120.635	3.041	422.105	1020.858	3.041	592.048	1254.765	3.041	978.202	383.582	335.125	964.810	216.481	-19.584	1130.645	453.318
127.041	554.930	1483.753	3.041	192.854	985.399	3.041	321.892	891.647	3.041	683.968	1390.001	3.041	760.872	363.705	431.125	649.538	65.663	-19.584	1002.861	570.261
127.041	554.930	1483.753	3.041	192.854	985.399	3.041	321.892	891.647	3.041	683.968	1390.001	3.041	628.579	456.337	431.125	517.245	158.295	-19.584	870.568	662.893
127.041	448.031	1345.339	3.041	291.460	1129.837	3.041	428.791	1030.061	3.041	585.362	1245.563	3.041	412.468	438.201	335.125	405.600	280.418	-19.584	558.387	498.620
127.041	454.717	1354.542	3.041	284.774	1120.635	3.041	422.105	1020.858	3.041	592.048	1254.765	3.041	572.926	667.359	335.125	559.534	500.258	-19.584	725.369	737.095
127.041	448.031	1345.339	3.041	291.460	1129.837	3.041	428.791	1030.061	3.041	585.362	1245.563	3.041	817.744	154.424	459.125	810.876	-3.359	104.416	963.663	214.843
127.041	454.717	1354.542	3.041	284.774	1120.635	3.041	422.105	1020.858	3.041	592.048	1254.765	3.041	978.202	383.582	459.125	964.810	216.481	104.416	1130.645	453.318
127.041	554.930	1483.753	3.041	192.854	985.399	3.041	321.892	891.647	3.041	683.968	1390.001	3.041	760.872	363.705	555.125	649.538	65.663	104.416	1002.861	570.261
127.041	554.930	1483.753	3.041	192.854	985.399	3.041	321.892	891.647	3.041	683.968	1390.001	3.041	628.579	456.337	555.125	517.245	158.295	104.416	870.568	662.893
127.041	448.031	1345.339	3.041	291.460	1129.837	3.041	428.791	1030.061	3.041	585.362	1245.563	3.041	412.468	438.201	459.125	405.600	280.418	104.416	558.387	498.620
127.041	454.717	1354.542	3.041	284.774	1120.635	3.041	422.105	1020.858	3.041	592.048	1254.765	3.041	572.926	667.359	459.125	559.534	500.258	104.416	725.369	737.095
119.541	448.031	1345.339	3.041	291.460	1129.837	3.041	428.791	1030.061	3.041	585.362	1245.563	3.041	817.744	154.424	575.625	810.876	-3.359	220.916	963.663	214.843
119.541	454.717	1354.542	3.041	284.774	1120.635	3.041	422.105	1020.858	3.041	592.048	1254.765	3.041	978.202	383.582	575.625	964.810	216.481	220.916	1130.645	453.318
119.541	554.930	1483.753	3.041	192.854	985.399	3.041	321.892	891.647	3.041	683.968	1390.001	3.041	760.872	363.705	671.625	649.538	65.663	220.916	1002.861	570.261
119.541	554.930	1483.753	3.041	192.854	985.399	3.041	321.892	891.647	3.041	683.968	1390.001	3.041	628.579	456.337	671.625	517.245	158.295	220.916	870.568	662.893
119.541	448.031	1345.339	3.041	291.460	1129.837	3.041	428.791	1030.061	3.041	585.362	1245.563	3.041	412.468	438.201	575.625	405.600	280.418	220.916	558.387	498.620
119.541	454.717	1354.542	3.041	284.774	1120.635	3.041	422.105	1020.858	3.041	592.048	1254.765	3.041	572.926	667.359	575.625	559.534	500.258	220.916	725.369	737.095
127.041	448.031	1345.339	3.041	291.460	1129.837	3.041	428.791	1030.061	3.041	585.362	1245.563	3.041	1139.493	1822.603	306.125	981.710	1829.471	-48.584	1199.912	1676.684
127.041	454.717	1354.542	3.041	284.774	1120.635	3.041	422.105	1020.858	3.041	592.048	1254.765	3.041	1368.650	1662.145	306.125	1201.549	1675.537	-48.584	1438.386	1509.702
127.041	554.930	1483.753	3.041	192.854	985.399	3.041	321.892	891.647	3.041	683.968	1390.001	3.041	1348.773	1879.475	402.125	1050.731	1990.809	-48.584	1555.329	1637.486
127.041	554.930	1483.753	3.041	192.854	985.399	3.041	321.892	891.647	3.041	683.968	1390.001	3.041	1441.406	2011.768	402.125	1143.364	2123.102	-48.584	1647.962	1769.779
127.041	448.031	1345.339	3.041	291.460	1129.837	3.041	428.791	1030.061	3.041	585.362	1245.563	3.041	1423.270	2227.879	306.125	1265.487	2234.747	-48.584	1483.689	2081.960
127.041	454.717	1354.542	3.041	284.774	1120.635	3.041	422.105	1020.858	3.041	592.048	1254.765	3.041	1652.427	2067.421	306.125	1485.326	2080.813	-48.584	1722.163	1914.978
127.041	448.031	1345.339	3.041	291.460	1129.837	3.041	428.791	1030.061	3.041	585.362	1245.563	3.041	1139.493	1822.603	430.125	981.710	1829.471	75.416	1199.912	1676.684
127.041	454.717	1354.542	3.041	284.774	1120.635	3.041	422.105	1020.858	3.041	592.048	1254.765	3.041	1368.650	1662.145	430.125	1201.549	1675.537	75.416	1438.386	1509.702
127.041	554.930	1483.753	3.041	192.854	985.399	3.041	321.892	891.647	3.041	683.968	1390.001	3.041	1348.773	1879.475	526.125	1050.731	1990.809	75.416	1555.329	1637.486
127.041	554.930	1483.753	3.041	192.854	985.399	3.041	321.892	891.647	3.041	683.968	1390.001	3.041	1441.406	2011.768	526.125	1143.364	2123.102	75.416	1647.962	1769.779
127.041	448.031	1345.339	3.041	291.460	1129.837	3.041	428.791	1030.061	3.041	585.362	1245.563	3.041	1423.270	2227.879	430.125	1265.487	2234.747	75.416	1483.689	2081.960
127.041	454.717	1354.542	3.041	284.774	1120.635	3.041	422.105	1020.858	3.041	592.048	1254.765	3.041	1652.427	2067.421	430.125	1485.326	2080.813	75.416	1722.163	1914.978
119.541	448.031	1345.339	3.041	291.460	1129.837	3.041	428.791	1030.061	3.041	585.362	1245.563	3.041	1139.493	1822.603	546.625	981.710	1829.471	191.916	1199.912	1676.684
119.541	454.717	1354.542	3.041	284.774	1120.635	3.041	422.105	1020.858	3.041	592.048	1254.765	3.041	1368.650	1662.145	546.625	1201.549	1675.537	191.916	1438.386	1509.702
119.541	554.930	1483.753	3.041	192.854	985.399	3.041	321.892	891.647	3.041	683.968	1390.001	3.041	1348.773	1879.475	642.625	1050.731	1990.809	191.916	1555.329	1637.486
119.541	554.930	1483.753	3.041	192.854	985.399	3.041	321.892	891.647	3.041	683.968	1390.001	3.041	1441.406	2011.768	642.625	1143.364	2123.102	191.916	1647.962	1769.779
119.541	448.031	1345.339	3.041	291.460	1129.837	3.041	428.791	1030.061	3.041	585.362	1245.563	3.041	1423.270	2227.879	546.625	1265.487	2234.747	191.916	1483.689	2081.960
119.541	454.717	1354.542	3.041	284.774	1120.635	3.041	422.105	1020.858	3.041	592.048	1254.765	3.041	1652.427	2067.421	546.625	1485.326	2080.813	191.916	1722.163	1914.978
127.041	448.031	1345.339	3.041	291.460	1129.837	3.041	428.791	1030.061	3.041	585.362	1245.563	3.041	1522.771	245.425	143.125	1364.988	252.293	-211.584	1583.190	99.506
127.041	454.717	1354.542	3.041	284.774	1120.635	3.041	422.105	1020.858	3.041	592.048	1254.765	3.041	1751.928	84.967	143.125	1584.827	98.359	-211.584	1821.664	-67.476
127.041	554.930	1483.753	3.041	192.854	985.399	3.041	321.892	891.647	3.041	683.968	1390.001	3.041	1732.051	302.297	239.125	1434.009	413.631	-211.584	1938.607	60.308
127.041	554.930	1483.753	3.041	192.854	985.399	3.041	321.892	891.647	3.041	683.968	1390.001	3.041	1824.684	434.590	239.125	1526.642	545.924	-211.584	2031.240	192.601
127.041	448.031	1345.339	3.041	291.460	1129.837	3.041	428.791	1030.061	3.041	585.362	1245.563	3.041	1806.548	650.701	143.125	1648.765	657.569	-211.584	1866.967	504.782
127.041	454.717	1354.542	3.041	284.774	1120.635	3.041	422.105	1020.858	3.041	592.048	1254.765	3.041	2035.705	490.243	143.125	1868.604	503.635	-211.584	2105.441	337.800
127.041	448.031	1345.339	3.041	291.460	1129.837	3.041	428.791	1030.061	3.041	585.362	1245.563	3.041	1522.771	245.425	267.125	1364.988	252.293	-87.584	1583.190	99.506
127.041	454.717	1354.542	3.041	284.774	1120.635	3.041	422.105	1020.858	3.041	592.048	1254.765	3.041	1751.928	84.967	267.125	1584.827	98.359	-87.584	1821.664	-67.476
127.041	554.930	1483.753	3.041	192.854	985.399	3.041	321.892	891.647	3.041	683.968	1390.001	3.041	1732.051	302.297	363.125	1434.009	413.631	-87.584	1938.607	60.308
127.041	554.930	1483.753	3.041	192.854	985.399	3.041	321.892	891.647	3.041	683.968	1390.001	3.041	1824.684	434.590	363.125	1526.642	545.924	-87.584	2031.240	192.601
127.041	448.031	1345.339	3.041	291.460	1129.837	3.041	428.791	1030.061	3.041	585.362	1245.563	3.041	1806.548	650.701	267.125	1648.765	657.569	-87.584	1866.967	504.782
127.041	454.717	1354.542	3.041	284.774	1120.635	3.041	422.105	1020.858	3.041	592.048	1254.765	3.041	2035.705	490.243	267.125	1868.604	503.635	-87.584	2105.441	337.800
119.541	448.031	1345.339	3.041	291.460	1129.837	3.041	428.791	1030.061	3.041	585.362	1245.563	3.041	1522.771	245.425	391.125	1364.988	252.293	36.416	1583.190	99.506
119.541	454.717	1354.542	3.041	284.774	1120.635	3.041	422.105	1020.858	3.041	592.048	1254.765	3.041	1751.928	84.967	391.125	1584.827	98.359	36.416	1821.664	-67.476
119.541	554.930	1483.753	3.041	192.854	985.399	3.041	321.892	891.647	3.041	683.968	1390.001	3.041	1732.051	302.297	487.125	1434.009	413.631	36.416	1938.607	60.308
119.541	554.930	1483.753	3.041	192.854	985.399	3.041	321.892	891.647	3.041	683.968	1390.001	3.041	1824.684	434.590	487.125	1526.642	545.924	36.416	2031.240	192.601
119.541	448.031	1345.339	3.041	291.460	1129.837	3.041	428.791	1030.061	3.041	585.362	1245.563	3.041	1806.548	650.701	391.125	1648.765	657.569	36.416	1866.967	504.782
119.541	454.717	1354.542	3.041	284.774	1120.635	3.041	422.105	1020.858	3.041	592.048	1254.765	3.041	2035.705	490.243	391.125	1868.604	503.635	36.416	2105.441	337.800
127.041	448.031	1345.339	3.041	291.460	1129.837	3.041	428.791	1030.061	3.041	585.362	1245.563	3.041	2277.770	2075.103	236.125	2284.638	2232.886	-118.584	2131.851	2014.684
127.041	454.717	1354.542	3.041	284.774	1120.635	3.041	422.105	1020.858	3.041	592.048	1254.765	3.041	2117.312	1845.945	236.125	2130.704	2013.046	-118.584	1964.869	1776.209
127.041	554.930	1483.753	3.041	192.854	985.399	3.041	321.892	891.647	3.041	683.968	1390.001	3.041	2334.642	1865.822	332.125	2445.976	2163.864	-118.584	2092.653	1659.266
127.041	554.930	1483.753	3.041	192.854	985.399	3.041	321.892	891.647	3.041	683.968	1390.001	3.041	2466.935	1773.190	332.125	2578.269	2071.232	-118.584	2224.946	1566.634
127.041	448.031	1345.339	3.041	291.460	1129.837	3.041	428.791	1030.061	3.041	585.362	1245.563	3.041	2683.450	1791.326	236.125	2690.318	1949.109	-118.584	2537.531	1730.907
127.041	454.717	1354.542	3.041	284.774	1120.635	3.041	422.105	1020.858	3.041	592.048	1254.765	3.041	2522.587	1562.168	236.125	2535.979	1729.269	-118.584	2370.144	1492.432
127.041	448.031	1345.339	3.041	291.460	1129.837	3.041	428.791	1030.061	3.041	585.362	1245.563	3.041	2277.770	2075.103	360.125	2284.638	2232.886	5.416	2131.851	2014.684
127.041	454.717	1354.542	3.041	284.774	1120.635	3.041	422.105	1020.858	3.041	592.048	1254.765	3.041	2117.312	1845.945	360.125	2130.704	2013.046	5.416	1964.869	1776.209
127.041	554.930	1483.753	3.041	192.854	985.399	3.041	321.892	891.647	3.041	683.968	1390.001	3.041	2334.642	1865.822	456.125	2445.976	2163.864	5.416	2092.653	1659.266
127.041	554.930	1483.753	3.041	192.854	985.399	3.041	321.892	891.647	3.041	683.968	1390.001	3.041	2466.935	1773.190	456.125	2578.269	2071.232	5.416	2224.946	1566.634
127.041	448.031	1345.339	3.041	291.460	1129.837	3.041	428.791	1030.061	3.041	585.362	1245.563	3.041	2683.450	1791.326	360.125	2690.318	1949.109	5.416	2537.531	1730.907
127.041	454.717	1354.542	3.041	284.774	1120.635	3.041	422.105	1020.858	3.041	592.048	1254.765	3.041	2522.587	1562.168	360.125	2535.979	1729.269	5.416	2370.144	1492.432
119.541	448.031	1345.339	3.041	291.460	1129.837	3.041	428.791	1030.061	3.041	585.362	1245.563	3.041	2277.770	2075.103	476.625	2284.638	2232.886	121.916	2131.851	2014.684
119.541	454.717	1354.542	3.041	284.774	1120.635	3.041	422.105	1020.858	3.041	592.048	1254.765	3.041	2117.312	1845.945	476.625	2130.704	2013.046	121.916	1964.869	1776.209
119.541	554.930	1483.753	3.041	192.854	985.399	3.041	321.892	891.647	3.041	683.968	1390.001	3.041	2334.642	1865.822	572.625	2445.976	2163.864	121.916	2092.653	1659.266
119.541	554.930	1483.753	3.041	192.854	985.399	3.041	321.892	891.647	3.041	683.968	1390.001	3.041	2466.935	1773.190	572.625	2578.269	2071.232	121.916	2224.946	1566.634
119.541	448.031	1345.339	3.041	291.460	1129.837	3.041	428.791	1030.061	3.041	585.362	1245.563	3.041	2683.450	1791.326	476.625	2690.318	1949.109	121.916	2537.531	1730.907
119.541	454.717	1354.542	3.041	284.774	1120.635	3.041	422.105	1020.858	3.041	592.048	1254.765	3.041	2522.587	1562.168	476.625	2535.979	1729.269	121.916	2370.144	1492.432

SET-POSITION ($XXsp_X$)

ject Top Points ($TXsp_X$)							Object Bottom Points ($BXsp_X$)											
	T_C			T_B			B_A			B_B			B_C			B_D		
z	x	y	z	x	y	z	x	y	z	x	y	z	x	y	z	x	y	z
86.416	208.554	1668.793	86.416	-9.648	1807.844	86.416	-107.012	1668.793	-37.584	111.190	1516.006	-37.584	208.554	1668.793	-37.584	-9.648	1807.844	-37.584
86.416	447.030	1514.859	86.416	210.193	1653.910	86.416	112.828	1514.859	-37.584	349.665	1349.024	-37.584	447.030	1514.859	-37.584	210.193	1653.910	-37.584
86.416	558.094	1830.131	86.416	53.496	1960.786	86.416	-37.990	1830.131	-37.584	466.608	1476.808	-37.584	558.094	1830.131	-37.584	53.496	1960.786	-37.584
86.416	650.726	1962.424	86.416	146.128	2093.079	86.416	54.642	1962.424	-37.584	559.240	1609.101	-37.584	650.726	1962.424	-37.584	146.128	2093.079	-37.584
86.416	492.331	2074.069	86.416	274.129	2213.120	86.416	176.765	2074.069	-37.584	394.967	1921.282	-37.584	492.331	2074.069	-37.584	274.129	2213.120	-37.584
86.416	730.807	1920.135	86.416	493.970	2059.186	86.416	396.605	1920.135	-37.584	633.442	1754.300	-37.584	730.807	1920.135	-37.584	493.970	2059.186	-37.584
210.416	208.554	1668.793	210.416	-9.648	1807.844	210.416	-107.012	1668.793	86.416	111.190	1516.006	86.416	208.554	1668.793	86.416	-9.648	1807.844	86.416
210.416	447.030	1514.859	210.416	210.193	1653.910	210.416	112.828	1514.859	86.416	349.665	1349.024	86.416	447.030	1514.859	86.416	210.193	1653.910	86.416
210.416	558.094	1830.131	210.416	53.496	1960.786	210.416	-37.990	1830.131	86.416	466.608	1476.808	86.416	558.094	1830.131	86.416	53.496	1960.786	86.416
210.416	650.726	1962.424	210.416	146.128	2093.079	210.416	54.642	1962.424	86.416	559.240	1609.101	86.416	650.726	1962.424	86.416	146.128	2093.079	86.416
210.416	492.331	2074.069	210.416	274.129	2213.120	210.416	176.765	2074.069	86.416	394.967	1921.282	86.416	492.331	2074.069	86.416	274.129	2213.120	86.416
210.416	730.807	1920.135	210.416	493.970	2059.186	210.416	396.605	1920.135	86.416	633.442	1754.300	86.416	730.807	1920.135	86.416	493.970	2059.186	86.416
558.416	208.554	1668.793	558.416	-9.648	1807.844	558.416	-107.012	1668.793	441.916	111.190	1516.006	441.916	208.554	1668.793	441.916	-9.648	1807.844	441.916
558.416	447.030	1514.859	558.416	210.193	1653.910	558.416	112.828	1514.859	441.916	349.665	1349.024	441.916	447.030	1514.859	441.916	210.193	1653.910	441.916
558.416	558.094	1830.131	558.416	53.496	1960.786	558.416	-37.990	1830.131	441.916	466.608	1476.808	441.916	558.094	1830.131	441.916	53.496	1960.786	441.916
558.416	650.726	1962.424	558.416	146.128	2093.079	558.416	54.642	1962.424	441.916	559.240	1609.101	441.916	650.726	1962.424	441.916	146.128	2093.079	441.916
558.416	492.331	2074.069	558.416	274.129	2213.120	558.416	176.765	2074.069	441.916	394.967	1921.282	441.916	492.331	2074.069	441.916	274.129	2213.120	441.916
558.416	730.807	1920.135	558.416	493.970	2059.186	558.416	396.605	1920.135	441.916	633.442	1754.300	441.916	730.807	1920.135	441.916	493.970	2059.186	441.916
-19.584	824.612	312.207	-19.584	671.825	94.005	-19.584	810.876	-3.359	-143.584	963.663	214.843	-143.584	824.612	312.207	-143.584	671.825	94.005	-143.584
-19.584	991.594	550.683	-19.584	825.759	313.846	-19.584	964.810	216.481	-143.584	1130.645	453.318	-143.584	991.594	550.683	-143.584	825.759	313.846	-143.584
-19.584	872.206	661.747	-19.584	518.883	157.149	-19.584	649.538	65.663	-143.584	1002.861	570.261	-143.584	872.206	661.747	-143.584	518.883	157.149	-143.584
-19.584	739.913	754.379	-19.584	386.590	249.781	-19.584	517.245	158.295	-143.584	870.568	662.893	-143.584	739.913	754.379	-143.584	386.590	249.781	-143.584
-19.584	419.336	595.984	-19.584	266.549	377.782	-19.584	405.600	280.418	-143.584	558.387	498.620	-143.584	419.336	595.984	-143.584	266.549	377.782	-143.584
-19.584	586.318	834.460	-19.584	420.483	597.623	-19.584	559.534	500.258	-143.584	725.369	737.095	-143.584	586.318	834.460	-143.584	420.483	597.623	-143.584
104.416	824.612	312.207	104.416	671.825	94.005	104.416	810.876	-3.359	-19.584	963.663	214.843	-19.584	824.612	312.207	-19.584	671.825	94.005	-19.584
104.416	991.594	550.683	104.416	825.759	313.846	104.416	964.810	216.481	-19.584	1130.645	453.318	-19.584	991.594	550.683	-19.584	825.759	313.846	-19.584
104.416	872.206	661.747	104.416	518.883	157.149	104.416	649.538	65.663	-19.584	1002.861	570.261	-19.584	872.206	661.747	-19.584	518.883	157.149	-19.584
104.416	739.913	754.379	104.416	386.590	249.781	104.416	517.245	158.295	-19.584	870.568	662.893	-19.584	739.913	754.379	-19.584	386.590	249.781	-19.584
104.416	419.336	595.984	104.416	266.549	377.782	104.416	405.600	280.418	-19.584	558.387	498.620	-19.584	419.336	595.984	-19.584	266.549	377.782	-19.584
104.416	586.318	834.460	104.416	420.483	597.623	104.416	559.534	500.258	-19.584	725.369	737.095	-19.584	586.318	834.460	-19.584	420.483	597.623	-19.584
220.916	824.612	312.207	220.916	671.825	94.005	220.916	810.876	-3.359	104.416	963.663	214.843	104.416	824.612	312.207	104.416	671.825	94.005	104.416
220.916	991.594	550.683	220.916	825.759	313.846	220.916	964.810	216.481	104.416	1130.645	453.318	104.416	991.594	550.683	104.416	825.759	313.846	104.416
220.916	872.206	661.747	220.916	518.883	157.149	220.916	649.538	65.663	104.416	1002.861	570.261	104.416	872.206	661.747	104.416	518.883	157.149	104.416
220.916	739.913	754.379	220.916	386.590	249.781	220.916	517.245	158.295	104.416	870.568	662.893	104.416	739.913	754.379	104.416	386.590	249.781	104.416
220.916	419.336	595.984	220.916	266.549	377.782	220.916	405.600	280.418	104.416	558.387	498.620	104.416	419.336	595.984	104.416	266.549	377.782	104.416
220.916	586.318	834.460	220.916	420.483	597.623	220.916	559.534	500.258	104.416	725.369	737.095	104.416	586.318	834.460	104.416	420.483	597.623	104.416
-48.584	1297.276	1829.471	-48.584	1079.074	1968.522	-48.584	981.710	1829.471	-172.584	1199.912	1676.684	-172.584	1297.276	1829.471	-172.584	1079.074	1968.522	-172.584
-48.584	1535.751	1675.537	-48.584	1298.914	1814.588	-48.584	1201.549	1675.537	-172.584	1438.386	1509.702	-172.584	1535.751	1675.537	-172.584	1298.914	1814.588	-172.584
-48.584	1646.815	1990.809	-48.584	1142.217	2121.464	-48.584	1050.731	1990.809	-172.584	1555.329	1637.486	-172.584	1646.815	1990.809	-172.584	1142.217	2121.464	-172.584
-48.584	1739.448	2123.102	-48.584	1234.850	2253.757	-48.584	1143.364	2123.102	-172.584	1647.962	1769.779	-172.584	1739.448	2123.102	-172.584	1234.850	2253.757	-172.584
-48.584	1581.053	2234.747	-48.584	1362.851	2373.798	-48.584	1265.487	2234.747	-172.584	1483.689	2081.960	-172.584	1581.053	2234.747	-172.584	1362.851	2373.798	-172.584
-48.584	1819.528	2080.813	-48.584	1582.691	2219.864	-48.584	1485.326	2080.813	-172.584	1722.163	1914.978	-172.584	1819.528	2080.813	-172.584	1582.691	2219.864	-172.584
75.416	1297.276	1829.471	75.416	1079.074	1968.522	75.416	981.710	1829.471	-48.584	1199.912	1676.684	-48.584	1297.276	1829.471	-48.584	1079.074	1968.522	-48.584
75.416	1535.751	1675.537	75.416	1298.914	1814.588	75.416	1201.549	1675.537	-48.584	1438.386	1509.702	-48.584	1535.751	1675.537	-48.584	1298.914	1814.588	-48.584
75.416	1646.815	1990.809	75.416	1142.217	2121.464	75.416	1050.731	1990.809	-48.584	1555.329	1637.486	-48.584	1646.815	1990.809	-48.584	1142.217	2121.464	-48.584
75.416	1739.448	2123.102	75.416	1234.850	2253.757	75.416	1143.364	2123.102	-48.584	1647.962	1769.779	-48.584	1739.448	2123.102	-48.584	1234.850	2253.757	-48.584
75.416	1581.053	2234.747	75.416	1362.851	2373.798	75.416	1265.487	2234.747	-48.584	1483.689	2081.960	-48.584	1581.053	2234.747	-48.584	1362.851	2373.798	-48.584
75.416	1819.528	2080.813	75.416	1582.691	2219.864	75.416	1485.326	2080.813	-48.584	1722.163	1914.978	-48.584	1819.528	2080.813	-48.584	1582.691	2219.864	-48.584
191.916	1297.276	1829.471	191.916	1079.074	1968.522	191.916	981.710	1829.471	75.416	1199.912	1676.684	75.416	1297.276	1829.471	75.416	1079.074	1968.522	75.416
191.916	1535.751	1675.537	191.916	1298.914	1814.588	191.916	1201.549	1675.537	75.416	1438.386	1509.702	75.416	1535.751	1675.537	75.416	1298.914	1814.588	75.416
191.916	1646.815	1990.809	191.916	1142.217	2121.464	191.916	1050.731	1990.809	75.416	1555.329	1637.486	75.416	1646.815	1990.809	75.416	1142.217	2121.464	75.416
191.916	1739.448	2123.102	191.916	1234.850	2253.757	191.916	1143.364	2123.102	75.416	1647.962	1769.779	75.416	1739.448	2123.102	75.416	1234.850	2253.757	75.416
191.916	1581.053	2234.747	191.916	1362.851	2373.798	191.916	1265.487	2234.747	75.416	1483.689	2081.960	75.416	1581.053	2234.747	75.416	1362.851	2373.798	75.416
191.916	1819.528	2080.813	191.916	1582.691	2219.864	191.916	1485.326	2080.813	75.416	1722.163	1914.978	75.416	1819.528	2080.813	75.416	1582.691	2219.864	75.416
-211.584	1680.554	252.293	-211.584	1482.352	391.344	-211.584	1364.988	252.293	-335.584	1583.190	99.506	-335.584	1680.554	252.293	-335.584	1482.352	391.344	-335.584
-211.584	1919.029	98.359	-211.584	1682.192	237.410	-211.584	1584.827	98.359	-335.584	1821.664	-67.476	-335.584	1919.029	98.359	-335.584	1682.192	237.410	-335.584
-211.584	2030.093	413.631	-211.584	1525.495	544.286	-211.584	1434.009	413.631	-335.584	1938.607	60.308	-335.584	2030.093	413.631	-335.584	1525.495	544.286	-335.584
-211.584	2122.726	545.924	-211.584	1618.128	676.579	-211.584	1526.642	545.924	-335.584	2031.240	192.601	-335.584	2122.726	545.924	-335.584	1618.128	676.579	-335.584
-211.584	1964.331	657.569	-211.584	1746.129	796.620	-211.584	1648.765	657.569	-335.584	1866.967	504.782	-335.584	1964.331	657.569	-335.584	1746.129	796.620	-335.584
-211.584	2202.806	503.635	-211.584	1965.969	642.686	-211.584	1868.604	503.635	-335.584	2105.441	337.800	-335.584	2202.806	503.635	-335.584	1965.969	642.686	-335.584
-87.584	1680.554	252.293	-87.584	1482.352	391.344	-87.584	1364.988	252.293	-211.584	1583.190	99.506	-211.584	1680.554	252.293	-211.584	1482.352	391.344	-211.584
-87.584	1919.029	98.359	-87.584	1682.192	237.410	-87.584	1584.827	98.359	-211.584	1821.664	-67.476	-211.584	1919.029	98.359	-211.584	1682.192	237.410	-211.584
-87.584	2030.093	413.631	-87.584	1525.495	544.286	-87.584	1434.009	413.631	-211.584	1938.607	60.308	-211.584	2030.093	413.631	-211.584	1525.495	544.286	-211.584
-87.584	2122.726	545.924	-87.584	1618.128	676.579	-87.584	1526.642	545.924	-211.584	2031.240	192.601	-211.584	2122.726	545.924	-211.584	1618.128	676.579	-211.584
-87.584	1964.331	657.569	-87.584	1746.129	796.620	-87.584	1648.765	657.569	-211.584	1866.967	504.782	-211.584	1964.331	657.569	-211.584	1746.129	796.620	-211.584
-87.584	2202.806	503.635	-87.584	1965.969	642.686	-87.584	1868.604	503.635	-211.584	2105.441	337.800	-211.584	2202.806	503.635	-211.584	1965.969	642.686	-211.584
36.416	1680.554	252.293	36.416	1482.352	391.344	36.416	1364.988	252.293	-80.084	1583.190	99.506	-80.084	1680.554	252.293	-80.084	1482.352	391.344	-80.084
36.416	1919.029	98.359	36.416	1682.192	237.410	36.416	1584.827	98.359	-80.084	1821.664	-67.476	-80.084	1919.029	98.359	-80.084	1682.192	237.410	-80.084
36.416	2030.093	413.631	36.416	1525.495	544.286	36.416	1434.009	413.631	-80.084	1938.607	60.308	-80.084	2030.093	413.631	-80.084	1525.495	544.286	-80.084
36.416	2122.726	545.924	36.416	1618.128	676.579	36.416	1526.642	545.924	-80.084	2031.240	192.601	-80.084	2122.726	545.924	-80.084	1618.128	676.579	-80.084
36.416	1964.331	657.569	36.416	1746.129	796.620	36.416	1648.765	657.569	-80.084	1866.967	504.782	-80.084	1964.331	657.569	-80.084	1746.129	796.620	-80.084
36.416	2202.806	503.635	36.416	1965.969	642.686	36.416	1868.604	503.635	-80.084	2105.441	337.800	-80.084	2202.806	503.635	-80.084	1965.969	642.686	-80.084
-118.584	2270.902	1917.320	-118.584	2423.689	2135.522	-118.584	2284.638	2232.886	-242.584	2131.851	2014.684	-242.584	2270.902	1917.320	-242.584	2423.689	2135.522	-242.584
-118.584	2103.920	1678.844	-118.584	2269.755	1915.681	-118.584	2130.704	2013.046	-242.584	1964.869	1776.209	-242.584	2103.920	1678.844	-242.584	2269.755	1915.681	-242.584
-118.584	2223.308	1567.780	-118.584	2576.631	2072.378	-118.584	2445.976	2163.864	-242.584	2092.653	1659.266	-242.584	2223.308	1567.780	-242.584	2576.631	2072.378	-242.584
-118.584	2355.601	1475.148	-118.584	2708.924	1979.746	-118.584	2578.269	2071.232	-242.584	2224.946	1566.634	-242.584	2355.601	1475.148	-242.584	2708.924	1979.746	-242.584
-118.584	2676.582	1633.543	-118.584	2829.369	1851.745	-118.584	2690.318	1949.109	-242.584	2537.531	1730.907	-242.584	2676.582	1633.543	-242.584	2829.369	1851.745	-242.584
-118.584	2509.195	1395.067	-118.584	2675.030	1631.904	-118.584	2535.979	1729.269	-242.584	2370.144	1492.432	-242.584	2509.195	1395.067	-242.584	2675.030	1631.904	-242.584
5.416	2270.902	1917.320	5.416	2423.689	2135.522	5.416	2284.638	2232.886	-118.584	2131.851	2014.684	-118.584	2270.902	1917.320	-118.584	2423.689	2135.522	-118.584
5.416	2103.920	1678.844	5.416	2269.755	1915.681	5.416	2130.704	2013.046	-118.584	1964.869	1776.209	-118.584	2103.920	1678.844	-118.584	2269.755	1915.681	-118.584
5.416	2223.308	1567.780	5.416	2576.631	2072.378	5.416	2445.976	2163.864	-118.584	2092.653	1659.266	-118.584	2223.308	1567.780	-118.584	2576.631	2072.378	-118.584
5.416	2355.601	1475.148	5.416	2708.924	1979.746	5.416	2578.269	2071.232	-118.584	2224.946	1566.634	-118.584	2355.601	1475.148	-118.584	2708.924	1979.746	-118.584
5.416	2676.582	1633.543	5.416	2829.369	1851.745	5.416	2690.318	1949.109	-118.584	2537.531	1730.907	-118.584	2676.582	1633.543	-118.584	2829.369	1851.745	-118.584
5.416	2509.195	1395.067	5.416	2675.030	1631.904	5.416	2535.979	1729.269	-118.584	2370.144	1492.432	-118.584	2509.195	1395.067	-118.584	2675.030	1631.904	-118.584
121.916	2270.902	1917.320	121.916	2423.689	2135.522	121.916	2284.638	2232.886	5.416	2131.851	2014.684	5.416	2270.902	1917.320	5.416	2423.689	2135.522	5.416
121.916	2103.920	1678.844	121.916	2269.755	1915.681	121.916	2130.704	2013.046	5.416	1964.869	1776.209	5.416	2103.920	1678.844	5.416	2269.755	1915.681	5.416
121.916	2223.308	1567.780	121.916	2576.631	2072.378	121.916	2445.976	2163.864	5.416	2092.653	1659.266	5.416	2223.308	1567.780	5.416	2576.631	2072.378	5.416
121.916	2355.601	1475.148	121.916	2708.924	1979.746	121.916	2578.269	2071.232	5.416	2224.946	1566.634	5.416	2355.601	1475.148	5.416	2708.924	1979.746	5.416
121.916	2676.582	1633.543	121.916	2829.369	1851.745	121.916	2690.318	1949.109	5.416	2537.531	1730.907	5.416	2676.582	1633.543	5.416	2829.369	1851.745	5.416
121.916	2509.195	1395.067	121.916	2675.030	1631.904	121.916	2535.979	1729.269	5.416	2370.144	1492.432	5.416	2509.195	1395.067	5.416	2675.030	1631.904	5.416

Appendix A-06, Boom Envelope Position Vector Plane Layout

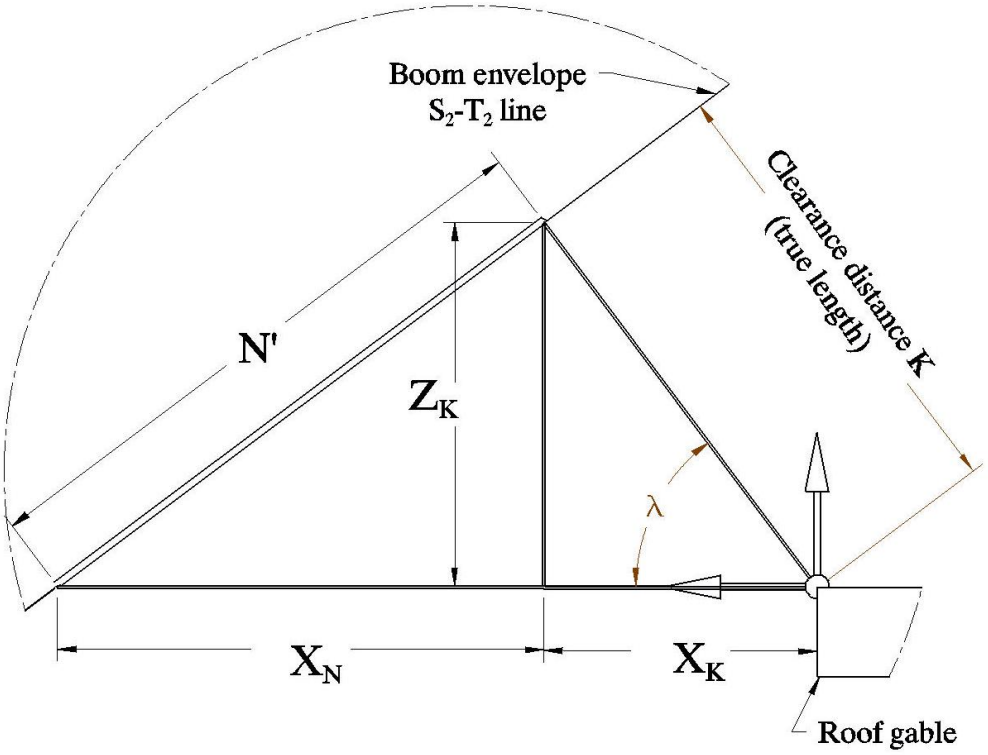

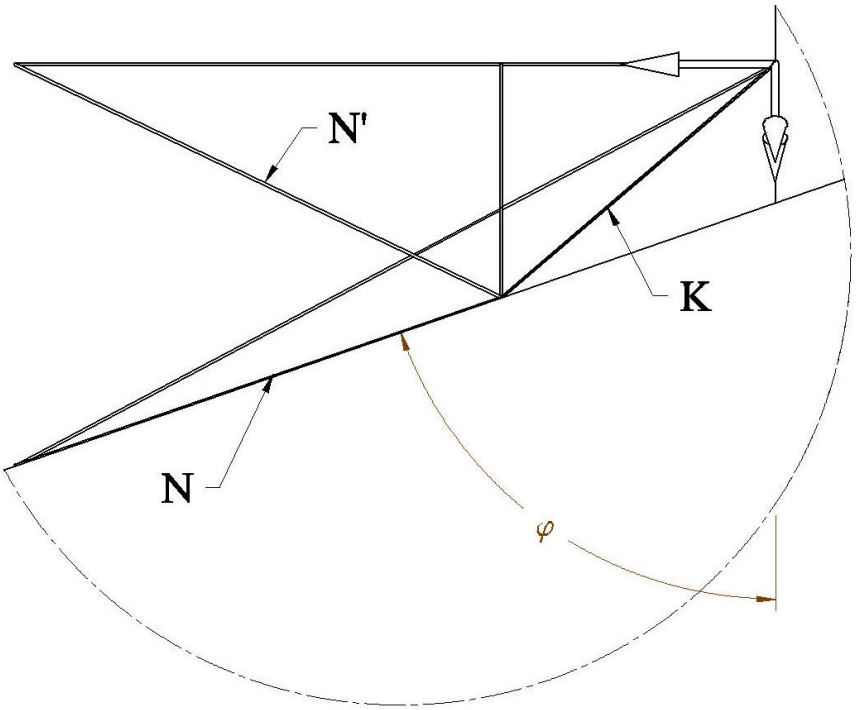

Appendix A-07, Object Trajectories Spatial Points Coordinates

Point	X	Y	Z
101	-881.62	-12.34	688.00
102	-733.73	-10.27	688.00
103	-718.27	-150.15	688.00
104	-1370.38	-286.47	688.00
105	-706.99	-196.55	688.00
106	-437.90	-121.74	688.00
107	-303.80	-338.05	688.00
108	-324.21	-360.75	688.00
109	-310.53	-372.59	688.00
110	-321.03	-385.18	688.00
111	-312.02	-392.51	688.00
112	-320.27	-402.89	688.00
113	-311.95	-409.37	688.00
114	-319.69	-419.53	688.00
115	-310.66	-426.25	688.00
116	-319.05	-437.76	688.00
117	-307.60	-445.88	688.00
118	-318.23	-461.29	688.00
119	-300.46	-473.06	688.00
120	-316.92	-498.96	688.00
121	-285.35	-517.66	688.00
122	-354.23	-642.63	688.00
123	-355.50	-641.93	688.00
124	-678.26	-1224.73	688.00
125	-277.19	-679.43	688.00
126	-528.85	-1296.27	688.00
127	-244.32	-691.93	688.00
128	-215.15	-609.32	688.00
129	128.67	-633.24	688.00
130	146.12	-719.10	688.00
131	168.98	-714.08	688.00
132	322.39	-1362.37	688.00
133	486.55	-549.30	688.00
134	486.55	-549.30	349.38
135	-551.35	484.22	688.00
136	-261.48	229.64	688.00
137	-508.15	529.38	688.00
138	-667.20	695.07	688.00
139	-787.32	820.21	688.00
140	579.86	977.94	688.00
141	374.26	631.18	688.00
142	371.73	632.68	688.00
143	176.29	300.04	688.00
201	-881.62	-12.34	805.75
202	-733.73	-10.27	805.75
203	-718.27	-150.15	805.75
204	-706.99	-196.55	805.75
205	-355.50	-641.93	805.75
206	-354.23	-642.63	805.75
207	-277.19	-679.43	805.75
208	-528.85	-1296.27	805.75
209	-244.32	-691.93	805.75
210	-215.15	-609.32	805.75
211	128.67	-633.24	805.75
212	146.12	-719.10	805.75
213	168.98	-714.08	805.75
214	322.39	-1362.37	805.75
215	486.55	-549.30	805.75
216	-551.35	484.22	805.75
217	-261.48	229.64	805.75
218	-508.15	529.38	805.75
219	-667.20	695.07	805.75
220	310.66	912.02	805.75
221	236.60	694.61	805.75
222	330.31	655.25	805.75
223	156.65	310.75	805.75
224	371.73	632.68	805.75
225	374.26	631.18	805.75
301	-881.62	-12.34	1035.75
302	-733.73	-10.27	1035.75
303	-718.27	-150.15	1035.75
304	-706.99	-196.55	1035.75
305	-355.50	-641.93	1035.75
306	-354.23	-642.63	1035.75
307	-277.19	-679.43	1035.75
308	-244.32	-691.93	1035.75
309	146.12	-719.10	1035.75
310	168.98	-714.08	1035.75
311	486.55	-549.30	1035.75
312	-551.35	484.22	1035.75
313	-261.48	229.64	1035.75
314	-508.15	529.38	1035.75
315	-667.20	695.07	1035.75
316	310.66	912.02	1035.75
317	236.60	694.61	1035.75
318	330.31	655.25	1035.75
319	156.65	310.75	1035.75
320	371.73	632.68	1035.75
321	374.26	631.18	1035.75
401	-881.62	-12.34	1196.35
402	-733.73	-10.27	1196.35
403	-718.27	-150.15	1196.35
404	-706.99	-196.55	1196.35
405	-355.50	-641.93	1196.36
406	-354.23	-642.63	1196.35
407	-277.19	-679.43	1196.35
408	-244.32	-691.93	1196.35
409	146.12	-719.10	1196.35
410	168.98	-714.08	1196.35
411	486.55	-549.30	1196.35
412	-551.35	484.22	1196.35
413	-261.48	229.64	1196.35
414	-508.15	529.38	1196.35
415	-667.20	695.07	1196.35
416	310.66	912.02	1196.35
417	236.60	694.61	1196.35
418	330.31	655.25	1196.35
419	156.65	310.75	1196.35
420	371.73	632.68	1196.35
421	374.26	631.18	1196.35
501	-881.62	-12.34	1234.00
502	-733.73	-10.27	1234.00
503	-718.27	-150.15	1234.00
504	-706.99	-196.55	1234.00
505	-355.50	-641.93	1234.00
506	-354.23	-642.63	1234.00
507	-277.19	-679.43	1234.00
508	-244.32	-691.93	1234.00
509	146.12	-719.10	1234.00
510	168.98	-714.08	1234.00
511	486.55	-549.30	1234.00
512	-551.35	484.22	1234.00
513	-508.15	529.38	1234.00
514	236.60	694.61	1234.00
515	330.31	655.25	1234.00
516	371.73	632.68	1234.00
517	374.26	631.18	1234.00
601	-881.62	-12.34	1277.38
602	-733.73	-10.27	1277.38
603	-718.27	-150.15	1277.38
604	-706.99	-196.55	1277.38
605	-355.50	-641.93	1277.38
606	-354.23	-642.63	1277.38
607	-277.19	-679.43	1277.38
608	-244.32	-691.93	1277.38
609	146.12	-719.10	1277.38
610	168.98	-714.08	1277.38
611	486.55	-549.30	1277.38
612	-551.35	484.22	1277.38
613	-508.15	529.38	1277.38
614	236.60	694.61	1277.38
615	330.31	655.25	1277.38
616	371.73	632.68	1277.38
617	374.26	631.18	1277.38

Appendix A-08, Paths Connections Database

ID	Start	End	Type	Dist
1	101	102	L	147.91
2	102	103	C	140.95
3	103	104	L	666.20
4	103	105	C	47.76
5	105	106	L	279.30
6	106	107	C	257.95
7	107	108	L	30.53
8	108	109	C	18.09
9	109	110	L	16.39
10	110	111	C	11.61
11	111	112	L	13.26
12	112	113	C	10.54
13	113	114	L	12.77
14	114	115	C	11.26
15	115	116	L	14.24
16	116	117	C	14.04
17	117	118	L	18.72
18	118	119	C	21.31
19	119	120	L	30.69
20	120	121	C	36.70
21	121	122	L	142.70
22	122	123	C	1.45
23	123	124	L	666.20
24	123	122	C	1.45
25	122	125	C	85.42
26	125	126	L	666.20
27	125	127	C	35.17
28	127	128	L	87.61
29	128	129	C	348.87
30	129	130	L	87.61
31	130	131	C	23.41
32	131	132	L	666.20
33	131	133	C	361.42
34	133	134	Vd	338.63
35	102	135	C	539.09
36	135	136	L	385.80
37	135	137	C	62.51
38	137	138	L	229.68
39	138	139	L	173.45
40	139	140	C	1478.18
41	140	141	L	403.13
42	141	142	C	2.94
43	142	143	L	385.80
44	142	141	C	2.94
45	141	133	C	1380.63
46	201	202	L	147.91
47	202	203	C	140.95
48	203	204	C	47.76
49	204	205	C	582.54
50	205	206	C	1.45
51	206	207	C	85.42
52	207	208	L	666.20
53	207	209	C	35.17
54	209	210	L	87.61
55	210	211	C	348.87
56	211	212	L	87.61
57	212	213	C	23.41
58	213	214	L	666.20
59	213	215	C	361.42
60	202	216	C	539.09
61	216	217	L	385.80
62	216	218	C	62.51
63	218	219	L	229.68
64	219	220	C	1053.31
65	220	221	L	229.68
66	221	222	C	101.72
67	222	223	L	385.80
68	222	224	C	47.17
69	224	225	C	2.94
70	225	215	C	1380.63
71	101	201	Vu	117.75
72	201	101	Vd	117.75
73	102	202	Vu	117.75
74	202	102	Vd	117.75
75	103	203	Vu	117.75
76	203	103	Vd	117.75
77	105	204	Vu	117.75
78	204	105	Vd	117.75
79	123	205	Vu	117.75
80	205	123	Vd	117.75
81	122	206	Vu	117.75
82	206	122	Vd	117.75
83	125	207	Vu	117.75
84	207	125	Vd	117.75
85	126	208	Vu	117.75
86	208	126	Vd	117.75
87	127	209	Vu	117.75
88	209	127	Vd	117.75
89	128	210	Vu	117.75
90	210	128	Vd	117.75
91	129	211	Vu	117.75
92	211	129	Vd	117.75
93	130	212	Vu	117.75
94	212	130	Vd	117.75
95	131	213	Vu	117.75
96	213	131	Vd	117.75
97	132	214	Vu	117.75
98	214	132	Vd	117.75
99	133	215	Vu	117.75
100	215	133	Vd	117.75
101	141	225	Vu	117.75
102	225	141	Vd	117.75
103	142	224	Vu	117.75
104	224	142	Vd	117.75
105	138	219	Vu	117.75
106	219	138	Vd	117.75
107	137	218	Vu	117.75
108	218	137	Vd	117.75
109	135	216	Vu	117.75
110	216	135	Vd	117.75
111	136	217	Vu	117.75
112	217	136	Vd	117.75
113	301	302	L	147.91
114	302	303	C	140.95
115	303	304	C	47.76
116	304	305	C	582.54
117	305	306	C	1.45
118	306	307	C	85.42
119	307	308	C	35.17
120	308	309	C	396.18
121	309	310	C	23.41
122	310	311	C	361.42
123	302	312	C	539.09
124	312	313	L	385.80
125	312	314	C	62.51
126	314	315	L	229.68
127	315	316	C	1053.31
128	316	317	L	229.68
129	317	318	C	101.72

ID	Start	End	Type	Dist
130	318	319	L	385.80
131	318	320	C	47.17
132	320	321	C	2.94
131	318	320	C	47.17
132	320	321	C	2.94
133	321	311	C	1380.63
134	201	301	Vu	230.00
135	301	201	Vd	230.00
136	202	302	Vu	230.00
137	302	202	Vd	230.00
138	203	303	Vu	230.00
139	303	203	Vd	230.00
140	204	304	Vu	230.00
141	304	204	Vd	230.00
142	205	305	Vu	230.00
143	305	205	Vd	230.00
144	206	306	Vu	230.00
145	306	206	Vd	230.00
146	207	307	Vu	230.00
147	307	207	Vd	230.00
148	209	308	Vu	230.00
149	308	209	Vd	230.00
150	212	309	Vu	230.00
151	309	212	Vd	230.00
152	213	310	Vu	230.00
153	310	213	Vd	230.00
154	215	311	Vu	230.00
155	311	215	Vd	230.00
156	225	321	Vu	230.00
157	321	225	Vd	230.00
158	224	320	Vu	230.00
159	320	224	Vd	230.00
160	222	318	Vu	230.00
161	318	222	Vd	230.00
162	223	319	Vu	230.00
163	319	223	Vd	230.00
164	221	317	Vu	230.00
165	317	221	Vd	230.00
166	220	316	Vu	230.00
167	316	220	Vd	230.00
168	219	315	Vu	230.00
169	315	219	Vd	230.00
170	218	314	Vu	230.00
171	314	218	Vd	230.00
172	216	312	Vu	230.00
173	312	216	Vd	230.00
174	217	313	Vu	230.00
175	313	217	Vd	230.00
176	401	402	L	147.91
177	402	403	C	140.95
178	403	404	C	47.76
179	404	405	C	582.54
180	405	406	C	1.45
181	406	407	C	85.42
182	407	408	C	35.17
183	408	409	C	396.18
184	409	410	C	23.41
185	410	411	C	361.42
186	402	412	C	539.09
187	412	413	L	385.80
188	412	414	C	62.51
189	414	415	L	229.68
190	415	416	C	1053.31
191	416	417	L	229.68
192	417	418	C	101.72
193	418	419	L	385.80
194	418	420	C	47.17
195	420	421	C	2.94
196	421	411	C	1380.63
197	301	401	Vu	160.60
198	401	301	Vd	160.60
199	302	402	Vu	160.60
200	402	302	Vd	160.60
201	303	403	Vu	160.60
202	403	303	Vd	160.60
203	304	404	Vu	160.60
204	404	304	Vd	160.60
205	305	405	Vu	160.61
206	405	305	Vd	160.61
207	306	406	Vu	160.60
208	406	306	Vd	160.60
209	307	407	Vu	160.60
210	407	307	Vd	160.60
211	308	408	Vu	160.60
212	408	308	Vd	160.60
213	309	409	Vu	160.60
214	409	309	Vd	160.60
215	310	410	Vu	160.60
216	410	310	Vd	160.60
217	311	411	Vu	160.60
218	411	311	Vd	160.60
219	321	421	Vu	160.60
220	421	321	Vd	160.60
221	320	420	Vu	160.60
222	420	320	Vd	160.60
223	318	418	Vu	160.60
224	418	318	Vd	160.60
225	319	419	Vu	160.60
226	419	319	Vd	160.60
227	317	417	Vu	160.60
228	417	317	Vd	160.60
229	316	416	Vu	160.60
230	416	316	Vd	160.60
231	315	415	Vu	160.60
232	415	315	Vd	160.60
233	314	414	Vu	160.60
234	414	314	Vd	160.60
235	312	412	Vu	160.60
236	412	312	Vd	160.60
237	313	413	Vu	160.60
238	413	313	Vd	160.60
239	501	502	L	147.91
240	502	503	C	140.95
241	503	504	C	47.76
242	504	505	C	582.54
243	505	506	C	1.45
244	506	507	C	85.42
245	507	508	C	35.17
246	508	509	C	396.18
247	509	510	C	23.41
248	510	511	C	361.42
249	502	512	C	539.09
250	512	513	C	62.51
251	513	514	C	802.22
252	514	515	C	101.72
253	515	516	C	47.17
254	516	517	C	2.94
255	517	511	C	1380.63
256	401	501	Vu	37.65

ID	Start	End	Type	Dist	ID	Start	End	Type	Dist
257	501	401	Vd	37.65	299	610	611	C	361.42
258	402	502	Vu	37.65	300	602	612	C	539.09
259	502	402	Vd	37.65	301	612	613	C	62.51
260	403	503	Vu	37.65	302	613	614	C	802.22
261	503	403	Vd	37.65	303	614	615	C	101.72
262	404	504	Vu	37.65	304	615	616	C	47.17
263	504	404	Vd	37.65	305	616	617	C	2.94
264	405	505	Vu	37.64	306	617	611	C	1380.63
265	505	405	Vd	37.64	307	501	601	Vu	43.38
266	406	506	Vu	37.65	308	601	501	Vd	43.38
267	506	406	Vd	37.65	309	502	602	Vu	43.38
268	407	507	Vu	37.65	310	602	502	Vd	43.38
269	507	407	Vd	37.65	311	503	603	Vu	43.38
270	408	508	Vu	37.65	312	603	503	Vd	43.38
271	508	408	Vd	37.65	313	504	604	Vu	43.38
272	409	509	Vu	37.65	314	604	504	Vd	43.38
273	509	409	Vd	37.65	315	505	605	Vu	43.38
274	410	510	Vu	37.65	316	605	505	Vd	43.38
275	510	410	Vd	37.65	317	506	606	Vu	43.38
276	411	511	Vu	37.65	318	606	506	Vd	43.38
277	511	411	Vd	37.65	319	507	607	Vu	43.38
278	412	512	Vu	37.65	320	607	507	Vd	43.38
279	512	412	Vd	37.65	321	508	608	Vu	43.38
280	414	513	Vu	37.65	322	608	508	Vd	43.38
281	513	414	Vd	37.65	323	509	609	Vu	43.38
282	417	512	Vu	37.65	324	609	509	Vd	43.38
283	514	417	Vd	37.65	325	510	610	Vu	43.38
284	418	515	Vu	37.65	326	610	510	Vd	43.38
285	515	418	Vd	37.65	327	511	611	Vu	43.38
286	420	516	Vu	37.65	328	611	511	Vd	43.38
287	516	420	Vd	37.65	329	512	612	Vu	43.38
288	421	517	Vu	37.65	330	612	512	Vd	43.38
289	517	421	Vd	37.65	331	513	613	Vu	43.38
290	601	602	L	147.91	332	613	513	Vd	43.38
291	602	603	C	140.95	333	514	614	Vu	43.38
292	603	604	C	47.76	334	614	514	Vd	43.38
293	604	605	C	582.54	335	515	615	Vu	43.38
294	605	606	C	1.45	336	615	515	Vd	43.38
295	606	607	C	85.42	337	516	616	Vu	43.38
296	607	608	C	35.17	338	616	516	Vd	43.38
297	608	609	C	396.18	339	517	617	Vu	43.38
298	609	610	C	23.41	340	617	517	Vd	43.38

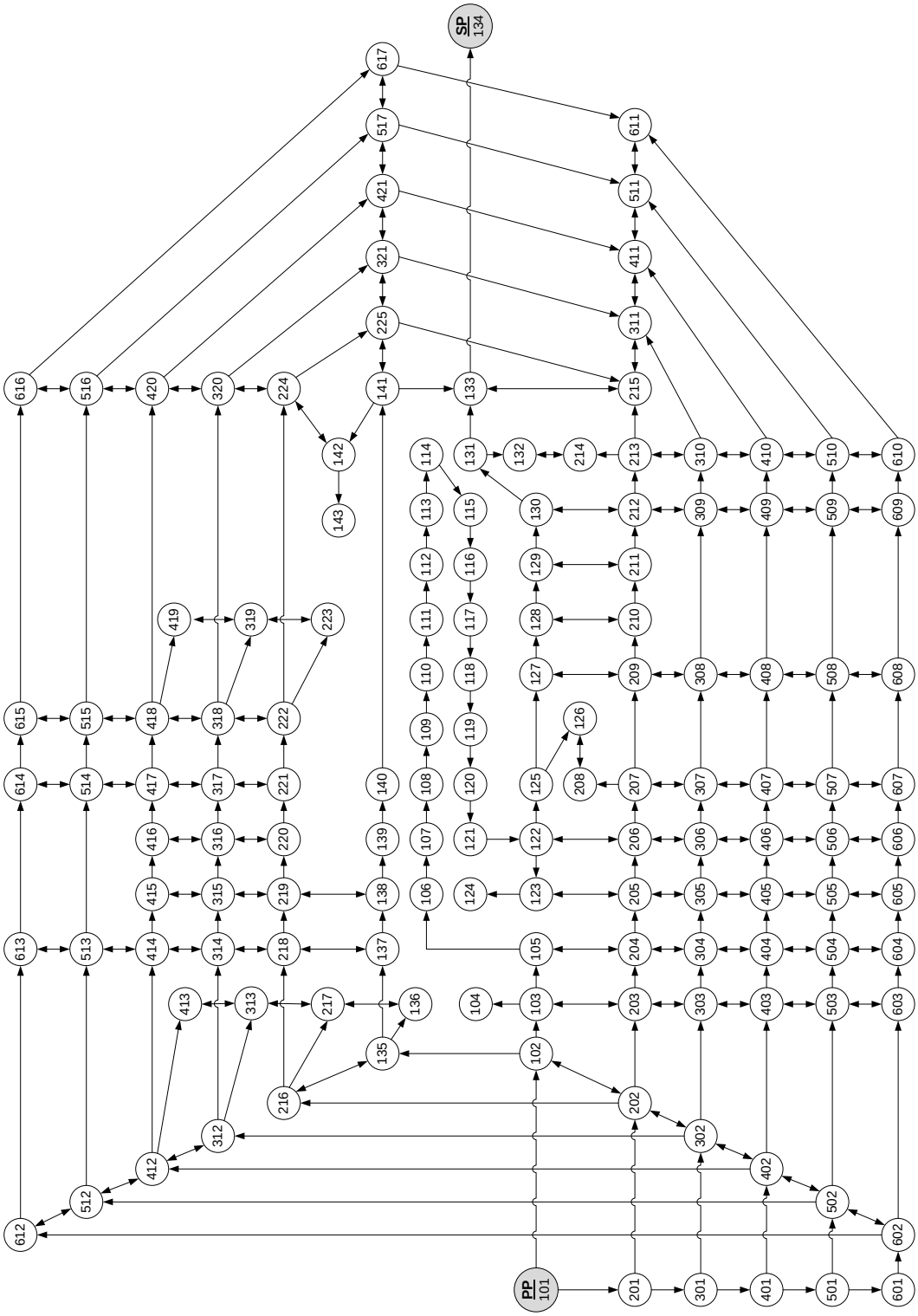

Appendix A-09, Methodology sample – Node Graph Flowchart

Appendix A-10, Methodology lifted objects centroid point.

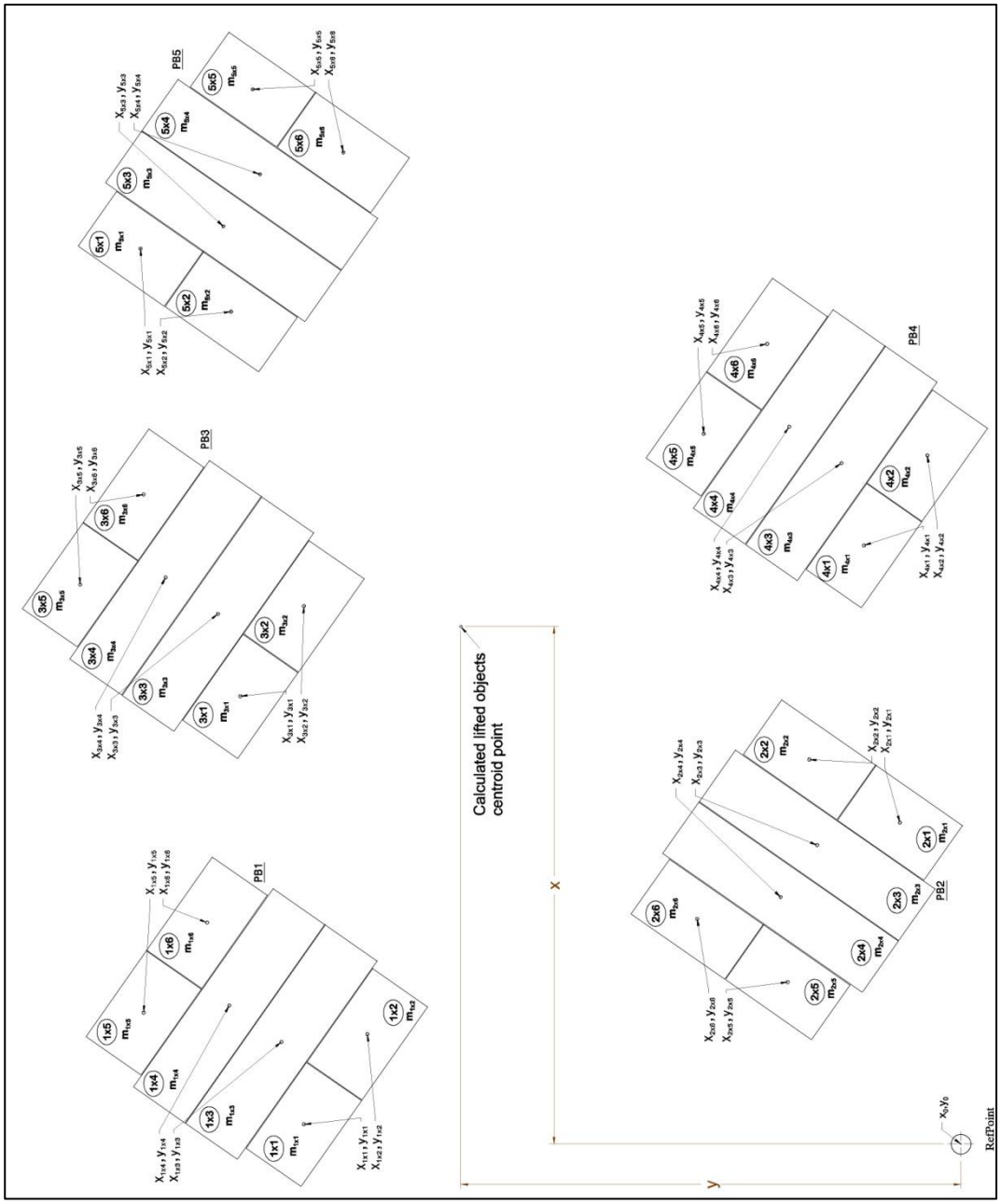

Appendix A-11, Methodology lifted objects set-point radiuses.

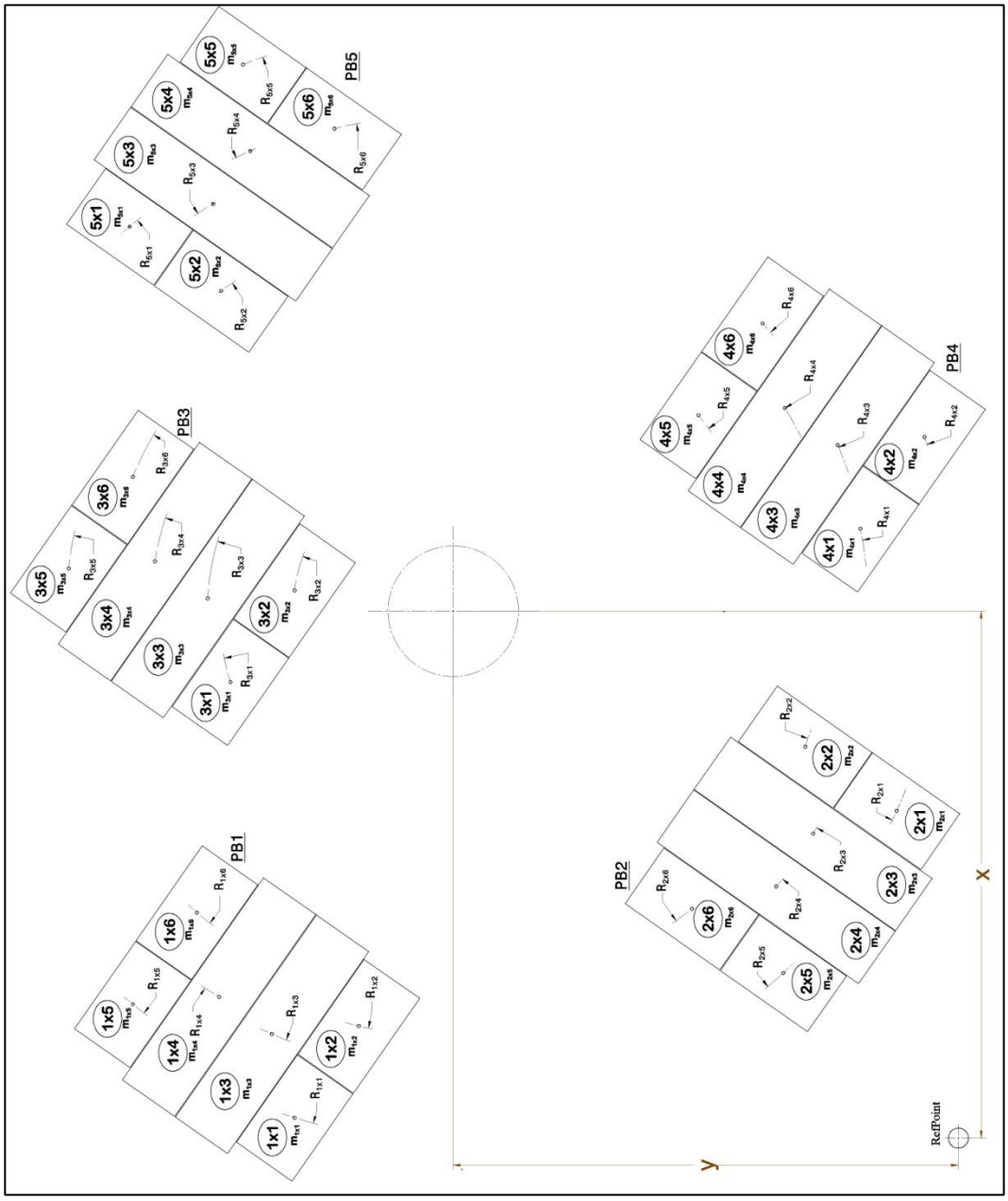

Appendix A-12, Numerical case lifted objects centroid point.

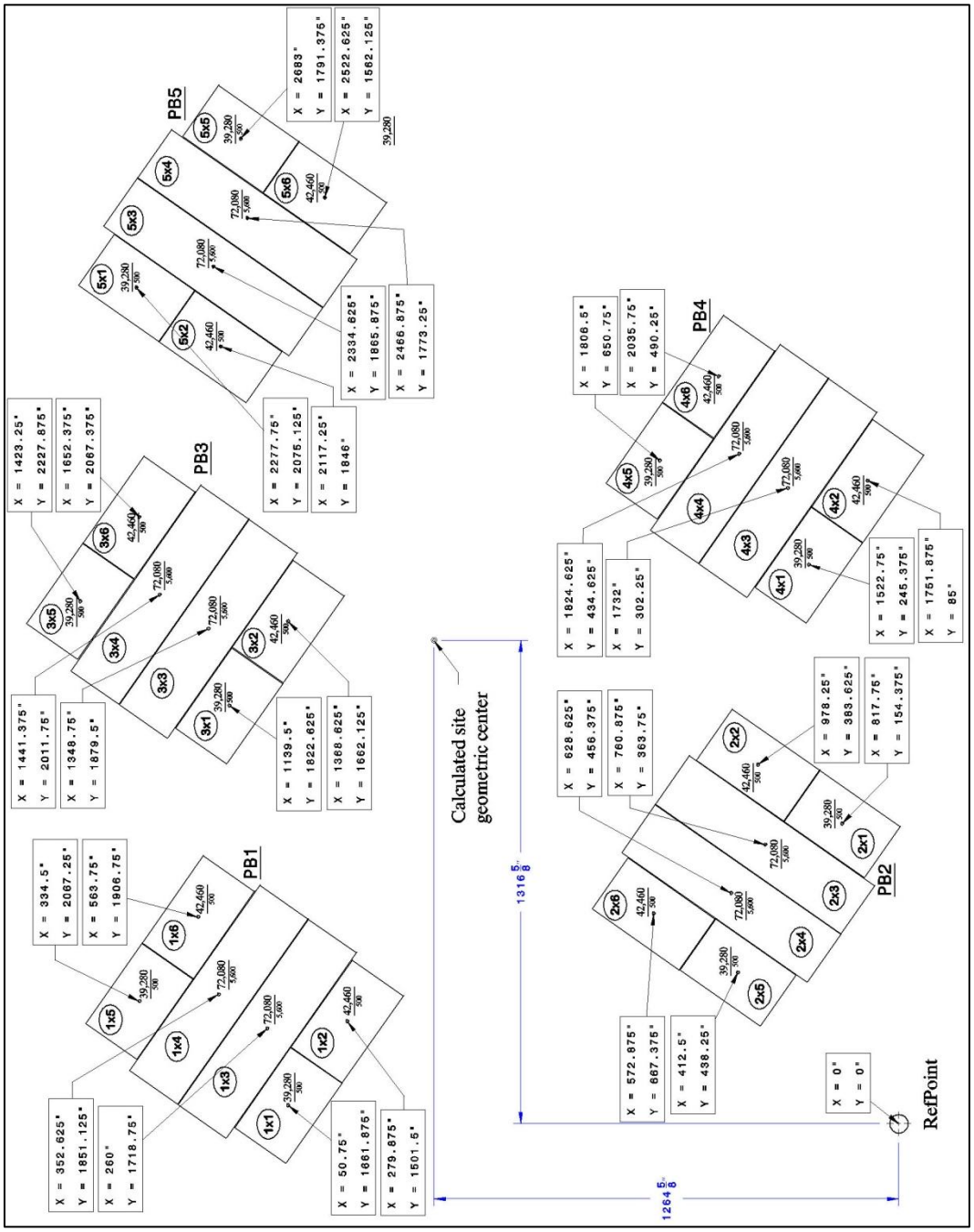

Appendix A-13, Numerical lifted objects set-point radiuses.

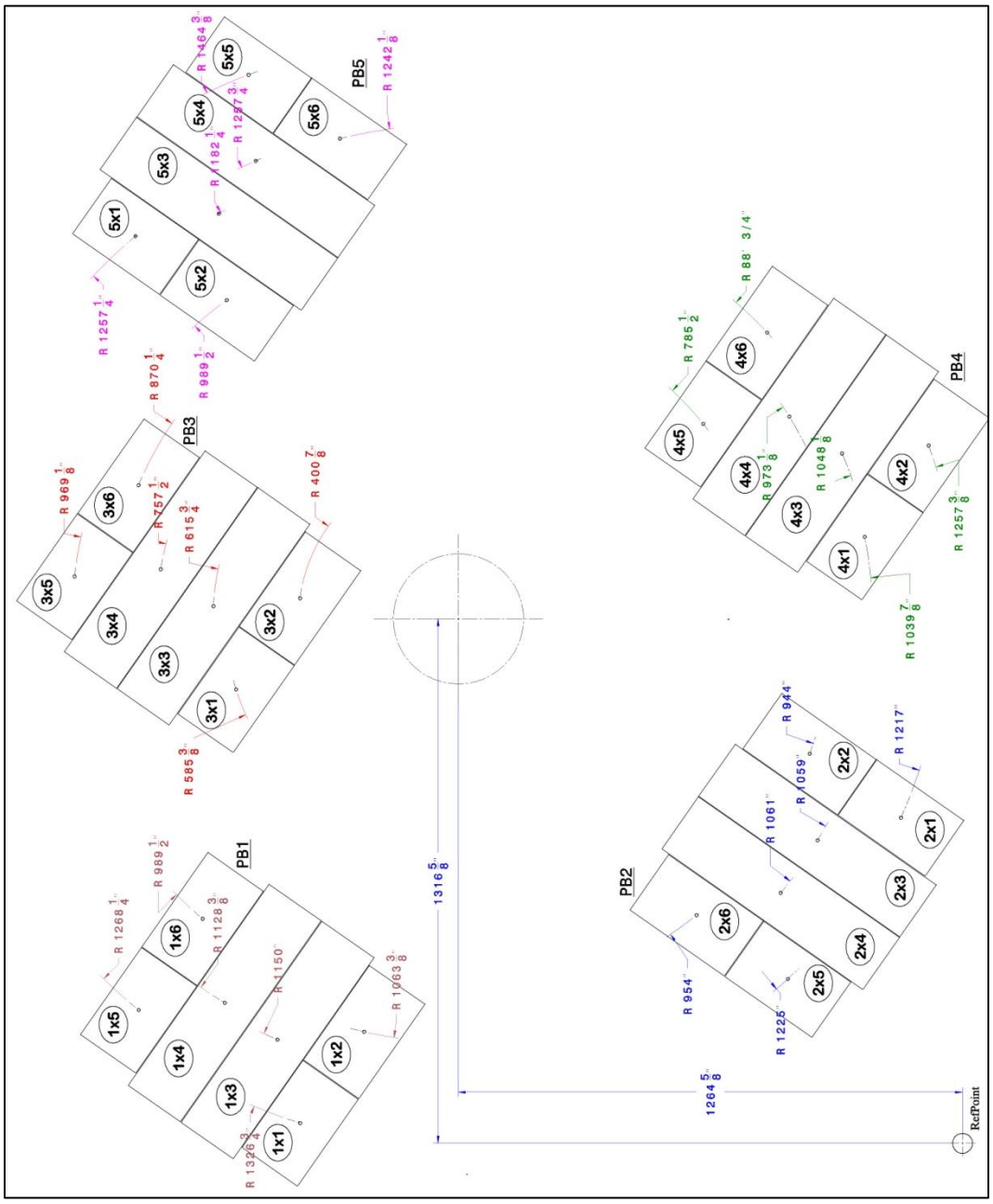

Lifting capacities main boom with Superlift

396,900 lb | 360° | 85%

Main boom

Radius	ft	108.9	124.3	139.4	154.9	170.0	183.7	Radius
ft				1,000 lb				ft
19		410.1	-	-	-	-	-	19
23		396.6	357.0	321.8	-	-	-	23
26		380.5	346.9	317.7	262.8	-	-	26
29		362.5	335.0	311.9	256.7	214.9	183.3	29
33		329.2	318.5	301.3	250.9	206.9	180.5	33
39		282.8	282.2	279.1	238.8	198.9	172.4	39
46		242.1	240.0	237.8	222.5	187.3	165.2	46
52		211.9	213.8	211.6	208.3	179.2	157.1	52
59		181.0	183.2	185.4	185.3	169.8	149.9	59
65		160.8	163.0	165.2	167.2	161.7	143.9	65
72		147.9	141.6	147.9	146.0	148.0	136.8	72
79		136.1	125.1	136.1	129.5	131.7	129.6	79
85		124.0	113.0	124.0	117.4	119.6	119.5	85
92		112.2	102.3	112.2	106.5	108.9	109.1	92
98		105.0	93.4	103.3	97.6	99.8	100.2	98
105		-	84.4	94.3	88.6	90.8	91.0	105
111		-	77.7	87.4	81.7	83.9	84.1	111
118		-	-	80.5	74.6	76.8	77.0	118
124		-	-	75.1	69.3	71.3	71.8	124
131		-	-	-	63.6	65.6	66.1	131
138		-	-	-	58.6	60.7	60.9	138
144		-	-	-	51.7	56.8	56.9	144
151		-	-	-	-	52.6	52.8	151
157		-	-	-	-	47.5	49.6	157
164		-	-	-	-	-	46.1	164
170		-	-	-	-	-	41.0	170
177		-	-	-	-	-	-	177

Appendix A-15, Maximum radii for three different module types.

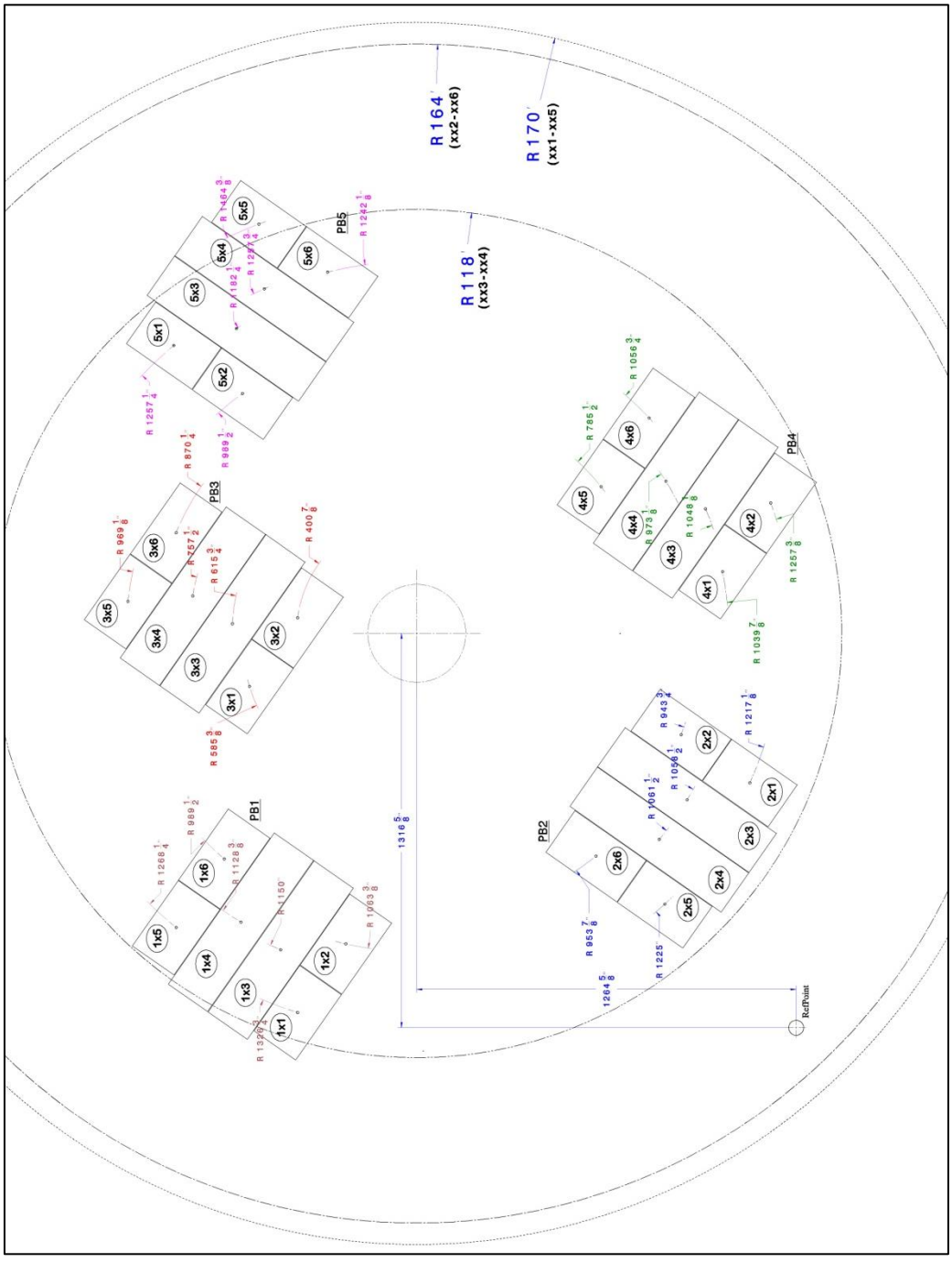

Appendix A-16, Elevation k_2 path and obstruction recognition.

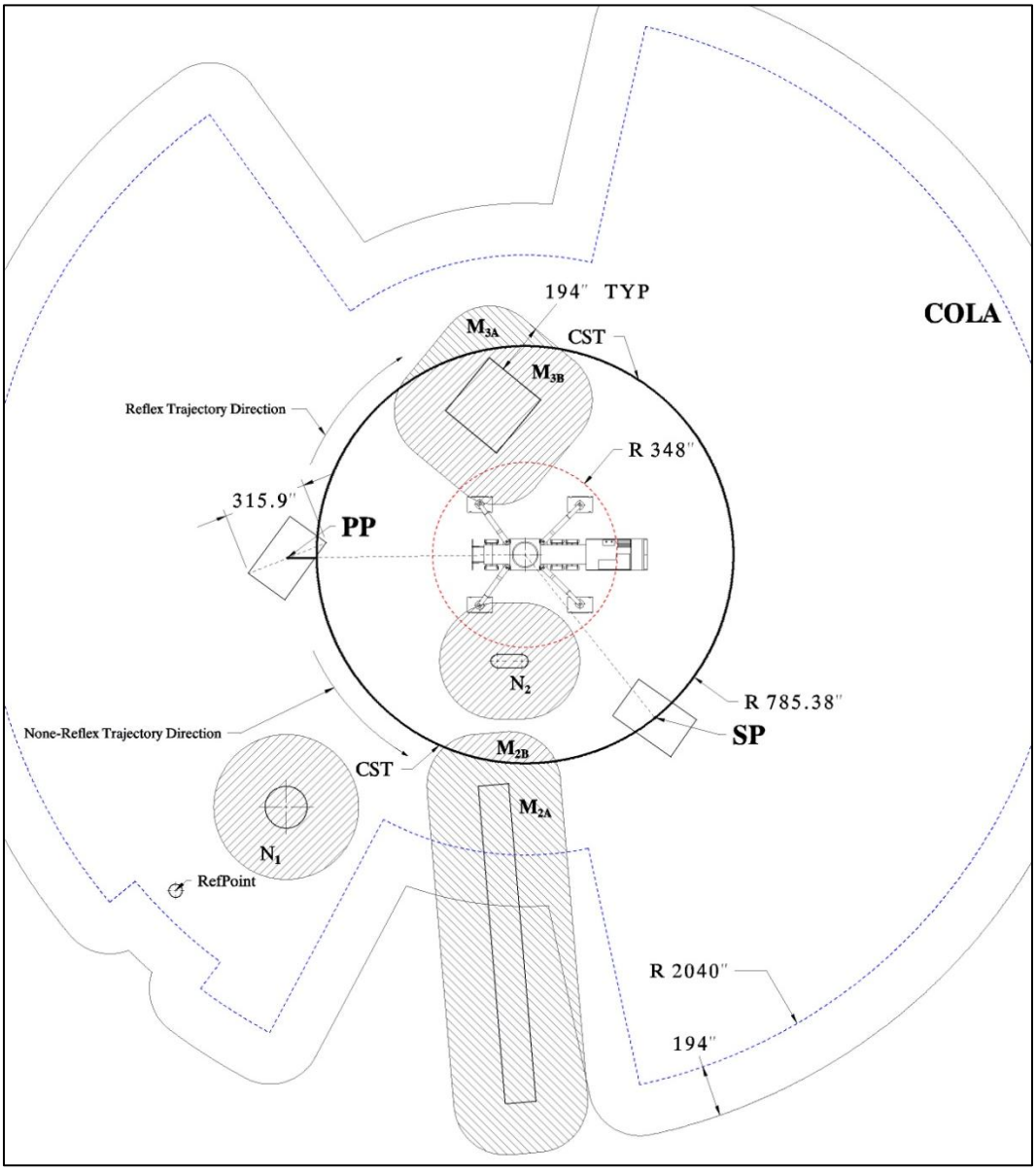

Appendix A-17, Elevation k_3 path and obstruction recognition.

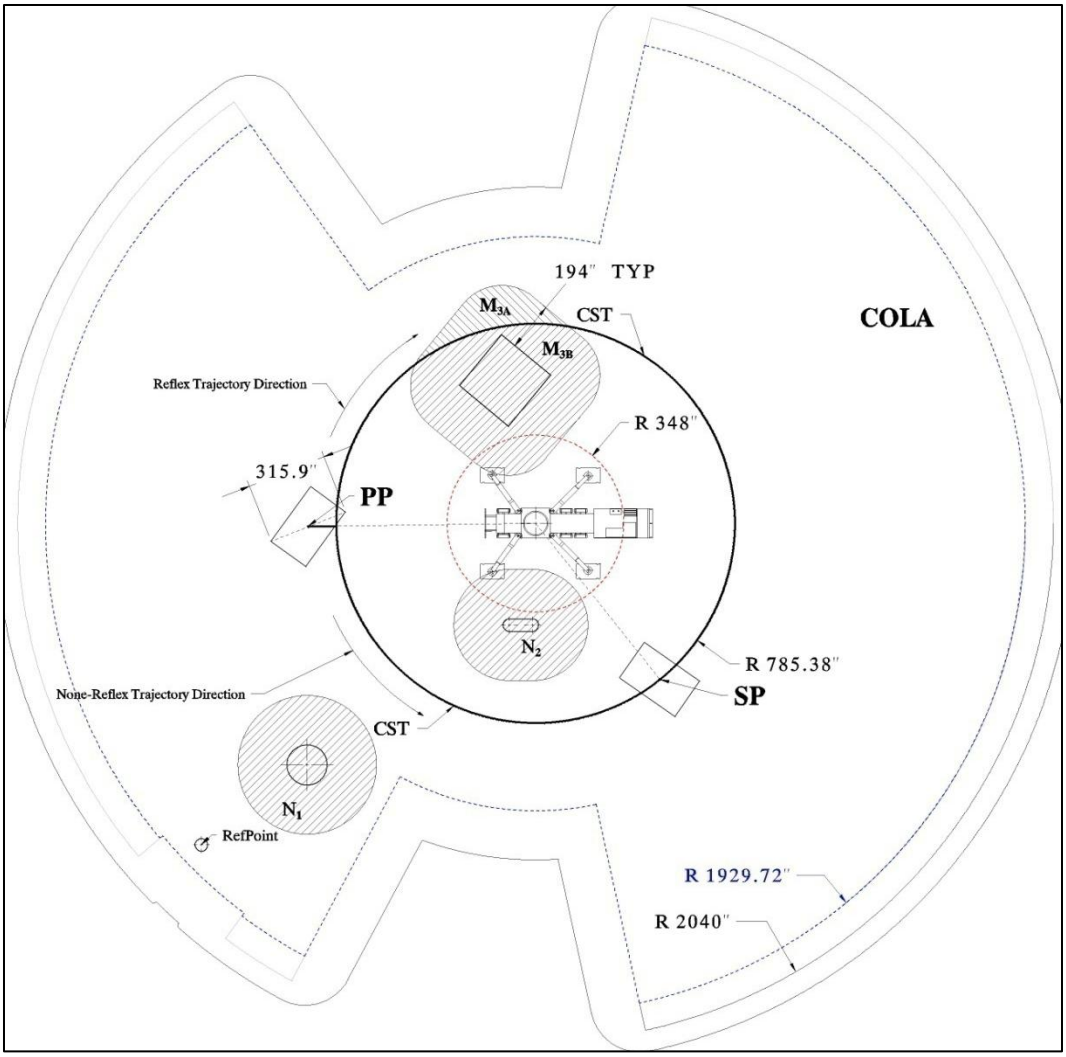

Appendix A-18, Elevation k_4 path and obstruction recognition.

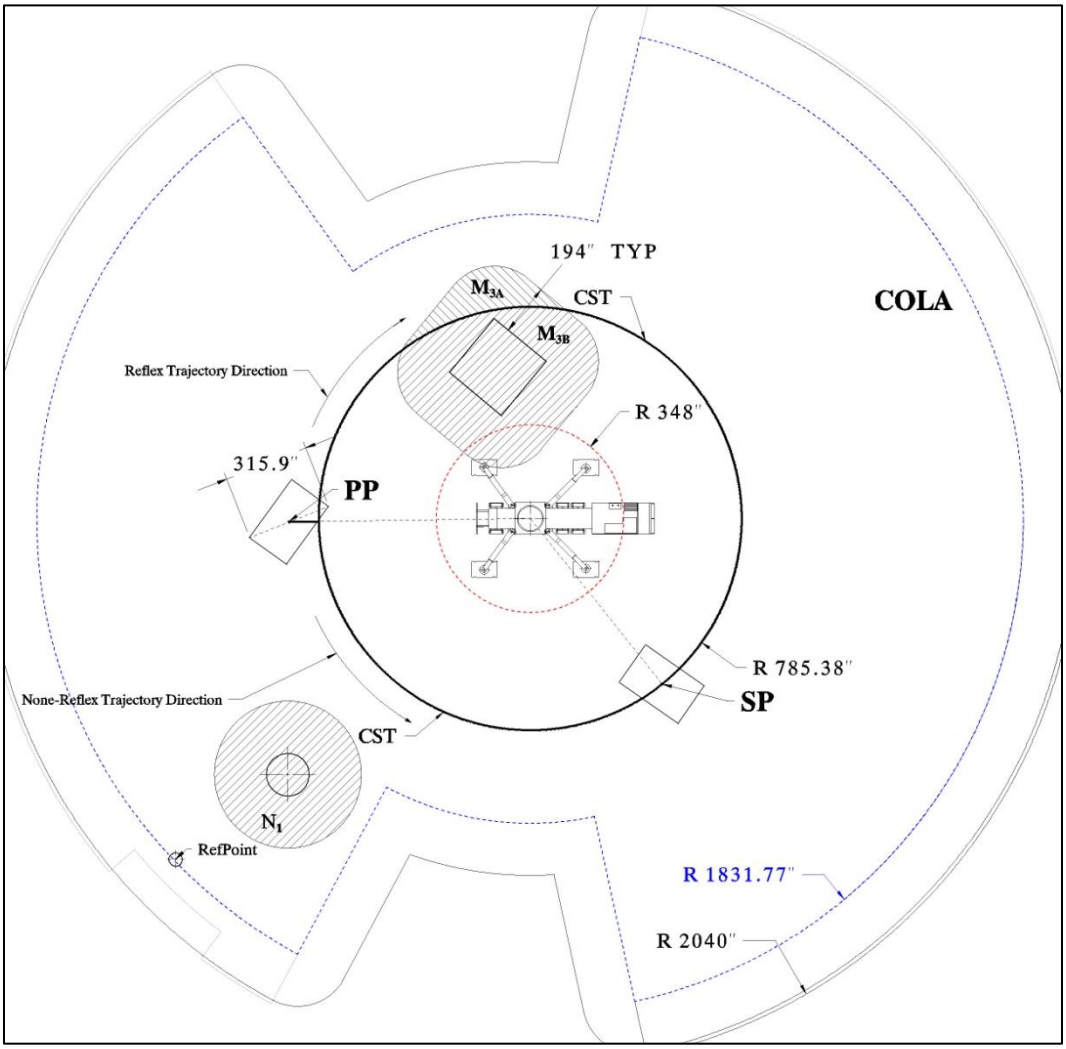

Appendix A-19, Elevation k_5 path and obstruction recognition.

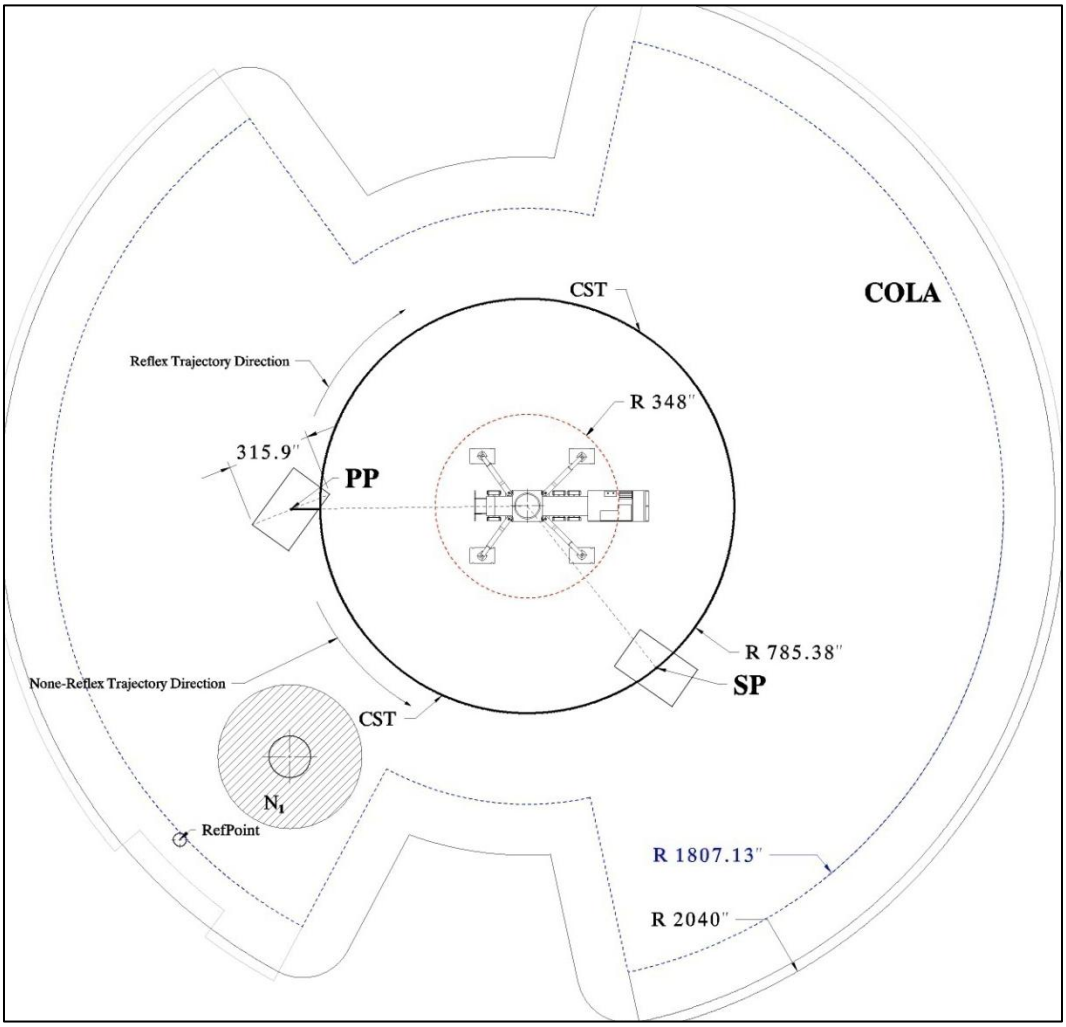

Appendix A-20, Elevation k_6 path and obstruction recognition.

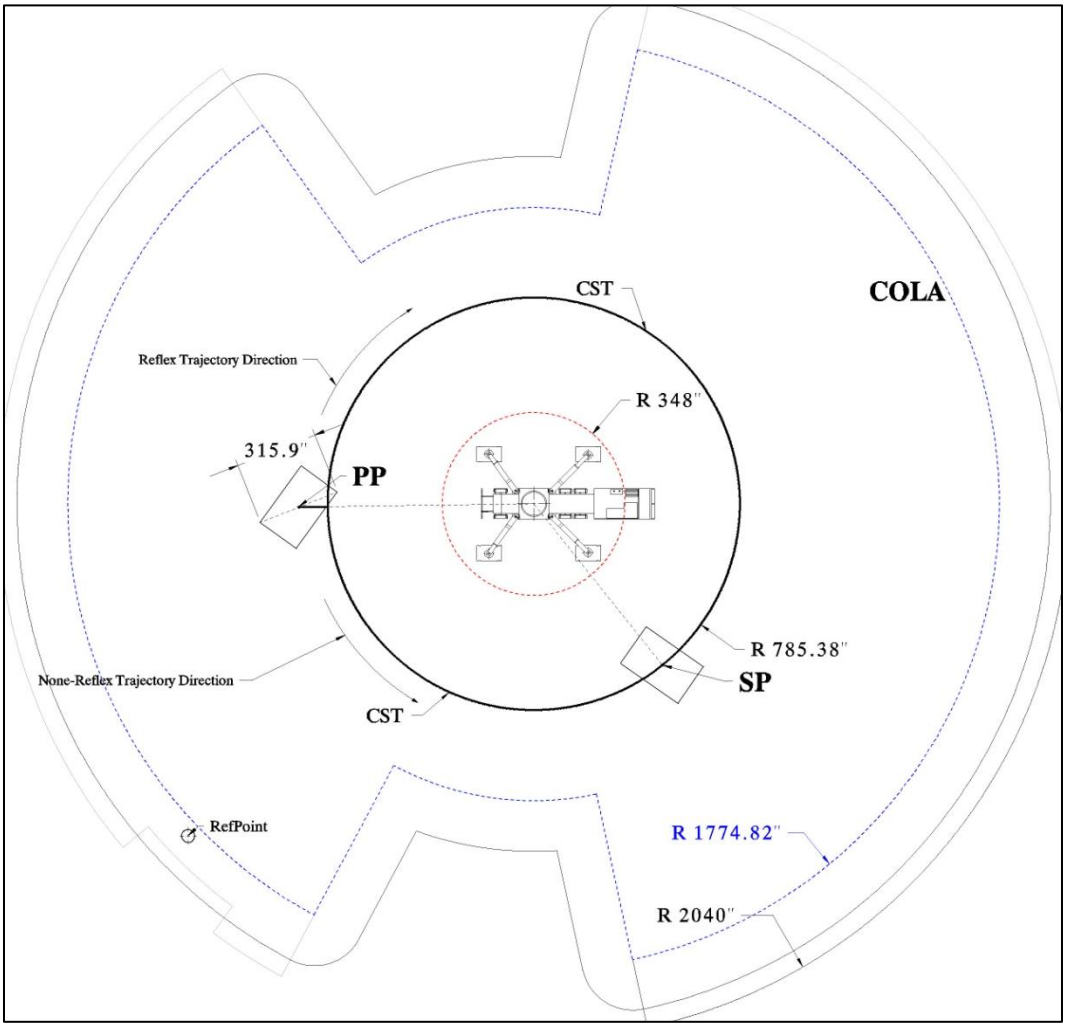

Appendix A-21, Elevation k_2 trajectory path development.

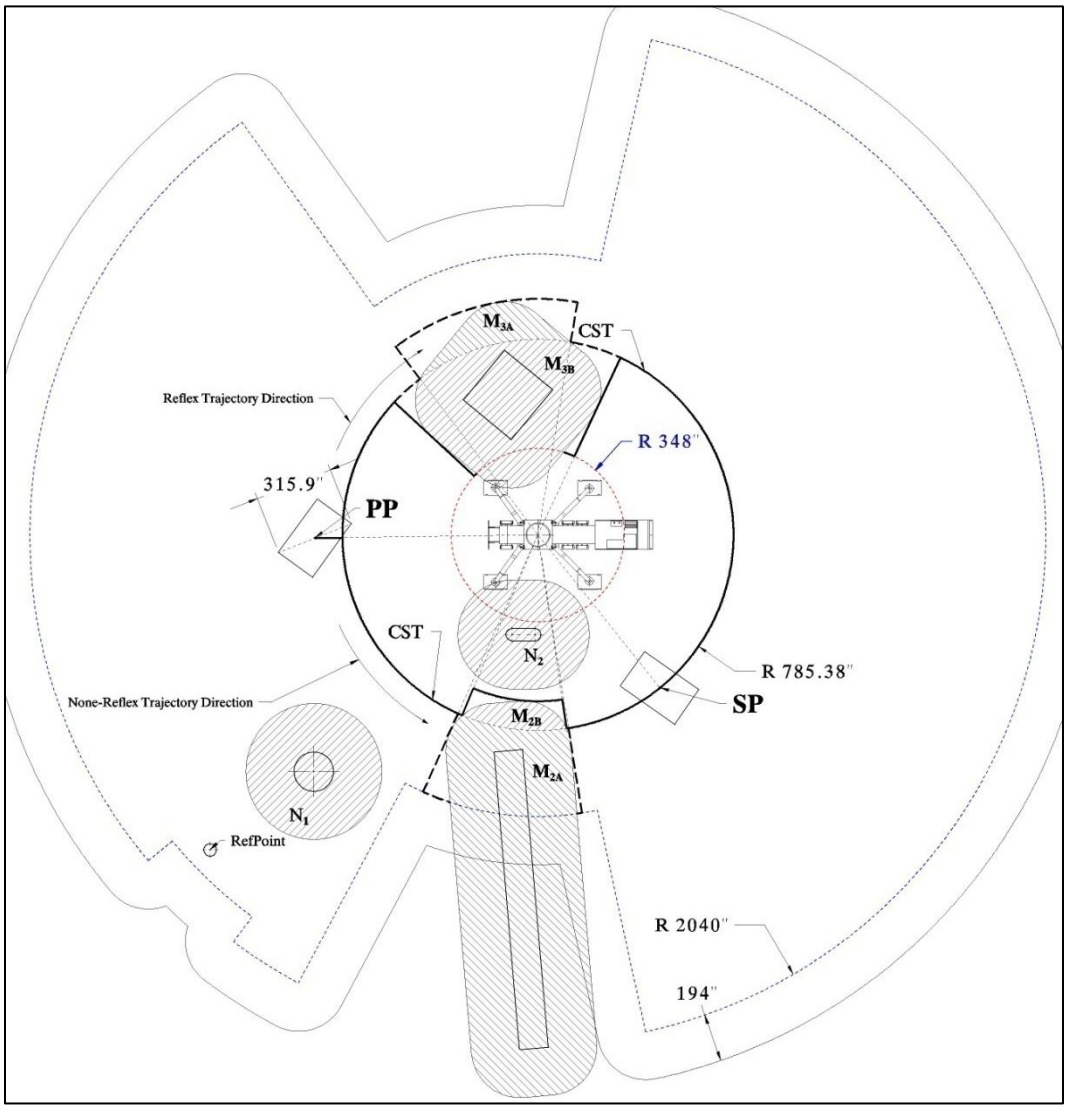

Appendix A-22, Elevation k_3 trajectory path development.

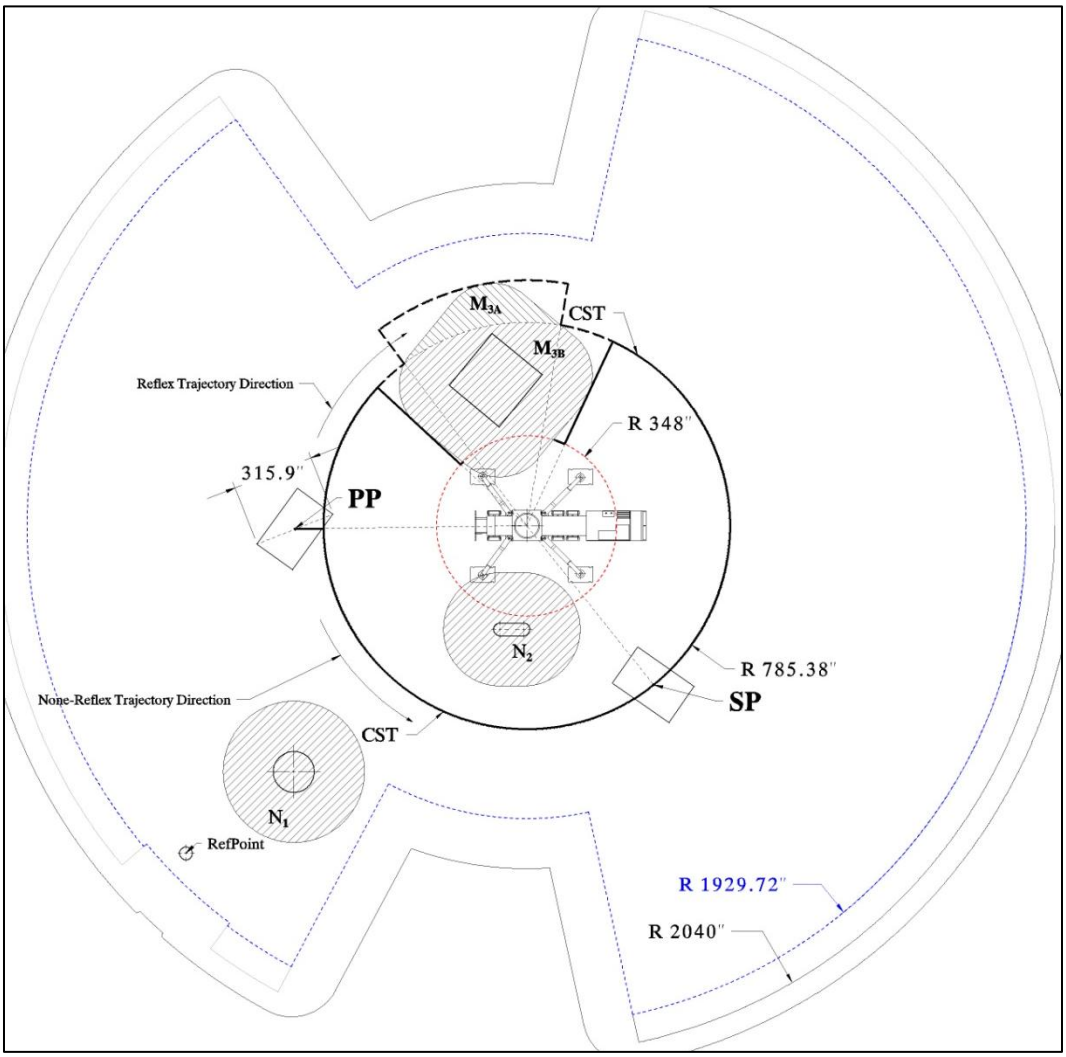

Appendix A-23, Elevation k_4 trajectory path development.

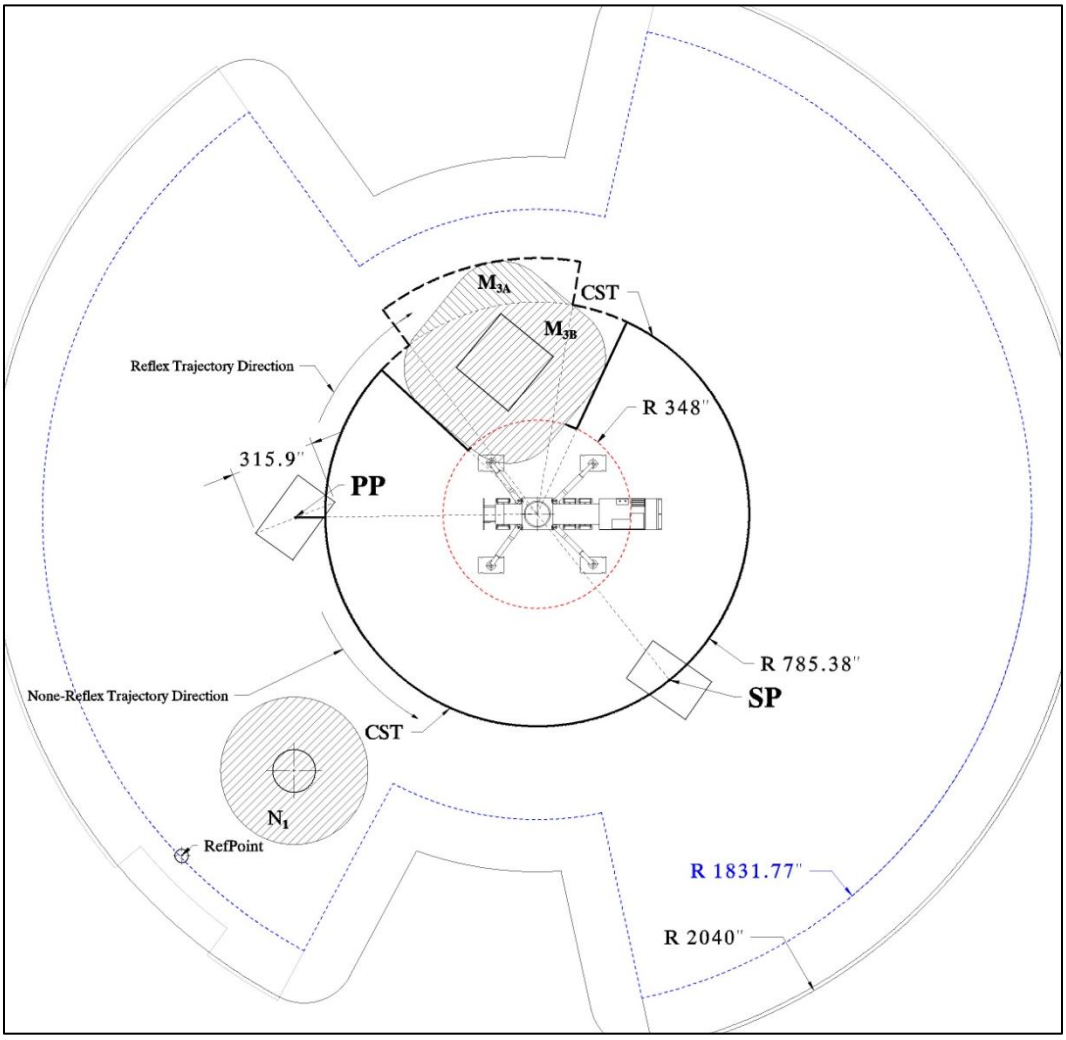

Appendix A-24, Elevation k_5 trajectory path development.

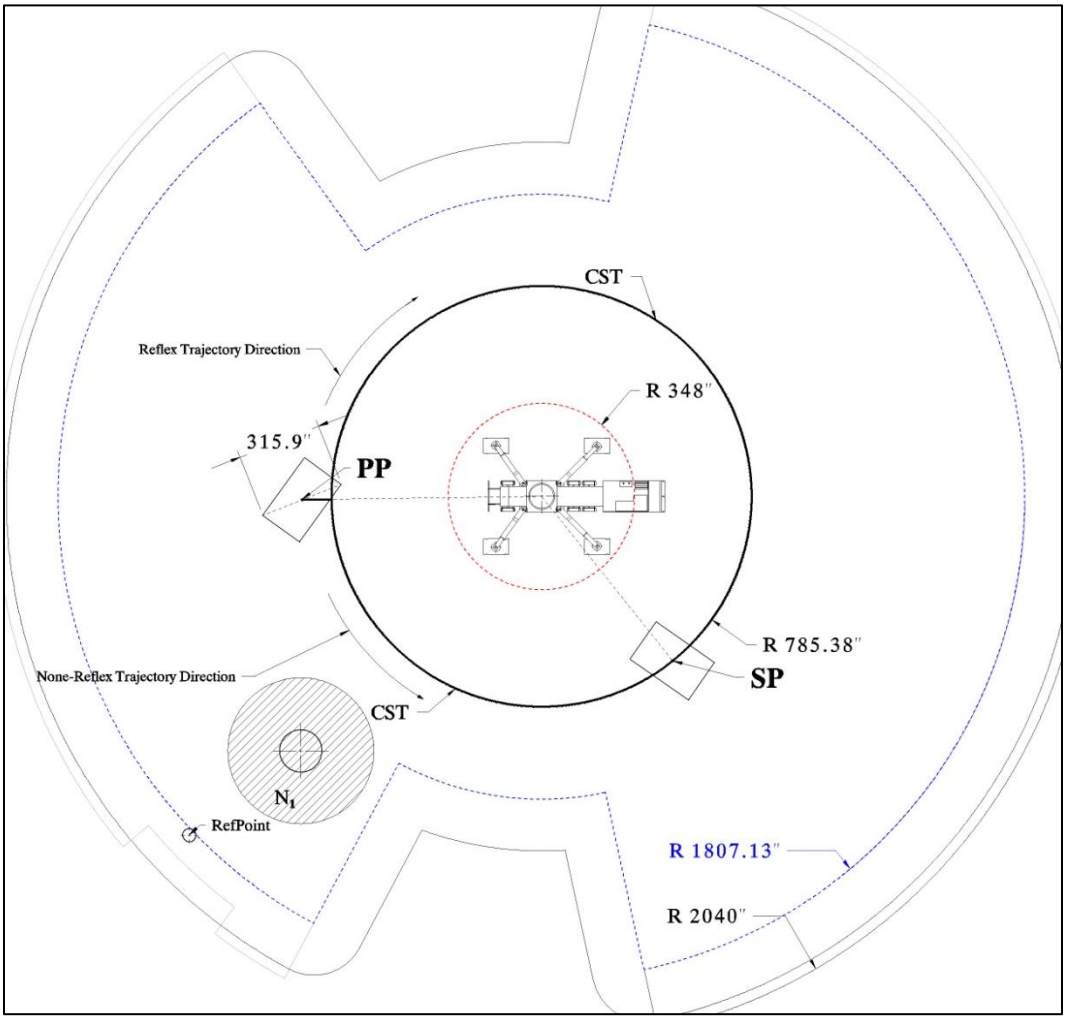

Appendix A-25, Elevation k_6 trajectory path development.

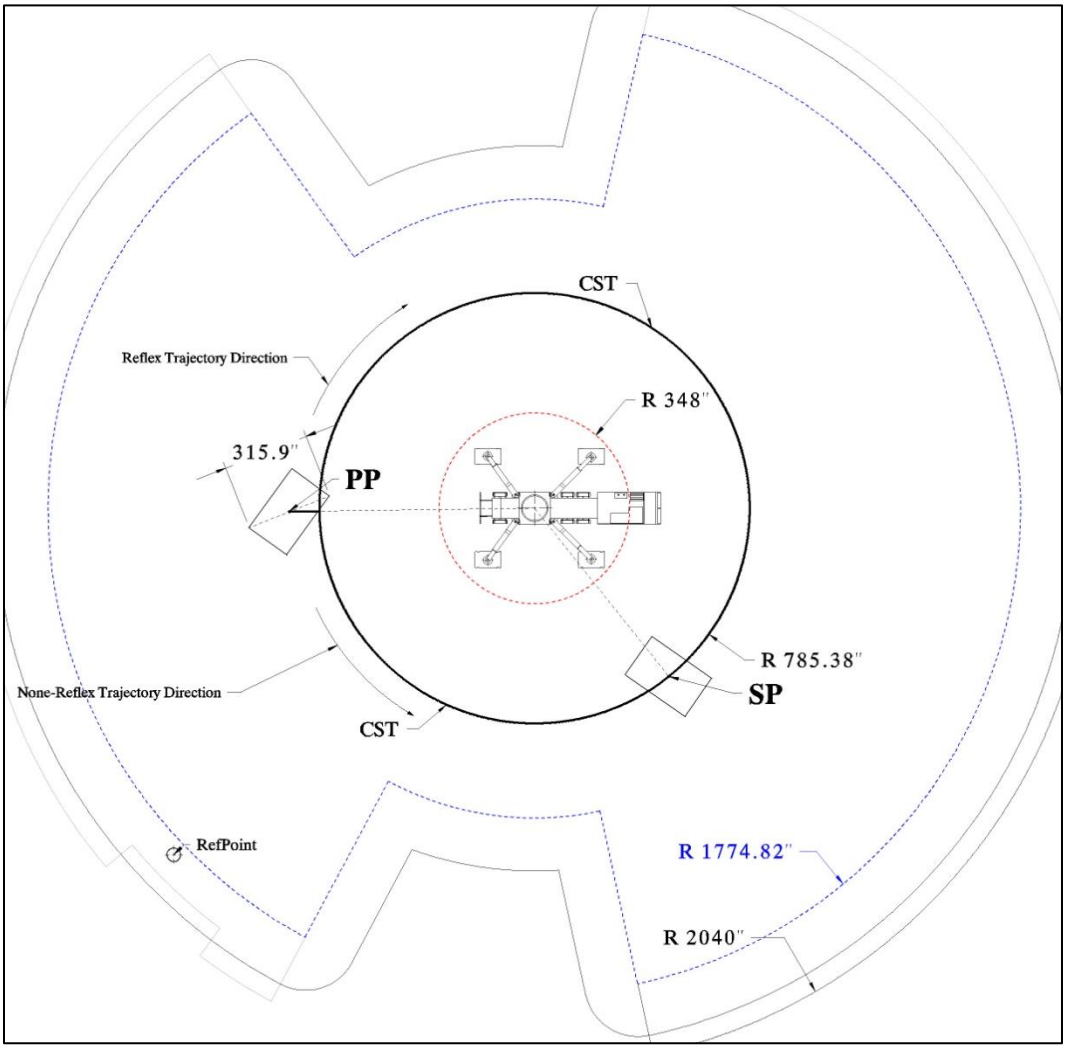

Appendix A-26, Elevations trajectory directional points coordinates.

Point	X	Y	Z
102	421.71	1252.13	688.00
701	1806.50	650.75	349.38
103	421.71	1252.13	723.00
104	531.33	1253.66	723.00
105	550.38	1092.35	723.00
106	560.90	1050.86	723.00
107	864.37	1136.70	723.00
108	1000.75	916.60	723.00
109	978.65	892.25	723.00
110	994.90	878.12	723.00
111	980.86	861.25	723.00
112	994.98	849.91	723.00
113	981.85	832.97	723.00
114	999.05	820.16	723.00
115	983.08	797.81	723.00
116	1012.23	778.30	723.00
117	984.52	734.03	723.00
118	1002.58	723.15	723.00
119	86.63	988.08	723.00
120	278.11	549.88	723.00
121	359.07	605.59	723.00
122	374.09	584.29	723.00
123	405.79	607.18	723.00
124	420.35	587.60	723.00
125	448.13	608.66	723.00
126	468.37	582.68	723.00
127	498.94	607.25	723.00
128	541.79	557.24	723.00
129	552.33	566.86	723.00
130	781.84	378.61	723.00
131	910.78	592.24	723.00
132	922.60	585.24	723.00
133	996.65	547.39	723.00
134	856.21	232.59	723.00
135	963.70	191.07	723.00
136	1012.83	540.39	723.00
137	1058.20	648.54	723.00
138	1414.63	603.76	723.00
139	1431.84	487.75	723.00
140	1439.60	488.94	723.00
141	1493.58	148.49	723.00
142	1473.45	145.48	723.00
143	1473.45	145.48	723.00
144	1806.50	650.75	723.00
145	1650.48	1975.51	723.00
146	1464.56	1579.62	723.00
147	1420.60	1596.73	723.00
148	1448.76	2038.81	723.00
149	1476.09	2198.91	723.00
150	745.58	2021.09	723.00
151	843.44	1891.45	723.00
152	740.47	1798.34	723.00
153	1061.33	1501.12	723.00
154	1070.57	1510.72	723.00
201	531.33	1253.66	804.80
202	550.38	1092.35	804.80
203	560.90	1050.86	804.80
204	910.78	592.24	804.80
205	922.60	585.24	804.80
206	996.65	547.39	804.80
207	856.21	232.59	804.80
208	963.70	191.07	804.80
209	1012.83	540.39	804.80
210	1058.20	648.54	804.80
211	1414.63	603.76	804.80
212	1431.84	487.75	804.80
213	1439.60	488.94	804.80
214	1493.58	148.49	804.80
215	1473.45	145.48	804.80
216	1806.50	650.75	804.80
217	1650.48	1975.51	804.80
218	1464.56	1579.62	804.80
219	1420.60	1596.73	804.80
220	1448.76	2038.81	804.80
221	1476.09	2198.91	804.80
222	745.58	2021.09	804.80
223	843.44	1891.45	804.80
224	740.47	1798.34	804.80
225	1061.33	1501.12	804.80
227	1070.57	1510.72	804.80
301	531.33	1253.66	1034.80
302	550.38	1092.35	1034.80
303	560.90	1050.86	1034.80
304	910.78	592.24	1034.80
305	922.60	585.24	1034.80
306	996.65	547.39	1034.80
307	1012.83	540.39	1034.80
308	1431.84	487.75	1034.80
309	1439.60	488.94	1034.80
310	1806.50	650.75	1034.80
311	1650.48	1975.51	1034.80
312	1464.56	1579.62	1034.80
313	1420.60	1596.73	1034.80
314	1448.76	2038.81	1034.80
315	1476.09	2198.91	1034.80
316	745.58	2021.09	1034.80
317	843.44	1891.45	1034.80
318	740.47	1798.34	1034.80
319	1061.33	1501.12	1034.80
320	1070.57	1510.72	1034.80
401	531.33	1253.66	1195.40
402	550.38	1092.35	1195.40
403	560.90	1050.86	1195.40
404	910.78	592.24	1195.40
405	922.60	585.24	1195.40
406	996.65	547.39	1195.40
407	1012.83	540.39	1195.40
408	1431.84	487.75	1195.40
409	1439.60	488.94	1195.40
410	1806.50	650.75	1195.40
411	1650.48	1975.51	1195.40
412	1464.56	1579.62	1195.40
413	1420.60	1596.73	1195.40
414	1448.76	2038.81	1195.40
415	1476.09	2198.91	1195.40
416	745.58	2021.09	1195.40
417	843.44	1891.45	1195.40
418	740.47	1798.34	1195.40
419	1061.33	1501.12	1195.40
420	1070.57	1510.72	1195.40
501	531.33	1253.66	1231.40
502	550.38	1092.35	1231.40
503	560.90	1050.86	1231.40
504	910.78	592.24	1231.40
505	922.60	585.24	1231.40
506	996.65	547.39	1231.40
507	1012.83	540.39	1231.40
508	1431.84	487.75	1231.40
509	1439.60	488.94	1231.40
510	1806.50	650.75	1231.40
511	1650.48	1975.51	1231.40
512	1448.76	2038.81	1231.40
513	843.44	1891.45	1231.40
514	740.47	1798.34	1231.40
601	531.33	1253.66	1276.40
602	550.38	1092.35	1276.40
603	560.90	1050.86	1276.40
604	910.78	592.24	1276.40
605	922.60	585.24	1276.40
606	996.65	547.39	1276.40
607	1012.83	540.39	1276.40
608	1431.84	487.75	1276.40
609	1439.60	488.94	1276.40
610	1806.50	650.75	1276.40
611	1650.48	1975.51	1276.40
612	1448.76	2038.81	1276.40
613	843.44	1891.45	1276.40
614	740.47	1798.34	1276.40

Appendix A-27, Trajectory points connection data.

ID	Start	End	Type	Dist	ID	Start	End	Type	Dist	ID	Start	End	Type	Dist	ID	Start	End	Type	Dist
1	102	103	L	35.00	44	152	153	L	437.37	87	204	131	Vd	81.80	130	147	219	Vu	81.80
2	103	104	L	109.63	45	153	154	C	13.33	88	132	205	Vu	81.80	131	219	147	Vd	81.80
3	104	105	C	162.72	46	152	151	C	139.01	89	205	132	Vd	81.80	132	301	302	C	162.72
4	105	106	C	42.80	47	151	150	L	162.42	90	133	206	Vu	81.80	133	302	303	C	42.80
5	106	107	L	315.37	48	150	149	C	773.09	91	206	133	Vd	81.80	134	303	304	C	590.67
6	107	108	C	262.32	49	149	148	L	162.42	92	134	207	Vu	81.80	135	304	305	C	13.73
7	108	109	L	32.88	50	148	145	C	212.06	93	207	134	Vd	81.80	136	305	306	C	83.20
8	109	110	C	21.54	51	145	146	L	437.38	94	135	208	Vu	81.80	137	306	307	C	17.64
9	110	111	L	21.95	52	146	147	C	47.20	95	208	135	Vd	81.80	138	307	308	C	427.56
10	111	112	C	18.12	53	145	144	C	1593.54	96	136	209	Vu	81.80	139	308	309	C	7.86
11	112	113	L	21.43	54	201	202	C	162.72	97	209	136	Vd	81.80	140	309	310	C	405.48
12	113	114	C	21.45	55	202	203	C	42.80	98	137	210	Vu	81.80	141	301	318	C	597.78
13	114	115	L	27.47	56	203	204	C	590.67	99	210	137	Vd	81.80	142	318	319	L	437.37
14	115	116	C	35.08	57	204	205	C	13.73	100	138	211	Vu	81.80	143	319	320	C	13.33
15	116	117	L	52.22	58	205	206	C	83.20	101	211	138	Vd	81.80	144	318	317	C	139.01
16	117	118	C	21.09	59	206	207	L	344.70	102	139	212	Vu	81.80	145	317	316	L	162.42
17	105	119	L	475.33	60	207	208	C	115.29	103	212	139	Vd	81.80	146	316	315	C	773.09
18	119	120	C	481.12	61	206	209	C	17.64	104	140	213	Vu	81.80	147	315	314	L	162.42
19	120	121	L	98.28	62	209	210	L	117.28	105	213	140	Vd	81.80	148	314	311	C	212.06
20	121	122	C	26.07	63	210	211	C	363.71	106	141	214	Vu	81.80	149	311	312	L	437.38
21	122	123	L	39.11	64	211	212	L	117.28	107	214	141	Vd	81.80	150	312	313	C	47.20
22	123	124	C	24.39	65	212	213	C	7.86	108	142	215	Vu	81.80	151	311	310	C	1593.54
23	124	125	L	34.85	66	213	214	L	344.71	109	215	142	Vd	81.80	152	201	301	Vu	230.00
24	125	126	C	32.94	67	214	215	C	20.35	110	144	216	Vu	81.80	153	301	201	Vd	230.00
25	126	127	L	39.22	68	213	216	C	405.48	111	216	144	Vd	81.80	154	202	302	Vu	230.00
26	127	128	C	65.87	69	201	224	C	597.78	112	152	244	Vu	81.80	155	302	202	Vd	230.00
27	128	129	L	14.27	70	224	225	L	437.37	113	244	152	Vd	81.80	156	203	303	Vu	230.00
28	129	130	C	297.86	71	225	227	C	13.33	114	153	225	Vu	81.80	157	303	203	Vd	230.00
29	130	131	L	249.52	72	224	223	C	139.01	115	225	153	Vd	81.80	158	204	304	Vu	230.00
30	131	132	C	13.73	73	223	222	L	162.42	116	154	227	Vu	81.80	159	304	204	Vd	230.00
31	132	133	C	83.20	74	222	221	C	773.09	117	227	154	Vd	81.80	160	205	305	Vu	230.00
32	133	134	L	344.70	75	221	220	L	162.42	118	151	223	Vu	81.80	161	305	205	Vd	230.00
33	134	135	C	115.29	76	220	217	C	212.06	119	223	151	Vd	81.80	162	206	306	Vu	230.00
34	133	136	C	17.64	77	217	218	L	437.38	120	150	222	Vu	81.80	163	306	206	Vd	230.00
35	136	137	L	117.28	78	218	219	C	47.20	121	222	150	Vd	81.80	164	209	307	Vu	230.00
36	137	138	C	363.71	79	217	216	C	1593.54	122	149	221	Vu	81.80	165	307	209	Vd	230.00
37	138	139	L	117.28	80	104	201	Vu	81.80	123	221	149	Vd	81.80	166	212	308	Vu	230.00
38	139	140	C	7.86	81	201	104	Vd	81.80	124	148	220	Vu	81.80	167	308	212	Vd	230.00
39	140	141	L	344.71	82	105	202	Vu	81.80	125	220	148	Vd	81.80	168	213	309	Vu	230.00
40	141	142	C	20.35	83	202	105	Vd	81.80	126	145	217	Vu	81.80	169	309	213	Vd	230.00
41	140	144	C	405.48	84	106	203	Vu	81.80	127	217	145	Vd	81.80	170	216	310	Vu	230.00
42	144	701	L	373.63	85	203	106	Vd	81.80	128	146	218	Vu	81.80	171	310	216	Vd	230.00
43	104	152	C	597.78	86	131	204	Vu	81.80	129	218	146	Vd	81.80	172	224	318	Vu	230.00

ID	Start	End	Type	Dist
173	318	224	Vd	230.00
174	225	319	Vu	230.00
175	319	225	Vd	230.00
176	227	320	Vu	230.00
177	320	227	Vd	230.00
178	223	317	Vu	230.00
179	317	223	Vd	230.00
180	222	316	Vu	230.00
181	316	222	Vd	230.00
182	221	315	Vu	230.00
183	315	221	Vd	230.00
184	220	314	Vu	230.00
185	314	220	Vd	230.00
186	217	311	Vu	230.00
187	311	217	Vd	230.00
188	218	312	Vu	230.00
189	312	218	Vd	230.00
190	219	313	Vu	230.00
191	313	219	Vd	230.00
192	401	402	C	162.72
193	402	403	C	42.80
194	403	404	C	590.67
195	404	405	C	13.73
196	405	406	C	83.20
197	406	407	C	17.64
198	407	408	C	427.56
199	408	409	C	7.86
200	409	410	C	405.48
201	401	418	C	597.78
202	418	419	L	437.37
203	419	420	C	13.33
204	418	417	C	139.01
205	417	416	L	162.42
206	416	415	C	773.09
207	415	414	L	162.42
208	414	411	C	212.06
209	411	412	L	437.38
210	412	413	C	47.20
211	411	410	C	1593.54
212	301	401	Vu	160.60
213	401	301	Vd	160.60
214	302	402	Vu	160.60
215	402	302	Vd	160.60
216	303	403	Vu	160.60
217	403	303	Vd	160.60
218	304	404	Vu	160.60
219	404	304	Vd	160.60
220	305	405	Vu	160.60
221	405	305	Vd	160.60
222	306	406	Vu	160.60
223	406	306	Vd	160.60
224	309	407	Vu	160.60
225	407	309	Vd	160.60
226	312	408	Vu	160.60
227	408	312	Vd	160.60
228	313	409	Vu	160.60
229	409	313	Vd	160.60
230	316	410	Vu	160.60
231	410	316	Vd	160.60
232	324	418	Vu	160.60
233	428	324	Vd	160.60
234	325	419	Vu	160.60
235	419	325	Vd	160.60
236	327	420	Vu	160.60
237	420	327	Vd	160.60
238	323	417	Vu	160.60
239	417	323	Vd	160.60
240	322	416	Vu	160.60
241	416	322	Vd	160.60
242	321	415	Vu	160.60
243	415	321	Vd	160.60
244	320	414	Vu	160.60
245	414	320	Vd	160.60
246	317	411	Vu	160.60
247	411	317	Vd	160.60
248	318	412	Vu	160.60
249	412	318	Vd	160.60
250	319	413	Vu	160.60
251	414	319	Vd	160.60
252	501	502	C	162.72
253	502	503	C	42.80
254	503	504	C	590.67
255	504	505	C	13.73
256	505	506	C	83.20
257	506	507	C	17.64
258	507	508	C	427.56
259	508	509	C	7.86
260	509	510	C	405.48
261	501	514	C	597.78
262	514	513	C	139.01
263	513	512	C	640.61
264	512	511	C	212.06
265	511	510	C	1593.54
266	401	501	Vu	36.00
267	501	401	Vd	36.00
268	402	502	Vu	36.00
269	502	402	Vd	36.00
270	403	503	Vu	36.00
271	503	403	Vd	36.00
272	404	504	Vu	36.00
273	504	404	Vd	36.00
274	405	505	Vu	36.00
275	505	405	Vd	36.00
276	406	506	Vu	36.00
277	506	406	Vd	36.00
278	407	507	Vu	36.00
279	507	407	Vd	36.00
280	408	508	Vu	36.00
281	508	408	Vd	36.00
282	409	509	Vu	36.00
283	509	409	Vd	36.00
284	410	510	Vu	36.00
285	510	410	Vd	36.00
286	418	514	Vu	36.00
287	514	418	Vd	36.00
288	417	513	Vu	36.00
289	513	417	Vd	36.00
290	414	512	Vu	36.00
291	512	414	Vd	36.00
292	411	511	Vu	36.00
293	511	411	Vd	36.00
294	601	602	C	162.72
295	602	603	C	42.80
296	603	604	C	590.67
297	604	605	C	13.73
298	605	606	C	83.20
299	606	607	C	17.64
300	607	608	C	427.56
301	608	609	C	7.86
302	609	610	C	405.48
303	601	614	C	597.78
304	614	613	C	139.01
305	613	612	C	640.61
306	612	611	C	212.06
307	611	610	C	1593.54
308	501	601	Vu	45.00
309	601	501	Vd	45.00
310	502	602	Vu	45.00
311	602	502	Vd	45.00
312	503	603	Vu	45.00
313	603	503	Vd	45.00
314	504	604	Vu	45.00
315	604	504	Vd	45.00
316	505	605	Vu	45.00
317	605	505	Vd	45.00
318	506	606	Vu	45.00
319	606	506	Vd	45.00
320	507	607	Vu	45.00
321	607	507	Vd	45.00
322	508	608	Vu	45.00
323	608	508	Vd	45.00
324	509	609	Vu	45.00
325	609	509	Vd	45.00
326	510	610	Vu	45.00
327	610	510	Vd	45.00